

**DESIGN OF FACTS CONTROLLER AND PSS USING  
INTELLIGENT TECHNIQUES FOR STABILITY  
ANALYSIS IN RESTRUCTURED MARKET**

By

**PIMAL R.GANDHI**



**DEPARTMENT OF ELECTRICAL ENGINEERING  
FACULTY OF TECHNOLOGY & ENGINEERING  
THE M. S. UNIVERSITY OF BARODA  
JANUARY, 2014**

**DESIGN OF FACTS CONTROLLER AND PSS USING  
INTELLIGENT TECHNIQUES FOR STABILITY  
ANALYSIS IN RESTRUCTURED MARKET**

*A Thesis submitted for the Award of the*

*Degree of*

**Doctor of PHILOSOPHY**

in

Electrical Engineering

By

**PIMAL R.GANDHI**



**DEPARTMENT OF ELECTRICAL ENGINEERING  
FACULTY OF TECHNOLOGY & ENGINEERING  
THE M. S. UNIVERSITY OF BARODA  
JANUARY, 2014**

## **CERTIFICATE**

This is to certify that the thesis entitled **DESIGN OF FACTS CONTROLLER AND PSS USING INTELLIGENT TECHNIQUES FOR STABILITY ANALYSIS IN RESTRUCTURED MARKET** submitted by *Pimal R.Gandhi* in fulfilment of the degree of **DOCTOR OF PHILOSOPHY** in Electrical Engineering Department, Faculty of Technology & Engineering, The M. S. University of Baroda, Vadodara is a bonafide record of investigations carried out by his in the Department of Electrical Engineering, Faculty of Technology & Engineering, The M. S. University of Baroda, Vadodara under my guidance and supervision. In my opinion the standards fulfilling the requirements of the Ph.D. Degree as prescribed in the regulations of the University has been attained.

**(Prof. S. K. Joshi)**

Professor  
Electrical Engineering Department  
Faculty of Technology & Engineering  
The Maharaja Sayajirio University of Baroda  
Vadodara 390 001

January, 2014

**Head**

Electrical Engineering Department  
Faculty of Tech. & Engg.

**Dean**

Faculty of Tech. & Engg.

## **DECLARATION**

I, Mr. Pimal R.Gandhi hereby declare that the work reported in this thesis entitled DESIGN OF FACTS CONTROLLER AND PSS USING INTELLIGENT TECHNIQUES FOR STABILITY ANALYSIS IN RESTRUCTURED MARKET submitted for the award of the degree of DOCTOR OF PHILOSOPHY in Electrical Engineering Department, Faculty of Technology & Engineering, The M. S. University of Baroda, Vadodara is original and has been carried out in the Department of Electrical Engineering, Faculty of Technology & Engineering, M. S. University of Baroda, Vadodara. I further declare that this thesis is not substantially the same as one, which has already been submitted in part or in full for the award of any degree or academic qualification of this University or any other Institution or examining body in India or abroad.

*(Pimal R.Gandhi)*

January, 2014.

**dedicated to my Parents,  
my Wife and my adorable Children**

# Synopsis

---

Name of Student: Pimal R.Gandhi

Roll No: 463

Degree for which submitted: Ph.D.

Department: Electrical Engineering

Thesis Title: **DESIGN OF FACTS CONTROLLER AND PSS USING  
INTELLIGENT TECHNIQUES FOR STABILITY ANALYSIS  
IN RESTRUCTURED MARKET**

Name of thesis supervisor: Professor S. K. Joshi

---

The electric utility industries have undergone unprecedented changes in its structure worldwide. New issues in power system operation and planning are inevitable due to the advent of an open market environment and restructuring of the industry into separate generation, transmission, and distribution entities [1] [2]. One of the major consequences of this new electric utility environment is the greater emphasis on stable, secure, controlled, momentary and high quality electric power in restructured power scenario. In restructure market consist generation companies (GENCOS), transmission companies (TRANCOS), distribution companies (GENCOs) and independent system operators (ISO). The ISO is independent and disassociated agent for market participation and perform the various ancillary services. The ISO uses ancillary services for [3] [4] maintaining the frequency, voltage profile, stability of the system and preventing the overloading as well as restoring the system after the black out.

The small signal stability analysis and transient stability analysis have become essential ingredient of for stable and secure operation of power system [5]. The stability of the power system has been affected by the disturbances like a sudden change in load, loss of generator or switching of a transmission line during the fault and wide spread use of the high gain

fast acting excitation system. The instability and low frequency oscillations limit the power transmission capability and the eventually breakdown of the entire power system under the certain operating conditions and configurations. The ancillary controllers play very important role in deregulated electric market to enhance the stability of the power system with their good controlling characteristics. The ancillary service such as power system stabilizer (PSS) [3] and Flexible Alternating Current Transmission system (FACTS) controller [4] [6] in deregulated electric market has been addressed. Significance and impact of small signal stability and transient stability issues in restructured electric market has been reported [3] [7].

The Power system stabilizer provides the supplementary control signal for the excitation system of the synchronous generator to damp the low frequency oscillations and to improve power system stability. The power system stabilizers have been designed very extensively using phase compensation techniques and parameters of PSS have been calculated based on linearized Philips–Heffron model of the power system for the small signal stability analysis [5] [8] [9]. The small signal stability and transient stability with concepts of synchronizing and damping torques has been explained in [10]. The conventional control techniques based PSS can provide optimal performance for the normal operating conditions and normal system parameters. However, a modern power system has become large, tight and highly dynamic, hence to difficult to solve low frequency oscillations problem through conventional and linear optimal control approaches. For the different loading conditions and configuration of power network, the parameters of PSS controllers are needed to be modified. To overcome these limitations, computational intelligent techniques such as Fuzzy Logic (FL), Artificial Neural Network (ANN), Genetics Algorithm (GA), Particle Swarm Optimization (PSO) etc. based PSS have been proposed in different literature.

The FACTS controller plays very important role in deregulated electric market to enhance the stability of the power system with their fast control characteristics and continuous compensating capability. FACTS devices can be effectively used for load flow control, loop power flow control, load dispatched, voltage regulation, enhancement of transient stability

and mitigation of system oscillation [11] [12]. One of the most important devices of series FACTS controller is thyristor controlled series capacitor (TCSC) [13] in order to enhance the stability and load ability of the transmission network.

In large power system, abnormal phenomena have been frequently observed such as tie-line power deviation, rotor speed deviation and outage of generation under various loading conditions. Automatic generation control (AGC) is an essential control loop in electric power system which maintain balances between generated power and demand power in each control area. For the conventional Load Frequency controller, the integral of area control error (ACE) is utilized as the control signal for conventional control strategy. An integral controller provides zero steady state deviation, but it produces poor dynamic performance. Therefore advanced control techniques are needed to handle abnormal situation in power system. The application of FACTS controllers [14] in multiarea AGC under deregulated electric market [15] has been reported by recent research paper.

Therefore achievement of desired performance of power system under contingencies, the intelligent techniques based adaptive PSS and FACTS damping controllers are required to be designed. The controllers accompany load frequency control (LFC) in multiple area generation (AGC) system in deregulated environment have been an attraction in ongoing research work.

The motivation behind the work presented in this thesis are:

1. To develop the linearized model of fifth order synchronous machine from non linear model and to derive the different constants follows block diagram of the synchronous machine connected to single machine infinite system.
2. To develop the mathematical model of the machine in state space form with conventional power system stabilizer (CPSS), proportional integral derivative PSS, and TCSC individually and simultaneously.
3. To design the PSS using different intelligent techniques such as Genetic Algorithm, Levenberg Marquardt neural network (LMNN), adaptive neuro fuzzy inference system

(ANFIS), genetics algorithm based artificial neural network hybrid algorithm (GA-ANN), Neural Network based non linear auto regressive moving average (NARMA)-L2 controller.

4. To design the stability control loop of TCSC using GA, ANN and ANFIS techniques. To analyze the simultaneous and individual application of PSS and TCSC using programming and to carry out non linear simulations under different operating conditions and disturbances in power system .
5. To develop linear model and block diagram of the two area automatic generation control system with the first order and fifth order power system model under the restructured electric environment.
6. To build the model of two area power system with multiple PSS, individual tie-line TCSC and combining PSSs and TCSC.
7. To study the effectiveness of an ancillary controllers such as multiple PSSs and TCSC in restructured electric market.
8. To evaluate the performance of smart control techniques based ancillary controller using linear analysis and non linear simulation.

A brief description of the work reported in the thesis is given below:

In present Chapter 1 introduces the restructured electric market, stability issue and application of ancillary controllers in restructured market. It represents the relevant state-of-the-art survey and sets the motivation behind the research work carried out in this thesis.

Chapter 2 presents, detail modeling of the system components and linerization of non linear equations using Taylor's series method. The state space form of power system with conventional power system stabilizer and PID- power system stabilizer have been described. The linearized state space form of power system with individual TCSC and simultaneous CPSS and TCSC have been also derived.

Chapter 3 presents, Genetic Algorithm based control strategies for designing of CPSS, PID-PSS and TCSC damping controller. The individual PSSs and simultaneous designed TCSC and PSS have been applied to the dynamical power system. The small signal stability analysis and non-linear simulation for the transient stability analysis are carried out for details investigation of the power system stability issue.

Chapter 4 discusses Adaptive Neuro-Fuzzy Inference System and Levenberg-Marquardt Artificial Neural Network algorithm for development of the control strategy for thyristor control series capacitor based damping controller and power system stabilizer. The non-linear simulations of single machine infinite bus system have been carried out using individual and simultaneously application of PSS and TCSC. The comparisons between intelligent control strategies based damping controllers also have been carried out.

Chapter 5 discusses Non Linear Auto regressive Moving Average-L2 controller and hybrid Genetic Algorithm based Network Network for development of the control strategy for power system stabilizer. In order to achieve appreciable damping, developed ANFIS based Thyristor control series capacitor has been suggested in addition to power system stabilizer. The non-linear simulations of single machine infinite bus system have been carried out using individual and simultaneously application of PSS and TCSC.

Chapter 6 presents, performance and role of ancillary controllers such as PSS and TCSC in two area control system under restructured electric market. Low order power system model and higher order power system model have been considered for depth analysis of two area system with ancillary controllers. The small signal stability analysis and non-linear simulation for the transient stability analysis are carried out for investigation of the power system stability issue.

Chapter 7 concludes the main finding and significant contribution of the thesis and provides a few suggestion for further scope of research work in this area.

## References

- [1] F.D. Galiana and M. Ilic,. A Mathematical Framework for the Analysis and Management of Power Transactions Under Open Access,. IEEE Trans. on Power Systems, vol. 13, no. 2, pp. 68- 687, 1998.
- [2] Joe H. Chow, Felix F. Wu, James A Momoh, Applied Mathematics for Restructured Electric Power Systems: Optimization, Control and Computational intelligence, Springer,2005.
- [3] Adrian andreoiu,Kamkar Bhattacharya, PSS-Control as an Ancillary Service , International Journal on Electric Power System Research, Vol.74, pp. 391-399, 2005.
- [4] C.K. Panigrahi, P.K. Chattopadhyay, R.N. Chakrabarti, FACTS in Deregulated Market Scenario, inaugural IEEE PES Conference and Exposition in Africa, IEEE, 2005.
- [5] P. Kundur, Power System Stability and Control, McGraw-Hill, 1994.
- [6] N.G.Hingorani, Role of FACTS in a Deregulated Market, IEEE, pp. 1463-1467, 2000.
- [7] Vijay Vittal, Consequence and impact of Electric Utility industry Restructuring on Transient Stability and Small Signal Stability Analysis, Proceedings of the IEEE, Vol.88, No. 2, pp. 196-207, 2002.
- [8] K.R.Padiyar, Power System Dynamics Stability and control, BS Publications, 2nd Hyderabad, India, 2002.
- [9] P.M.anderson, A.A.Fouad , Power System Control and Stability, Wiley Interscience, IEEE Press, Second Edition, 2003.
- [10] Michael J. Basler, Richard C. Schaefer, Understanding Power-System Stability, IEEE Transaction on industry Applications, Vol. 44, No. 2, pp. 463-474, 2008.
- [11] N.G.Hingorani and L.Gyugyi, Understanding FACTS: Concepts and Technology of Flexible AC Transmission System, IEEE Press, 2000.
- [12] R.Mohan Mathur, Rajiv K. Verma, Thyristor-Based FACTS controllers for Electrical Transmission Systems, IEEE Press, 2003.
- [13] Alberto D.Del Rosso, Claudio A.Canizares, Victor M.Dona, A Study of TCSC Controller Design for Power System Stability Improvement, IEEE transactions on power system, Vol. 18, No.4, pp: 1487-1496, 2003.

- [14] C.Srinivasa Rao, S.Siva Nagaraju, P.SAngameswara Raju, Automatic Generation Control of TCPS Based Hydrothermal System Under Open Market Scenario: A Fuzzy Logic Approach, Vol. 31, pp. 315-322, 2009.
- [15] Vaibhav Donde, M.A.Pai, An A.Hiskens, Simulation and Optimization in an AGC System After Deregulation, IEEE Transaction on Power System, Vol. 16, No. 3, pp.481-489, 2001.

# Acknowledgements

It is my proud privilege to express my deep sense of gratitude and indebtedness towards my thesis supervisor Prof.S.K. Joshi, for his invaluable guidance, unfailing support and constant encouragement, which were the vital factors in successful completion of the present work. I am heartily thankful to him for his deep concern towards my academics and personal welfare. His painstaking support and exhaustive involvement in preparation of manuscript, mathematical modelling of system, conduction of simulation studies is gratefully acknowledged. I sincerely appreciate his pronounced individualities, humanistic and warm personal approach, which has given me strength to carry out this research work on steady and smooth course. I humbly acknowledge a lifetime's gratitude to him.

I would like to convey my sincer thank to Board of Management, Sardar Vallabhbhai Patel Institute of Technology, Vasad for giving me a golden opportunity to pursue doctoral program. I am extremely grateful to Chairman,S.V.I.T.,Vasad, Principal,S.V.I.T.,Vasad and H.O.D.,Electrical Department, for sanctioning my study leave, support and encouragement throughout my study. It is a pleasure to acknowledge the sincere support given by my friends and colleagues at S.V.I.T., Vasad.,

I express my deep sense of reverence and profound gratitude to my Parents for their pains and sufferings they have undergone to bring me up to this level. I respectfully thank to my grandmother, parents-in-law and my sister for their blessing and encouragement.

I express my heartiest gratitude to my beloved wife Namrata, my daughter Swara and son Mantra for their unconditional support in every aspects of my life. I would like to cordially thank my wife Namrata for her loving support, patience and unfailing enthusiasm in keeping continuity of this research work.

At the end I acknowledge my sincere thanks for one all who have helped me directly or indirectly during the pursue of my studies.

**Pimal Gandhi**

# Contents

<b>Synopsis</b>	<b>iv</b>
<b>Acknowledgements</b>	<b>xi</b>
<b>List of Figures</b>	<b>xvii</b>
<b>List of Tables</b>	<b>xxiii</b>
<b>1 Introduction</b>	<b>1</b>
1.1 General . . . . .	1
1.2 State-of-the Art . . . . .	3
1.3 Motivation . . . . .	12
1.4 Thesis Organization . . . . .	15
<b>2 Mathematical Modeling of Power System</b>	<b>17</b>
2.1 General . . . . .	17
2.2 Generator model . . . . .	17
2.3 Excitation System . . . . .	19
2.3.1 Initial Conditions . . . . .	19
2.4 Linearization and Eigen Properties . . . . .	20
2.4.1 Linearization . . . . .	20
2.4.2 Sate Space Representation . . . . .	22
2.4.3 Eigen Values . . . . .	23
2.4.3.1 Eigen Vector . . . . .	24
2.4.3.2 Participation Factor . . . . .	25

2.4.3.3	Eigen value and Stability . . . . .	26
2.5	Linear model of power system . . . . .	27
2.5.1	Calculation of $K_1$ to $K_{10}$ Constants . . . . .	27
2.5.2	State Space Representation of System . . . . .	29
2.6	Power System Stabilizer . . . . .	31
2.6.1	Conventional Power system stabilizer . . . . .	31
2.6.1.1	Model of Power System with CPSS . . . . .	32
2.6.2	Proportional Integral Derivative Power System Stabilizer . . . . .	33
2.6.2.1	Model of Power System with PID-PSS . . . . .	33
2.7	Thyristor Control Series Capacitor . . . . .	34
2.7.1	Model of Power system with Inclusion of TCSC . . . . .	36
2.7.2	Model of Power System with Inclusion of TCSC and PSS . . . . .	38
2.8	Conclusion . . . . .	40
<b>3</b>	<b>Design of PSS and TCSC Using Genetic Algorithm</b>	<b>42</b>
3.1	Introduction . . . . .	42
3.2	GA based Design of CPSS and PID-PSS . . . . .	43
3.2.1	Genetic Algorithm . . . . .	43
3.2.2	Problem Formulation and Optimization Function . . . . .	44
3.2.3	Calculation of Initial Conditions . . . . .	45
3.2.4	Eigen values and Participation Factor . . . . .	47
3.2.5	Results . . . . .	47
3.3	GA based Design of TCSC and PSS . . . . .	53
3.3.1	Problem Formulation and Optimization Function . . . . .	53
3.3.2	Calculation of $K_1$ to $K_{10}$ Constants . . . . .	55
3.3.3	Eigen values and Participation factor . . . . .	55
3.3.4	Results . . . . .	56
3.4	Non-linear Simulation . . . . .	60
3.4.1	Case I . . . . .	61
3.4.2	Case II . . . . .	65
3.4.3	Case III . . . . .	67

3.4.4	Case IV . . . . .	70
3.4.5	Case V . . . . .	72
3.4.6	Case VI . . . . .	74
3.5	Conclusion . . . . .	76
<b>4</b>	<b>Design of PSS and TCSC Using ANFIS and ANN</b>	<b>77</b>
4.1	Introduction . . . . .	77
4.2	Adaptive Neuro-Fuzzy Inference System (ANFIS) . . . . .	78
4.2.1	ANFIS- Architecture . . . . .	78
4.3	Steps for Designing of ANFIS based PSS and TCSC . . . . .	81
4.3.1	ANFIS-Power System Stabilizer . . . . .	81
4.3.2	ANFIS-Thyristor Control Series Capacitor . . . . .	85
4.4	Levenberge-Marquardt Neural Network . . . . .	88
4.4.1	Levenberg-Marquardt Algorithm . . . . .	88
4.5	Steps for Designing of LMNN based PSS and TCSC . . . . .	90
4.5.1	ANN-Power System Stabilizer . . . . .	90
4.5.2	Design of LMNN-TCSC . . . . .	92
4.6	Non Linear Simulation . . . . .	93
4.6.1	Case I . . . . .	94
4.6.2	case II . . . . .	94
4.6.3	Case III . . . . .	95
4.6.4	Case IV . . . . .	96
4.6.5	Case V . . . . .	97
4.7	Conclusion . . . . .	97
<b>5</b>	<b>Design of PSS Using NARMA-L2 and GA-ANN Controller with TCSC</b>	<b>99</b>
5.1	Introduction . . . . .	99
5.2	Nonlinear Auto regressive Moving average -L2 Controller . . . . .	100
5.2.1	NARMA-L2 (Feedback Linearization) Control . . . . .	100
5.2.1.1	Identification Stage . . . . .	100
5.2.1.2	Controller Stage . . . . .	102
5.3	NARMA-L2 Controller based Power System Stabilizer . . . . .	102

5.3.1	Neural Network Identifier . . . . .	103
5.3.2	Neural Network Controller . . . . .	105
5.4	GA-ANN Hybrid-Power System Stabilizer . . . . .	105
5.4.1	Genetic Algorithm . . . . .	106
5.4.2	Neural Network . . . . .	108
5.5	Non Linear Simulation . . . . .	110
5.5.1	Case I . . . . .	110
5.5.2	Case II . . . . .	112
5.5.3	Case III . . . . .	113
5.5.4	Case IV . . . . .	114
5.5.5	Case V . . . . .	115
5.5.6	Case VI . . . . .	115
5.6	Simulation of System with Intelligent Techniques based PSS and ANFIS-TCSC . . . . .	116
5.6.1	Case I . . . . .	117
5.6.2	Case II . . . . .	118
5.6.3	Case III . . . . .	119
5.6.4	Case IV: . . . . .	120
5.7	Conclusion . . . . .	121
<b>6</b>	<b>Design of Ancillary Controllers for Restructured Electric Market</b>	<b>123</b>
6.1	Introduction . . . . .	123
6.2	Restructured Power System . . . . .	124
6.3	Design of TCSC Controller with First Order Power System Model . . . . .	126
6.3.1	Power system model . . . . .	127
6.3.2	Tie Line Power Flow Model With TCSC . . . . .	127
6.3.3	Block Diagram and Model of Interconnected Two area System . . . . .	129
6.3.4	GA- tie line TCSC Controller: Problem Formulation and Optimization Function . . . . .	134
6.3.5	ANFIS- Tie Line TCSC Controller . . . . .	135
6.3.6	Simulation and Results . . . . .	136

6.3.7	Discussion . . . . .	141
6.4	Design of PSS and TCSC Controller with Fourth order Power System Model	142
6.4.1	Power System Model . . . . .	143
6.4.1.1	Model of Power System with multiple PSS . . . . .	143
6.4.1.2	Model of Power System with PSSs and TCSC . . . . .	143
6.4.2	Design of Ancillary controllers using GA . . . . .	148
6.4.2.1	GA based Multiple PSS : Problem Formulation and Optimization Function . . . . .	148
6.4.2.2	GA based PSSs and TCSC : Problem Formulation and Optimization Function . . . . .	149
6.4.3	Design of Ancillary controllers using ANFIS . . . . .	150
6.4.3.1	ANFIS based Multiple PSS . . . . .	151
6.4.3.2	ANFIS based PSSs and TCSC . . . . .	151
6.4.4	Analysis . . . . .	151
6.4.5	Non Linear Simulation . . . . .	153
6.5	Conclusion . . . . .	161
<b>7</b>	<b>Conclusions</b>	<b>164</b>
7.1	General . . . . .	164
7.2	Summary of Important Findings . . . . .	165
7.3	Scope of Future Research . . . . .	170
	<b>Bibliography</b>	<b>172</b>
	<b>A Data of Single machine Infinite Bus system</b>	<b>183</b>
	<b>B Numerical Values of the Restructured Model</b>	<b>184</b>

# List of Figures

2.1	Block diagram of State Space Representation . . . . .	22
2.2	Single Machine Infinite Bus System . . . . .	27
2.3	Block diagram representaion of SMIB system . . . . .	30
2.4	SMIB with PSS . . . . .	31
2.5	CPSS with state variables . . . . .	31
2.6	Block diagram represntaion of SMIB with PSS . . . . .	34
2.7	Basic module of TCSC . . . . .	35
2.8	Model of TCSC . . . . .	36
2.9	SMIB wiht PSS and TCSC . . . . .	36
2.10	TCSC state diagram . . . . .	37
2.11	TCSC delay Equation . . . . .	37
2.12	Block diagram of System with PSS and TCSC . . . . .	40
3.1	Flow Chart of GA based PSSs . . . . .	46
3.2	Numbers of population versus convergence of fitness function with PSS at Normal operating condition . . . . .	50
3.3	Flow chart of GA based PSS and TCSC . . . . .	54
3.4	Numbers of population versus convergence of Fitness Function with TCSC at Normal Operating Condition . . . . .	57
3.5	Numbers of population versus convergence of Fitness Function with PSS and TCSC at Normal Operating Condition . . . . .	57
3.6	Case I: Speed deviation between 0s to 10s with damping coefficient $D = 0$ and without controller (PSS and TCSC) . . . . .	61

3.7	Case I : Speed deviation between 0s to 30s with damping coefficient $D = 0$ and without controller (PSS and TCSC) . . . . .	62
3.8	Case I : Speed deviation between 30s to 60s with damping coefficient $D = 0$ and without controllers(PSS and TCSC) . . . . .	62
3.9	Case I : Speed deviation between 60s to 90s with damping coefficient $D = 0$ and without controller (PSS and TCSC) . . . . .	63
3.10	Case I : Speed deviation between 1s to 1.2s with zero damping coefficient $D = 0$ and without controller(PSS and TCSC) . . . . .	63
3.11	Case I: Rotor angle with GA based PSSs . . . . .	63
3.12	Case I: Speed deviation with GA based PSSs . . . . .	64
3.13	Case I: Speed deviation with GA based TCSC and PSS-TCSC . . . . .	64
3.14	Case I: Line reactance with GA based TCSC and PSS-TCSC . . . . .	64
3.15	Case II: Speed deviation with damping coefficient $D = 0$ and without controller (PSS and TCSC) . . . . .	65
3.16	Case II: Rotor angle with GA based PSSs . . . . .	66
3.17	Case II: Speed deviation with GA based PSSs . . . . .	66
3.18	Case II: Speed deviation with GA based TCSC and PSS-TCSC . . . . .	67
3.19	Case III : Speed deviation between 1s to 1.2s with damping coefficient $D = 0$ and without controller(PSS and TCSC) . . . . .	68
3.20	Case III : Speed deviation between 1s to 2s with damping coefficient $D = 0$ and without controllers (PSS and TCSC) . . . . .	68
3.21	Case III : Speed deviation between 2s to 7s with damping coefficient $D = 0$ and without controller(PSS and TCSC) . . . . .	69
3.22	Case III: Speed deviation between 0s to 10s with damping coefficient $D = 0$ and without controller (PSS and TCSC) . . . . .	69
3.23	Case III: Speed deviation with GA based PSSs . . . . .	69
3.24	Case III: Speed deviation with GA based TCSC and PSS-TCSC . . . . .	70
3.25	Case IV: Speed deviation between 1s to 4s with damping coefficient $D = 0$ and without controller (PSS and TCSC) . . . . .	71
3.26	Case IV: Speed deviation between 0s to 10s with damping coefficient $D = 0$ and without controller (PSS and TCSC) . . . . .	71

3.27	Case IV: Speed deviation with GA based PSSs . . . . .	71
3.28	Case IV: Speed deviation with GA based TCSC and PSS-TCSC . . . . .	72
3.29	Case V: Speed deviation between 1s to 4s with damping coefficient $D = 0$ and without controller (PSS and TCSC) . . . . .	72
3.30	Case V: Speed response between 0s to 10s with damping coefficient $D = 0$ and without controller (PSS and TCSC) . . . . .	73
3.31	Case V: Speed deviation with GA based PSSs . . . . .	73
3.32	Case V: Speed deviation with GA based PSS and PSS-TCSC . . . . .	73
3.33	Case VI: Speed deviation between 1s to 3s with damping coefficient $D = 0$ and without controller (PSS and TCSC) . . . . .	74
3.34	Case VI: Speed deviation between 0s to 10s with damping coefficient $D = 0$ and without controller (PSS and TCSC) . . . . .	74
3.35	Case VI: Rotor angle with GA based PSSs . . . . .	75
3.36	Case VI: Speed deviation with GA based PSSs . . . . .	75
3.37	Case VI: Speed deviation with GA based PSS and PSS-TCSC . . . . .	75
4.1	Takagi-Sugeno Fuzzy Model . . . . .	79
4.2	Adaptive Neuro Fuzzy Architecture . . . . .	79
4.3	Fuzzy Logic Control based PSS . . . . .	82
4.4	ANFIS-PSS Structure . . . . .	84
4.5	Membership Functions of Speed (Input :1)-PSS . . . . .	84
4.6	Membership Functions of Change in Speed (Input :2)-PSS . . . . .	84
4.7	Decision-Surface Viewer of PSS . . . . .	85
4.8	ANFIS-TCSC Structure . . . . .	86
4.9	Membership Functions of Speed (Input: 1)-TCSC . . . . .	87
4.10	Membership Functions of Change in Speed (Input :2)-TCSC . . . . .	87
4.11	Decision-Surface Viewer of TCSC . . . . .	87
4.12	Training data and Actual data PSS . . . . .	92
4.13	Mean Square Error . . . . .	92
4.14	Case I: Speed response of ANFIS and LMNN based PSS-TCSC . . . . .	94
4.15	Case II: Speed response of ANFIS and LMNN based PSS-TCSC . . . . .	95

4.16	Case III: Speed response of ANFIS and LMNN based PSS-TCSC . . . . .	96
4.17	Case IV: Speed response of ANFIS and LMNN based PSS-TCSC . . . . .	96
4.18	Case V: Speed response of ANFIS and LMNN based PSS-TCSC . . . . .	97
5.1	Identification Stage . . . . .	102
5.2	NARMA-L2 Controller . . . . .	102
5.3	Identification of the Plant . . . . .	103
5.4	Plant Input, Plant Output, NN Output and Error . . . . .	104
5.5	Implementation of NARMA-L2 Controller . . . . .	105
5.6	Convergence rate of GA . . . . .	107
5.7	Best Value of NN Parameters . . . . .	108
5.8	Error Between Actual and Target Value . . . . .	109
5.9	Output of GANN . . . . .	110
5.10	Case I: Speed response of NARMA-L2 and GA-ANN based PSS . . . . .	111
5.11	Case I: Speed response of NARMA-L2 and GA-ANN based PSS and ANFIS-TCSC . . . . .	111
5.12	Case II: Speed response of NARMA-L2 and GA-ANN based PSS . . . . .	112
5.13	Case II: Speed response of NARMA-L2 and GA-ANN based PSS and ANFIS-TCSC . . . . .	113
5.14	Case III: Speed response of NARMA-L2 and GA-ANN based PSS . . . . .	113
5.15	Case III: Speed response of NARMA-L2 and GA-ANN based PSS and ANFIS-TCSC . . . . .	114
5.16	Case IV: Speed response of NARMA-L2 and GA-ANN based PSS and ANFIS-TCSC . . . . .	114
5.17	Case V: Speed response of NARMA-L2 and GA-ANN based PSS and ANFIS-TCSC . . . . .	115
5.18	Case VI: Speed response of NARMA-L2 and GA-ANN based PSS and ANFIS-TCSC . . . . .	116
5.19	Case I: All Intelligent Techniques based PSS . . . . .	117
5.20	Case I: ANFIS-TCSC with Intelligent Techniques based PSS . . . . .	117
5.21	Case II: All Intelligent Techniques based PSS . . . . .	118

5.22	Case II: ANFIS-TCSC with Intelligent Techniques based PSS . . . . .	118
5.23	Case III: All Intelligent Techniques based PSS . . . . .	119
5.24	Case III: ANFIS-TCSC with Intelligent Techniques based PSS . . . . .	119
5.25	Case IV: All Intelligent Techniques based PSS . . . . .	120
5.26	Case IV: ANFIS-TCSC with Intelligent Techniques based PSS . . . . .	120
6.1	Schematic Diagram of Two area system in Restructured Market . . . . .	124
6.2	Restructured System with TCSC in Series with Tie-Line . . . . .	125
6.3	First Order Power System . . . . .	127
6.4	Intelligent techniques based TCSC for two area system under restructured market . . . . .	133
6.5	Case I: Speed deviation in Restructured Market without Tie Line Controller	138
6.6	Case I: Speed deviation in Restructured Market with GA-TCSC Tie Line controller . . . . .	138
6.7	Case I: Speed Deviation in Restructured Market with ANFIS-TCSC Tie Line controller . . . . .	139
6.8	Case I: Tie Line Power Change with Controllers . . . . .	139
6.9	Case II: Speed deviation In Restructured Market without Tie Line Controller	139
6.10	Case II: Speed deviation in Restructured Market with GA-TCSC Tie Line Controller . . . . .	140
6.11	Case II : Speed deviation in Restructured Market with ANFIS-TCSC Tie Line Controller . . . . .	140
6.12	Case II: Tie Line Power Change With Controllers . . . . .	140
6.13	Two area interconnection system with multiple PSS in restructured market .	144
6.14	Case I: First O.C. : Response of speed deviation in Area 1 and Area 2 . . .	155
6.15	Case I : First O.C.: Response of speed deviation in Area 1 with Multiple PSS and TCSC . . . . .	155
6.16	Case I: First O.C.: Response of speed deviation in Area 2 with Multiple PSS and TCSC . . . . .	155
6.17	Case I: First O.C.: Change in Tie Line Power with Controllers . . . . .	156
6.18	Case I: Second O.C.: Response of speed deviation in Area 1 and Area 2 . .	156

6.19 Case I: Second O.C.: Response of speed deviation in Area 1 with Multiple PSS and TCSC . . . . .	156
6.20 Case I: Second O.C.: Response of speed deviation in Area 2 with Multiple PSS and TCSC . . . . .	157
6.21 Case I: Second O. C.: Change in Tie Line Power with Controllers . . . . .	157
6.22 Case II: First O.C.: Response of Apeed deviation in Area 1 and Area 2 . . .	158
6.23 Case II: First O.C.: Response of Apeed deviation in Area 1 with Multiple PSS and TCSC . . . . .	159
6.24 Case II: First O.C.: Response of Speed deviation in Area 2 with Multiple PSS and TCSC . . . . .	159
6.25 Case II: First O.C.: Change in Tie Line Power with Controllers . . . . .	159
6.26 Case II: Second O.C.: Response of Speed deviation in Area 1 and Area 2 . .	160
6.27 Case II: Second O.C.: Response of Speed deviation in Area 1 with Multiple PSS and TCSC . . . . .	160
6.28 Case II: Second O.C.: Response of speed deviation in Area 2 with Multiple PSS and TCSC . . . . .	160
6.29 Case II: Second O.C.: Change in Tie Line Power with Controllers . . . . .	161

# List of Tables

3.1	Calculation of Initial Conditions . . . . .	46
3.2	Value of $K_1$ to $K_{10}$ Constant . . . . .	47
3.3	GA Parameters and Values . . . . .	48
3.4	Optimized Parameters of CPSS . . . . .	48
3.5	Optimized Parameters of PID-PSS . . . . .	49
3.6	Participation Factor (first operating condition)-CPSS . . . . .	49
3.7	Participation Factor (second operating condition)-CPSS . . . . .	49
3.8	Participation Factor (third operating condition)-CPSS . . . . .	49
3.9	Participation Factor(Fourth operating condition)-CPSS . . . . .	50
3.10	Eigen values and Damping Factor of CPSS and PID-PSS . . . . .	52
3.11	Values of $K_1$ to $K_{10}$ Constant after inclusion of TCSC . . . . .	55
3.12	Optimized Parameter of TCSC and PSS . . . . .	58
3.13	Eigen values and Damping factor of PSS and TCSC . . . . .	58
3.14	Eigen values and Damping factor of PSS and TCSC....Contd... . . . . .	59
4.1	Membership Function of ANFIS-PSS . . . . .	83
4.2	Membership Function of ANFIS-TCSC . . . . .	86
4.3	Mean Square Error of ANN based PSS . . . . .	91
5.1	GA Parameter and Value . . . . .	107
6.1	Eigen values without TCSC and with TCSC . . . . .	136
6.2	Optimized Parameters of TCSC . . . . .	136
6.3	Time Response Parameters without Tie-Line TCSC Controller . . . . .	141
6.4	Time Response Parameters with Tie-line GA-TCSC Controller . . . . .	142

6.5	Time Response Parameters with Tie-line ANFIS-TCSC Controller . . . . .	142
6.6	Optimized Parameters of PSSs . . . . .	152
6.7	Eigen values without PSSs . . . . .	152
6.8	Eigen values with PSSs . . . . .	152
6.9	Eigen values with TCSC . . . . .	152
6.10	Eigen values with PSSs and TCSC . . . . .	153

# Chapter 1

## Introduction

### 1.1 General

The electric power industries, throughout the world, have undergone unprecedented changes in its structure. In the restructured environment, the electric energy industries have changed from vertical integrated utilities into number of entities in each spectrum of power system. With the advent of an open market scenario, competition in the industries and restructuring in separate generation, transmission and distribution entities, new issues in power system operation and planning have to be anticipated. The reformulation of planning and operation in electric utility industry as per technical aspects are required. One of the major consequences of this new electrical utility environment has greater emphasis on reliability, security and stability of power system [59, 29]. Restructured market consists of generation companies (GENCOS), distribution companies (DISCOs), transmission companies (TRAN-COS) and independent system operators (ISO). The ISO is independent and disassociated agent for market participation and performs the various ancillary services.

The small signal stability analysis and transient stability analysis have become essential ingredient of stable operation and secure operation of power system [15]. The power system stability is defined [50] as that property of a power system that enables it to remain in a state of operating equilibrium under normal operating conditions and to regain an acceptable state of equilibrium after being subjected to a disturbance. The disturbances can be an intended

one, such as an operator action, or a fault due to natural causes or maloperation of the protection system.

Stability is condition of equilibrium between opposing forces. The mechanism by which interconnected synchronous machines maintain synchronism with one another is through restoring forces, which act whenever there are forces tending to accelerate or decelerate one or more machines with respect to other machine. Under the steady-state conditions, there is balance between input mechanical torque and the output electrical torque of each machine and the speed remains constant. If the system is perturbed, this equilibrium is upset, resulting in acceleration and deceleration of rotors of machines. This tends to increase the speed difference and hence the angular separation. Beyond the certain limit, an increase in angular separation is accompanied by a decrease in power transfer. This increases angular separation further and leads to instability. With electric power systems, the change in electrical torque of a synchronous machine following a perturbation can be resolved into two components [15, 6]:

$$\Delta T_e = T_s \Delta \delta + T_D \Delta \omega \quad (1.1)$$

where  $T_s \Delta \delta$  is the component of torque change in phase with rotor angle perturbation  $\Delta \delta$  and is referred to as synchronising torque component;  $T_s$  is the synchronizing torque coefficient.

$T_D \Delta \omega$  is the components of torque in phase with speed deviation  $\Delta \omega$  and is referred to as the damping torque component;  $T_D$  is the damping torque coefficient.

System stability depends in the existence of the both components of torque for every synchronous machine. The Lack of sufficient synchronizing torque results in instability through an aperiodic drift in rotor angle and the lack of sufficient damping torque results in oscillatory instability.

The power system stabilizer (PSS) has been recognized as an ancillary service in restructured electrical market [54], and important control device that is essential for enhancing system stability. The PSS is used to add damping to the generator rotor oscillations by

controlling its excitation using auxiliary stabilizing signal. To provide damping, the stabilizer produces a component of electrical torque in phase with the rotor speed deviation. The control action provided by PSS to enhance system stability is considered as one of the system ancillary services.

Flexible Alternating Current Transmission System (FACTS) controllers are another ancillary service in deregulated electric market. The FACTS controller plays very important role in deregulated electric market to enhance the stability of the power system [55, 26]. FACTS devices can be effectively used for load flow control, loop power flow control, load dispatched, voltage regulation, enhancement of transient stability and mitigation of system oscillation [55, 25, 26, 44]. The Thyristor Control Series Capacitor (TCSC) is the versatile FACTS device which can nullify many problems of power system operation due to its faster control action and adaptive capabilities [44].

For achievement of desired performance of power system under contingencies, the intelligent techniques based adaptive PSS and TCSC damping controllers are required to be designed. The controllers accompany load frequency control (LFC) in multiple area generation (AGC) system in deregulated environment have been an attraction in ongoing research work.

## 1.2 State-of-the Art

The worldwide electric energy industries have undergone the changes from vertical integrated utilities to restructured electric market. The restructured market provides platform to sell the electric energy to various customer at competitive price. In restructured market, reformulation of planning and operation in electric industry as per technical aspects have required [21, 59, 29]. However, the essential ideas remain the unchanged. The open market consists of generation companies (GENCOs), distribution companies (DISCOs), transmission companies (TRANCOs) and independent system operators (ISO).

GENCOs generate electricity and have the opportunity to sell the electricity to entities with which they have negotiated sales contracts. Generally GENCOs consist of a group

of generating units within a single company ownership structure with the sole objective of producing electrical power. In addition to active power, they may sell reactive power (ancillary services) and operating reserves.

TRANCOSs transport electricity using a high voltage, bulk transmission system from GENCOs to Distribution Companies (DISCOs)/retailers for delivering power to customers. A TRANCOS has role of building, owning, maintaining and operating the transmission system in a certain geographical region to provide services for maintaining the overall reliability of the electrical power systems and provides open access of transmission wires to all market entities in the system. The investment and operating costs of transmission facilities are recovered using access charges, which are usually paid by every user within the area/region, and transmission usage charges based on line flows contributed by each user.

A distribution company (DISCO) distributes the electricity, through its facilities, to customers in a certain geographical region. They buy wholesale electricity either through the spot markets or through direct contracts with GENCOs and supply electricity to the enduser customers. A DISCO is a regulated utility that constructs and maintains distribution wires connecting the transmission grid to the end user customers. A DISCO is responsible for building and operating its electric system to maintain a desired degree of reliability and availability.

Several market structure and transactions exist to achieve a competitive electricity environment. Three basic models exist based on the types of transactions [22]. First is a PoolCo, which is defined as a centralized market place that clears the market for the buyers and sellers. Electric power sellers/buyers submit bids to the pool for the amount of power that they are willing to trade in the market. Second is Bilateral Contract model, a bilateral transaction is an exchange of power between buying and selling entities [21]. These transactions can be defined for a particular time interval of the day and its value may be time varying. It may be either firm or non-firm and can be a short term and long term transaction. Third model is the hybrid model, which combines various features of the previous two models. In the hybrid model, the utilization of the PoolCo is not obligatory, and any customer would

be allowed to negotiate a power supply agreement directly with the suppliers or choose to accept power at the pool market price.

A competitive market would necessitate an independent operation and control of the grid. Due to this reason, most of the utilities have established an entity called Independent System Operator. It is entrusted with responsibility of ensuring the reliability, security and efficient operation of an open access transmission system. It is an independent authority and does not participate in trading of electricity. The ISO has the authority to commit and redispatch the system resources and to curtail loads for maintaining the system security.

An ancillary service is an interconnected operation service that is necessary to support a transfer of electricity between purchasing and selling entities. Ancillary services are needed to ensure that the system operators are able to meet their responsibilities, although also aim at enhancing system reliability and maintaining adequate quality standards. In the deregulated market, the ancillary services are mandated to be unbundled from the energy services. Ancillary services are procured through the market competitively. The ISO uses ancillary services for the following tasks [54, 55]:

- Keeping the frequency of the system within certain bounds
- Controlling the voltage profile of the system
- Maintaining the stability of the system
- Preventing the overloads in the transmission system
- Restoring the system after the black out.

The instability in a power system can occur in a variety of ways depending on the system configuration and operating conditions. Traditionally, the stability problem has been associated with maintaining synchronous operation. In the evaluation of stability, the concern is the behavior of the power system when subjected to a disturbance. The disturbance may be small or large. This aspect of stability is influenced by the dynamics of the generator rotor angles and the power-angle relationships and is referred to as rotor angle stability. The details of rotor angle stability analysis can be found in [33, 15, 43, 31, 6]. This stability problem deals with the study of the electromechanical oscillations inherent in power

systems. The fundamental factor in this analysis is the characterization of the variation of the power or torque outputs of synchronous machines as their rotors oscillate. In general, the components of the power system that influence the electrical and mechanical torques of the synchronous machines are included in the model. These components are listed below.

- The transmission network before, during, and after the disturbance.
- The loads and their characteristics.
- The parameters of the synchronous machines.
- The control components of the synchronous machines (excitation systems, power system stabilizers).
- The mechanical turbine and the speed governor.
- Other power plant components that influence the mechanical torque.
- Other control devices, such as supplementary controls, special protection schemes and FACTS (Flexible AC Transmission System) devices that are deemed necessary in the mathematical description of the system.

Small signal stability is ability of the power system to maintain synchronism under small disturbances. Such disturbances occur continually on the system because of small variations in loads and generation. The disturbances are considered sufficiently small for linearization of system equations to be permissible for purpose of analysis. Instability that may result can be of two forms: (i) steady increase in rotor angle due to lack of sufficient synchronising torque, or(ii) rotor oscillations of increasing amplitude due to lack of sufficient damping torque. The nature of the system response to small disturbances depends on a number of factors including the initial operating, the transmission strength, and the type of generator excitation control used. For a generator connected radially to power system, in the absence of automatic voltage regulators (i.e.with constant field voltage) the instability is due to lack of sufficient synchronising torque. With continuously acting voltage regulators, the small disturbance stability problem is one of ensuring sufficient damping of system oscillation. Instability is normally through oscillations of increasing amplitude. The small signal stability is largely a problem of insufficient damping of oscillations.

Transient stability is the ability of the power system to maintain synchronism when subjected to a severe transient disturbance. The resulting system response involves large excursion of generator rotor angles and is influenced by the non linear power angle relationship. The non linear algebraic differential equations are used for analysis of transient stability. The numerical solutions of the non linear algebraic differential equations are obtained.

The Power system stabilizer (PSS) generates the supplementary control signal for the excitation system to damp the low frequency oscillations and to improve power system stability. The power system stabilizers have been designed very extensively using phase compensation techniques and parameters of PSS have been calculated based on linearized Philips–Heffron model of the power system for the small signal stability analysis [2, 43, 15, 33]. The small signal stability and transient stability with concepts of synchronizing and damping torques has been explained by [74]. Different types of arrangement of phase compensator based PSSs have been used for detail analysis of the power system [56, 33, 43, 15]. The coordinated design of PSS and automatic voltage regulator (AVR) [84] can handle power system stability problem under certain operating conditions. The paper [80] presents artificial neural network (ANN) based controller model to simulate the automatic voltage regulator (AVR) response for the transient stability analysis.

Modulation of generation excitation can produce transient change in the generator's electrical output power. Fast responding exciters equipped with high gain AVR's use their speed and forcing to increase a generator's synchronizing torque coefficient  $T_s$ , result in improved steady-state and transient stability limits. Improvements in synchronizing torque are often achieved at the expense of damping torque, hence in reduced levels of oscillatory or small signal stability. To counteract this effect, many units that utilize high-gain AVRs are also equipped with PSSs to increase the damping coefficient  $T_D$  and to improve oscillatory stability.

The modern and conventional control techniques based PSS can provide optimal performance for the normal operating conditions and normal system parameters. However, a modern power system has become large, tight and highly dynamic, hence too difficult to

solve low frequency oscillations problem through conventional and linear optimal control approaches. For the different loading conditions and configuration of power network, the parameters of PSS needed to be modify.

The proportional integral improved adaptive control law [81], H-infinity control technique [35] and robust control based [46] power system stabilizer can overcome the time consuming and non optimal damping. However, it required complex computation for implementation in the dynamic power system. To overcome these limitations, computational intelligent techniques such as Fuzzy Logic (FL), Artificial Neural Network (ANN), Genetic Algorithm (GA), Particle Swarm Optimization (PSO) etc. based PSS have been proposed in the literature.

Fuzzy logic is very attractive technique for model free design of the plant. Fuzzy logic based power system stabilizer [28, 51], adaptive fuzzy logic base power system stabilizer [61] for maintaining the stability of the power system cover a wide range of operating conditions. But the linguistic or user defined variables are needed to design the rule based of fuzzy inference system. The gain and time constants of conventional PSS are optimized under the different operating conditions through different computational optimization techniques like: Genetic algorithm, particle swarm optimization and bacterial foraging and simulated annealing have been explained by [83, 24, 108]. For each and individual operating condition, the individual PSS parameters are needed to be tune. The parameters of PSS have to be calculated and evaluated through Artificial Neural Network [52] under the different operating conditions of the power system. The adaptive neural network based power system stabilizer has been proposed by [45]. By combining the generalized neuron predictor and a fuzzy logic controller based adaptive fuzzy logic power system stabilizer [68] and the two level fuzzy and adaptive neurofuzzy inference systems based power system stabilizer [106] have been applied to the power system dynamics.

Many applications of computational intelligent techniques in power system engineering have been mentioned by literature. The voltage stability [17, 104, 91], load flow analysis [67], power system security [70], load and price forecasting [60, 101, 109], reactive power compensation [73], transmission loss allocation [95], harmonic estimation [98], fault detection

in distribution network [82], induction generator and wind power forecasting [64, 69, 86, 72], and state estimation [18] have been discussed.

During the last decade, a number of the Flexible Alternating Current Transmission System (FACTS) control devices have been proposed and implemented in real power system [25, 44]. An Adaptive Neuro-Fuzzy Inference System (ANFIS) method based on the Artificial Neural Network (ANN) to design a Static Synchronous Series Compensator (SSSC)-based controller for the improvement of transient stability has been suggested in paper [107]. The proposed ANFIS controller combines the advantages of a fuzzy controller as well as the quick response and adaptability nature of an ANN. The ANFIS structures were trained using the generated database by the fuzzy controller of the SSSC. It is observed that the proposed SSSC controller improves greatly the voltage profile of the system under severe disturbances. The results prove that the proposed SSSC-based ANFIS controller is found to be robust to fault location and changes in operating conditions.

The laboratory implementation and test results of an advanced TCSC ANN-based inverse control system to enhance power system transient stability has been presented by [47]. Satisfactory performance and robustness of the TCSC control are demonstrated by the test results on a laboratory power system subject to different disturbances under various operating conditions

A supplementary damping controller for a unified power flow controller (UPFC) is designed for power system dynamic performance enhancement has been discussed in paper [39].

The paper [93] presents a new control method based on Neural Network technique to damp out the power system low frequency oscillations using STATCOM controller. The main objective of this paper is to investigate the power system dynamic stability enhancement by using neural network based FACTS (STATCOM) Controller.

An integrated approach of radial basis function neural network (RBFNN) and Takagi-Sugeno (TS) fuzzy scheme with a genetic optimization of their parameters has been developed to design intelligent adaptive controllers for improving the transient stability performance of power systems has been presented by [36].

Nowadays the FACTS controller plays very important role in deregulated electric market,

which has been explained in literature [55, 26, 62].

In general, FACTS controllers can be divided into four categories:

Series controller

Shunt controller

Combined series-series controller

Combined series-shunt controller

One of the most important devices of series FACTS controller is thyristor controlled series capacitor (TCSC) [38] in order to enhance the stability and loadability of the transmission network. The nonlinear  $H_\infty$  controller and LQR/LTR controllers based TCSC have been presented by [63, 30]. The various computational intelligent algorithms based TCSC [102, 75, 99, 47] are being designed to cope up the stability of the power system under the different system configuration as well as load variation. The self tuning fuzzy-PI controller and type-2 fuzzy controller for TCSC has been proposed by [75, 99]. The artificial neural network and search algorithms based TCSC have been presented by [102, 47]. For the performance enhancement of the dynamical power system, the new area of the research is build up on coordinated design of PSS and TCSC. The different computational intelligent techniques based coordinated design of PSS and TCSC have been mentioned in literature [103, 66].

The power system stability in deregulated electric market has been addressed [37]. The ancillary services such as power system stabilizer (PSS) [54] and Flexible Alternating Current Transmission System (FACTS) controllers [55, 26] in deregulated electric market have been addressed. Nowadays, by increasing complexity in power system, it is important to provide stable, secure, controlled, monetary and high quality electric power in restructured environment. The FACTS controller plays very important role in deregulated electric market to enhance the stability of the power system with their fast control characteristics and continuous compensating capability. FACTS devices can be effectively used for load flow control, loop power flow control, load dispatched, voltage regulation, enhancement of transient stability and mitigation of system oscillation [55, 26, 25, 44].

Large scale power systems are composed of control areas or regions representing coher-

ent groups of generators. In large power system abnormal phenomena have been frequently observed such as tie-line power deviation, rotor speed deviation and outage of generators under various loading conditions. Automatic generation control (AGC) is an essential control loop in electric power system which maintains balance between generated power and demand power in each control area. For the conventional Load Frequency controller, the integral of area control error (ACE) is utilized as the control signal for conventional control strategy. Literature [3, 92, 41, 57, 5] has addressed the area generation control with ACE in conventional LFC loop. An integral controller provides zero steady state deviation, but it produces poor dynamic performance. Therefore advanced control techniques are needed to cope up with abnormal situation in power system. Nowadays, smart controllers have been introduced and are replacing conventional controller. They have fast, adaptive and good dynamic characteristics for load frequency control issue. Genetic algorithm, bacteria foraging, [40, 79], fuzzy logic [53], neural network [23, 100], adaptive neuro fuzzy inference system [76, 105] based LFC have been developed.

The Load frequency controller (LFC) is recognized as an ancillary service in deregulated electric market. The extensive details and modified block diagram of two area AGC under the restructured market has been discussed by [32, 85].

The adaptive neurofuzzy inference system based automatic generation control [76], genetic algorithms and linear matrix inequality [40], gradient Newton algorithm [32] are some published researches on minimization of ACE in deregulated LFC. The application of different FACTS controllers in deregulated market in multi area AGC system has been reported [77, 49, 78, 96] by recent research paper. The fuzzy logic based tie line power controller TCPS has been designed for the hydrothermal system [77], decentralized control law of SSSC devices [49] and particle swarm optimization based TCPS [78] have been designed. The superconducting energy devices with TCPS and SSSC using evolutionary algorithms for two area hydro system have been extensively designed in literature [96].

Intelligent computing consists of several computing paradigms [87, 89, 90], including neural networks [7, 12, 11, 10], fuzzy set theory [1], approximate reasoning, and derivative

free optimization methods such as genetic algorithm [8], swam optimization [27, 16], ant colony optimization [58], bacterial foraging [34], simulated annealing [87, 90] etc. have been reported. Each of these constituent methodologies has its own strengths. The integration of these methodologies have been formed the core of soft computing. The synergisms allow soft computing to incorporate human knowledge effectively, deal with imprecision and uncertainty and learn to adapt to unknown or changing environment. Main characteristic is its inherent capability to create hybrid systems that are based on an integration of the techniques. They have provided complementary learning, reasoning and searching methods to combine domain knowledge and empirical data to develop flexible computing tools and to solve complex problems. In confronting real world computing problems, it is frequently advantageous to use several intelligent computing techniques synergistically rather than exclusively, resulting in construction of hybrid intelligent system.

### 1.3 Motivation

The extensive survey of literature could give the information regarding to the application of the computational intelligent methods in field of power system stability but it could also divulge the growing interest of the researchers on the relatively new field of intelligent computing in restructured power industries.

The Third –order dynamic model and Philips-Heffron linear model of the synchronous machine is most preferable for a researcher for stability analysis of power system. The power system model only takes into account the generator main field winding. However, for the effective analysis of single machine infinite bus system, linear and non linear higher order power system model accompany of automatic voltage regulator are to be required for small signal stability and transient stability analysis. Computational intelligent method based Power system stabilizer [83, 24, 108] has been developed, but comparison between evolutionary algorithm based conventional power system stabilizer and proportional integral derivative power system stabilizer, and their application to linear and non linear with fourth order power system model have not been discussed. The eigen values analysis with

power system stabilizer and TCSC controller are required for effective analysis of closed loop stability. Mathematical modeling of individual power system, model of power system with PSS and model of power system with simultaneous PSS and TCSC are to be required for identification of power system stability. The paper [103, 66] shows the non linear simulation of power system with PSS and TCSC, but the closed loop system stability with controllers have not been discussed.

Artificial neural network based power system stabilizer [52, 45] has been discussed. The feed forward multilayer neural networks are the most common neural network architecture for solution of control problem. A widely used training method for feed forward multilayer neural network is the back propagation algorithm. The standard back propagation learning algorithm has several limitations. Most of all, a long and slow training process, when plant is non-linear and parameters of the plant are dynamic. The rate of convergence is seriously affected by the initial weights and the learning rate of parameters. So fast and adaptive algorithm has to be required to cope up with dynamical situation in power system.

The literature survey motivates to develop other intelligent techniques based power system stabilizer and Thyristor control series capacitor for single machine infinite bus system extensively. Literature survey reveals that no research work has been carried out for designing of PSS using hybrid genetic algorithm based neural network and neural network identification technique. Literature survey reveals that no any research work has been discussed the comparison between different intelligent methods for designing of PSS and TCSC and their simultaneously application in dynamical power system.

Literature survey shows linear single order transfer function of the synchronous generator used in Load frequency control loop for area generation control in convention and deregulated electric market. TCPS and SSSC have been used as tie line power controller [77, 78, 76, 96], which are designed using computational intelligent methods. But effect of FACTS controllers on frequency deviation with higher order power system model with automatic voltage regulator in multiarea control loop have not been discussed. Literature survey reveals that no research work has been carried out on the smart control techniques based TCSC

as tie line power controller in conventional and deregulated electric market. Literature survey reveals that no research work has discussed the effect of individual and simultaneous application of ancillary controllers such as PSS and TCSC on closed loop stability and transient stability of multiarea power system using intelligent methods under restructured electric market, with different correlative conditions between GENCOs and DISCOs and load variation in various control area. Mathematically justification for application of ancillary controllers in two area deregulated electric market with load frequency control loop has not been addressed in literature survey.

Hence, the main objectives behind the present work are as follows:

1. To develop the linearized model of fifth order synchronous machine from non linear model and to derive the different constants followed by block diagram of the synchronous machine connected to single machine infinite system.
2. To develop the mathematical model of the machine in state space form with conventional power system stabilizer (CPSS), proportional integral derivative PSS and TCSC individually and simultaneously.
3. To design the PSS using different intelligent techniques such as Genetic Algorithm, Levenberg Marquardt neural network (LMNN), adaptive neuro fuzzy inference system (ANFIS), genetic algorithm based artificial neural network hybrid algorithm (GA-ANN), Neural Network based non linear auto regressive moving average (NARMA)-L2 controller.
4. To design the stability control loop of TCSC using GA, ANN and ANFIS techniques. To analyze the simultaneous and individual application of PSS and TCSC using programming and to carry out non linear simulations under different operating conditions and disturbances in power system .
5. To develop linear model and block diagram of the two area automatic generation control system with the first order and fifth order power system model under the restructured electric environment.

6. To build the model of two area power system with multiple PSS, individual tie-line TCSC and combining PSSs and TCSC.
7. To study the effectiveness of ancillary controllers such as multiple PSSs and TCSC in restructured electric market.
8. To evaluate the performance of smart control techniques based ancillary controller using linear analysis and non linear simulation.

## 1.4 Thesis Organization

The present Chapter 1 introduces the restructured electric market, stability issue and application of ancillary controllers in restructured market. It represents the relevant state-of-the-art survey and sets the motivation behind the research work carried out in this thesis.

Chapter 2 presents, detail modeling of the system components and linearization of non linear equations using Taylor's series method. The state space form of power system with conventional power system stabilizer and PID- power system stabilizer have been described. The linearized state space form of power system with individual TCSC and simultaneous CPSS and TCSC have also been derived.

Chapter 3 presents, Genetics Algorithm based control strategies for designing of CPSS, PID-PSS and TCSC damping controller. The individual PSSs and simultaneous designed TCSC and PSS have been applied to the dynamic power system. The small signal stability analysis and non-linear simulation for the transient stability analysis have been carried out for detailed investigation of the power system stability issue.

Chapter 4 discusses Adaptive Neuro-Fuzzy Inference System and Levenberg-Marquardt Artificial Neural Network algorithm for development of the control strategy for thyristor control series capacitor based damping controller and power system stabilizer. The non-linear simulations of single machine infinite bus system have been carried out using individual and simultaneous application of PSS and TCSC. The comparisons between intelligent control strategies based damping controllers have also been carried out.

Chapter 5 discusses Non Linear Auto regressive Moving Average-L2 controller and hybrid Genetic Algorithm based Network Network for development of the control strategy for power system stabilizer. In order to achieve appreciable damping, developed ANFIS based Thyristor control series capacitor has been suggested in addition to power system stabilizer. The non-linear simulations of single machine infinite bus system have been carried out using individual and simultaneous application of PSS and TCSC.

Chapter 6 presents, performance and role of ancillary controllers such as PSS and TCSC in two area control system under restructured electric market. Low order power system model and higher order power system model have been considered for in depth analysis of two area system with ancillary controllers. The stability analysis and non-linear simulation for the transient stability analysis are carried out for investigation of the power system stability issue.

Chapter 7 summarizes the main finding and significant contribution of the thesis and provides a few suggestion for future scope of research work in this area.

# Chapter 2

## Mathematical Modeling of Power System

### 2.1 General

The mathematical model of synchronous machine can be described by a set of differential equations representing the dynamics of the machines, exciters and other controls and algebraic equations representing the network relation. The model considered for the stability analysis in this thesis are described below:

### 2.2 Generator model

Fourth order model of generator [33, 15, 43, 6] has been used in the present study as described below:

The dynamics of the synchronous generator can be represented by the following equations:

$$\dot{\delta} = \omega_B (\omega_m - \omega_{m0}) \quad (2.1)$$

$$\dot{\omega}_m = \frac{1}{2H} (-k_d ((\omega_m - \omega_{m0})) + T_m - T_e) \quad (2.2)$$

where  $\delta$  is generator's rotor angle,  $\omega_m$  the speed deviation,  $H$  machine inertia constant,  $T_m$  is the Mechanical power input to generator,  $T_e$  is the electrical power output of the generator,  $k_d$  the damping constant.

The electrical torque equation is represented by following algebraic equation:

$$T_e = E'_d i_d + E'_q i_q + (x'_d - x'_q) i_d i_q \quad (2.3)$$

where  $i_d$  and  $i_q$  are d-axis and q-axis current respectively,  $E'_d$  and  $E'_q$  are d-axis and q-axis transient voltage,  $x'_d$  and  $x'_q$  are d-axis and q-axis transient reactance.

The effect of saliency is considered, the changes in flux linkage of the field winding have to be accounted for along the d and q axes. Therefore, two more additional state equation (2.4) and (2.5) along with the swing equations (2.1) and (2.2) have to be considered.

$$\dot{E}'_q = \frac{1}{T'_{d0}} \left[ \left( -E'_q + (x_d - x'_d) i_d \right) + E_{fd} \right] \quad (2.4)$$

$$\dot{E}'_d = \frac{1}{T'_{q0}} \left[ \left( -E'_d - (x_q - x'_q) i_q \right) \right] \quad (2.5)$$

where  $T'_{d0}$  and  $T'_{q0}$  are d-axis and q-axis open circuit time constant,  $x_d$  and  $x_q$  d-axis and q-axis synchronous reactance,

The line resistance is considering very low, it equal to be zero ohms. The stator  $d$  and  $q$  axes current and voltage algebraic equations can written as follows:

$$i_d = \frac{E_b \cos \delta - E'_q}{(x_e + x'_d)} \quad (2.6)$$

$$i_q = \frac{E_b \sin \delta + E'_d}{(x_e + x'_q)} \quad (2.7)$$

$$v_q = -x_e i_d + E_b \cos \delta \quad (2.8)$$

$$v_d = -x_e i_q - E_b \sin \delta \quad (2.9)$$

$$V_t = \sqrt{v_d^2 + v_q^2} \quad (2.10)$$

where  $x_e$  is the line reactance,  $v_d$  and  $v_q$  are d-axis and q-axis voltage,  $V_t$  the terminal voltage and  $E_b$  infinite bus voltage.

## 2.3 Excitation System

The IEEE type –ST1 exciter [33, 43] has been considered in this study and equation governing the dynamics is given as follows:

$$\dot{E}_{fd} = -\frac{1}{T_A} E_{fd} + \frac{K_A}{T_A} (V_{ref} - V_t) \quad (2.11)$$

where  $E_{fd}$  = field excitation voltage

$K_A$  =Exciter gain

$T_A$  =Exciter time constant

$V_{ref}$  =Reference voltage setting

$V_t$  =Terminal voltage

### 2.3.1 Initial Conditions

The power system is described by set of non linear differential equations and is required to be solved numerically. It is assumed that the system is at a stable equilibrium point till  $t=0$ . It is necessary to calculate the initial conditions at time  $t=0$  based on power system operating points. Calculation of initial conditions [33, 43] are very important for power system stability analysis. The operating points are calculated from load flow analysis [41, 15].

The initial conditions are calculated from following set of Equations:

Calculation of  $\hat{I}_{a0}$  from Equation (2.12).

$$\hat{I}_{a0} = I_{a0} \angle \phi_0 = \frac{P_t - jQ_t}{V_{t0} \angle -\theta_0} \quad (2.12)$$

$\delta_0$  and  $E_{q0}$  are calculated from Equation (2.13).

$$E_{q0} \angle \delta_0 = V_{t0} \angle \theta_0 + (R_a + jx_q) I_{a0} \angle \phi_0 \quad (2.13)$$

The different variables  $i_{d0}$ ,  $i_{q0}$ ,  $v_{d0}$ ,  $E_{fd0}$ ,  $E'_{q0}$ ,  $E'_{d0}$  and  $T_{e0}$  are calculated from following Equations:

$$i_{d0} = -I_{a0} \sin(\delta_0 - \phi_0) \quad (2.14)$$

$$i_{q0} = I_{a0} \cos(\delta_0 - \phi_0) \quad (2.15)$$

$$v_{d0} = -V_{to} \sin(\delta_0 - \phi_0) \quad (2.16)$$

$$v_{q0} = V_{to} \cos(\delta_0 - \phi_0) \quad (2.17)$$

$$E_{fd0} = E_{q0} - (x_d - x_q) i_{d0} \quad (2.18)$$

$$E'_{q0} = E_{fd0} + (x_d - x'_d) i_{d0} \quad (2.19)$$

$$E'_{d0} = - (x_q - x'_q) i_{q0} \quad (2.20)$$

$$T_{e0} = E'_{q0} i_{q0} + E'_{d0} i_{d0} + (x'_d - x'_q) i_{d0} i_{q0} = T_{m0} \quad (2.21)$$

## 2.4 Linearization and Eigen Properties

### 2.4.1 Linearization

The dynamic system can be represented in a set of  $n$  first order non-linear differential equations [88, 15].

$$\dot{x} = f(x, u) \quad (2.22)$$

$$y = g(x, u) \quad (2.23)$$

Where  $x$  is the state vector with  $n$  state variable,  $u$  is input vector to the system, and  $y$  is the output vector.

To investigate the small-signal stability at one operating point, equation (2.22) and (2.23) need to be linearized. Assume  $x_0$  is the initial state vector at the current operating point and  $u_0$  is the corresponding input vector. As the perturbation is considered small, the nonlinear function  $f$  can be expressed in terms of Taylor's series expansion. With terms involving second and higher order powers of  $\Delta x$  and  $\Delta u$  are neglected, we may write

$$\dot{x}_i = \dot{x}_{i0} + \Delta \dot{x}_i = f_i [(x_0 + \Delta x), (u_0 + \Delta u)] \quad (2.24)$$

$$= f_i(x_0, u_0) + \frac{\partial f_i}{\partial x_1} \Delta x_1 + \dots + \frac{\partial f_i}{\partial x_n} \Delta x_n + \frac{\partial f_i}{\partial u_1} \Delta u_1 + \dots + \frac{\partial f_i}{\partial u_r} \Delta u_r \quad (2.25)$$

$$\dot{x}_{i0} = \dot{f}_i(x_0, u_0)$$

$$\Delta \dot{x}_i = \frac{\partial f_i}{\partial x_1} \Delta x_1 + \dots + \frac{\partial f_i}{\partial x_n} \Delta x_n + \frac{\partial f_i}{\partial u_1} \Delta u_1 + \dots + \frac{\partial f_i}{\partial u_r} \Delta u_r \quad (2.26)$$

$$\Delta y_j = \frac{\partial g_j}{\partial x_1} \Delta x_1 + \dots + \frac{\partial g_j}{\partial x_n} \Delta x_n + \frac{\partial g_j}{\partial u_1} \Delta u_1 + \dots + \frac{\partial g_j}{\partial u_r} \Delta u_r \quad (2.27)$$

Therefore, the linearized forms of Equation (2.26) and (2.27) are written as:

$$\Delta \dot{x} = A \Delta x + B \Delta u \quad (2.28)$$

$$\Delta y = C \Delta x + D \Delta u \quad (2.29)$$

Where  $A$  is the state matrix,  $B$  the control matrix,  $C$  the output matrix, and  $D$  is the feed forward matrix. For the stability analysis and eigen value analysis of the synchronous machine, the state matrix  $A$  is the most important. This matrix can be represented by Equations (2.30) and (2.31). The block diagram of state space is represented by Figure 2.1.

$$A = \begin{bmatrix} \frac{\partial f_1}{\partial x_1} & \cdot & \cdot & \cdot & \frac{\partial f_1}{\partial x_n} \\ \cdot & \cdot & \cdot & \cdot & \cdot \\ \cdot & \cdot & \cdot & \cdot & \cdot \\ \cdot & \cdot & \cdot & \cdot & \cdot \\ \frac{\partial f_n}{\partial x_1} & \cdot & \cdot & \cdot & \frac{\partial f_n}{\partial x_n} \end{bmatrix} \quad B = \begin{bmatrix} \frac{\partial f_1}{\partial u_1} & \cdot & \cdot & \cdot & \frac{\partial f_1}{\partial u_r} \\ \cdot & \cdot & \cdot & \cdot & \cdot \\ \cdot & \cdot & \cdot & \cdot & \cdot \\ \cdot & \cdot & \cdot & \cdot & \cdot \\ \frac{\partial f_n}{\partial u_1} & \cdot & \cdot & \cdot & \frac{\partial f_n}{\partial u_r} \end{bmatrix} \quad (2.30)$$

$$C = \begin{bmatrix} \frac{\partial g_1}{\partial x_1} & \cdot & \cdot & \cdot & \frac{\partial g_1}{\partial x_n} \\ \cdot & \cdot & \cdot & \cdot & \cdot \\ \cdot & \cdot & \cdot & \cdot & \cdot \\ \cdot & \cdot & \cdot & \cdot & \cdot \\ \frac{\partial g_m}{\partial x_1} & \cdot & \cdot & \cdot & \frac{\partial g_m}{\partial x_n} \end{bmatrix} \quad D = \begin{bmatrix} \frac{\partial g_1}{\partial u_1} & \cdot & \cdot & \cdot & \frac{\partial g_1}{\partial u_r} \\ \cdot & \cdot & \cdot & \cdot & \cdot \\ \cdot & \cdot & \cdot & \cdot & \cdot \\ \cdot & \cdot & \cdot & \cdot & \cdot \\ \frac{\partial g_m}{\partial u_1} & \cdot & \cdot & \cdot & \frac{\partial g_m}{\partial u_r} \end{bmatrix} \quad (2.31)$$

$\Delta x$  is the state vector of dimension  $n$

$\Delta y$  is the output vector of dimension  $m$

$\Delta u$  is the input vector of dimension  $r$

$A$  is the state or plant matrix of size  $n \times n$

$B$  is the control or input matrix of  $n \times r$

$C$  is the output matrix of size  $m \times n$

$D$  is the feedforward matrix  $m \times r$

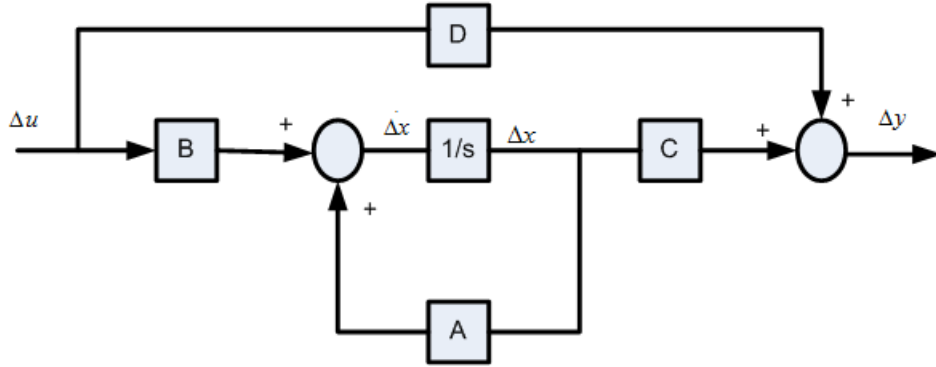


Figure 2.1: Block diagram of State Space Representation

### 2.4.2 State Space Representation

The Laplace transform of the equations (2.26) and (2.27), the state equations (2.32) and (2.33) are presented in the time domain as per follow [65, 88, 97]:

$$s\Delta x(s) - \Delta x(0) = A\Delta x(s) + B\Delta u(s) \quad (2.32)$$

$$\Delta y(s) = C\Delta x(s) + D\Delta u(s) \quad (2.33)$$

Rearranging Equation (2.32), we have

$$(SI - A)\Delta x(s) = \Delta x(0) + B\Delta u(s) \quad (2.34)$$

Hence

$$\Delta x(s) = (SI - A)^{-1} [\Delta x(0) + B\Delta u(s)] \quad (2.35)$$

$$= \frac{\text{adj}(SI - A)^{-1}}{\det(SI - A)^{-1}} [\Delta x(0) + Bu(s)] \quad (2.36)$$

and correspondingly,

$$\Delta y(s) = C \frac{\text{adj}(SI - A)^{-1}}{\det(SI - A)^{-1}} [\Delta x(0) + Bu(s)] + D\Delta u(s) \quad (2.37)$$

The Laplace transforms of  $\Delta x$  and  $\Delta y$  consist two component, one dependent on the initial conditions and the other on the inputs. These are the Laplace transforms of the free and zero-state components of the state and output vectors. The poles of  $\Delta x(s)$  and  $\Delta y(s)$  are the roots of the Equation:

$$\det(SI - A) = 0 \quad (2.38)$$

The values of  $s$  which satisfy the above are known as eigen values of matrix  $A$ , and Equation is referred as the characteristics Equation of matrix  $A$ .

### 2.4.3 Eigen Values

The eigen values of a matrix [88] are given by the values of the scalar parameter  $\lambda$  for which there exist non-trivial solutions to the equation

$$A\phi = \lambda\phi \quad (2.39)$$

where

$A$  is an  $n \times n$  matrix

$\phi$  is an  $n \times 1$  vector

For the calculation of eigen value, the equation (2.39) may be written in the form

$$(A - \lambda I)\phi = 0 \quad (2.40)$$

For a non-trivial solution

$$\det(A - \lambda I) = 0 \quad (2.41)$$

Expression of the determinant gives the characteristics equation. The  $r$  solution of (2.41)  $\lambda = \lambda_1, \lambda_2, \dots, \lambda_n$  are eigen values of  $A$ .

### 2.4.3.1 Eigen Vector

For any eigen value  $\lambda_p$  the  $n$ -column  $\phi_p$  which satisfies (2.39) is called the right eigen vector [15] of  $A$  associated with the eigen value  $\lambda_p$ .

$$A\phi_p = \lambda_p\phi_p \quad (2.42)$$

$$p = 1, 2, \dots, r$$

The right- eigen vector is represented by equation (2.43)

$$\phi_p = \begin{bmatrix} \phi_{1p} \\ \phi_{2p} \\ \cdot \\ \cdot \\ \cdot \\ \phi_{rp} \end{bmatrix} \quad (2.43)$$

Similarly, the  $r$  row vector  $\psi_p$  which satisfies the equation

$$\psi_p A = \lambda_p \psi_p \quad (2.44)$$

$p = 1, 2, \dots, r$  is called the left eigen vector associated with the eigenvalue  $\lambda_p$ .

$$\psi_p = \begin{bmatrix} \psi_{1p} & \psi_{2p} & \cdot & \cdot & \cdot & \psi_{rp} \end{bmatrix} \quad (2.45)$$

The left and right eigen vectors corresponding to different eigen values are orthogonal, i.e.

$$\psi_q \phi_p = 0 \quad (2.46)$$

$\lambda_p \neq \lambda_q$  and

$$\psi_q \phi_p = \alpha_p \quad (2.47)$$

where  $\lambda_p = \lambda_q$  and  $\alpha_p$  is a non zero constant. To normalized these vector so that

$$\psi_q \phi_p = 1 \quad (2.48)$$

### 2.4.3.2 Participation Factor

Participation factor [48, 4, 15] is used for identifying the state variables that have significant participation on a selected mode among many modes in a multigenerator power system. Participation matrix ( $P$ ), which combines the right and left eigen vectors entries and used as measure of the association between the state variables and the modes.

$$P = \begin{bmatrix} P_1 & P_2 & \cdot & \cdot & \cdot & P_r \end{bmatrix} \quad (2.49)$$

with

$$P_p = \begin{bmatrix} P_{1p} \\ P_{2p} \\ \cdot \\ \cdot \\ \cdot \\ P_{rp} \end{bmatrix} = \begin{bmatrix} \phi_{1p} \psi_{p1} \\ \phi_{2p} \psi_{p2} \\ \cdot \\ \cdot \\ \cdot \\ \phi_{1p} \psi_{pr} \end{bmatrix} \quad (2.50)$$

where

$\phi_{KP}$  = the element on the  $k$ th row and  $p$ th column of the modal matrix  $\phi$

=  $k$ th entry of the right eigen vector  $\phi_p$

$\psi_{PK}$  = the element on the  $p$ th row and  $k$ th column of the modal matrix  $\psi$

=  $k$ th entry of the right eigen vector  $\psi_p$

The element  $P_{KP} = \phi_{KP} \psi_{PK}$  is the termed as the participation factor.  $\phi_{KP}$  measures the activity of the variable  $X_K$  in the  $p$ th mode, and  $\psi_{PK}$  gives the weights of contribution of

this activity to the mode, the product  $P_{KP}$  measures the net participation. The effect of multiplying the element of the left and right eigen vectors makes the  $P_{KP}$  dimensionless.

### 2.4.3.3 Eigen value and Stability

The time dependent characteristics of a mode corresponding to an eigen value  $\lambda_i$  is given by  $e^{\lambda_i t}$  [88, 15]. Hence the stability of the system is determined by the eigen values as follows:

1. A real eigen value corresponds to a non-oscillatory mode. A negative real eigen value describes a decaying mode. The large its magnitude, the faster the decay. A positive real eigen value represents aperiodic instability.
2. Complex eigen values occur in conjugate pairs, and each pair corresponds to an oscillatory mode. The real components of the eigen values give the damping, and the imaginary components present the frequency of oscillation. A negative real part describes a damped oscillation, whereas a positive real part represents oscillation of increasing amplitude.

Thus  $\lambda$  for a complex pair of eigen values is represented by equation (2.51).

$$\lambda = \sigma \pm j\omega \quad (2.51)$$

where  $\sigma$  and  $\omega$  show the real part and imaginary part of the eigen value.

The frequency of oscillation in  $Hz$  is given by equation (2.52), which represents the actual of damped frequency.

$$f = \frac{\omega}{2\pi} \quad (2.52)$$

The equation (2.53) represents the damping factor

$$\zeta = \frac{-\sigma}{\sqrt{\sigma^2 + \omega^2}} \quad (2.53)$$

The damping ratio  $\zeta$  determines the rate of decay of the amplitude of the oscillation. The time constant of amplitude decay is  $\frac{1}{|\sigma|}$ .

## 2.5 Linear model of power system

The single machine infinite bus system (SMIB) is shown in Figure 2.2, where  $V_t$  and  $E_b$  are generator terminal voltage and infinite bus voltage respectively. The  $X_e$  and  $X_t$  are transmission line reactance and transformer reactance respectively. The dynamic model of the synchronous machine and exciter described by section 2.2 and 2.3 respectively are linearized about its initial conditions using linearization concept, which is described by section (2.4.1). After linearization of the equations (2.6) and (2.7) of  $i_d$  and  $i_q$  and substituting these equations in (2.8), (2.9) and (2.10) yield the linearized equations of  $V_q$ ,  $V_d$ ,  $V_t$  and  $T_e$ . The linearized equations are represented by equations (2.54) to (2.61).

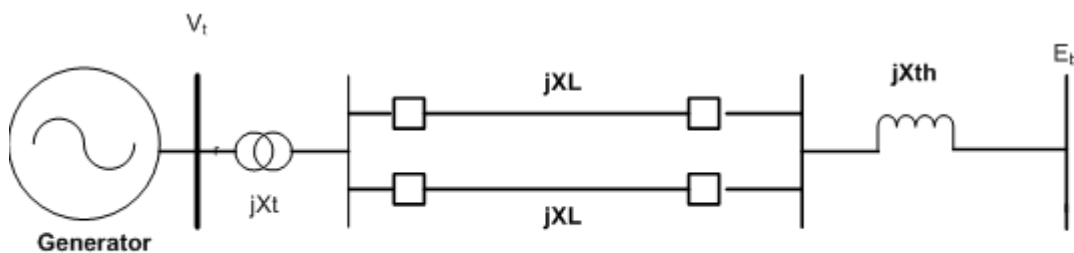


Figure 2.2: Single Machine Infinite Bus System

### 2.5.1 Calculation of $K_1$ to $K_{10}$ Constants

The linearized form of  $\Delta i_d$  and  $\Delta i_q$  are represented by equations (2.54) and (2.55).

$$\Delta i_d = P_1 \Delta \delta + P_2 \Delta E'_q \quad (2.54)$$

$$\Delta i_q = P_3 \Delta \delta + P_4 \Delta E'_d \quad (2.55)$$

Where

$$P_1 = \frac{-E_b \sin \delta_0}{x_e + x'_d}, \quad P_2 = -\frac{1}{x_e + x'_d}, \quad P_3 = \frac{E_b \cos \delta_0}{x_e + x'_q}, \quad P_4 = \frac{1}{x_e + x'_q} \quad (2.56)$$

The linearized equations of  $\Delta v_d$ ,  $\Delta v_q$ ,  $V_t$  and  $\Delta T_e$  are shown by equations (2.57) to (2.61).

$$\Delta V_d = (-E_b \cos \delta_0 + P_3 x_e) \Delta \delta + x_e P_4 \Delta E'_d \quad (2.57)$$

$$\Delta V_q = (-E_b \sin \delta_0 + P_1 x_e) \Delta \delta - x_e P_2 \Delta E'_q \quad (2.58)$$

$$\Delta T_e = K_1 \Delta \delta + K_2 \Delta E'_q + K_3 \Delta E'_d \quad (2.59)$$

$$\Delta V_t = \frac{V_{d0}}{V_{t0}} \Delta v_d + \frac{V_{q0}}{V_{t0}} \Delta v_q \quad (2.60)$$

$$\Delta V_t = K_8 \Delta \delta + K_9 \Delta E'_q + K_{10} E'_d \quad (2.61)$$

The fourth-order model of the synchronous machine is considered and  $K_1$  to  $K_{10}$  constant are derived by substituting the above equations in linearized form of the machine state equations (2.1), (2.2), (2.4), (2.5) and (2.11). The linearized forms of the machine state Equations are represented by equations (2.62) to (2.66).

$$\dot{\delta} = \omega_b \Delta \omega_m \quad (2.62)$$

$$\Delta \dot{\omega}_m = -\frac{k_d}{2H} \Delta \omega_m + \frac{1}{2H} \Delta T_m - \frac{K_1}{2H} \Delta \delta - \frac{K_2}{2H} \Delta E'_q - \frac{K_3}{2H} \Delta E'_d \quad (2.63)$$

$$\Delta \dot{E}'_q = \frac{1}{T'_{d0}} \left( \Delta E_{fd} - K_5 \Delta \delta - \frac{\Delta E'_q}{K_4} \right) \quad (2.64)$$

$$\Delta \dot{E}'_d = \frac{1}{T'_{q0}} \left( K_7 \Delta \delta - \frac{\Delta E'_d}{K_6} \right) \quad (2.65)$$

$$\Delta \dot{E}_{fd} = -\frac{K_A}{T_A} \Delta \delta - \frac{K_A K_9}{T_A} \Delta E'_q - \frac{K_A K_{10}}{T_A} \Delta E'_d + \frac{K_A}{T_A} \Delta V_{ref} + \frac{1}{T_A} \Delta f_d \quad (2.66)$$

## 2.5.2 State Space Representation of System

The expression (2.67) is described linearized power system model in state space form  $\Delta\dot{x} = A\Delta x + B\Delta u$  and machine constant  $K_1$  to  $K_{10}$  are described by equations (2.68) to (2.77). Figure 2.3 represents the block diagram of SMIB.

$$\begin{aligned}
 \begin{bmatrix} \Delta\dot{\delta} \\ \Delta\dot{\omega}_m \\ \Delta\dot{E}'_q \\ \Delta\dot{E}'_d \\ \Delta\dot{E}'_{fd} \end{bmatrix} &= \begin{bmatrix} 0 & \omega_B & 0 & 0 & 0 \\ -\frac{K_1}{2H} & -\frac{D}{2H} & -\frac{K_2}{2H} & -\frac{K_3}{2H} & 0 \\ -\frac{K_5}{T'_{d0}} & 0 & -\frac{1}{T'_{d0}K_4} & 0 & \frac{1}{T'_{d0}} \\ \frac{K_7}{T'_{q0}} & 0 & 0 & -\frac{1}{T'_{q0}K_6} & 0 \\ -\frac{K_A K_8}{T_A} & 0 & -\frac{K_A K_9}{T_A} & -\frac{K_A K_{10}}{T_A} & -\frac{1}{T_A} \end{bmatrix} \begin{bmatrix} \Delta\delta \\ \Delta\omega_m \\ \Delta E'_q \\ \Delta E'_d \\ \Delta E'_{fd} \end{bmatrix} \\
 + \begin{bmatrix} 0 \\ \frac{1}{2H} \\ 0 \\ 0 \\ \frac{K_A}{T_A} \end{bmatrix} & \begin{bmatrix} 0 & \Delta T_m & 0 & 0 & V_{ref} \end{bmatrix} \tag{2.67}
 \end{aligned}$$

where,

$$\begin{aligned}
 K_1 &= \frac{\partial T_e}{\partial \delta} = - \left[ E'_{d0} + \left( (x'_d - x'_q) i_{q0} \right) \right] \frac{E_{d0} E_b \sin \delta_0}{x_e + x'_d} + \\
 & \left[ (x'_d - x'_q) i_{d0} + E'_{q0} \right] \frac{E_b \cos \delta_0}{x_e + x'_{dq}} \tag{2.68}
 \end{aligned}$$

$$K_2 = \frac{\partial T_e}{\partial E'_q} = - \left[ E'_{d0} + \left( (x'_d - x'_q) i_{q0} \right) \right] \frac{1}{x_e + x'_d} + E'_{q0} \frac{1}{x_e + x'_q} + i_{q0} \tag{2.69}$$

$$K_3 = \frac{\partial T_e}{\partial E'_d} = \left[ i_{d0} + \left( (x'_d - x'_q) i_{d0} \right) \right] \frac{1}{x_e + x'_q} \tag{2.70}$$

$$K_4 = \frac{\partial E'_q}{\partial E_q} = \frac{x_e + x'_d}{(x_e + x'_d) + (x_d - x'_d)} \tag{2.71}$$

$$K_5 = \frac{\partial E'_q}{\partial \delta} = (x_d - x'_d) \frac{E_b \sin \delta_0}{x_e + x'_d} \tag{2.72}$$

$$K_6 = \frac{\partial E'_d}{\partial E_d} = \frac{x_e + x'_q}{(x_e + x'_q) + (x_q - x'_q)} \tag{2.73}$$

$$K_7 = \frac{\partial E'_d}{\partial \delta} = - \left( x_q - x'_q \right) \frac{E_b \cos \delta_0}{x_e + x'_q} \quad (2.74)$$

$$K_8 = \frac{\partial E_{fd}}{\partial \delta} = \frac{V_{d0}}{V_{t0}} \left( -E_b \cos \delta_0 + \frac{x_e E_b \cos \delta_0}{x_e + x'_d} \right) \quad (2.75)$$

$$K_9 = \frac{\partial E_{fd}}{\partial E'_q} = \frac{V_{q0} x_e}{V_{t0}} \frac{1}{x_e + x'_d} \quad (2.76)$$

$$K_{10} = \frac{\partial E_{fd}}{\partial E'_d} = \frac{V_{d0} x_e}{V_{t0}} \frac{1}{x_e + x'_q} \quad (2.77)$$

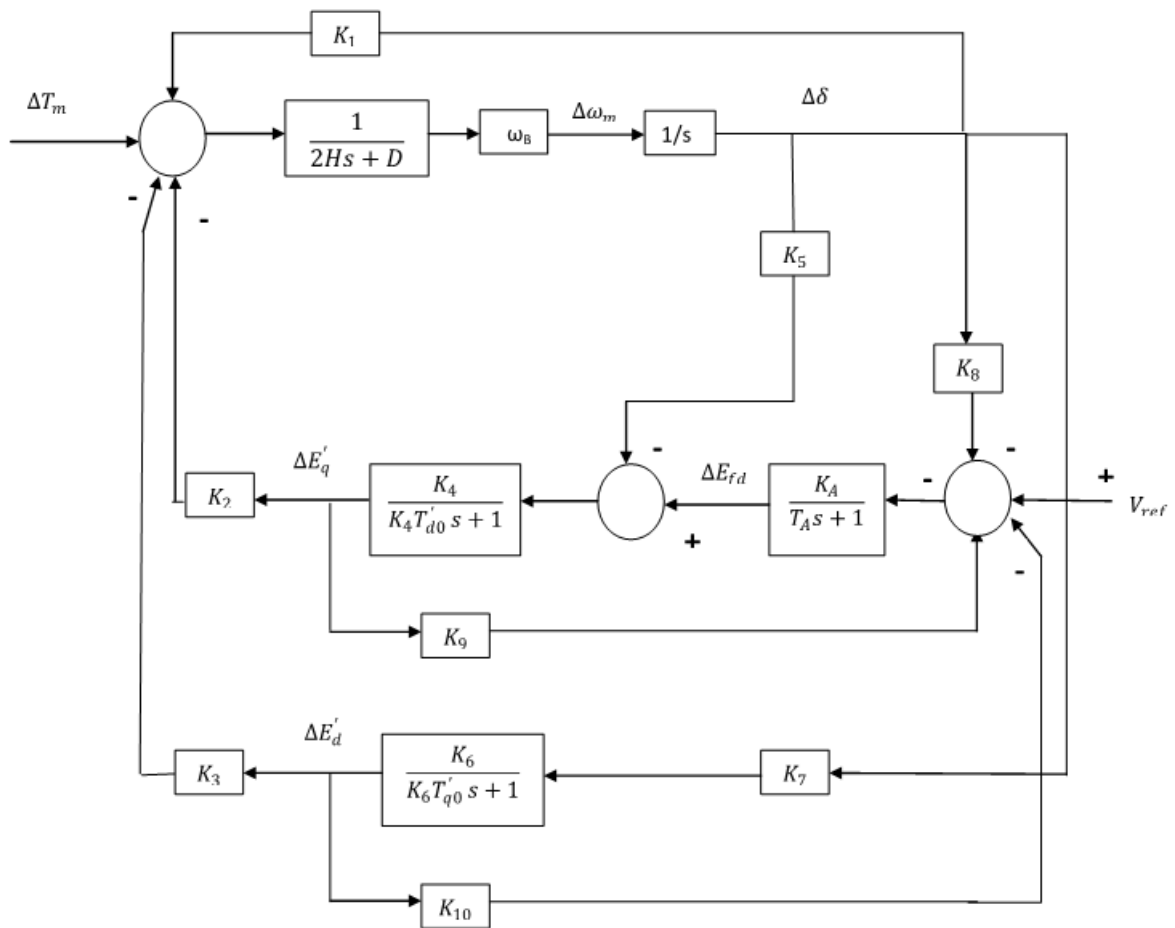


Figure 2.3: Block diagram representation of SMIB system

## 2.6 Power System Stabilizer

The single machine infinite bus system with generator connected PSS is shown in Figure 2.4.

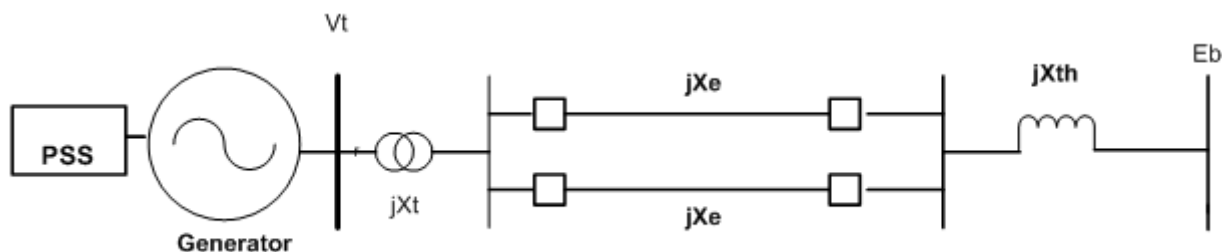


Figure 2.4: SMIB with PSS

### 2.6.1 Conventional Power system stabilizer

The output response of the PSS is shown as a feedback element from generator speed and is described in the form [56, 33, 15]. The conventional power system stabilizer is described by equation (2.78). The first term in equation (2.78) is a reset term that is used to washout the compensation effect after the time lag  $T_w$ . The second term of  $\Delta V_{pss}$  is a lead compensation pair that can be used to improve the phase lag through the system from  $V_{ref}$  to generator shaft speed  $\Delta\omega_m$ .

$$\Delta V_{pss} = \frac{K_{pss} T_w s}{1 + T_w s} \left[ \frac{(1 + T_1 s)(1 + T_2 s)}{(1 + T_3 s)(1 + T_4 s)} \right] \Delta\omega_m \quad (2.78)$$

The equation (2.78) is represented by state model of PSS which is shown by Figure 2.5.

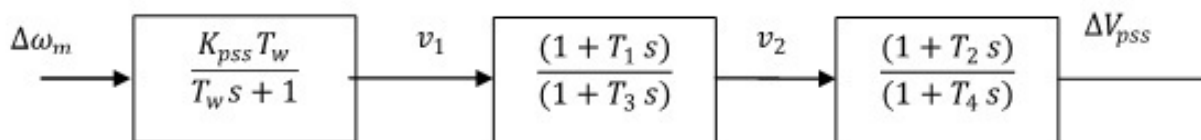


Figure 2.5: CPSS with state variables

The two new state  $v_1$ ,  $v_2$  and output variable  $\Delta V_{pss}$  of PSS are included in machine state equations. The CPSS new state equation are described as follow:

$$\Delta v_1 = -\frac{K_1 K_{pss}}{2H} \Delta\delta - \frac{DK_{pss}}{2H} \Delta\omega_m - \frac{K_2 K_{pss}}{2H} \Delta E'_q - \frac{K_3 K_{pss}}{2H} \Delta E'_d - \frac{1}{T_w} \Delta v_1 \quad (2.79)$$

$$\Delta \dot{v}_2 = -a_1 \Delta \delta - a_2 \Delta \omega_m - a_3 \Delta E'_q - a_4 \Delta E'_d - a_5 \Delta v_1 + a_6 v_2 \quad (2.80)$$

$$\Delta \dot{v}_{pss} = -b_1 \Delta \delta - b_2 \Delta \omega_m - b_3 \Delta E'_q - b_4 \Delta E'_d + b_5 \Delta v_1 + b_6 \Delta v_2 + b_7 \Delta v_{pss} \quad (2.81)$$

### 2.6.1.1 Model of Power System with CPSS

The Power system stabilizer provides the additional signal to excitation system. After the addition of PSS with excitation system, the exciter equation would be changed. The exciter equation is described by equations (2.82) and (2.83).

$$\dot{E}_{fd} = -\frac{1}{T_A} E_{fd} + \frac{K_A}{T_A} (V_{ref} - V_t + V_{pss}) \quad (2.82)$$

$$\Delta \dot{E}_{fd} = -\frac{K_A K_8}{T_A} \Delta \delta - \frac{K_A K_9}{T_A} \Delta E'_q - \frac{K_A K_{10}}{T_A} \Delta E'_d + \frac{K_A}{T_A} \Delta V_{ref} - \frac{1}{T_A} \Delta_{fd} + \frac{K_A}{T_A} V_{pss} \quad (2.83)$$

The state model of machine with PSS is described by equation (2.84).

$$A = \begin{bmatrix} 0 & \omega_B & 0 & 0 & 0 & 0 & 0 & 0 \\ -\frac{K_1}{2H} & -\frac{D}{2H} & -\frac{K_2}{2H} & -\frac{K_3}{2H} & 0 & 0 & 0 & 0 \\ -\frac{K_5}{T'_{d0}} & 0 & -\frac{1}{T'_{d0} K_4} & 0 & \frac{1}{T'_{d0}} & 0 & 0 & 0 \\ \frac{K_7}{T'_{q0}} & 0 & 0 & -\frac{1}{T'_{q0} K_6} & 0 & 0 & 0 & 0 \\ -\frac{K_A K_8}{T_A} & 0 & -\frac{K_A K_9}{T_A} & -\frac{K_A K_{10}}{T_A} & -\frac{1}{T_A} & 0 & 0 & \frac{K_A}{T_A} \\ -\frac{K_1 K_{pss}}{2H} & -\frac{DK_{pss}}{2H} & -\frac{K_2 K_{pss}}{2H} & -\frac{K_3 K_{pss}}{2H} & 0 & -\frac{1}{T_w} & 0 & 0 \\ a_1 & a_2 & a_3 & a_4 & 0 & a_5 & a_6 & 0 \\ b_1 & b_2 & b_3 & b_4 & 0 & b_5 & b_6 & b_7 \end{bmatrix}_{8 \times 8} \quad (2.84)$$

Where,

$$\dot{x} = \left[ \Delta \dot{\delta} \quad \Delta \dot{\omega}_m \quad \Delta \dot{E}'_q \quad \Delta \dot{E}'_d \quad \Delta \dot{E}_{fd} \quad \Delta \dot{v}_1 \quad \Delta \dot{v}_2 \quad \Delta \dot{V}_{pss} \right]'$$

$$a_1 = -\frac{T_1 K_{pss}}{T_2 2H}, a_2 = -\frac{T_1 DK_{pss}}{T_2 2H}, a_3 = -\frac{T_1 K_2 K_{pss}}{T_2 2H}, a_4 = -\frac{T_1 K_3 K_{pss}}{T_2 2H}, a_5 = \frac{1}{T_2} - \frac{T_1}{T_2 T_w}, a_6 = -\frac{1}{T_2}$$

$$b_1 = -\frac{T_1 T_3 K_1 K_{pss}}{T_2 T_4 2H}, b_2 = -\frac{T_2 T_4 DK_{pss}}{T_2 T_4 2H}, b_3 = -\frac{T_2 T_3 K_2 K_{pss}}{T_2 T_4 2H}, b_4 = -\frac{T_1 T_3 K_3 K_{pss}}{T_2 T_4 2H}, b_5 = \frac{T_3}{T_2 T_4} - \frac{T_1 T_3}{T_2 T_4 2H},$$

$$b_6 = \frac{1}{T_4} - \frac{T_3}{T_2 T_4}, b_7 = -\frac{1}{T_4}$$

## 2.6.2 Proportional Integral Derivative Power System Stabilizer

One of the most powerful but complex controller mode combines the proportional, integral and derivative mode. This mode eliminates the offset of the proportional mode and provides fast response [20, 88]. In present work PID based PSS is proposed with feedback element from generator speed and is represented by in Laplace form. The Laplace form of PID-PSS is represented by equation (2.85).

$$\Delta V_{pss} = \left[ K_p + \frac{K_I}{s} + K_D s \right] \Delta \omega_m \quad (2.85)$$

### 2.6.2.1 Model of Power System with PID-PSS

The state model of machine with PID-PSS is described by equation (2.86). Figure 2.6 represents block diagram of machine with CPSS and PID-PSS.

$$A = \begin{bmatrix} 0 & \omega_B & 0 & 0 & 0 & 0 \\ -\frac{K_1}{2H} & \frac{D}{-2H} & -\frac{K_2}{2H} & -\frac{K_3}{2H} & 0 & 0 \\ -\frac{K_5}{T'_{d0}} & 0 & -\frac{1}{T'_{d0}K_4} & 0 & \frac{1}{T'_{d0}} & 0 \\ \frac{K_7}{T_{q0}} & 0 & 0 & -\frac{1}{T_{q0}K_6} & 0 & 0 \\ -\frac{K_A K_8}{T_A} & 0 & -\frac{K_A K_9}{T_A} & -\frac{K_A K_{10}}{T_A} & -\frac{1}{T_A} & 0 \\ \left( \frac{K_1}{\omega_B} - \frac{K_1 K_{10}}{2H} \right) & \left( K_P - \frac{K_d k_d}{2H} \right) & -\frac{K_2 K_D}{2H} & \frac{-K_3 K_D}{2H} & 0 & 0 \end{bmatrix}_{6 \times 6} \quad (2.86)$$

Where,

$$\dot{x} = \left[ \Delta \dot{\delta} \quad \Delta \dot{\omega}_m \quad \Delta \dot{E}'_q \quad \Delta \dot{E}'_d \quad \Delta \dot{E}'_{fd} \quad \Delta \dot{V}_{pss} \right]'$$

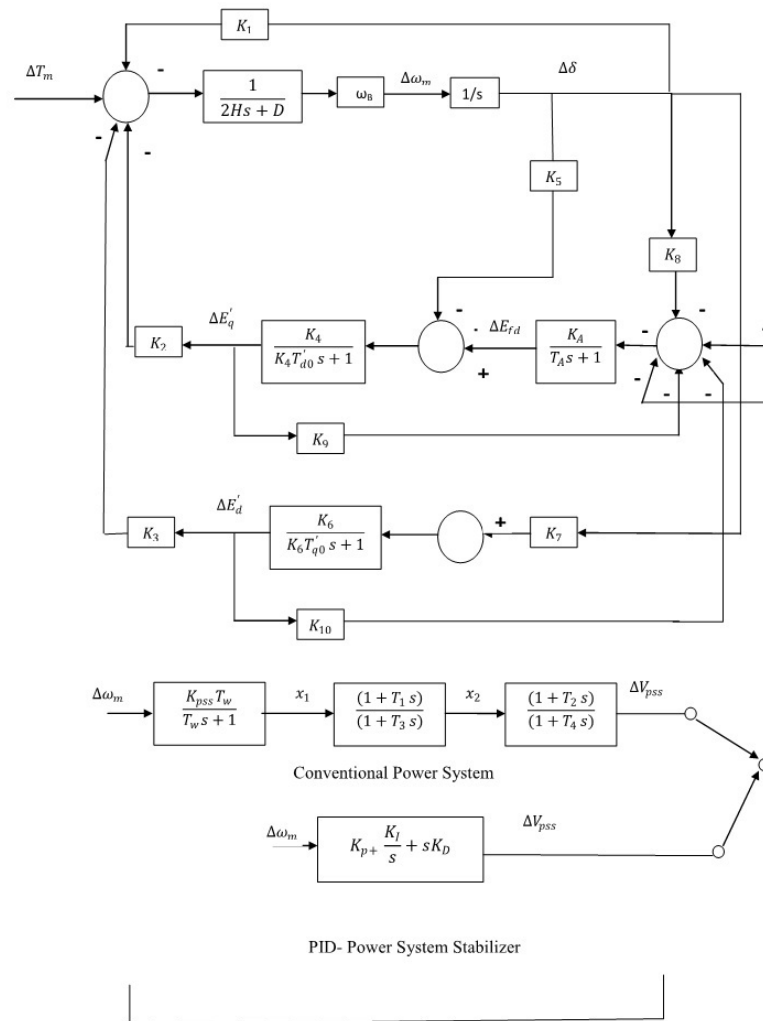


Figure 2.6: Block diagram representation of SMIB with PSS

## 2.7 Thyristor Control Series Capacitor

Thyristor controlled series capacitor provides the fast, continuous and dynamic control of power by varying the apparent reactance of the specific transmission line. The TCSC can enhance the oscillatory stability by damping of oscillation and improves the dynamic and transient stability of the power system [55, 25, 44, 62]. One line diagram of the basic module of the TCSC is shown in Figure 2.7. A TCSC is a parallel combination of a fixed

series capacitor and a variable thyristor controlled reactor. The TCSC has two operating ranges around its internal circuit resonance. One is  $\alpha_{min} \leq \alpha \leq 180$  where  $X_{TCSC(\alpha)}$  is capacitive, and other is the  $90 \leq \alpha \leq L_{lim}$  where  $X_{TCSC(\alpha)}$  is inductive. The internal circuit resonance depends on the ratio of inductor and capacitor reactance of TCSC. The steady state relationship between firing angle and the reactance  $X_{TCSC}$  can be described by the following equation [44].

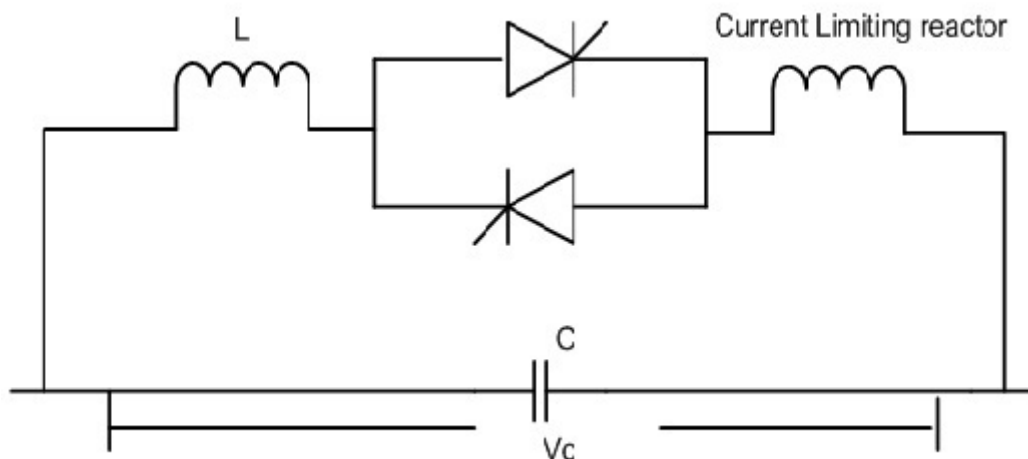


Figure 2.7: Basic module of TCSC

$$X_{TCSC(\alpha)} = X_C - \frac{X_C^2(\mu + \sin\mu)}{(X_C - X_L)\pi} + \frac{4X_C^2 \cos^2(\mu/2) [\operatorname{ptan}(\frac{p\pi}{2}) - \tan(\pi/2)]}{(X_C - X_L)(p^2 - 1)\pi} \quad (2.87)$$

Where  $X_C$  is reactance of the fixed capacitor,  $X_L$  is inductive reactance of inductor  $L$  connected in parallel to capacitor, compensation ratio  $p = \sqrt{\frac{X_C}{X_L}}$  and conduction angle of TCSC is  $\mu = \pi - \alpha$ . The model for the TCSC for the stability study is shown in Figure 2.8 and is based on the variation of the reactance of the TCSC in the capacitive region [38, 44]. In this Figure,  $X_{mod}$  is the stability control modulation reactance value as determined by the stability control loop, and  $X_{ref}$  denotes the TCSC steady state reactance or set point, whose value is calculated from power flow or steady state control loop. The sum of these two values produce  $X_{total}$  which is the final reactance offered by the external control block. This signal is passed through first order lag transfer function and produced the final value of the reactance  $X_{TCSC(\alpha)}$ . The time constant  $T_{TCSC}$  presents the natural response of the device and the delay

introduced by the internal control. The limits are given by  $X_{Cmin} = X_{TCSC}(180^\circ) = X_C$  and  $X_{Cmax} = X_{TCSC}(\alpha_{Cmin})$ . Here, the controller is assumed to operate in the capacitive region only, it means  $\alpha_{min} > \alpha_r$ , where  $\alpha_r$  correspond to the resonant point.

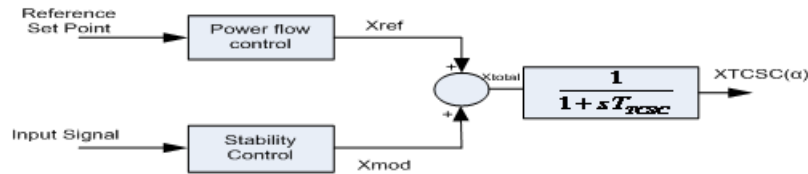


Figure 2.8: Model of TCSC

$$\dot{X}_{TCSC(\alpha)} = \frac{1}{T_{TCSC}} (X_{mod} + X_{ref}) - X_{TCSC(\alpha)} \quad (2.88)$$

The stability control loop of TCSC can be described by the Equation (2.89) .

$$X_{TCSC(\alpha)} = \frac{K_C T_{w1} s}{1 + T_{w1} s} \left[ \frac{(1 + T_{1T} s)(1 + T_{2T} s)}{(1 + T_{3T} s)(1 + T_{4T} s)} \right] \Delta\omega_m \quad (2.89)$$

Where  $T_{w1}$  and  $K_C$  are time constant and gain of the washout filter.  $T_{1T}, T_{2T}, T_{3T}$  and  $T_{4T}$  are time constant of the phase compensator, which provides appropriate phase-lead characteristics to compensate for the phase lag between input and output signals.

### 2.7.1 Model of Power system with Inclusion of TCSC

Figure 2.9 represents the single machine infinite bus system with generator connected PSS and transmission line equipped TCSC.

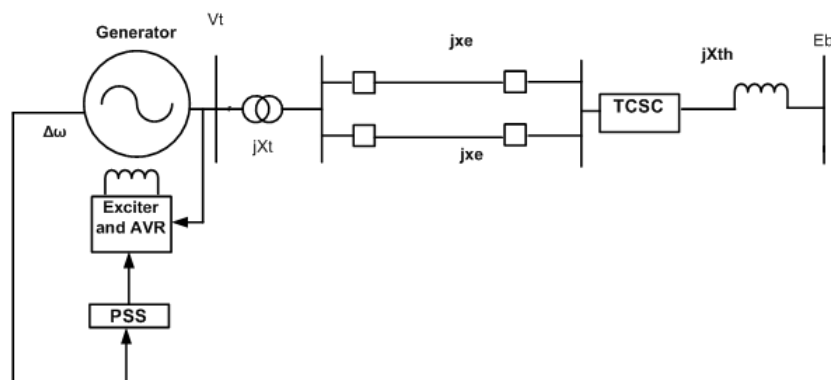


Figure 2.9: SMIB wiht PSS and TCSC

After the inclusion of TCSC in power system model, the line reactance would be changed as  $X_{net} = X_e - X_{TCSC}$ . The power transfer between the  $V_t$  and  $E_b$  is written as follows:

$$P_t = \frac{V_t E_b \sin \delta_0}{X_{net}} \quad (2.90)$$

The Current and voltage Equations of  $i_q, i_d, v_q$  and  $v_d$  would be changed. Hence electric torque  $T_e$  is also changed. The linearized model of the machine is derived after the inclusion of TCSC and new set of state Equations  $\Delta \dot{\delta}, \Delta \dot{\omega}_m, \Delta \dot{E}'_q, \Delta \dot{E}'_d, \Delta \dot{E}'_{fd}$  are obtained. Consequently  $K_1$  to  $K_{10}$  constants of the power system are recalculated using new line reactance  $X_{net}$  and initial conditions. After addition of TCSC, three new state variables and a state variable  $X_{TCSC(\alpha)}$  are required to be considered for stability control loop of TCSC. For the TCSC stability control loop the equation (2.88) and (2.89) are resolved using four state variables of TCSC model and then included in machine state equation. Figure 2.10 and 2.11 show stability control loop and time delay of TCSC. Equation (2.91) represents power system matrix  $A$  with TCSC stability control loop.

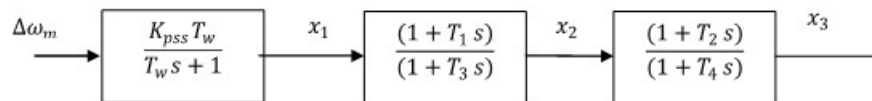


Figure 2.10: TCSC state diagram

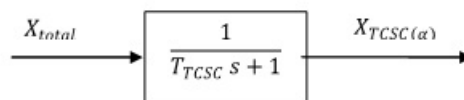


Figure 2.11: TCSC delay Equation

The matrix  $A$  is described as follow:

$$A = \begin{bmatrix} 0 & \omega_B & 0 & 0 & 0 & 0 & 0 & 0 & 0 \\ -\frac{K_1}{2H} & -\frac{D}{2H} & -\frac{K_2}{2H} & -\frac{K_3}{2H} & 0 & 0 & 0 & 0 & \frac{K_p}{2H} \\ -\frac{K_5}{T'_{d0}} & 0 & -\frac{1}{T'_{d0}K_4} & 0 & \frac{1}{T'_{d0}} & 0 & 0 & 0 & K_q \\ \frac{K_7}{T'_{q0}} & 0 & 0 & -\frac{1}{T'_{q0}K_6} & 0 & 0 & 0 & 0 & K_d \\ -\frac{K_A K_8}{T_A} & 0 & -\frac{K_A K_9}{T_A} & -\frac{K_A K_{10}}{T_A} & -\frac{1}{T_A} & 0 & 0 & 0 & \frac{K_A K_{Ed}}{T_A} \\ c_1 & c_2 & c_3 & c_4 & 0 & c_5 & 0 & 0 & 0 \\ d_1 & d_2 & d_3 & d_4 & 0 & d_5 & d_6 & 0 & 0 \\ e_1 & e_2 & e_3 & e_4 & 0 & e_5 & e_6 & e_7 & 0 \\ 0 & 0 & 0 & 0 & 0 & 0 & 0 & f_1 & f_2 \end{bmatrix}_{9 \times 9} \quad (2.91)$$

Where

$$\dot{x} = \left[ \Delta\delta \quad \Delta\omega_m \quad \Delta\dot{E}'_q \quad \Delta\dot{E}'_d \quad \Delta\dot{E}'_{fd} \quad \Delta x_1 \quad \Delta x_2 \quad \Delta x_3 \quad \Delta X_{TCSC} \right]'$$

## 2.7.2 Model of Power System with Inclusion of TCSC and PSS

The two state variables and  $\Delta V_{pss}$  of CPSS, and three state variables and  $X_{TCSC(\alpha)}$  of TCSC are included in power system model. After the inclusion of state variables of PSS and TCSC, the power system model is converted in  $12 \times 12$  matrix form. Equation (2.92) represents power system matrix  $A$  with PSS and TCSC stability control loop. Figure 2.12 represents the block diagram of power system with TCSC and  $\Delta V_{pss}$  signal coming from PSS.

$$\begin{bmatrix}
0 & \omega_B & 0 & 0 & 0 & 0 & 0 & 0 & 0 & 0 & 0 & 0 \\
-\frac{K_1}{2H} & -\frac{D}{2H} & -\frac{K_2}{2H} & -\frac{K_3}{2H} & 0 & 0 & 0 & 0 & 0 & 0 & 0 & \frac{K_p}{2H} \\
-\frac{K_5}{T'_{d0}} & 0 & -\frac{1}{T'_{d0}K_4} & 0 & \frac{1}{T'_{d0}} & 0 & 0 & 0 & 0 & 0 & 0 & K_q \\
\frac{K_7}{T'_{q0}} & 0 & 0 & -\frac{1}{T'_{q0}K_6} & 0 & 0 & 0 & 0 & 0 & 0 & 0 & K_d \\
-\frac{K_A K_8}{T_A} & 0 & -\frac{K_A K_9}{T_A} & -\frac{K_A K_{10}}{T_A} & -\frac{1}{T_A} & 0 & 0 & \frac{K_A}{T_A} & 0 & 0 & 0 & \frac{K_A K_{fed}}{T_A} \\
-\frac{K_1 K_{pss}}{2H} & -\frac{DK_{pss}}{2H} & -\frac{K_2 K_{pss}}{2H} & -\frac{K_3 K_{pss}}{2H} & 0 & -\frac{1}{T_w} & 0 & 0 & 0 & 0 & 0 & \frac{K_C K_{pss}}{2H} \\
a_1 & a_2 & a_3 & a_4 & 0 & a_5 & a_6 & 0 & 0 & 0 & 0 & \frac{K_C K_{pss} T_1}{2HT_2} \\
b_1 & b_2 & b_3 & b_4 & 0 & b_5 & b_6 & b_7 & 0 & 0 & 0 & \frac{K_C K_{pss} T_1 T_3}{2HT_2 T_4} \\
c_1 & c_2 & c_3 & c_4 & 0 & c_5 & 0 & 0 & 0 & 0 & 0 & 0 \\
d_1 & d_2 & d_3 & d_4 & 0 & d_5 & d_6 & 0 & 0 & 0 & 0 & 0 \\
e_1 & e_2 & e_3 & e_4 & 0 & e_5 & e_6 & e_7 & 0 & 0 & 0 & 0 \\
0 & 0 & 0 & 0 & 0 & 0 & 0 & f_1 & f_2 & 0 & 0 & 0
\end{bmatrix} \quad (2.92)$$

Where,

$$K_p = \frac{\partial T_e}{\partial X_{TCSC}}, \quad K_q = \frac{\partial E'_q}{\partial X_{TCSC}}, \quad K_d = \frac{\partial E'_d}{\partial X_{TCSC}}, \quad K_{fed} = \frac{\partial E_{fd}}{\partial X_{TCSC}}$$

$$c_1 = -\frac{K_C K_1}{2H}, \quad c_2 = -\frac{K_C D}{2H}, \quad c_3 = -\frac{K_C K_2}{2H}, \quad c_4 = -\frac{K_C K_3}{2H}, \quad c_5 = -\frac{1}{T_{w1}}$$

$$d_1 = -\frac{T_{1T} K_1 K_C}{T_{2T} 2H}, \quad d_2 = -\frac{T_{1T} D K_C}{T_{2T} 2H}, \quad d_3 = -\frac{T_{1T} K_2 K_C}{T_{2T} 2H}, \quad d_4 = -\frac{T_{1T} K_3 K_C}{T_{2T} 2H},$$

$$d_5 = \left[ \frac{1}{T_{2T}} - \frac{T_{1T}}{T_{2T} T_{w1}} \right], \quad d_6 = -\frac{1}{T_{2T}}$$

$$e_1 = -\frac{T_{1T} T_{3T} K_1 K_C}{T_{2T} T_{4T} 2H}, \quad e_2 = -\frac{T_{1T} T_{3T} D K_C}{T_{2T} T_{4T} 2H}, \quad e_3 = -\frac{T_{1T} T_{3T} K_2 K_C}{T_{2T} T_{4T} 2H}, \quad e_4 = -\frac{T_{1T} T_{3T} K_3 K_C}{T_{2T} T_{4T} 2H}$$

$$e_5 = \left[ \frac{T_{3T}}{T_{2T} T_{4T}} - \frac{T_{1T} T_{3T}}{T_{2T} T_{4T} T_{w1}} \right], \quad d_5 = \left[ \frac{1}{T_{4T}} - \frac{1}{T_{2T}} \right], \quad d_6 = -\frac{1}{T_{4T}}$$

$$f_1 = -\frac{1}{T_{TCSC}}, \quad f_2 = \frac{1}{T_{TCSC}}$$

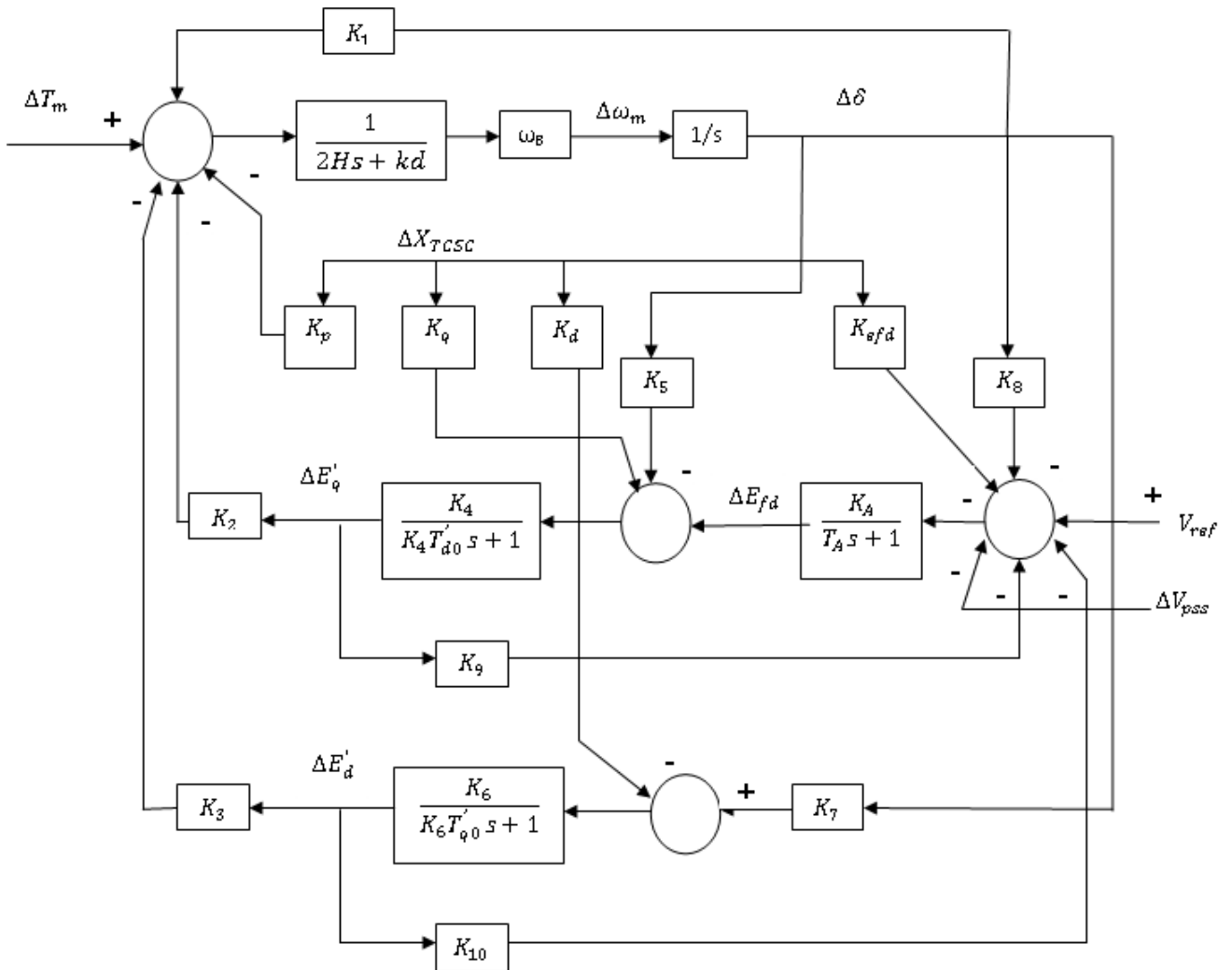


Figure 2.12: Block diagram of System with PSS and TCSC

## 2.8 Conclusion

For designing of computational intelligent techniques based PSS and TCSC, the mathematical model of the power system with different damping controllers are required. Calculation of eigen values, damping factors and participation of rotor mode are very important parameters for depth analysis of small signal stability issues. The transient stability analysis can be done by dynamical model of the power system.

This chapter has presented the fourth order non linear mathematical model of the power

system with IEEE-ST1 excitation system. The systematic procedure for conversion of non linear model into linear model with both PSS, TCSC and simultaneous designing of PSS and TCSC have been discussed. Using Taylor's series method, a new fourth order linearized model of the power system with exciter has been derived and the equations of machine constant  $K_1$  to  $K_{10}$  have been calculated. The linearized mathematical model and state space form of power system with conventional power system stabilizer and a new PID- power system stabilizer have been described. The linearized state space form of power system with individual TCSC and simultaneous CPSS and TCSC have been also derived. The block diagram representation of system with PSSs and TCSC has been included.

# Chapter 3

## Design of PSS and TCSC Using Genetic Algorithm

### 3.1 Introduction

This chapter deals with the individual and simultaneous application of thyristor controlled series capacitor and power system stabilizer for dynamic power system stability improvement. The Genetic Algorithm based Controllers have been designed for the development of the control strategy for thyristor control series capacitor and power system stabilizer. The parameters tuning of genetic algorithm based PSS and TCSC are considered as an optimization problem and the parameters are tuned using genetic search algorithm under different operating points. The non-linear and linearized model of the synchronous machine which includes both the generator main field winding and the damper winding on q-axis has been considered for the effective analysis of the system. The non-linear simulation of single machine infinite bus has been carried out, results of which show the efficacy and capability of simultaneous application both controllers under the various operating conditions and disturbances. The results demonstrate the improvement in the dynamic performance of the system with proposed control algorithms. The time response analysis have been performed under different operating conditions and contingencies.

## 3.2 GA based Design of CPSS and PID-PSS

### 3.2.1 Genetic Algorithm

Genetic Algorithms (GAs) are adaptive heuristic search algorithms introduced on the evolutionary themes of natural selection. The fundamental concept of the GA design is to model processes in a natural system that is required for evolution, specifically those that follow the principles posed by Charles Darwin to find the survival of the fittest. GAs constitute an intelligent development of a random search within a defined search space to solve a problem. GA was first pioneered by John Holland in the 1960s, and has been widely studied, experimented, and applied in numerous engineering disciplines. GA has been used for optimizing the parameters of the control system that are complex and difficult to solve by conventional optimization methods. GA maintains a set of candidate solutions called population and repeatedly modifies them. At each step, the GA selects individuals from the current population to be parents and uses them to produce the children for the next generation. Candidate solutions are usually represented as strings of fixed length, called chromosomes. A fitness or objective function is used to reflect the goodness of each member of the population. Given a random initial population, GA operates in cycles called generations, as follows [8]:

- Each member of the population is evaluated using a fitness function.
- The population undergoes reproduction in a number of iterations. One or more parents are chosen stochastically, but strings with higher fitness values have higher probability of contributing an offspring.
- Genetic operators, such as crossover and mutation, are applied to parents to produce offspring.
- The offspring are inserted into the population and the process is repeated.

Some of the advantages of GAs are as follows [90]:

1. GA is capable of parallel processing.

2. A large solution set can be obtained very quickly by GA.
3. GA is well suitable for complex, non linear and noisy fitness function.
4. GA is capable of converging to the local minima.

### 3.2.2 Problem Formulation and Optimization Function

Here, different parameters of the conventional PSS (Equ.2.78) and PID-PSS (Equ.2.85) are optimized under different operating conditions. For the conventional power system stabilizer the time constants  $T_1, T_2, T_3, T_4$ , and the gain  $K_{pss}$  are optimized using real coded genetic search algorithm. For the Proportional Integral Derivative - PSS, the gain  $K_p, K_I$  and  $K_D$  are optimized using real coded GA. In the both type of PSS input feedback signal is rotor speed, and under the steady state operation, the output of the PSS is zero. Under the disturbance conditions, the output of PSS is modified according to the change in the speed during dynamic environment. In this study, objective is to minimize the optimization function, which is described by equation (3.1).

$$J = \int_0^T t |\Delta\omega_m(t)| dt \quad (3.1)$$

The optimization function has been developed such that the damping factor of the system be improved and minimize real part of the eigen values associated with the rotor mode. The minimization of eigen values show that closed loop poles of the systems are located very far away in s-plane from origin. Hence time response parameters such as settling time to be improved and overshoots to be reduced. The Time Multiplied by Absolute Error (ITAE) [65, 97] has been used as the performance index. The optimization function  $J$  follows the optimized performance of CPSS and PID-PSS controlled system, and CPSS and PID-PSS gains for the system are adjusted such that the performance index to be minimized. The performance index is calculated over a time interval  $T$ , normally in the region of  $(0 \leq t \leq T)$ , where  $t$  is the settling time of the system. The best system response is obtained when the both PSS parameters are optimized by minimizing the maximum eigen values over a certain

range of operating conditions. The optimization flow chart of GA based CPSS and PID-PSS is shown in Figure 3.1.

Optimized  $J$  subject to:

For conventional Power system stabilizer

$$T_1^{min} \leq T_1 \leq T_1^{max} \quad (3.2)$$

$$T_2^{min} \leq T_2 \leq T_2^{max} \quad (3.3)$$

$$T_3^{min} \leq T_3 \leq T_3^{max} \quad (3.4)$$

$$T_4^{min} \leq T_4 \leq T_4^{max} \quad (3.5)$$

$$K_{pss}^{min} \leq K_{pss} \leq K_{pss}^{max} \quad (3.6)$$

For Proportional Integral Derivative - Power system stabilizer

$$K_p^{min} \leq K_p \leq K_p^{max} \quad (3.7)$$

$$K_I^{min} \leq K_I \leq K_I^{max} \quad (3.8)$$

$$K_D^{min} \leq K_D \leq K_D^{max} \quad (3.9)$$

### 3.2.3 Calculation of Initial Conditions

The initial conditions of the synchronous machine are calculated for different operating conditions. Four operating conditions are considered such as normal loading, slight heavy loading, heavy loading and very heavy loading. Here active power  $P_t = 0.6, 0.75, 0.9, 0.12$  and reactive power  $Q_t = 0.0224, 0.1, 0.15, 0.2$  are considered as different loading conditions. The initial conditions of different variables described by section (2.3.1) are calculated. The initial conditions of  $i_{d0}, i_{q0}, v_{d0}, v_{q0}, E'_{q0}, E'_d, \delta_0$  are given in Table 3.1. By using these values,  $K_1$  (Equ.2.68) to  $K_{10}$  (Equ. 2.77) constants of the machine are calculated. Then after the

eigen values, damping factor, right eigen vector, left eigen vector and participation factors (Section:2.4.3) of the machine have been calculated under four different operating conditions. Table 3.2 represents values of machine constant at different loading conditions.

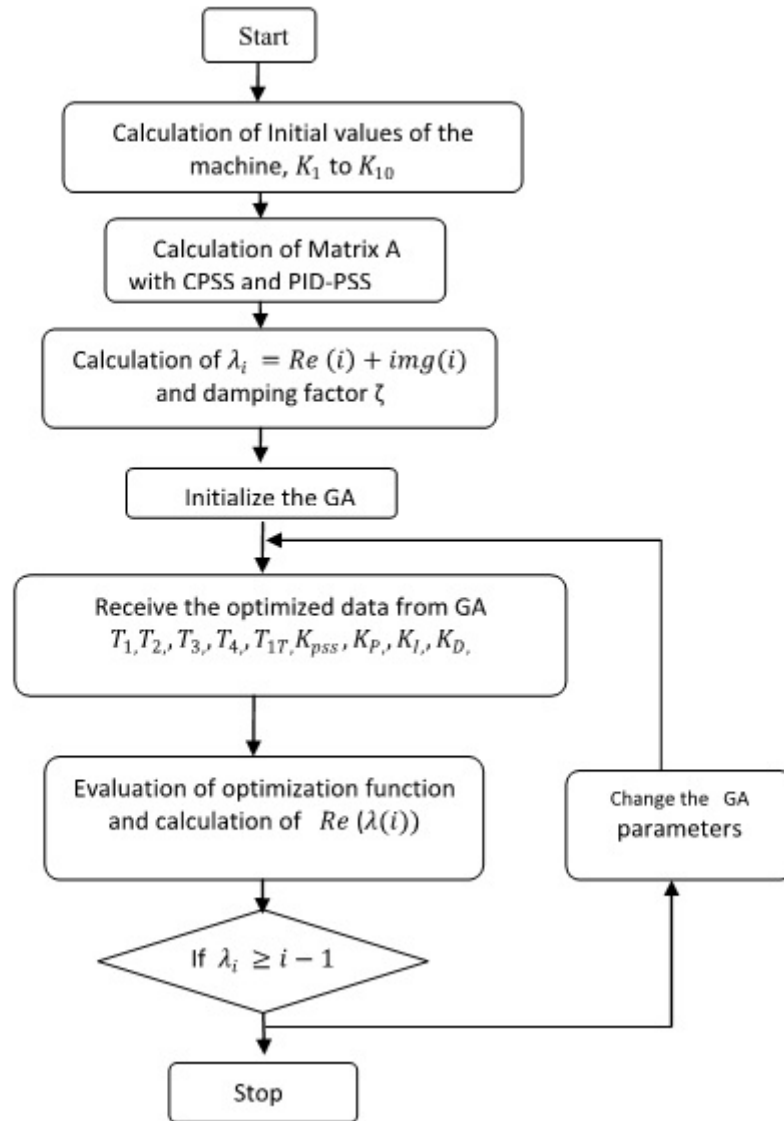


Figure 3.1: Flow Chart of GA based PSSs

Table 3.1: Calculation of Initial Conditions

Sr.No	Operating conditions	$i_{d0}$	$i_{q0}$	$v_{d0}$	$v_{q0}$	$E'_{d0}$	$E'_{q0}$	$\delta_0$
1	$P_t = 0.6, Q_t = 0.0224$	-0.383	0.425	-0.674	0.806	-0.232	0.969	61.52
2	$P_t = 0.75, Q_t = 0.1$	-0.553	0.455	-0.72	0.764	-0.248	1.0015	64.95
3	$P_t = 0.9, Q_t = 0.15$	-0.724	0.489	-0.765	0.7191	-0.2763	1.025	68.42
4	$P_t = 1.2, Q_t = 0.2$	-1.03	0.531	-0.841	0.628	-0.289	1.065	74.9

Table 3.2: Value of  $K_1$  to  $K_{10}$  Constant

Operating Conditions	$K_1$	$K_2$	$K_3$	$K_4$	$K_5$
$P_t = 0.6, Q_t = 0.0224$	0.726523	1.434816	0.317627	0.452937	1.061707
$P_t = 0.75, Q_t = 0.1$	0.764320	1.514948	0.223680	0.452937	1.094229
$P_t = 0.9, Q_t = 0.15$	0.786620	1.587298	0.132994	0.452937	1.123214
$P_t = 1.2, Q_t = 0.2$	0.796368	1.709019	-0.041301	0.452937	1.166157

Contd...

$K_6$	$K_7$	$K_8$	$K_9$	$K_{10}$
0.759433	-0.151024	-0.074594	0.472187	-0.253221
0.759433	-0.134110	-0.077964	0.447764	-0.270886
0.759433	-0.116467	-0.082909	0.421359	-0.287812
0.759433	-0.082475	-0.095970	0.368063	-0.316500

### 3.2.4 Eigen values and Participation Factor

The linear model of the system has been considered and eigen values of the Matrix  $A$  is calculated with both types of the PSSs under the different operating conditions. The matrix  $A$  of the different state space models described by equations (2.67), (2.84) and (2.86) are used for calculation of eigen values and eigen vectors. For the effective operation of the PSSs, the participation factor methods [4, 15] are used for identification of the eigen values associated with electromechanical modes. The magnitude of the participation factors are calculated using right eigen vector and left eigen vector.

### 3.2.5 Results

The linearized model presented by Figures 2.3 and 2.6 have been used for the small signal stability analysis of the SMIB system without PSS and with PSS respectively. For different operating conditions, the oscillations of the electromechanical modes of the machine are identified with GA based CPSS and PID-PSS, and small signal stability of the system has been analyzed.

The initial conditions, eigen values, damping factors and participation factors of the system are calculated using MATLAB programming. For four operating conditions, the objective function described by equations (3.2) to (3.9) are optimized. The time domain simulation is performed and fitness value is determined through equation (3.1) for each set of the gain and time constant parameters of CPSS and PID-PSS. By changing the GA parameters such as population size, crossover rate and function, mutation rate and function, number of generation, etc, the new set of gains and time constants are developed and best fitness values are selected. The parameters are selected for expected solution is given by Table 3.3 for the normal operating condition. The appropriate choice of the GAs parameters affects the convergence rate of the algorithm. Figure 3.2 shows the relationship between numbers of population versus convergence of fitness function under normal operating conditions. The optimized parameters of CPSS and PID-PSS are tuned for expected solution which is given by Table 3.4 and Table 3.5 respectively. All eigen values and corresponding damping factor without PSS and with GA based PSSs are shown in Table 3.10. The magnitude of participation factor of CPSS under the different operating conditions are shown in Table 3.6 to 3.9.

Table 3.3: GA Parameters and Values

GA Parameters	Values/function
Population size	50
Stopping Generation	65
Scaling function	rank
Selection function	Stochastic Uniform
Mutation function	Gaussian
Crossover function	Scattered

Table 3.4: Optimized Parameters of CPSS

Parameters	Operating Points			
	1	2	3	4
$K_{pss}$	4.562	4.691	4.962	5.232
$T_1$	0.97	1.089	1.83	2.11
$T_2$	0.994	0.849	2.419	2.821
$T_3$	0.633	0.362	0.432	0.523
$T_4$	0.0161	0.078	0.173	0.213

Table 3.5: Optimized Parameters of PID-PSS

Parameters	Operating Points			
	1	2	3	4
$K_P$	0.0256	0.0255	0.315	0.385
$K_I$	0.269	0.256	0.328	0.415
$K_D$	11.618	12.618	13.75	14.21

Table 3.6: Participation Factor (first operating condition)-CPSS

$P_t = 0.6, Q_t = 0.0224$							
0.0008	0.0039	0.0039	<b>0.5173</b>	<b>0.5173</b>	0.0051	0.0011	0.0269
0.0008	0.0039	0.0039	<b>0.5173</b>	<b>0.5173</b>	0.0051	0.0006	0.0269
0.1149	0.4974	0.4974	0.0298	0.0298	0.0000	0.0000	0.0056
0.0000	0.0000	0.0000	0.0398	0.0398	0.0000	0.0001	1.0630
0.2264	0.4174	0.4174	0.0031	0.0031	0.0000	0.0000	0.0004
0.0018	0.0061	0.0061	0.0654	0.0654	1.0105	0.0245	0.0058
0.0011	0.0038	0.0038	0.0401	0.0401	0.0002	1.0232	0.0083
0.6632	0.0405	0.0405	0.0211	0.0211	0.0000	0.0000	0.0004

Table 3.7: Participation Factor (second operating condition)-CPSS

$P_t = 0.75, Q_t = 0.1$							
0.0140	0.0140	0.0252	<b>0.5442</b>	<b>0.5442</b>	0.0054	0.0158	0.0157
0.0140	0.0140	0.0252	<b>0.5442</b>	<b>0.5442</b>	0.0054	0.0152	0.0157
0.6246	0.6246	0.1815	0.0424	0.0424	0.0000	0.0006	0.0073
0.0003	0.0003	0.0004	0.0386	0.0386	0.0000	0.0024	1.0545
0.4557	0.4557	0.4789	0.0050	0.0050	0.0000	0.0000	0.0005
0.0079	0.0079	0.0129	0.0582	0.0582	1.0111	0.0509	0.0004
0.0158	0.0158	0.0279	0.1133	0.1133	0.0003	1.0859	0.0305
0.2996	0.0761	0.0758	0.1345	0.1345	0.0000	0.0016	0.0002

Table 3.8: Participation Factor (third operating condition)-CPSS

$P_t = 0.9, Q_t = 0.15$							
0.0222	0.0222	0.2844	<b>0.6563</b>	<b>0.6563</b>	0.0066	0.0128	0.0159
0.0222	0.0222	0.2844	<b>0.6563</b>	<b>0.6563</b>	0.0066	0.0077	0.0159
0.8205	0.8205	0.2024	0.0847	0.0847	0.0000	0.0001	0.0068
0.0006	0.0006	0.0251	0.0336	0.0336	0.0000	0.0002	1.0475
0.7098	0.7098	0.0544	0.0128	0.0128	0.0000	0.0000	0.0005
0.0029	0.0029	0.0367	0.0285	0.0285	1.0151	0.0334	0.0007
0.0128	0.0128	0.2076	0.1263	0.1263	0.0018	1.0172	0.0183
0.1997	0.0450	0.0222	0.3545	0.3545	0.0001	1.0172	0.0183

Table 3.9: Participation Factor(Fourth operating condition)-CPSS

$P_t = 1.2, Q_t = 0.2$							
0.0523	0.0523	<b>0.8220</b>	<b>0.8220</b>	0.6051	0.0074	0.0219	0.0158
0.0523	0.0523	<b>0.8220</b>	<b>0.8220</b>	0.6051	0.0074	0.0078	0.0158
1.0148	1.0148	0.1705	0.1705	0.3595	0.0000	0.0001	0.0054
0.0011	0.0011	0.0344	0.0344	0.0500	0.0000	0.0001	1.0575
0.8070	0.8070	0.0289	0.0289	0.0865	0.0000	0.0000	0.0004
0.0050	0.0050	0.0385	0.0385	0.0603	1.0174	0.0336	0.0014
0.0219	0.0219	0.1725	0.1725	0.3222	0.0025	1.0171	0.0169
0.3668	0.0399	0.0068	0.7198	2.9158	0.0002	0.0006	0.0128

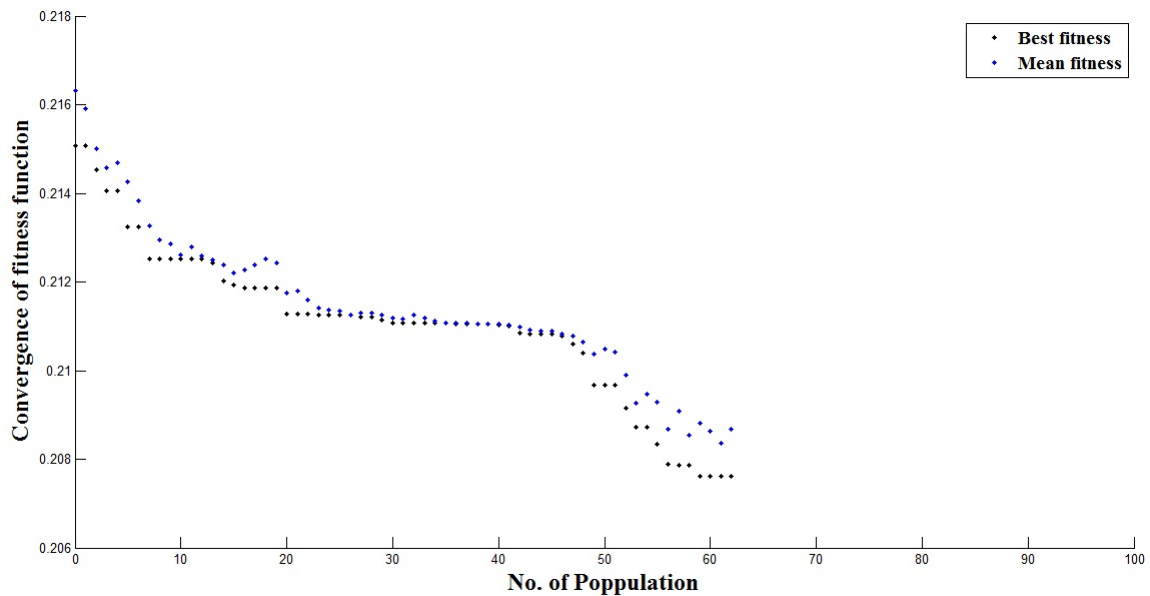


Figure 3.2: Numbers of population versus convergence of fitness function with PSS at Normal operating condition

Attention to Table 3.10, for all operating conditions, without application of PSS second pair of eigen value is positive and damping factor corresponding to same eigen value is negative. The positive eigen values show instability of system. While using of CPSS and PID-PSS, all the eigen values are negative with positive damping factor. This shows that system has become stable using power system stabilizer.

The eigen values associated to the only electromechanical mode (rotor mode) is evaluated using participation factor for all operating points. Attention to Table 3.10, the eigen values

associated with rotor mode are positive with negative damping factor without PSS. The damping factor are -0.0002, -0.0094, -0.0196,-0.0451 for four operating conditions. The oscillatory frequency of rotor mode is increased which shows instability of the system.

With CPSS, for first operating condition to third operating condition, the  $\lambda_4$  and  $\lambda_5$  have significant participation in rotor mode and for fourth operating condition,  $\lambda_3$  and  $\lambda_4$  have higher participation in rotor mode. eigen values and corresponding participation factor have been shown by bold font in Table 3.10, and Table 3.6 to 3.9 respectively. The damping factors associated to rotor mode are 0.1786, 0.2920, 0.3071, 0.4155 for all operating conditions using CPSS. Using right and left eigen vectors, the participation factors are calculated for PID-PSS.

With PID-PSS, second pair of eigen values (i.e.  $\lambda_3$  and  $\lambda_4$ ) have significant participation in rotor mode for all operating conditions. The bold font in Table 3.10 represents the eigen values and the damping factors 0.4483, 0.4109, 0.5726, 0.7484 associated to rotor mode for all operating conditions.

The CPSS and PID-PSS significantly improved the eigen values, damping factor and reduced oscillatory frequency in rotor mode. The eigen values of system have shown that the location of closed loop poles are in the left half of the s-pane and results show that the system has become stable using by CPSS and PID-PSS. Hence stability of power system has been improved using PSSs under different loading conditions.

Table 3.10: Eigen values and Damping Factor of CPSS and PID-PSS

O.C.	without PSS		With PSS			
	eigen value	$\xi$	CPSS		PID-PSS	
			eigen value	$\xi$	eigen value	$\zeta$
1	-20.3431 +27.1736i	0.5993	-80.8871	1.0000	-17.1033 +24.9993i	0.5647
	-20.3431 -27.1736i	0.5993	-10.1653 +42.3526i	0.2334	-17.1033 -24.9993i	0.5647
	<b>0.0012 + 6.4014i</b>	-0.0002	-10.1653 -42.3526i	0.2334	<b>-3.3149 + 6.6100i</b>	<b>0.4483</b>
	<b>0.0012 - 6.4014i</b>	-0.0002	<b>-0.7752 + 4.2697i</b>	<b>0.1786</b>	<b>-3.3149 - 6.6100i</b>	<b>0.4483</b>
	-2.6404	1.0000	<b>-0.7752 - 4.2697i</b>	<b>0.1786</b>	-2.4857	1.0000
			-2.6678	1.0000	-0.0021	1.0000
			-0.1005	1.0000		
2	-20.3826 +26.0738i	0.6159	-10.7327 +27.2905i	0.3660	-17.4124 +25.1619i	0.5690
	-20.3826 -26.0738i	0.6159	-10.7327 -27.2905i	0.3660	-17.4124 -25.1619i	0.5690
	<b>0.0623 + 6.6531i</b>	-0.0094	-29.0967	1.0000	<b>-2.9977 + 6.6512i</b>	<b>0.4109</b>
	<b>0.0623 - 6.6531i</b>	-0.0094	<b>-1.4417 + 4.7212i</b>	<b>0.2920</b>	<b>-2.9977 - 6.6512i</b>	<b>0.4109</b>
	-2.6836	1.0000	<b>-1.4417 - 4.7212i</b>	<b>0.2920</b>	-2.5007	1.0000
			-2.6813	1.0000	-0.0031	1.0000
			-1.1954	1.0000		
3	-20.4367 +24.8339i	0.6354	-16.8994 +22.3471i	0.6032	-15.4249 +21.4022i	0.5847
	-20.4367 -24.8339i	0.6354	-16.8994 -22.3471i	0.6032	-15.4249 -21.4022i	0.5847
	<b>0.1348 + 6.8749i</b>	-0.0196	-8.6414	1.0000	<b>-4.9546 + 7.0932i</b>	<b>0.5726</b>
	<b>0.1348 - 6.8749i</b>	-0.0196	<b>-1.9660 + 6.0933i</b>	<b>0.3071</b>	<b>-4.9546 - 7.0932i</b>	<b>0.5726</b>
	-2.7204	1.0000	<b>-1.9660 - 6.0933i</b>	<b>0.3071</b>	-2.5610	1.0000
			-2.7348	1.0000	-0.0040	1.0000
			-0.4103	1.0000		
4	-20.5971 +22.1444i	0.6811	-15.8036 +18.9297i	0.6409	-12.1260 +16.7328i	0.5868
	-20.5971 -22.1444i	0.6811	-15.8036 -18.9297i	0.6409	-12.1260 -16.7328i	0.5868
	<b>0.3284 + 7.2704i</b>	-0.0451	<b>-2.8438 + 6.2254i</b>	<b>0.4155</b>	<b>-8.2177 + 7.2835i</b>	<b>0.7484</b>
	<b>0.3284 - 7.2704i</b>	-0.0451	<b>-2.8438 - 6.2254i</b>	<b>0.4155</b>	<b>-8.2177 - 7.2835i</b>	<b>0.7484</b>
	-2.7868	1.0000	-7.9133	1.0000	-2.6315	1.0000
			-2.8131	1.0000	-0.0053	1.0000
			-0.1007	1.0000		
		-0.3518	1.0000			

### 3.3 GA based Design of TCSC and PSS

#### 3.3.1 Problem Formulation and Optimization Function

Different parameters of the PSS and TCSC are optimized using real coded genetic algorithm under four operating conditions. For the conventional power system stabilizer, the time constants  $T_1, T_2, T_3, T_4$ , and the gain  $K_{pss}$  are optimized. For the TCSC controller the time constant  $T_{1T}, T_{2T}, T_{3T}, T_{4T}$ , and  $K_C$  are tuned using real coded genetic search algorithm. For PSS and TCSC, the time constant of wash out filter  $T_w$  and  $T_{w1}$  has been selected to be 10. The rotor speed signal has been utilized as feedback signal for both the stabilizer. Here, it is objective to minimize the optimization function  $J$ . The optimization flow chart has been shown in Figure (3.3). The optimization function is described by equation (3.10).

$$J = \int_0^T t |\Delta\omega_m(t)| dt \quad (3.10)$$

The optimization function has been developed such that the damping factor of the system be improved by minimization of real part of the eigen values associated with the rotor mode. Hence time response parameters such as settling time is to be improved and overshoots is to be reduced. The Time Multiplied by Absolute Error (ITAE) has been used as the performance index. The optimization function  $J$  follows the optimized performance of PSS and TCSC controlled system. The CPSS and TCSC gains for the system are adjusted such that the performance index to be minimized. The performance index is calculated over a time interval  $T$ , normally in the region of  $(0 \leq t \leq T)$ , where  $t$  is the settling time of the system. The best system response is obtained when the PSS and TCSC parameters are optimized by minimizing the maximum eigen values over a certain range of operating conditions. The flow chart 3.3 shows the optimization of PSS and TCSC parameters. Optimize  $J$  subject to:

$$T_1^{min} \leq T_1 \leq T_1^{max} \quad (3.11)$$

$$T_2^{min} \leq T_2 \leq T_2^{max} \quad (3.12)$$

$$T_3^{min} \leq T_3 \leq T_3^{max} \quad (3.13)$$

$$T_4^{min} \leq T_4 \leq T_{14}^{max} \quad (3.14)$$

$$T_{1T}^{min} \leq T_{1T} \leq T_{1T}^{max} \quad (3.15)$$

$$T_{2T}^{min} \leq T_{2T} \leq T_{2T}^{max} \quad (3.16)$$

$$T_{3T}^{min} \leq T_{3T} \leq T_{4T}^{max} \quad (3.17)$$

$$T_{4T}^{min} \leq T_{4T} \leq T_{4T}^{max} \quad (3.18)$$

$$K_{pss}^{min} \leq K_{pss} \leq K_{pss}^{max} \quad (3.19)$$

$$K_C^{min} \leq K_C \leq K_C^{max} \quad (3.20)$$

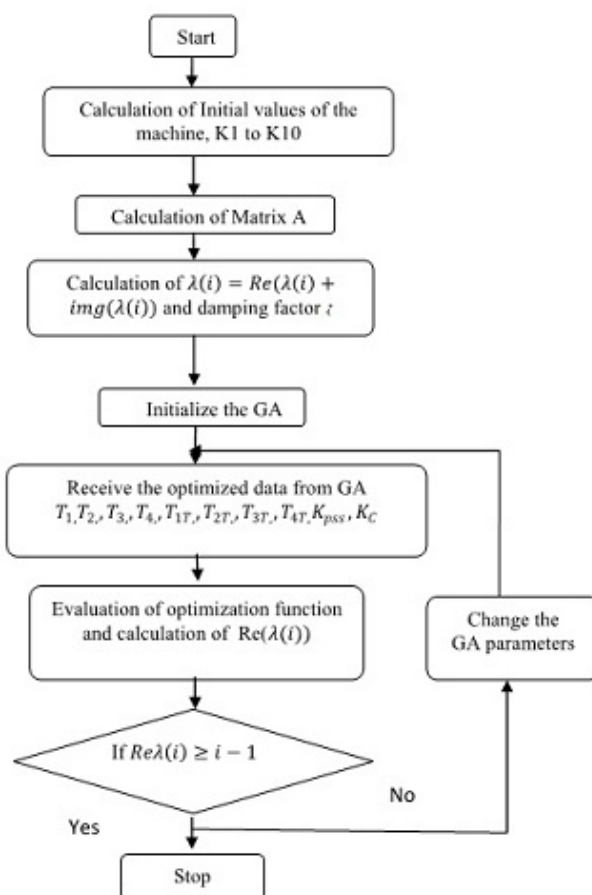


Figure 3.3: Flow chart of GA based PSS and TCSC

### 3.3.2 Calculation of $K_1$ to $K_{10}$ Constants

The initial conditions of the synchronous machine are calculated for different operating conditions. Four operating conditions are considered such as light loading, normal loading and heavy loading and very heavy loading. Here active power  $P_t = 0.6, 0.75, 0.9, 1.2$  and reactive power  $Q_t = 0.0224, 0.1, 0.15, 0.2$  are used as different loading conditions. The initial conditions of different variables described by section (2.3.1) are calculated. The initial conditions of  $i_{d0}, i_{q0}, v_{d0}, v_{q0}, E'_{q0}, E'_d, \delta_0$  are given in Table 3.1. After addition of TCSC, new values of  $K_1$  to  $K_{10}$  constants (Table: 3.11) are calculated using initial conditions. The constant of the machine are changed as line reactance of the system would be changed after changing of line reactance  $X_e$  to  $X_{net}$ . Then after the eigen values, damping factor, right eigen vector, left eigen vector and participation factors (Section: 2.4.3) of the machine are calculated under the four different operating conditions.

Table 3.11: Values of  $K_1$  to  $K_{10}$  Constant after inclusion of TCSC

Operating Conditions	$K_1$	$K_2$	$K_3$	$K_4$	$K_5$
$P_t = 0.6, Q_t = 0.0224$	0.800705	1.533198	0.371039	0.424146	1.193447
$P_t = 0.75, Q_t = 0.1$	0.843310	1.618670	0.283385	0.424146	1.230004
$P_t = 0.9, Q_t = 0.15$	0.869186	1.695800	0.198232	0.424146	1.262585
$P_t = 1.2, Q_t = 0.2$	0.882877	1.825553	0.034083	0.424146	1.310857

Contd...

$K_6$	$K_7$	$K_8$	$K_9$	$K_{10}$
0.745751	-0.162542	-0.092693	0.435552	-0.223638
0.745751	-0.144338	-0.096039	0.413023	-0.239239
0.745751	-0.125349	-0.100948	0.388668	-0.254187
0.745751	-0.088765	-0.113915	0.339507	-0.279524

### 3.3.3 Eigen values and Participation factor

The linear model of the system has been considered and eigen values of the state matrix  $A$  are calculated with individual application of TCSC, and simultaneously design of PSS and TCSC under the different operating conditions. The matrix  $A$  of the different state space models described by equations (2.91) and (2.92) are used for calculation of eigen values and

eigen vectors. For the effective operation of the PSS, the participation factor [4, 15] methods are used for identification of the eigen values associated with electromechanical modes. The magnitude of the participation factors are calculated using right eigen vector and left eigen vector.

### 3.3.4 Results

The linearized model presented by Figure 2.12 has been used for the small signal stability analysis of the SMIB system with TCSC and PSS. For different operating conditions, the oscillations of the electromechanical modes of the machine are identified with GA based CPSS and TCSC, and small signal stability of the system is analyzed.

The initial conditions, eigen values, damping factors and participation factors of the system are calculated using MATLAB programming. For four operating conditions, the objective function described by equation (3.11) to (3.20) have been optimized. The time domain simulation is performed and fitness value is determined through equation (3.10) for each set of the gain and time constant parameters of CPSS and TCSC. By changing the GA parameters such as population size, crossover rate and function, mutation rate and function, number of generation, etc, the new set of gains and time constants are developed and best fitness values have been selected. The GA parameters are selected for expected solution and are given by Table 3.3 for the normal operating condition. The appropriate choice of the GAs parameters affects the convergence rate of the algorithm. The relationship between numbers of population versus convergence of fitness function of TCSC and PSS-TCSC under normal operating conditions has been shown by Figures 3.4 and 3.5 respectively. The optimized parameters of CPSS and TCSC are tuned for expected solution which is given by Table 3.12. All eigen values and damping factor with individual application of TCSC and simultaneous application of PSS and TCSC is shown in Table 3.13 .

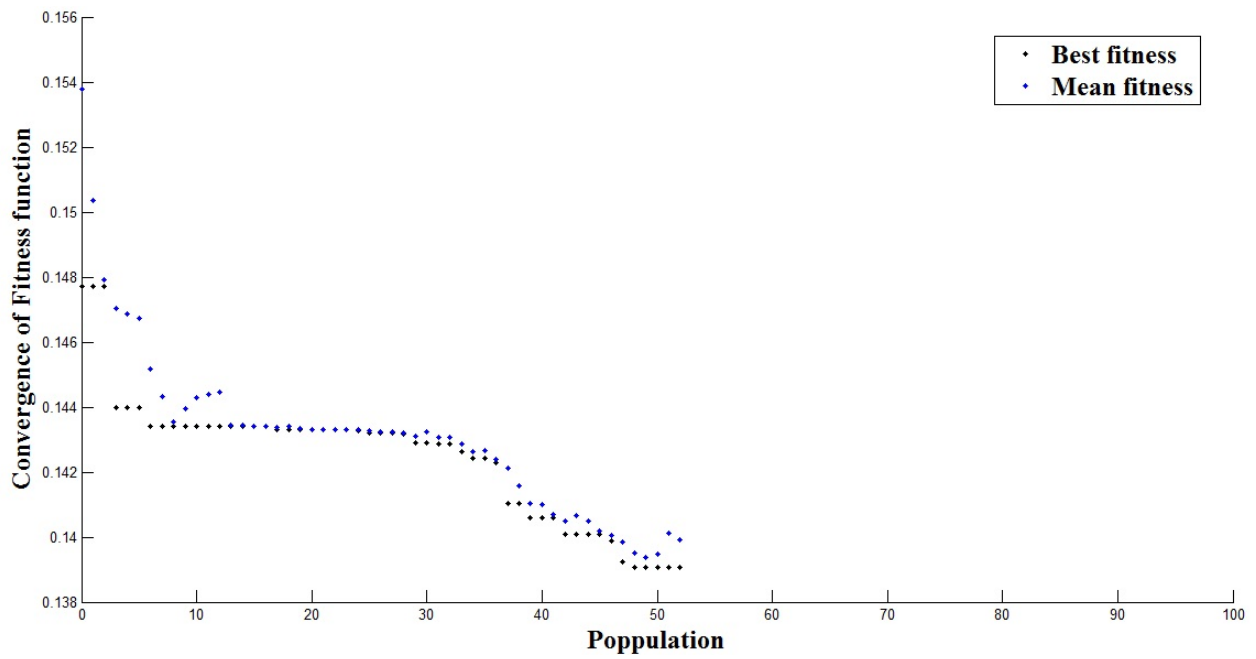


Figure 3.4: Numbers of population versus convergence of Fitness Function with TCSC at Normal Operating Condition

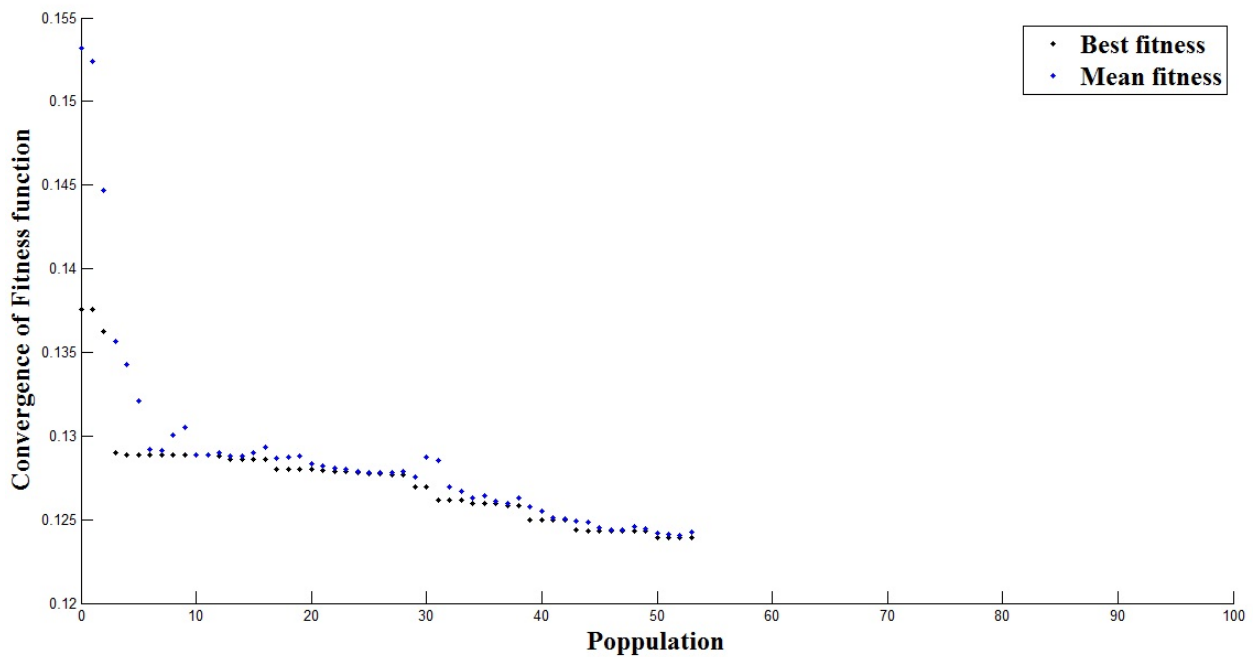


Figure 3.5: Numbers of population versus convergence of Fitness Function with PSS and TCSC at Normal Operating Condition

Table 3.12: Optimized Parameter of TCSC and PSS

Parameter	Operating Conditions			
	1	2	3	4
$K_C$	50.253	70.256	85.256	95.256
$T_{1T}$	0.1382	0.1464	0.1589	0.1682
$T_{2T}$	0.1091	0.1402	0.1358	2.1423
$T_{3T}$	0.1135	0.1235	0.1125	0.1323
$T_{4T}$	0.1645	0.1524	0.1687	2.1789
$K_{pss}$	4.562	4.691	4.962	5.232
$T_1$	0.97	1.089	1.83	2.111
$T_2$	0.994	0.849	2.419	2.821
$T_3$	0.633	0.362	0.432	0.523
$T_4$	0.0161	0.078	0.173	0.213

Table 3.13: Eigen values and Damping factor of PSS and TCSC

O.C.	TCSC		PSS and TCSC		
	eigen values	$\zeta$	eigen values	$\zeta$	
1	-68.6920	1.0000	-84.2000	1.0000	
	-16.9056 +15.2140i	0.7433	-66.3827	1.0000	
	-16.9056 -15.2140i	0.7433	-7.4441 +39.2017i	0.1866	
	<b>-2.7191 + 9.8082i</b>	<b>0.2671</b>	-7.4441 -39.2017i	0.1866	
	<b>-2.7191 - 9.8082i</b>	<b>0.2671</b>	-9.2578	1.0000	
	-9.4529	1.0000	<b>-2.1424 + 4.2892i</b>	<b>0.4469</b>	
	-4.9141	1.0000	<b>-2.1424 - 4.2892i</b>	<b>0.4469</b>	
	-3.0040	1.0000	-5.4183	1.0000	
	-0.1008	1.0000	-3.0116	1.0000	
			-0.9809	1.0000	
			-0.1068	1.0000	
			-0.0000	1.0000	
	2	-71.3735	1.0000	-71.7830	1.0000
		-17.8289 +12.4113i	0.8207	-36.0467	1.0000
-17.8289 -12.4113i		0.8207	-3.1731 +23.4427i	0.1341	
<b>-0.6254 +10.5403i</b>		<b>0.0592</b>	-3.1731 -23.4427i	0.1341	
<b>-0.6254 -10.5403i</b>		<b>0.0592</b>	<b>-3.0735 + 4.2816i</b>	<b>0.5832</b>	
-0.1003		1.0000	<b>-3.0735 - 4.2816i</b>	<b>0.5832</b>	
-3.3571		1.0000	-5.9775	1.0000	
-5.1883		1.0000	-6.9985	1.0000	
-6.9348		1.0000	-3.3244	1.0000	
			-1.1287	1.0000	
			-0.1088	1.0000	
			0.0000	-1.0000	

Table 3.14: Eigen values and Damping factor of PSS and TCSC....Contd...

3	-73.7957	1.0000	-73.9565	1.0000
	-18.9081 +13.5580i	0.8127	-20.7877	1.0000
	-18.9081 -13.5580i	0.8127	-1.9973 +12.6794i	0.1556
	<b>1.9050 + 9.1233i</b>	<b>-0.2044</b>	-1.9973 -12.6794i	0.1556
	<b>1.9050 - 9.1233i</b>	<b>-0.2044</b>	<b>-6.0822 + 4.1356i</b>	<b>0.8269</b>
	-0.0995	1.0000	<b>-6.0822 - 4.1356i</b>	<b>0.8269</b>
	-3.6162	1.0000	-8.8109	1.0000
	-5.0999	1.0000	-3.4876	1.0000
	-6.8422	1.0000	-5.9690	1.0000
			-0.3711	1.0000
			-0.1116	1.0000
			-0.0000	1.0000
4	-66.7339	1.0000	-66.7363	1.0000
	-20.8003 +20.5770i	0.7109	-14.5965 +16.0765i	0.6722
	-20.8003 -20.5770i	0.7109	-14.5965 -16.0765i	0.6722
	<b>0.5379 + 7.8571i</b>	<b>-0.0683</b>	<b>-3.7172 + 6.8400i</b>	<b>0.4775</b>
	<b>0.5379 - 7.8571i</b>	<b>-0.0683</b>	<b>-3.7172 - 6.8400i</b>	<b>0.4775</b>
	-2.8547	1.0000	-8.5977	1.0000
	-0.4421 + 0.1715i	0.9323	-2.8793	1.0000
	-0.4421 - 0.1715i	0.9323	-0.4277 + 0.1625i	0.9348
	-0.0962	1.0000	-0.4277 - 0.1625i	0.9348
			-0.3381	1.0000
			-0.1090	1.0000
			-0.0000	1.0000

The participation factor method is used for identification of eigen values and damping factor associated to electromechanical mode using TCSC and PSS-TCSC. Attention to Table 3.13, for all operating conditions, the damping factor of system has been improved with application of TCSC and PSS-TCSC. The eigen values and damping factors related to rotor mode shown by bold font in Table 3.13. With TCSC, for the two operating conditions the eigen values associated with rotor mode is negative and damping factor is positive. For remaining last two operating conditions, the eigen values associated with rotor mode is positive and damping factor are negative. With TCSC, the damping factor associated to rotor mode are 0.2671, 0.0592, -0.2044, -0.0683 for four operating conditions, while with simultaneous application of PSS and TCSC, damping factors associated to rotor mode are 0.4469, 0.5832, 0.8269, 0.4775 for four operating conditions. The application of PSS-TCSC,

significantly improved the eigen values, damping factors and reduced oscillatory frequency in rotor mode. The simultaneous application of PSS and TCSC have provided good stability to the system as eigen values and damping factors are improved compare to individual application of PSS and TCSC. The closed poles are very far away in the left half of the s-plane using PSS-TCSC compare to individual damping controller.

### 3.4 Non-linear Simulation

The nonlinear model of the power system has been used for the transient stability analysis of the SMIB system with generator attached PSS and transmission line connected TCSC. The initial conditions of the different variables are calculated using MATLAB programming. The non-linear simulation is carried out using non-linear dynamic model described by equations (2.6) to (2.11), which has been implemented using MATLAB/simulink environment. The detailed data of the power system used in this study is given by Appendix A. Comparison analysis between CPSS and PID-PSS, and individual and simultaneous application of TCSC and CPSS are carried out under different operating conditions, faults and disturbance. These disturbances are considered such as the three phase short circuit at sending end and middle of transmission line, outage of transmission line, suddenly changes in mechanical input and step changes in terminal voltage reference.

For case 1 to case 6, the time response of rotor speed deviation  $\omega_m$ (rad/sec), rotor angle  $\delta$  (degree), terminal voltage  $V_t$  (p.u.) and net line reactance  $X_{net}$  (p.u.) have been shown in figures. Without application of controllers, oscillations in rotor speed deviation have been observed, which shows the marginal stability and instability of the system. While PSS and TCSC have provided damping to the synchronous machine and have improved the power system stability. With application of damping controllers, the system becomes stable and different time response parameters have been improved.

### 3.4.1 Case I

Considering operating condition 1 as defined in table 3.1  $P_t = 0.6, Q_t = 0.0224$ . A three phase fault is created at 1s at the sending end of one the circuits of the transmission line and cleared after 100ms [33]. The original system restored after the fault clearance. The response of the rotor speed deviation between 0s to 10s with damping coefficient  $D = 0$  and without PSS and TCSC damping controllers has been shown in Figure 3.6. Figures 3.7, 3.8 and 3.9 have shown the response of speed deviation between 0s to 30s, 30s to 60s and 60s to 90s respectively with zero damping coefficient and without damping controllers. The transient response during faulted condition between 1s to 2s has been shown in Figure 3.10. The response of the  $\delta$  and  $\omega_m$  with presence of GA based CPSS and PID-PSS have been shown in Figure 3.11 and 3.12 respectively. The response of  $\omega_m$  and  $X_{net}$  with individual and simultaneously application of GA based TCSC and PSS have been shown in Figure 3.13 and 3.14 respectively. Figures 3.6, 3.7, 3.8 and 3.9 have shown that the oscillations in rotor speed deviation are growing. While using individual PSSs and TCSC and simultaneous application of GA based PSS-TCSC significantly diminished this oscillation in the system and provided very good damping characteristics.

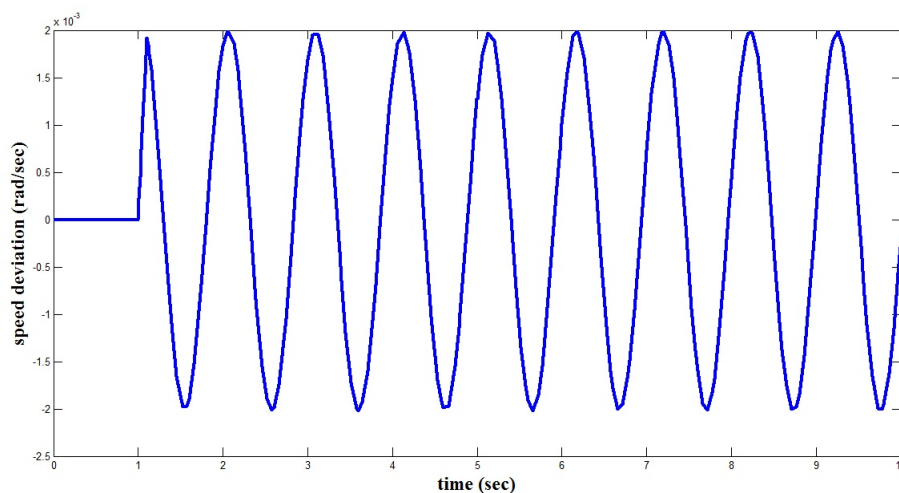


Figure 3.6: Case I: Speed deviation between 0s to 10s with damping coefficient  $D = 0$  and without controller (PSS and TCSC)

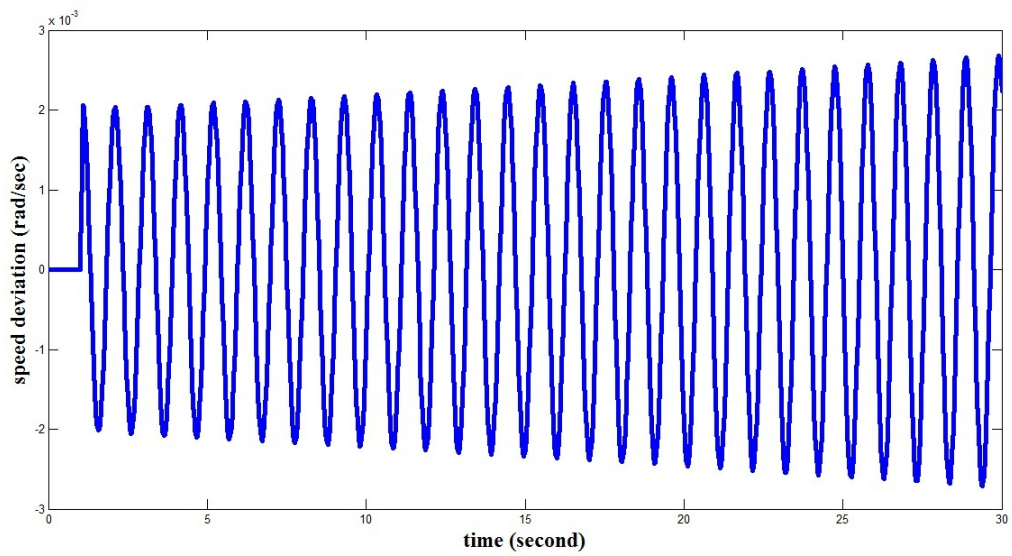


Figure 3.7: Case I : Speed deviation between 0s to 30s with damping coefficient  $D = 0$  and without controller (PSS and TCSC)

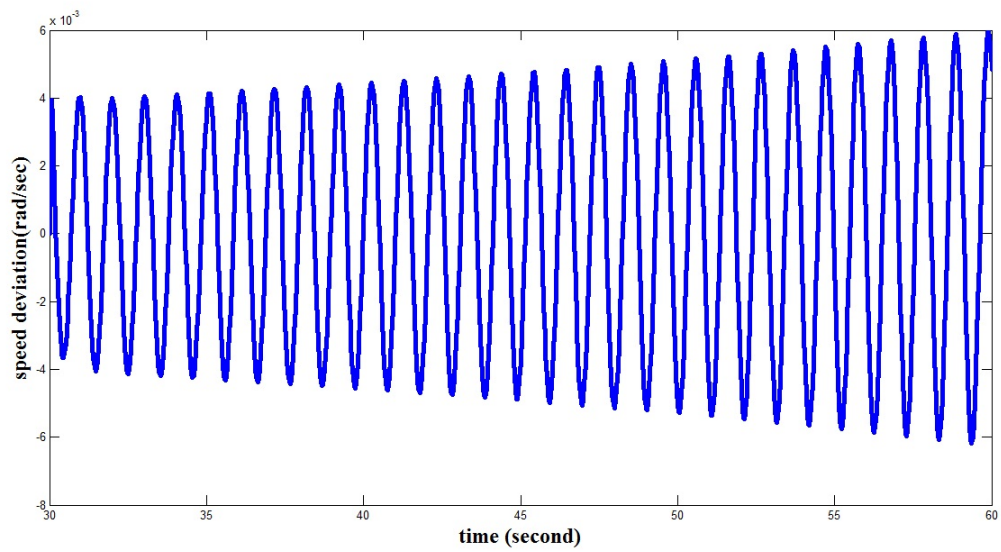


Figure 3.8: Case I : Speed deviation between 30s to 60s with damping coefficient  $D = 0$  and without controllers(PSS and TCSC)

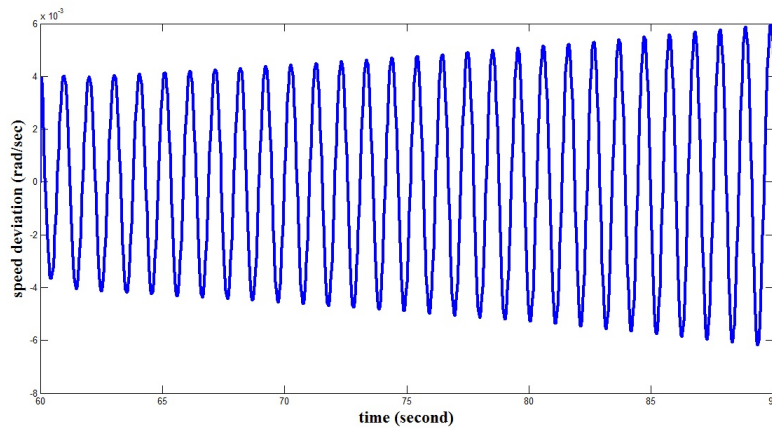


Figure 3.9: Case I : Speed deviation between 60s to 90s with damping coefficient  $D = 0$  and without controller (PSS and TCSC)

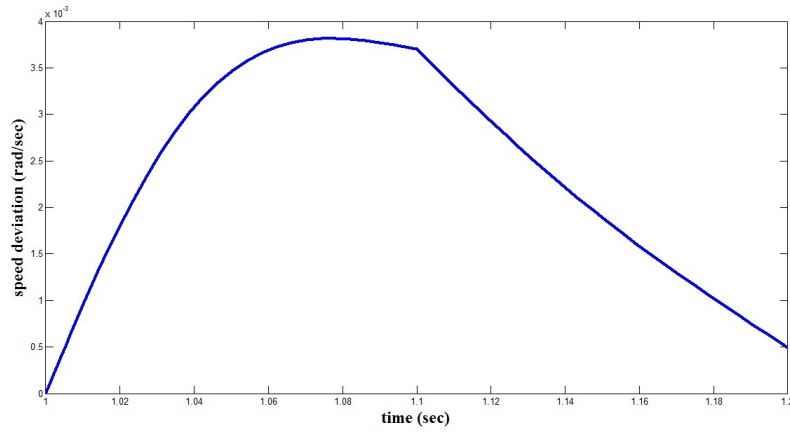


Figure 3.10: Case I : Speed deviation between 1s to 1.2s with zero damping coefficient  $D = 0$  and without controller(PSS and TCSC)

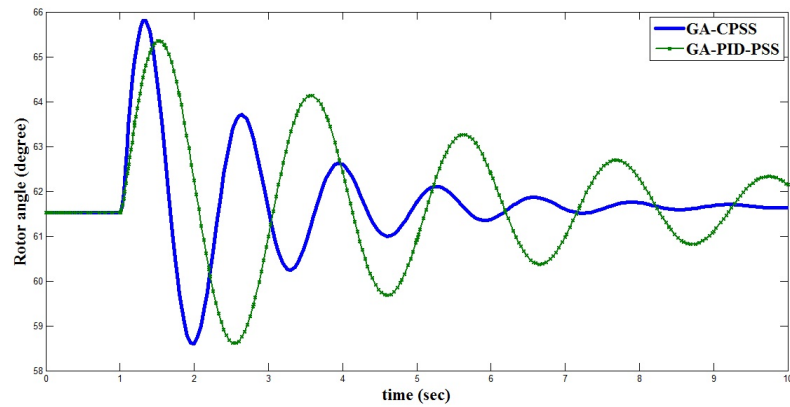


Figure 3.11: Case I: Rotor angle with GA based PSSs

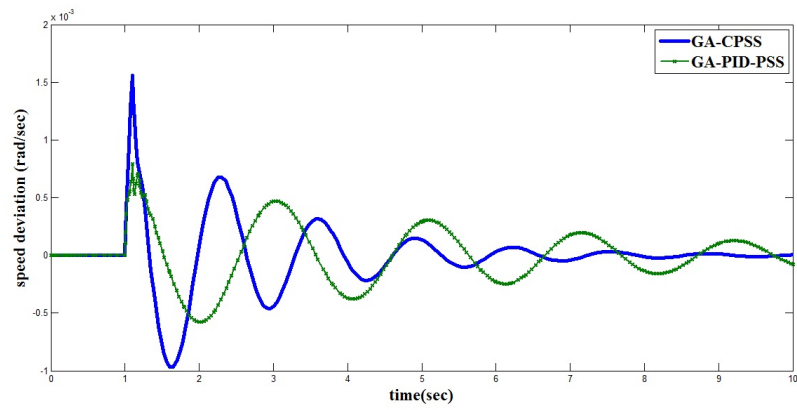


Figure 3.12: Case I: Speed deviation with GA based PSSs

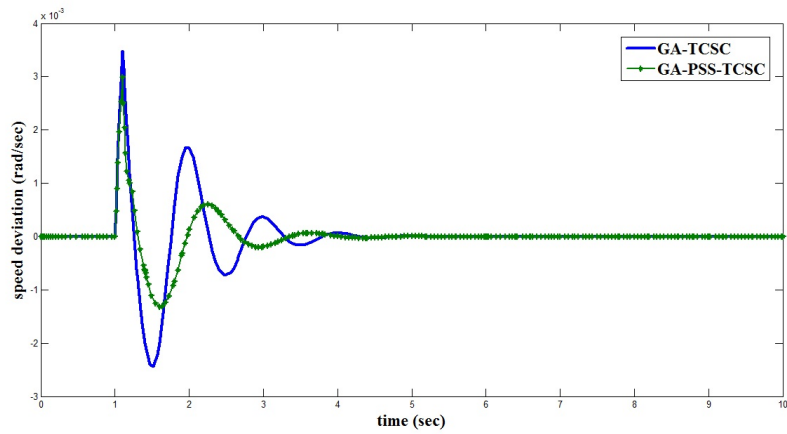


Figure 3.13: Case I: Speed deviation with GA based TCSC and PSS-TCSC

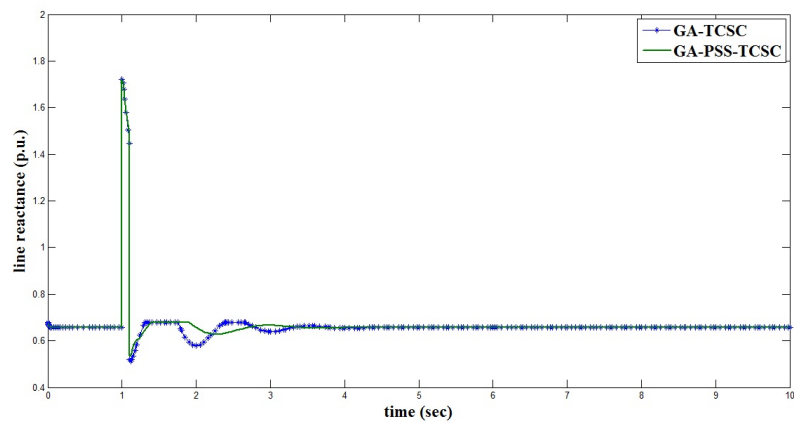


Figure 3.14: Case I: Line reactance with GA based TCSC and PSS-TCSC

### 3.4.2 Case II

$P_t = 0.6, Q_t = 0.0224$ , A three phase fault is created at 1s at the middle of one transmission line and cleared after 50 ms by the disconnection of the faulted line, and then successfully reclosed at 5s [71]. Figure 3.15 shows the response of the rotor speed deviation with damping coefficient  $D = 0$  and without PSS and TCSC damping controllers. The response of the  $\delta$  and  $\omega_m$  with the presence of GA based CPSS and PID-PSS have been shown in Figure 3.16 and 3.17 respectively. The response of  $\omega_m$  with individual and simultaneously application of GA based TCSC and PSS has been shown in Figure 3.18. Without application of damping controllers, the oscillations in speed deviation have been observed. These oscillations are continuous growing, which shows instability of system after 10s. While using the individual PSSs and TCSC and simultaneous application of GA based PSS-TCSC significantly diminished this oscillations and improved stability of the system.

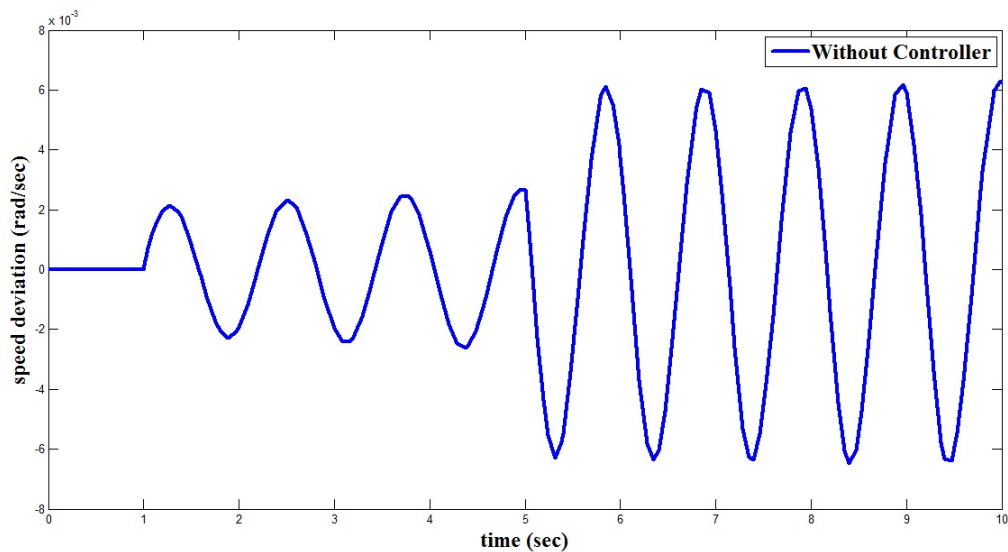


Figure 3.15: Case II: Speed deviation with damping coefficient  $D = 0$  and without controller (PSS and TCSC)

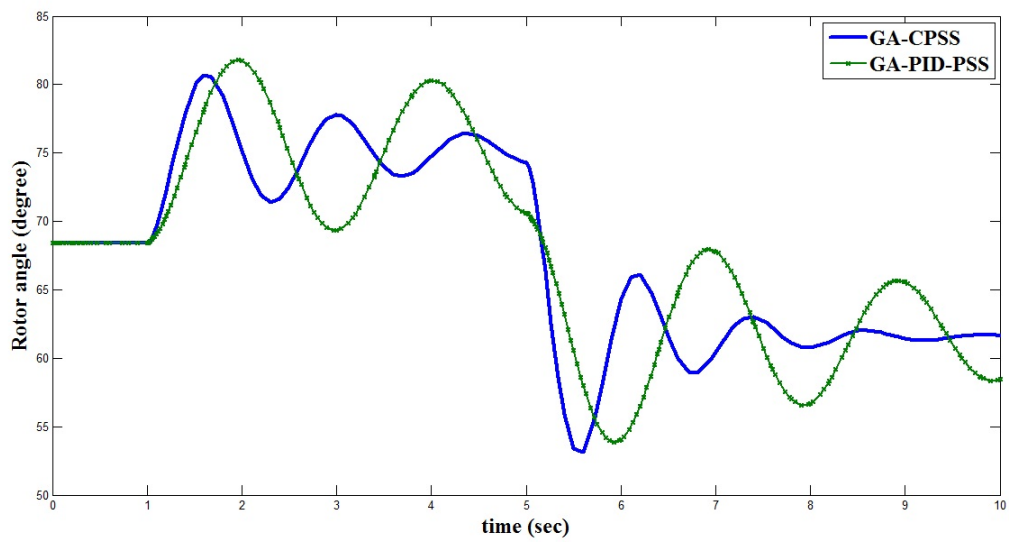


Figure 3.16: Case II: Rotor angle with GA based PSSs

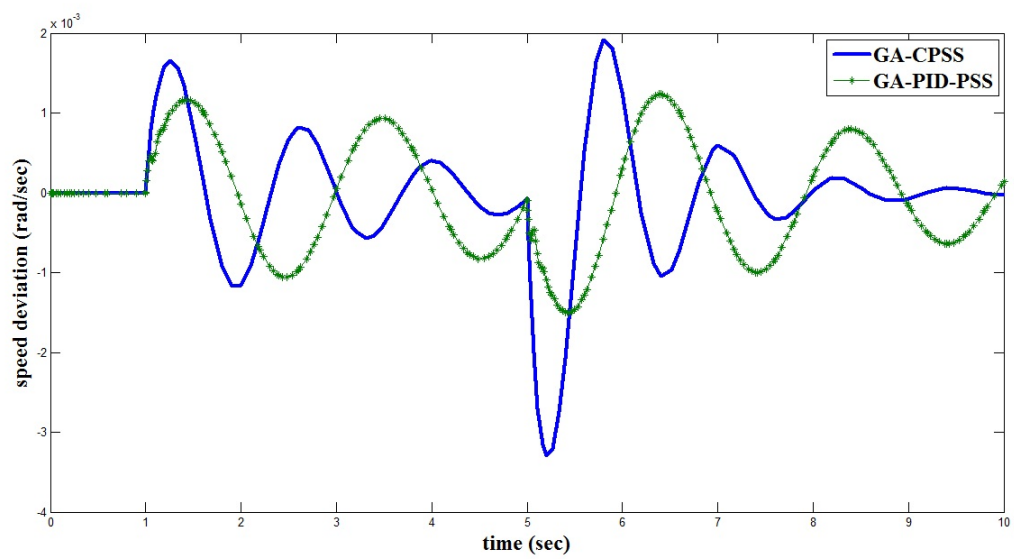


Figure 3.17: Case II: Speed deviation with GA based PSSs

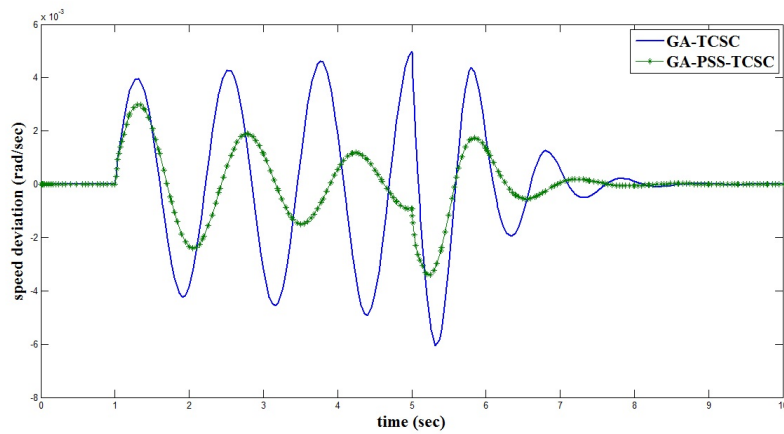


Figure 3.18: Case II: Speed deviation with GA based TCSC and PSS-TCSC

### 3.4.3 Case III

$P_t = 0.9, Q_t = 0.12$ , Here heavy loading condition is considered. A three phase fault is created at 1s at the sending end of one of the circuits of the transmission line and cleared after 50ms. Figures 3.19, 3.20, 3.21 and 3.22 have shown the response of speed deviation between 1s to 1.2s, 1s to 2s, 2s to 7s and 0s to 10s respectively with damping coefficient  $D = 0$  and without damping controllers. Under heavy loading condition, the system lost its stability very quickly and system became unstable. Figure 3.23 shows the response of the  $\omega_m$  with the presence of GA based CPSS and PID-PSS. Figure 3.24 shows the response of  $\omega_m$  with individual and simultaneous application of GA based TCSC and PSS. While using individual GA based PSSs and TCSC and simultaneous application of GA based PSS-TCSC provided excellent damping characteristics.

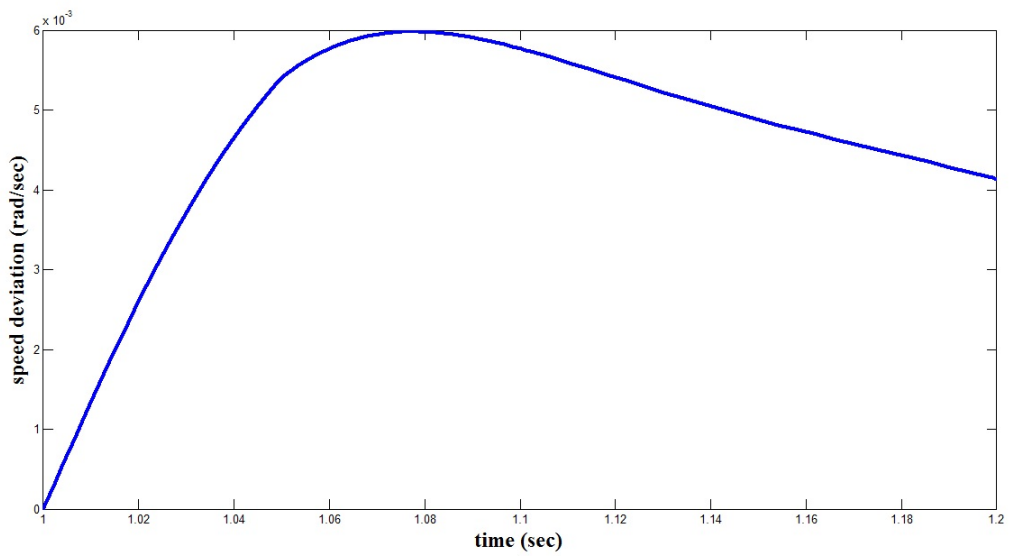


Figure 3.19: Case III : Speed deviation between 1s to 1.2s with damping coefficient  $D = 0$  and without controller(PSS and TCSC)

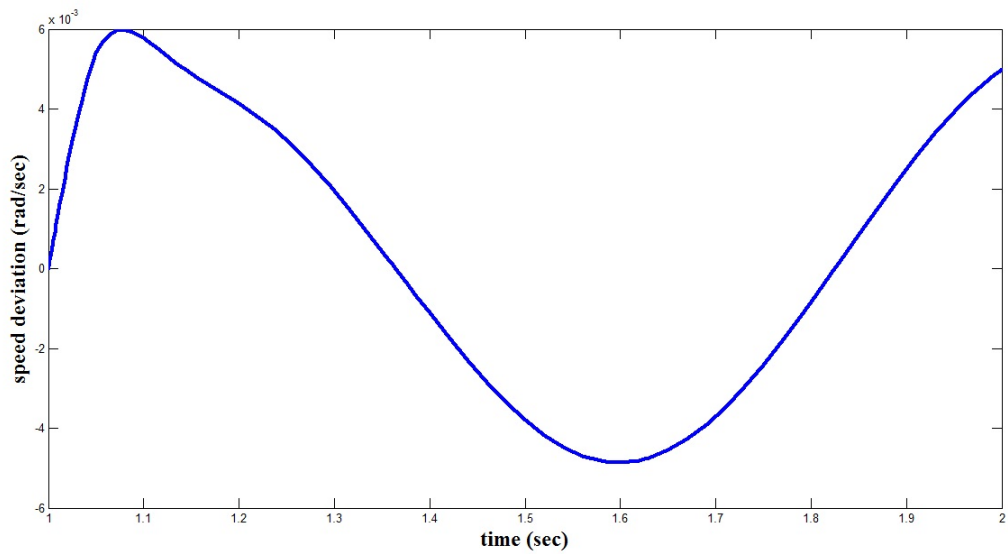


Figure 3.20: Case III : Speed deviation between 1s to 2s with damping coefficient  $D = 0$  and without controllers (PSS and TCSC)

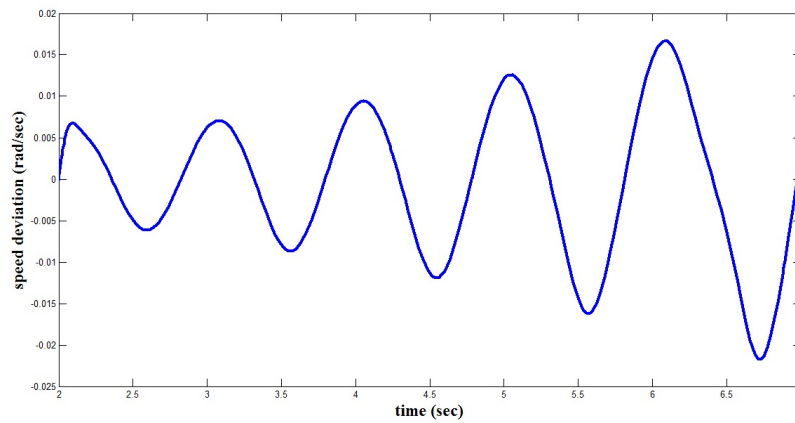


Figure 3.21: Case III : Speed deviation between 2s to 7s with damping coefficient  $D = 0$  and without controller(PSS and TCSC)

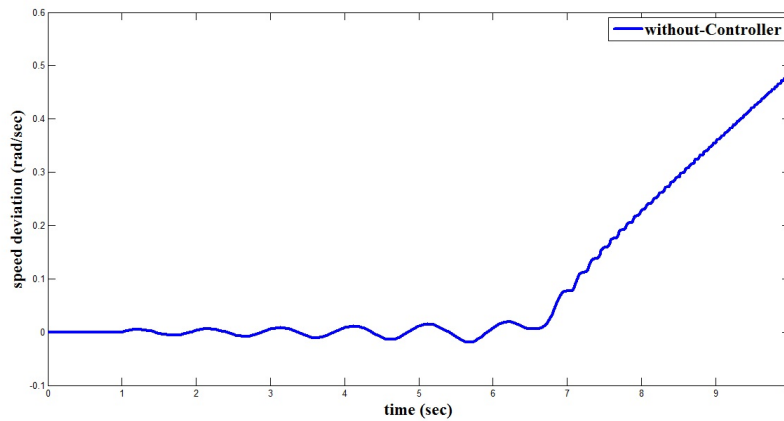


Figure 3.22: Case III: Speed deviation between 0s to 10s with damping coefficient  $D = 0$  and without controller (PSS and TCSC)

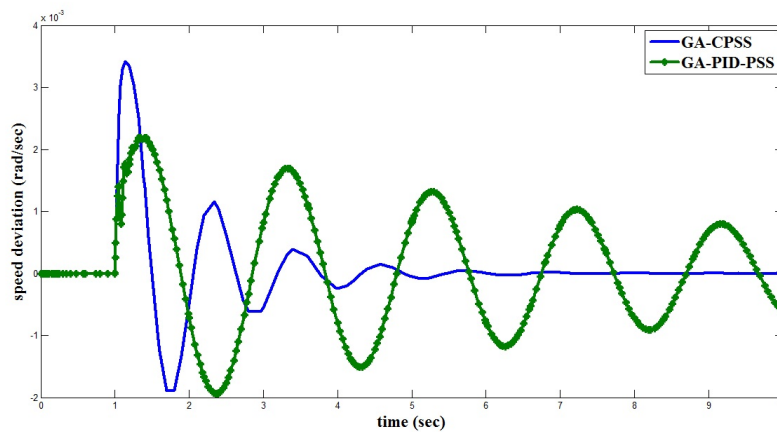


Figure 3.23: Case III: Speed deviation with GA based PSSs

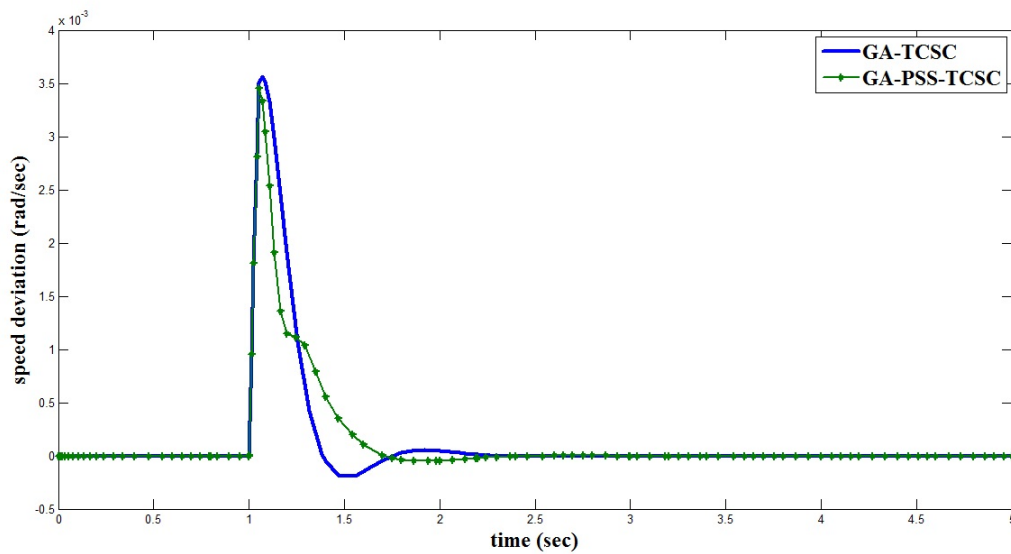


Figure 3.24: Case III: Speed deviation with GA based TCSC and PSS-TCSC

### 3.4.4 Case IV

$P_t = 0.9, Q_t = 0.12$ , Under the heavy loading condition, a 10% mechanical change applied at 1s and removed at 5s is considered. The response of rotor speed deviation between 1s to 4s and 0s to 10s has been shown in Figure 3.25 and Figure 3.26 respectively with damping coefficient  $D = 0$  and without application of PSS and TCSC damping controllers. The system lost its stability at 4s which has been shown by Figure 3.26. The response of the  $\omega_m$  with the presence of GA based CPSS and PID-PSS has been shown in Figure 3.27. The response of  $\omega_m$  with individual and simultaneously application of GA based TCSC and PSS has been shown in Figure 3.28. Variations in the speed response are observed at 1s and 5s with controllers because mechanical change is applied at same instant. The simultaneous application of PSS and TCSC has been provided very good stability to system compared to individual application of PSS and TCSC.

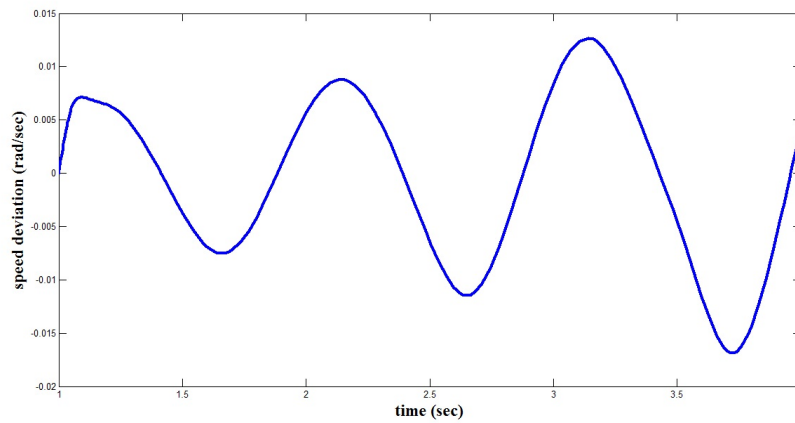


Figure 3.25: Case IV: Speed deviation between 1s to 4s with damping coefficient  $D = 0$  and without controller (PSS and TCSC)

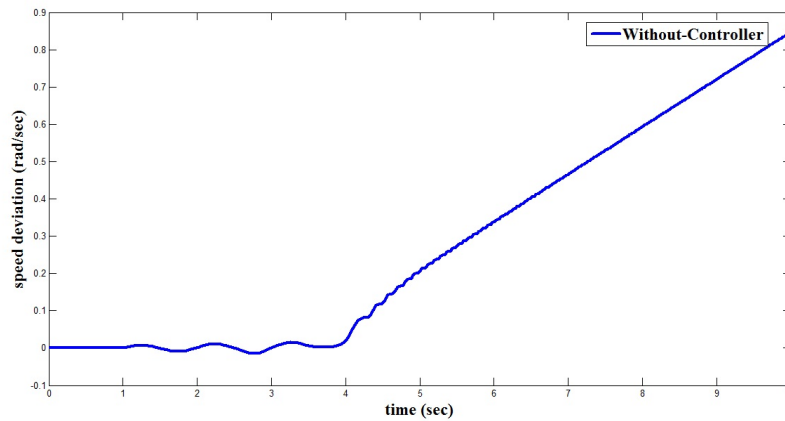


Figure 3.26: Case IV: Speed deviation between 0s to 10s with damping coefficient  $D = 0$  and without controller (PSS and TCSC)

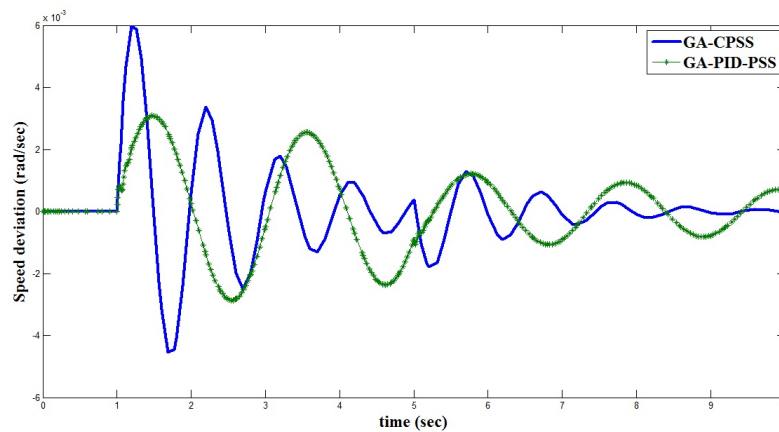


Figure 3.27: Case IV: Speed deviation with GA based PSSs

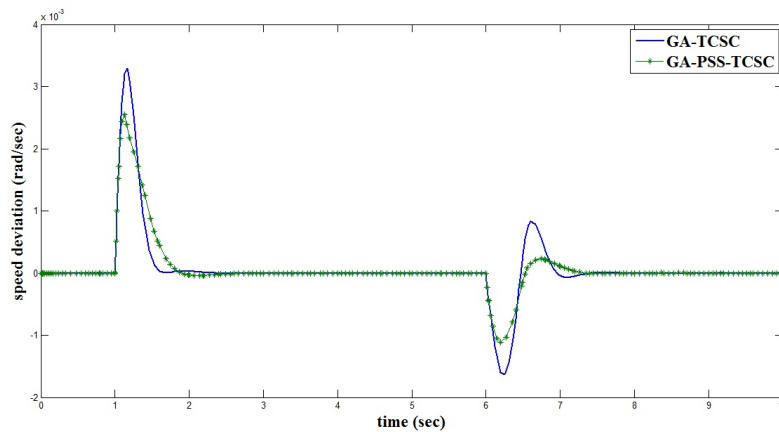


Figure 3.28: Case IV: Speed deviation with GA based TCSC and PSS-TCSC

### 3.4.5 Case V

$P_t = 1.2, Q_t = 0.2$ , Under very heavy loading condition, a 10% input terminal voltage applied at 1s and removed at 5s is considered. The response of the rotor speed deviation with damping coefficient  $D = 0$  without controllers has been shown in Figure 3.29 and Figure 3.30. Under heavy loading condition, the system lost its stability very quickly and system became unstable. Figure 3.31 shows the response of the  $\omega_m$  with the presence of GA based CPSS and PID-PSS. Figure 3.32 shows that the system lost its stability using the individual application of TCSC with continuous growing of oscillation, while simultaneous application of GA based TCSC and PSS provides stability to system.

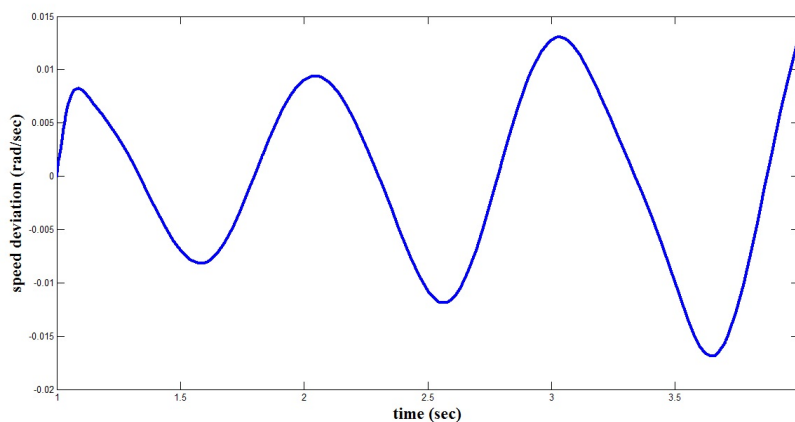


Figure 3.29: Case V: Speed deviation between 1s to 4s with damping coefficient  $D = 0$  and without controller (PSS and TCSC)

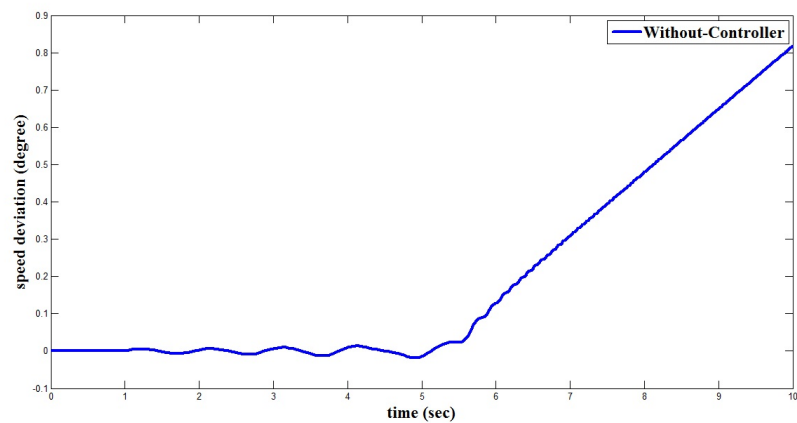


Figure 3.30: Case V: Speed response between 0s to 10s with damping coefficient  $D = 0$  and without controller (PSS and TCSC)

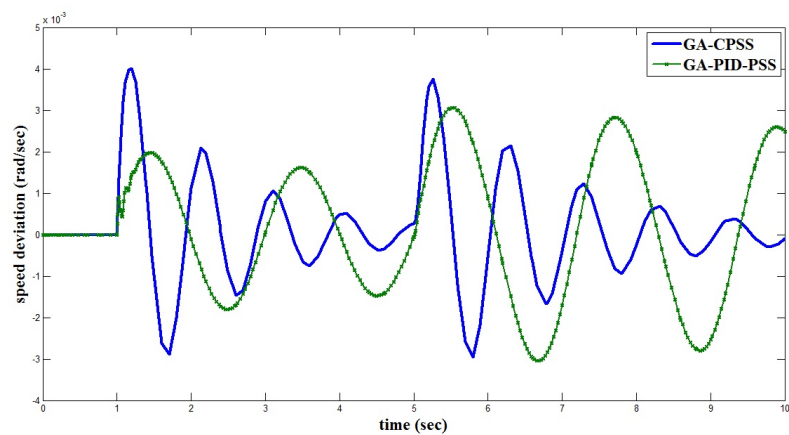


Figure 3.31: Case V: Speed deviation with GA based PSSs

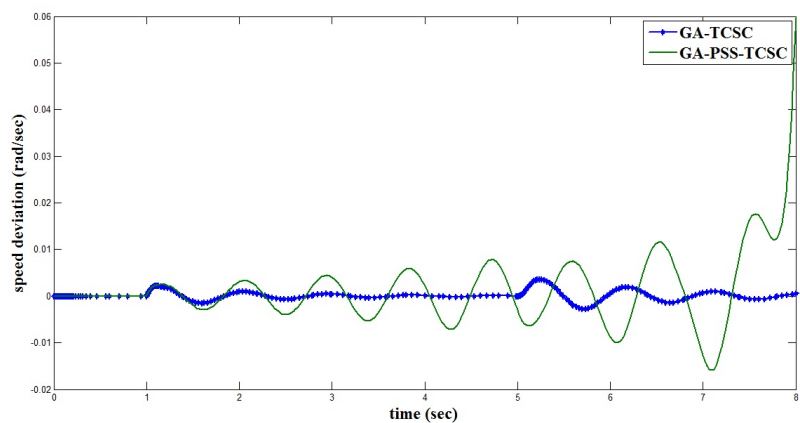


Figure 3.32: Case V: Speed deviation with GA based PSS and PSS-TCSC

### 3.4.6 Case VI

$P_t = 0.75, Q_t = 0.1$ , In this case another severe disturbance is considered. One of the transmission lines is permanently tripped at 1s. The transmission line reactance is suddenly increased and system lost its stability very rapidly. The response of the rotor speed deviation with damping coefficient  $D = 0$  and without controllers has been shown in Figure 3.33 and Figure 3.34. The response of the  $\delta$  and  $\omega_m$  with the presence of GA based CPSS and PID-PSS have been shown in Figure 3.35 and 3.36 respectively. The response of  $\omega_m$  with individual and simultaneous application of GA based TCSC and PSS has been shown in Figure 3.37.

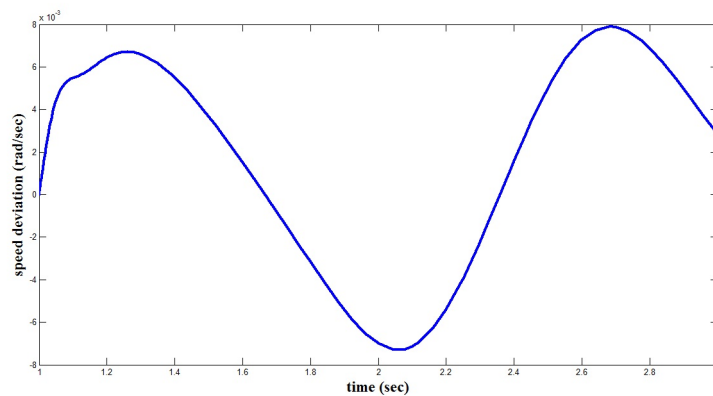


Figure 3.33: Case VI: Speed deviation between 1s to 3s with damping coefficient  $D = 0$  and without controller (PSS and TCSC)

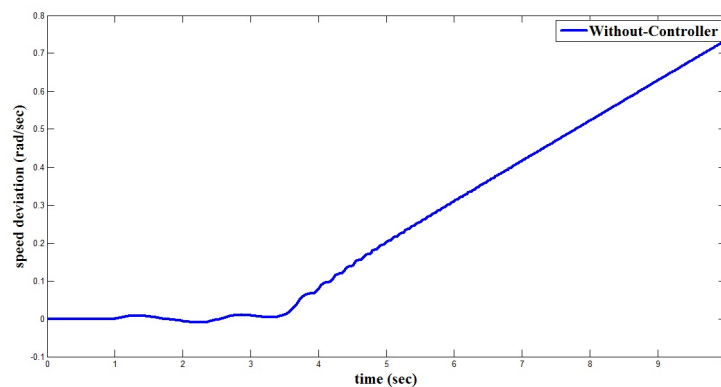


Figure 3.34: Case VI: Speed deviation between 0s to 10s with damping coefficient  $D = 0$  and without controller (PSS and TCSC)

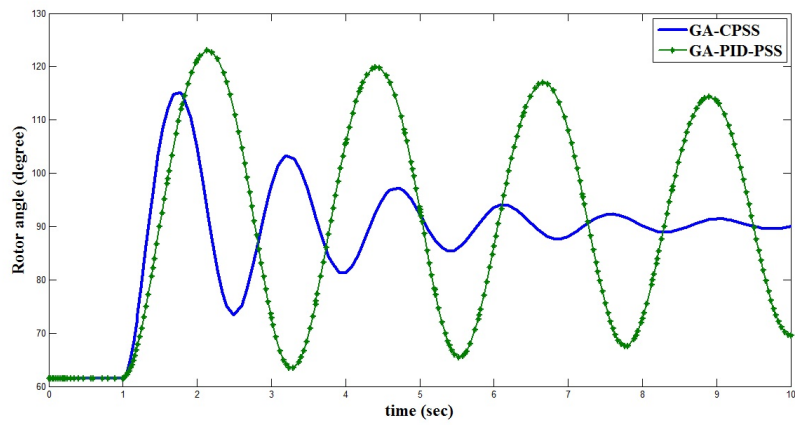


Figure 3.35: Case VI: Rotor angle with GA based PSSs

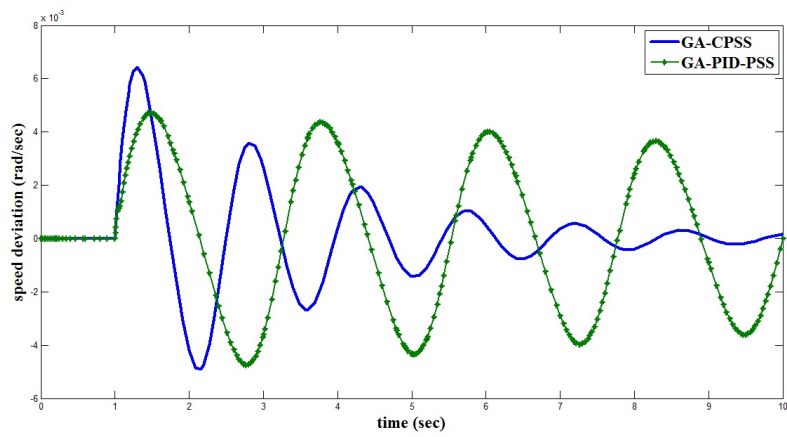


Figure 3.36: Case VI: Speed deviation with GA based PSSs

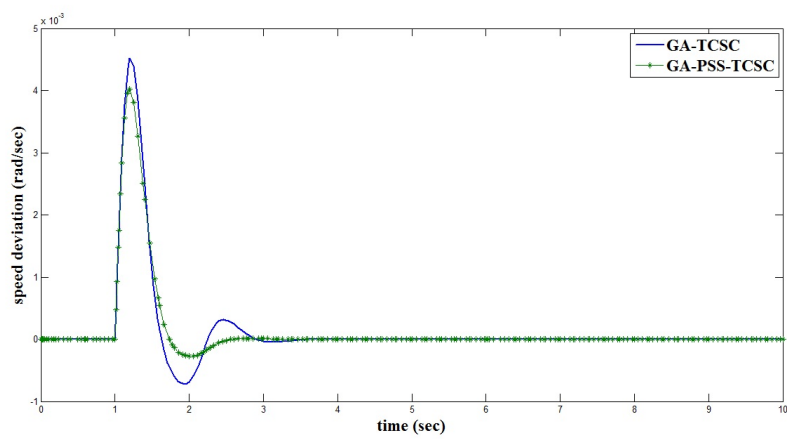


Figure 3.37: Case VI: Speed deviation with GA based PSS and PSS-TCSC

### 3.5 Conclusion

In this study, Genetic Algorithm based control strategies have been developed for designing of PSSs and TCSC damping controller. The PSSs and simultaneous designed TCSC and PSS have been applied to the dynamical power system. The small signal stability analysis and non-linear simulation for the transient stability analysis have been carried out for detailed investigation of the power system stability issue. Four different operating conditions have been taken and the responses of the rotor angle, rotor speed deviation, terminal voltage and net reactance have been analyzed under different types of the disturbances and faults.

It has been shown that the eigen values associated to the electromechanical mode are more negative with presence of CPSS and PID-PSS in power system and poles in s-plane are far away from origin. The damping factor has been improved with PSSs compare to the without PSSs, which shown that the system is more stable and PSSs have been provided good damping to oscillation in power system. It has been also observed that with the simultaneous application of PSS and TCSC in power system, the eigen values are more negative and damping factor has been improved significantly, which shows good stability of system compare to the individual application of PSS and TCSC.

From the non - linear analysis, without the application of the controllers in the system, the oscillations in rotor angle, rotor speed deviation have been observed. Under the heavy loading conditions, it has been cleared that if the active power and reactive power are increased, the oscillation in rotor angle and speed deviation are continuously growing which creates the instability of the system under the contingencies. The simultaneously designed TCSC and PSS damping controller have been significantly diminished oscillations in system. Simultaneously application of TCSC and PSS have been provided very good damping characteristics compare to the individual application of PSSs or TCSC and almost eliminate the oscillations in system. Application of GA based TCSC and PSSs have improved the time response parameters such as settling time, rise time and delay time appreciably and also decreased the overshoot in the system.

# Chapter 4

## Design of PSS and TCSC Using ANFIS and ANN

### 4.1 Introduction

The Adaptive Neuro-Fuzzy Inference System and Levenberg-Marquardt Artificial Neural Network algorithm for the development of the control strategy for thyristor control series capacitor based damping controller and power system stabilizer has been discussed in this chapter. In order to achieve the appreciable damping, the series capacitor has been suggested in addition to power system stabilizer. The non-linear simulations of single machine infinite bus system (SMIB) have been carried out using individual and simultaneous application of PSS and TCSC. The comparison between intelligent control strategies based damping controllers has been carried out. The results have shown efficacy and capability of proposed control schemes under the various operating conditions, disturbances and fault conditions, and also have demonstrated the improvement in the dynamic performance of the system with proposed control algorithm.

## 4.2 Adaptive Neuro-Fuzzy Inference System (ANFIS)

Combining the learning power of neural network with knowledge representation of Fuzzy logic gives a Neuro-Fuzzy system. It gives the advantage of neural networks as well as of fuzzy logic system and it removes the individual disadvantages by combining them on the common features. Fuzzy logic has tolerance for imprecision of data, while neural networks have tolerance for noisy data. Fuzzy logic provides a structure within which the learning ability of neural networks is employed and neural network can be used to generate the membership functions for a fuzzy system and to tune them. There are two ways of hybridization; one is to endow NNs with fuzzy capabilities, thereby increasing the network's expressiveness and flexibility to adapt to uncertain environment. The second aspect is to apply neuronal learning capabilities to fuzzy system to make the fuzzy systems more adaptive to changing environment.

### 4.2.1 ANFIS- Architecture

It is assumed that the fuzzy inference system under consideration has two inputs  $x$  and  $y$  and one output  $z$ . For a first order Sugeno fuzzy model, a common rule set with two fuzzy if-then rules is the following:

Rule 1: If  $x$  is  $A_1$  and  $y$  is  $B_1$  then  $f_1 = p_1x + q_1y + r_1$

Rule 2: If  $x$  is  $A_2$  and  $y$  is  $B_2$  then  $f_2 = p_2x + q_2y + r_2$

The reasoning mechanism for the Sugeno model has been shown in Figure 4.1 and corresponding equivalent ANFIS architecture has been shown in Figure 4.2. The ANFIS algorithm has been described in literature [13, 87].

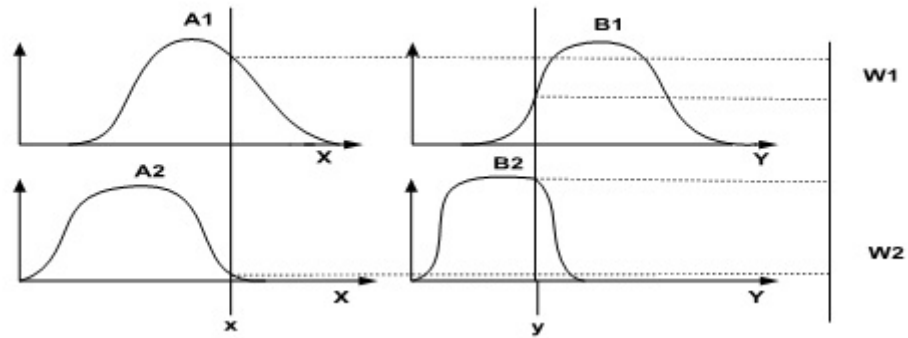


Figure 4.1: Takagi-Sugeno Fuzzy Model

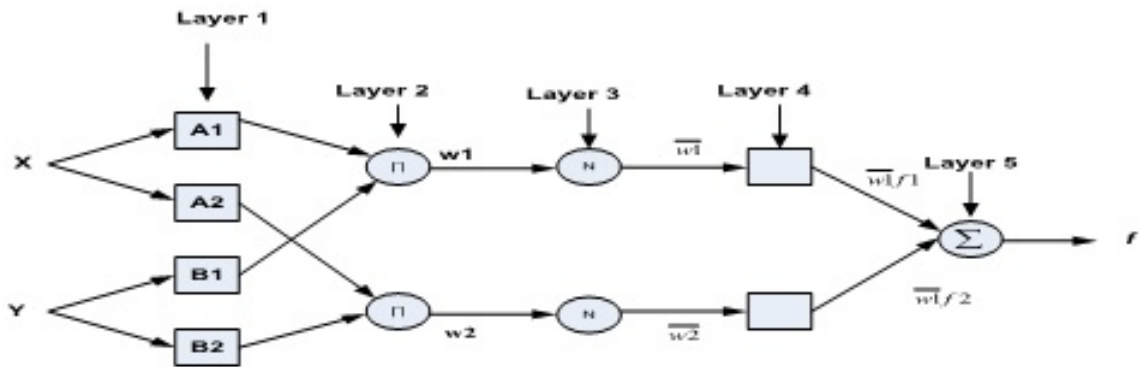


Figure 4.2: Adaptive Neuro Fuzzy Architecture

Layer 1: Every node  $i$  in this layer is an adaptive node with a node function

$$O_{1,i} = \mu A_i(x), \text{ for } i = 1, 2 \text{ or}$$

$$O_{1,i} = \mu B_{i-2}(y), \text{ for } i = 3, 4$$

Where  $x$  (or  $y$ ) is the input to node  $A_i$  (or  $B_{i-2}$ ) is a linguistic label associated with this node. Here the membership functions of  $A$  can be appropriate parameterized membership function such as generalized bell function:

$$\mu_{A(x)} = \frac{1}{1 + \left| \frac{x-c_i}{a_i} \right|^{2b}} \tag{4.1}$$

Where  $\{a_i, b_i, c_i\}$  is the parameter set. As the values of these parameters change, the bell-shaped function varies accordingly, thus exhibiting various forms of membership functions for fuzzy set  $A$ . Parameters in this layer are referred to as premise parameters.

Layer 2: Every node in this layer is a fixed node labeled  $II$ , whose output is the product of all the incoming signals:

$$O_{2,i} = w_i = \mu_{A_i}(x)\mu_{B_i}(y), \quad i = 1, 2. \quad (4.2)$$

Each node output represents the firing strength of a rule. In general, any other T-norm operators that perform fuzzy AND can be used as the node function in this layer.

Layer 3: Every node in this layer is a fixed node labeled  $N$ . The  $i$ th node calculates the ratio of the  $i$ th rule's firing strength to the sum of all rules's firing strengths:

$$O_{3,i} = \bar{w}_i = \frac{w_i}{w_1 + w_2}, \quad i = 1, 2. \quad (4.3)$$

Outputs of this layer are called normalized firing strengths.

Layer 4: Every node  $i$  in this layer is an adaptive node with a node function:

$$O_{4,i} = \bar{w}_i f_i = \bar{w}_i(p_i x + q_i y + r_i) \quad (4.4)$$

Where  $(\bar{w}_i)$  is a normalized firing strength from layer 3 and  $\{p_i, q_i, r_i\}$  is the parameter set of this node. Parameters in this layer are referred to as consequent parameters.

Layer 5: The single node in this layer is a fixed node labeled  $\Sigma$ , which computes the overall output and the summation of all incoming signals :

$$O_{5,i} = \sum_i \bar{w}_i f_i = \frac{\sum_i w_i f_i}{\sum_i w_i} \quad (4.5)$$

From the ANFIS architecture as shown in Figure 4.2, we observe that when the values of the premise parameters are fixed, the overall output can be expressed as a linear combination of the consequent parameters. The output  $f$  in Figure 4.1 can be expressed as below:

$$\begin{aligned} f &= \frac{w_1}{w_1 + w_2} f_1 + \frac{w_2}{w_1 + w_2} f_2 \\ &= \bar{w}_1(p_1 x + q_1 y + r_1) + \bar{w}_2(p_2 x + q_2 y + r_2) \\ &= (\bar{w}_1 x)p_1 + (\bar{w}_1 y)q_1 + \bar{w}_1 r_1 + (\bar{w}_2 x)p_2 + (\bar{w}_2 y)q_2 + \bar{w}_2 r_2 \end{aligned} \quad (4.6)$$

### 4.3 Steps for Designing of ANFIS based PSS and TCSC

1. To generate the input data pattern and corresponding the target data pattern.
2. To develop the fuzzy inference system (FIS).
3. To select the number and type of the membership functions.
4. Application of rules extracted algorithm to initialize the rules of FIS.
5. Training of the FIS using learning algorithm such as hybrid learning or backpropagation learning algorithm [87, 13].
6. Testing of FIS through testing data.
7. If desired solution is achieved then stop training, else to change the fuzzy membership functions, fuzzy membership function types, change the rules extracted algorithm, FIS learning algorithm, no. of epochs, error tolerance and repeat the algorithm from the step 2.
8. Implementation of ANFIS in real system and compute the output of the system.

#### 4.3.1 ANFIS-Power System Stabilizer

In this work, CPSS is replaced by the ANFIS based PSS. The mathematical model of the CPSS has been used for the generation of the training data for the ANFIS. The Takagi-Sugeno FIS [87] is used for the design of ANFIS based PSS. Sugeno has high computational efficiency and it works well with optimization and adaptive techniques [89, 90]. The network has been trained using 2000 sample training data, which are generated under the consideration of the different operating conditions and dynamic behavior of the power system. The two inputs and one output have been used for the training of ANFIS. The dynamic inputs are speed  $\Delta\omega_m(t)$  and change in speed ( $\frac{\Delta d\omega_m(t)}{dt}$ ) and corresponding  $\Delta V_{pss}$  has been selected

as output value of the ANFIS. Figure 4.3 shows the fuzzy logic controller (FLC) based PSS with inputs and output.

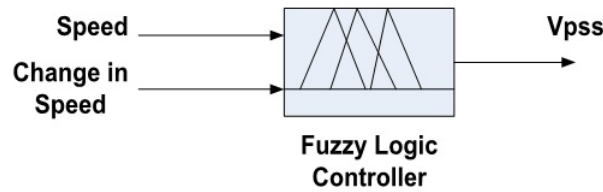


Figure 4.3: Fuzzy Logic Control based PSS

Generally gbell and gauss types membership functions (MFs) are preferable for ANFIS controller. No any convention for selection of type of MFs. The general rule is to produce a satisfactory response of the system with ANFIS controller in minimum time and also to obtain minimization of error with minimum ANFIS training parameters. The selection of number of membership function such that less number of membership function produce satisfactory response of the system. Consequently memory utilization should be reduced and ANFIS controller should produce quick response in less time. Table 4.1 shows the generating error after the execution of PSS-ANFIS structure with inputs and output data. Here four types of membership functions such that gbell, gauss, gauss2 and dsig are selected with different number of rules for designing of inputs and output variables of ANFIS controller. The triangle and trapezoidal membership functions are not suitable for ANFIS structure. Normally they are used for design of fuzzy logic controller based system. For two inputs, 3, 4, 5 and 7 variables are selected and corresponding 9, 16, 25 and 49 rules are developed. Here forty nine rules based structure of the PSS-ANFIS controller is not preferable as it takes high computational time for the execution compared to the other ANFIS structures. The best ANFIS-PSS structure has been selected after the testing with real power system. The gbell type four membership functions are selected and total sixteen rules are developed for inputs and output.

Speed signal range is selected between -0.002527 to 0.003344 and change in speed signal -0.06441 to 0.1094 for defining the inputs membership functions. The output membership

functions are varied between -0.09217 to 0.1112. Figure 4.4 represents the ANFIS-PSS structure with inputs and output. Figure 4.5 and 4.6 have represented gbell type four linguistic membership functions. Figure 4.7 shows the decision surface viewer of inputs and output of the PSS.

For initializing of FIS rules, the grid partition method has been used and the initial rules are extracted. The hybrid learning algorithm has been used for training to modify FIS parameters after obtaining the application of grid partition method. The hybrid algorithm combines the least square and backpropagation gradient descent algorithm. In the hybrid algorithm [87], as shown in Figure 4.2, the node outputs go forward until layer 4 and consequence parameters are estimated by least-squares method. In the backward phase, the error signals propagate backward and the algorithm iteratively learns the premise parameters by gradient descent. The training is continued until the error becomes constant. 10 numbers of epochs are selected for training of ANFIS based PSS. The numbers of epochs are selected such that expected goal may be achieved with minimum value of error. After the 10 number of iteration, the error between actual output and ANFIS output is minimized. The training is continued until the desired error becomes constant. The training is completed when the constant error 0.00248381 has been reached.

Table 4.1: Membership Function of ANFIS-PSS

No.of Rules	Type of Membership Functions			
	gbell	gauss	gauss2	dsig
	Error			
9	0.00305385	0.00295805	0.00265287	0.00287214
16	0.00248381	0.00303126	0.00298624	0.00320831
25	0.00325109	0.00285967	0.00240166	0.00406903
49	0.0016727	0.00158654	0.00207032	0.0033497

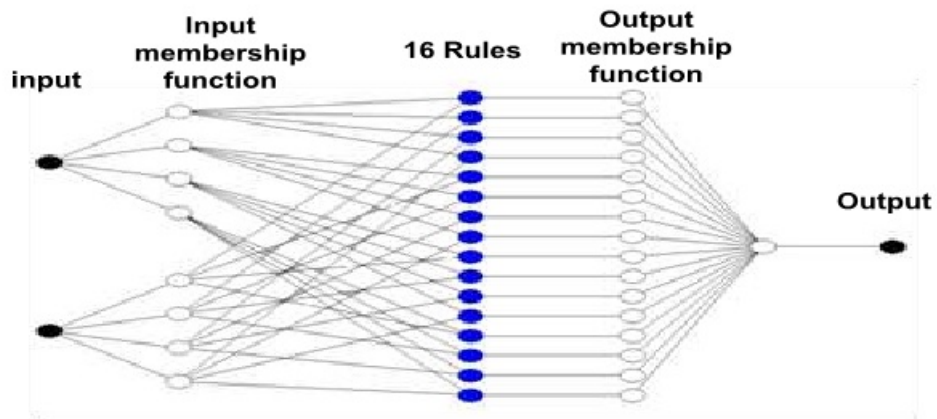


Figure 4.4: ANFIS-PSS Structure

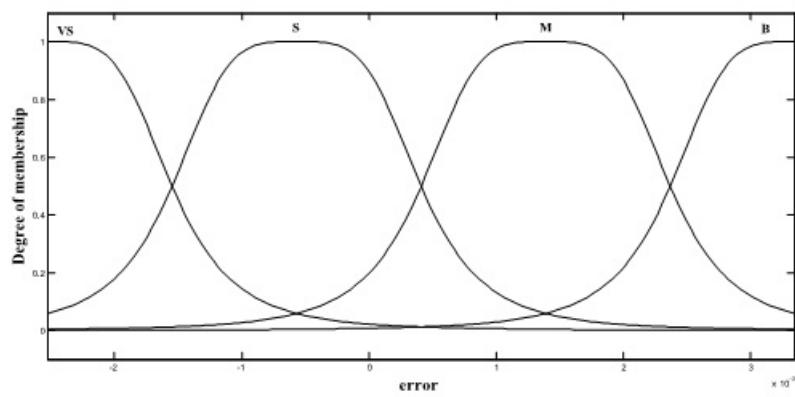


Figure 4.5: Membership Functions of Speed (Input :1)-PSS

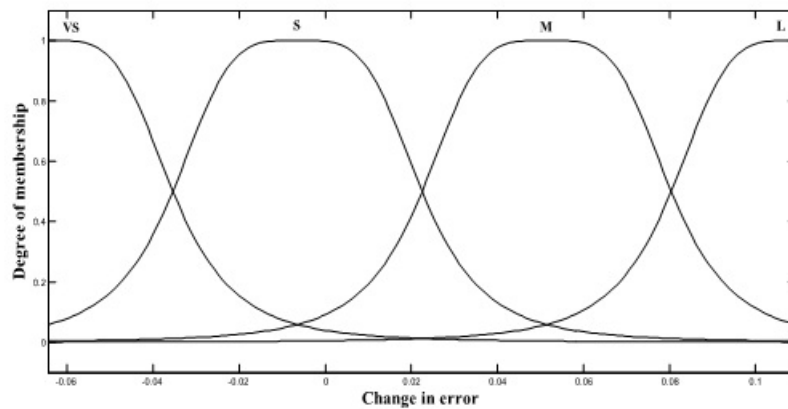


Figure 4.6: Membership Functions of Change in Speed (Input :2)-PSS

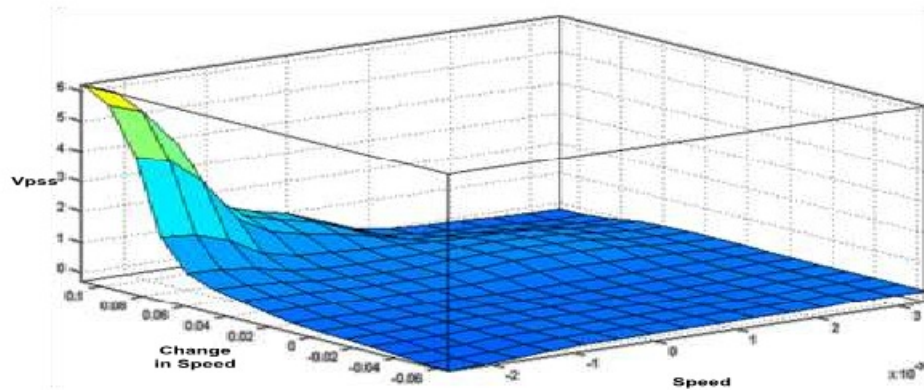


Figure 4.7: Decision-Surface Viewer of PSS

### 4.3.2 ANFIS-Thyristor Control Series Capacitor

Here, the stability control loop of the TCSC has been designed and replaced by sugeno ANFIS. The stability control loop of the TCSC has been used for generation of the training data pair of ANFIS under the consideration of plant dynamics. The inputs are speed  $\Delta\omega_m(t)$  and change in speed  $\frac{\Delta d\omega_m(t)}{dt}$ , and corresponding  $X_{mod}$  has been selected as output value of the ANFIS. The input signals of TCSC are speed and acceleration, so communication delay has been taken into consideration to compensate the time lag between generator signal and transmission side input of the TCSC. The first order transfer function with 0.5 second delay has been used as communication time delay for generation of input and output data. The comparative analysis between types of MFs with different number of rules are illustrated by Table 4.2. Table 4.2 shows the generating error after the execution of ANFIS structure with inputs and output data. Here three types of membership functions are selected with different number of rules for designing of inputs and output variables of ANFIS controller. It has been experimentally verified that forty nine rules based structure of the ANFIS controller is not preferable as it takes high computational time for the execution compared to the other ANFIS structures. Type of MFs, number of MFs and number of FIS rules are selected such that generating error should be minimized. The best ANFIS-TCSC structure has been selected after the testing with real power system. The TCSC model has been implemented in

power system with ANFIS based stability control loop. Here the gauss type five membership functions are selected and total twenty five rules are designed for inputs and output. Speed signal range is selected between -0.003313 to 0.003808 and change in speed signal -0.05169 to 0.1172 for defining the input membership functions. The output membership functions are varied between -0.2143 to 0.234. After 10 number of epochs, the error between actual output and ANFIS output is minimized. Figure 4.8 represents structure of ANFIS based TCSC controller. Membership functions for the ANFIS based TCSC controller have been represented in Figure 4.9 and 4.10. The decision surface viewer of ANFIS-TCSC controller has been presented by Figure 4.11. The training is continued until the desired error becomes constant. The training is completed when the constant error 0.000805447 has been reached.

Table 4.2: Membership Function of ANFIS-TCSC

No.of Rules	Type of Membership Functions		
	gbell	gauss	dsig
	Error		
9	0.00169247	0.00084397	0.00115811
16	0.00029095	0.000753772	0.00158915
25	0.00131741	0.000805447	0.000930369
49	0.000256792	0.000494053	0.00674250

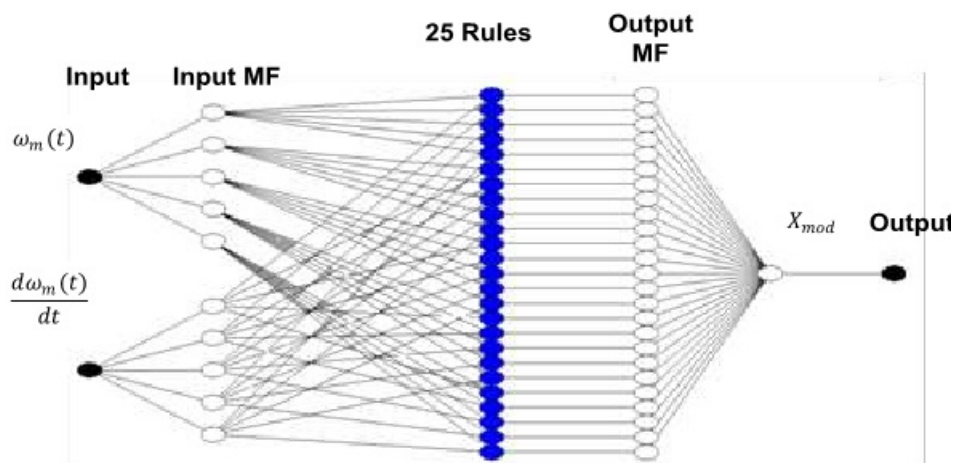


Figure 4.8: ANFIS-TCSC Structure

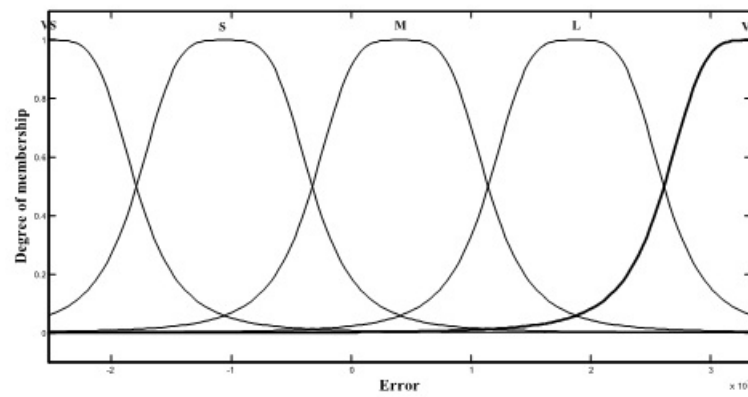


Figure 4.9: Membership Functions of Speed (Input: 1)-TCSC

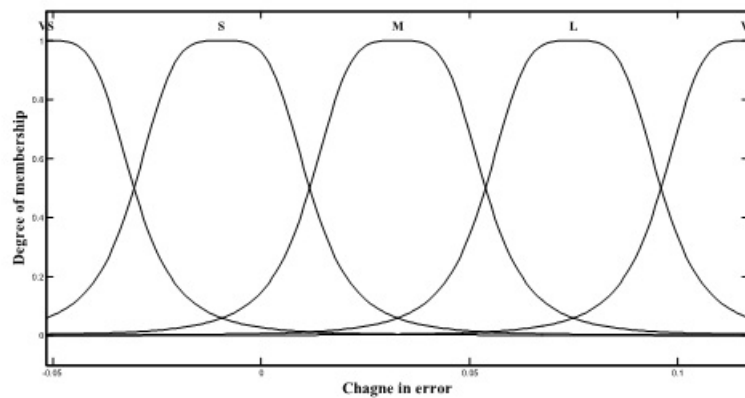


Figure 4.10: Membership Functions of Change in Speed (Input :2)-TCSC

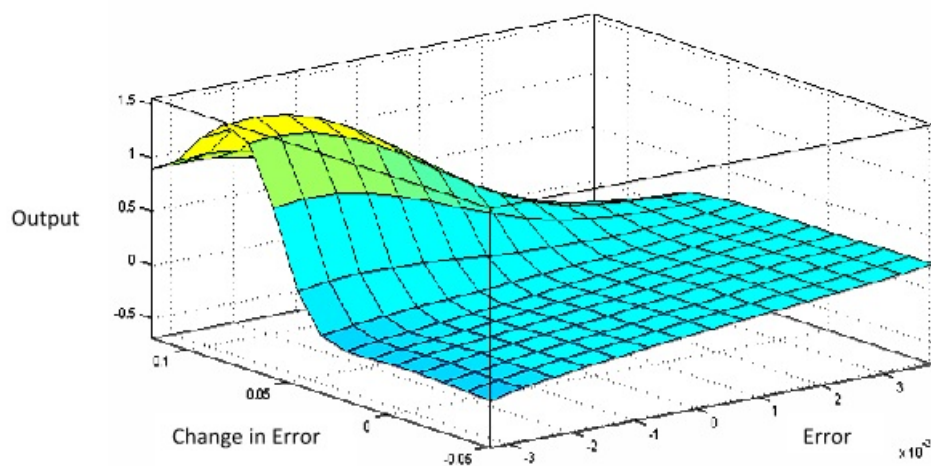


Figure 4.11: Decision-Surface Viewer of TCSC

## 4.4 Levenberge-Marquardt Neural Network

Artificial Neural Network has been one of the most interesting topics in the control community because they have the ability to treat many problems that cannot be handled by traditional analytical techniques. There are several approaches to neural network training, for determining an appropriate set of weights. The feedforward multilayer neural networks are the most common neural network architecture for solution of control problem. A widely used training method for feedforward multilayer neural network is the back propagation algorithm; the standard back propagation learning algorithm has several limitations. Most of all, a long and slow training process when plant is non-linear and parameters of the plant are dynamic i.e. the rate of convergence is seriously affected by the initial weights and the learning rate of parameters. Here, the learning rule is common to a standard nonlinear optimization or least-squares technique. The adjustment of weight is done at the end of each iteration and the sum of squares of all errors is used as the objective function for the optimization problem. In this problem derivative –based optimization Levenberg-Marquardt method [87, 14] is used for solving the nonlinear least squares problem. The Gauss Newton Levenberg-Marquardt method works well in practice and has become standard of nonlinear least squares routines.

### 4.4.1 Levenberg-Marquardt Algorithm

To implement the Levenberg–Marquardt algorithm [87, 14, 94] for neural network training, the first step is calculation of Jacobin matrix and second step is organize the training process iteratively for weight updating. Suppose that we have a function  $V(k)$  to minimize with respect to the parameter  $k$  vector, and then Newton’s method would be

$$\Delta k = - [\nabla^2 V(k)^{-1}] \nabla V(k) \quad (4.7)$$

Where is  $\nabla^2 V(k)^{-1}$  Hessian matrix and  $\nabla V(k)$  is the gradient.

$\nabla\omega(k)$  - sum of square function

$$V(k) = \sum_{i=1}^N e_i^2(k) \quad (4.8)$$

Then it can be shown that

$$\nabla V(k) = J^T(k)e(k) \quad (4.9)$$

$$\nabla^2 V(k) = J^T(k)J(k) + s(k) \quad (4.10)$$

$$J(k) = \begin{bmatrix} \frac{\partial e_1(k)}{\partial \theta_1} & \frac{\partial e_1(k)}{\partial \theta_2} & \cdot & \cdot & \cdot & \frac{\partial e_1(k)}{\partial \theta_n} \\ \frac{\partial e_2(k)}{\partial \theta_1} & \frac{\partial e_2(k)}{\partial \theta_2} & \cdot & \cdot & \cdot & \frac{\partial e_2(k)}{\partial \theta_n} \\ \cdot & \cdot & \cdot & \cdot & \cdot & \cdot \\ \cdot & \cdot & \cdot & \cdot & \cdot & \cdot \\ \cdot & \cdot & \cdot & \cdot & \cdot & \cdot \\ \frac{\partial e_N(k)}{\partial \theta_1} & \frac{\partial e_N(k)}{\partial \theta_2} & \cdot & \cdot & \cdot & \frac{\partial e_N(k)}{\partial \theta_n} \end{bmatrix} \quad (4.11)$$

$$s(k) = \sum_{i=1}^N e_i(k)\nabla^2 e_i(k) \quad (4.12)$$

The updated rule of Levenberg Marquardt to the Gauss-Newton method is

$$\theta_{k+1} = \theta_k - [J(k)^T J(k) + \alpha I]^{-1} J(k)e(k) \quad (4.13)$$

Where  $J(k)$  is Jacobian matrix,  $\alpha$  is always positive called combination coefficient,  $I$  is the identity matrix. As the combination of the steepest descent algorithm and the Gauss-Newton algorithm, the Levenberg-Marquardt algorithm switches between the two algorithms during the training process. When the combination coefficient  $\alpha$  is very small, the Gauss-Newton algorithm is used while combination coefficient  $\alpha$  is very large; the steepest descent method is used. With the update rule of the Levenberg-Marquardt algorithm equation (4.13) and the computation of Jacobian matrix, the next step is to organize the training process.

## 4.5 Steps for Designing of LMNN based PSS and TCSC

1. To generate the input data pattern and corresponding the target data pattern.
2. To Develop the feedforward neural net
3. Training of the neural network using Levenberg-Marquardt algorithm
4. To Update the NN parameters through equation (4.13).
5. Calculating mean square error between actual output and targeted output.
6. Computing the output of the NN.
7. If desired solution is achieved then stop, else change the NN goal, learning rate, no. of epochs and repeat the algorithm from the step 4.

### 4.5.1 ANN-Power System Stabilizer

In this work, CPSS is replaced by the ANN based PSS. The time constants and gain of lag-lead compensator based CPSS has been tuned by genetic algorithm [8] and genetic algorithm tuned model of the CPSS has been used for the generation of the training data for the artificial neural network. The network has been trained using 8000 sample data, which are generated under the consideration of the different operating conditions and dynamic behavior of the power system. The training pattern for the feedforward neural network is dynamic inputs  $u(t)$  and corresponding outputs  $y(t)$  such that  $\omega_m(t), \omega_m(t-1), \omega_m(t-2), \omega_m(t-3)$  and  $V_{pss}$  respectively and targeted value of the neural network is  $\hat{y}(t)$ .

Table 4.3 represents the mean square error (mse), number of iteration and training time in second with different learning rate and different combination of neurons in input layer, hidden layer and output layer. The different combinations of neurons are selected and trained the neural network such that error should be reduced with less number of iteration and less time. Each trained neural network has been tested with real power system and

performance has been analyzed. Here dynamic data are used for training of neural network so large number of neurons is required for satisfactory performance of the system. Hence the feedforward network has been developed with 50 neurons in first layer, 30 neurons in hidden layer and 1 neuron in output layer with hyperbolic tangent sigmoidal transfer function in first layer and hidden layer, and linear transfer functions in output layer. The selection of [50 30 1] neurons with higher learning rate neural network has produced better response.

Table 4.3: Mean Square Error of ANN based PSS

No.of neurons	Learning rate					
	0.05			0.1		
	Iteration	t (sec)	mse	Iteration	t (sec)	mse
[10: 5:1]	35	6	$2.64 \times 10^{-5}$	11	2	$3.01 \times 10^{-5}$
[20: 10: 1]	89	24	$2.72 \times 10^{-5}$	25	7	$2.96 \times 10^{-5}$
[30: 20: 1]	16	10	$2.96 \times 10^{-5}$	12	8	$2.80 \times 10^{-5}$
[50: 30: 1]	24	11	$3.06 \times 10^{-5}$	27	12	$2.98 \times 10^{-5}$

Contd..

0.3			0.5		
Iteration	t (sec)	mse	Iteration	t (sec)	mse
39	7	$2.83 \times 10^{-5}$	32	6	$2.98 \times 10^{-5}$
108	29	$2.81 \times 10^{-5}$	11	3	$2.96 \times 10^{-5}$
26	16	$2.60 \times 10^{-5}$	13	8	$2.97 \times 10^{-5}$
15	34	$2.88 \times 10^{-5}$	5	24	$3.84 \times 10^{-5}$

During the training of ANN, the weights and bias of the network are adjusted such that the error between the actual output and targeted output is minimized and desired goal is achieved through Levenberg-Marquardt derivatives –based optimization. The optimization function can be represented by the following equation.

$$J_i(k) = \frac{1}{2} [\Delta\omega_m(k) - \Delta\hat{\omega}_m(k)]^2 \quad (4.14)$$

The Levenberg-Marquardt's direction is determined by the updated rule of Levenberg Marquardt to the Gauss-Newton method. Which one is an intermediate between the Gauss-Newton direction and the steepest descent direction. Figure 4.12 shows relation between training data versus output data and targeted data. Figure 4.13 shows the minimizing of the cost function  $J_i(k)$  described by the equation (4.14). The selected structure has produced

$3.84 \times 10^{-5}$  mse in 24 second with 0.5 learning rate. The training is performed for 5 number of iteration through appropriate adjustment of weight and bias of neural network.

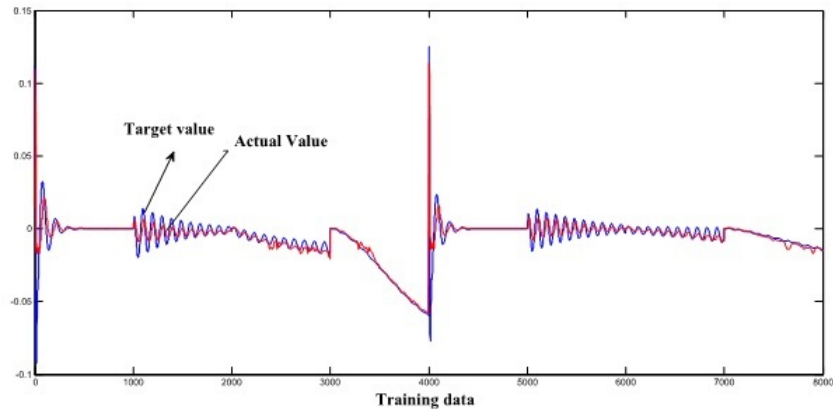


Figure 4.12: Training data and Actual data PSS

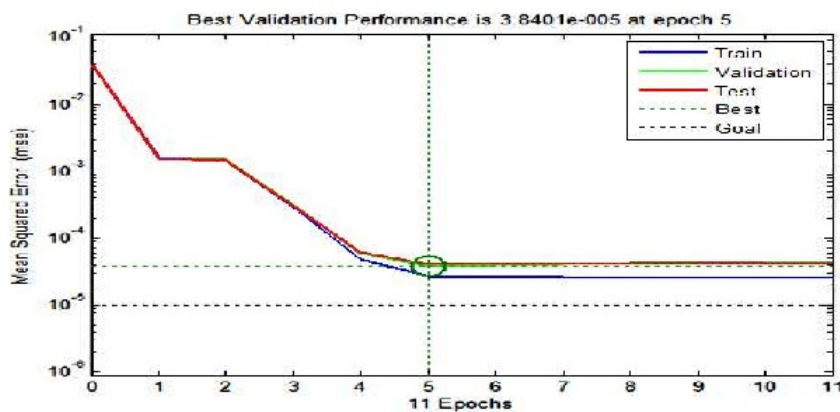


Figure 4.13: Mean Square Error

#### 4.5.2 Design of LMNN-TCSC

Here, the stability control loop of the TCSC has been trained by artificial neural network. The gain and time constant of TCSC controller has been tuned by GA and the tuned model of the TCSC described by the equation (2.87), (2.88) and (2.89) have been used to generate the training data for the NN under the different operating condition and dynamic behavior of the power system. Procedure for selection of number of neurons in different layers of ANN-TCSC is similar to the ANN-PSS. The training pattern for the feedforward neural

network is dynamic inputs  $u_1(t)$  and corresponding outputs  $y_1(t)$  such that  $\omega_m(t), \omega_m(t - 1), \omega_m(t - 2), \omega_m(t - 3)$  and  $X_{mod}$  respectively and targeted value of the neural network is  $\hat{y}_1(t)$ . The first order transfer function with 0.5 second delay has been used as communication time delay. The feedforward network has been developed with 30 neurons in first layer, 10 neurons in hidden layer and 1 neuron in output layer with hyperbolic tangent sigmoidal transfer function in first layer and hidden layer, and linear transfer functions in output layer. The optimization function can be represented by the following equation.

$$J_i(k) = \frac{1}{2} [y(k) - \hat{y}_1(k)]^2 \quad (4.15)$$

The mean square error  $0.00002947 \times 10^{-5}$  has been reached after the 13 iterations through appropriate adjustment of weight and bias of neural network using Levenberg-Marquardt algorithm.

## 4.6 Non Linear Simulation

The nonlinear model of the power system has been used for the stability analysis of the SMIB system with generator attached PSS and transmission line connected TCSC. The initial conditions have been calculated using MATLAB programming. The non-linear simulation is carried out using non-linear dynamic model, which has been implemented using MATLAB/simulink environment. The non linear model and detail data of the power system used in this study is given in Appendix A. The comparison analysis between ANFIS and LMNN based PSS and, simultaneous application of ANFIS and ANN based TCSC - PSS are carried out under different operating condition, faults and disturbance. These disturbances are considered such as the three phase short circuit at the infinite bus, outage of transmission line, suddenly changes in mechanical input and step change in terminal voltage reference. The comparison study of intelligent techniques based TCSC and PSS has been carried out.

### 4.6.1 Case I

Considering operating condition 1 as defined in table 3.1  $P_t = 0.6, Q_t = 0.0224$ . A three phase fault is created at 1s at the sending end of one the circuits of the transmission line and cleared after 100ms [33]. The original system restored after fault clearance. The response of speed deviation without the application of controllers and with application of intelligent controllers have been shown in Figure 3.6 and 4.14 respectively. Figures 3.6 shows that without application of controllers, the oscillation in speed deviation has been observed while using simultaneously application of ANFIS and ANN based TCSC-PSS, and individually PSS significantly diminished this oscillation in the system and provided very good damping characteristics.

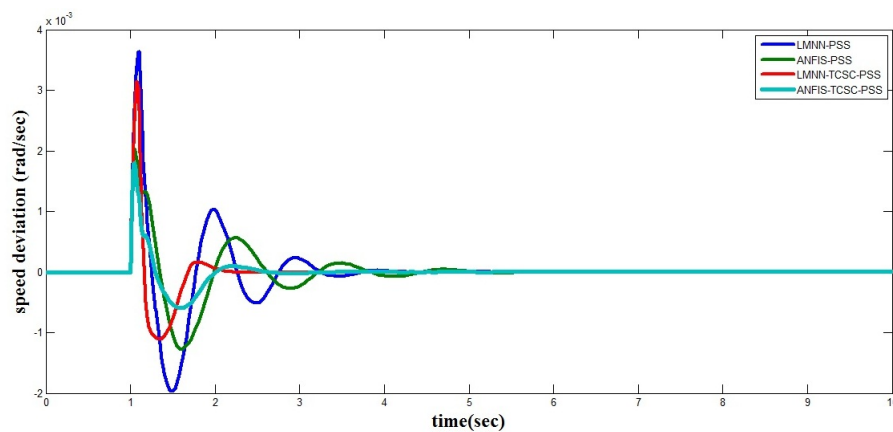


Figure 4.14: Case I: Speed response of ANFIS and LMNN based PSS-TCSC

### 4.6.2 case II

$P_t = 0.9, Q_t = 0.12$ , Here heavy loading condition is considered. A three phase fault is created at 1s at the sending end of one of the circuits of the transmission line and cleared after 50ms.. The original system restored after the fault clearance. The response of the  $\omega_m(t)$  without controller has been shown in Figure 3.22, the oscillation in the power system continuously growing with respect to the time and system has become unstable. The speed response with LMNN and ANFIS based PSS and simultaneous application of LMNN and ANFIS based TCSC-PSS has been shown in Figure 4.15. The simultaneous application of ANFIS and

ANN based TCSC-PSS, and individual applications of PSS reduced the oscillations in the system and improved stability.

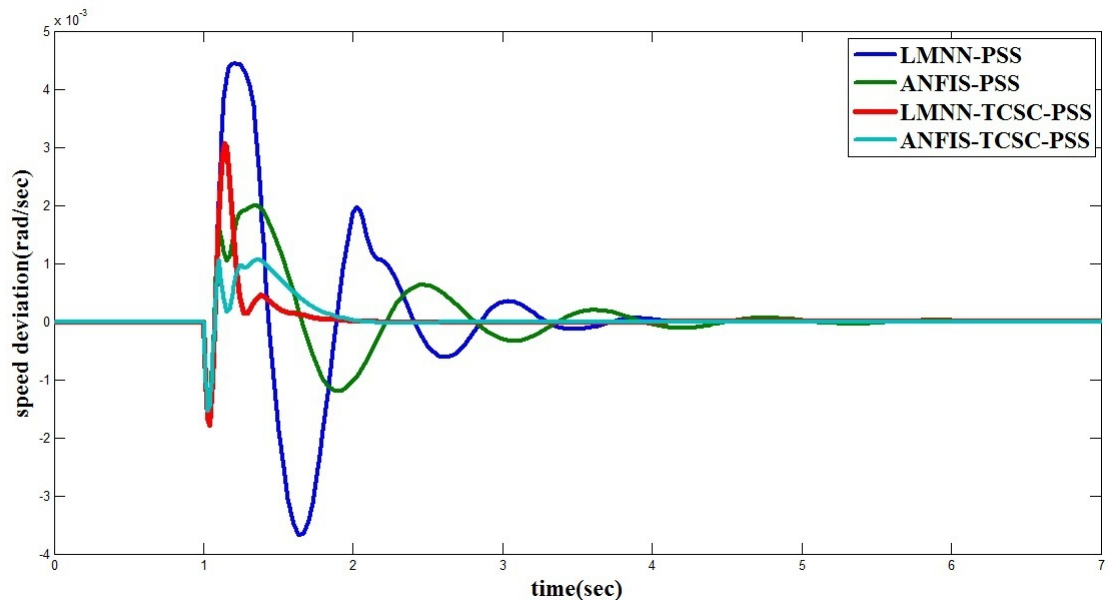


Figure 4.15: Case II: Speed response of ANFIS and LMNN based PSS-TCSC

### 4.6.3 Case III

$P_t = 0.9, Q_t = 0.12$ , Under the heavy loading condition a 10% mechanical change applied at 1s and removed at 5 s is considered. The system lost its stability at 4s without application of controllers, which has been shown by Figure 3.26. The response of  $\omega_m$  with and simultaneous application of LMNN and ANFIS based PSS-TCSC has been shown in Figure 4.16. The simultaneous application of ANFIS and ANN based TCSC-PSS, and individual applications of PSS reduced the oscillations in the system and improved stability.

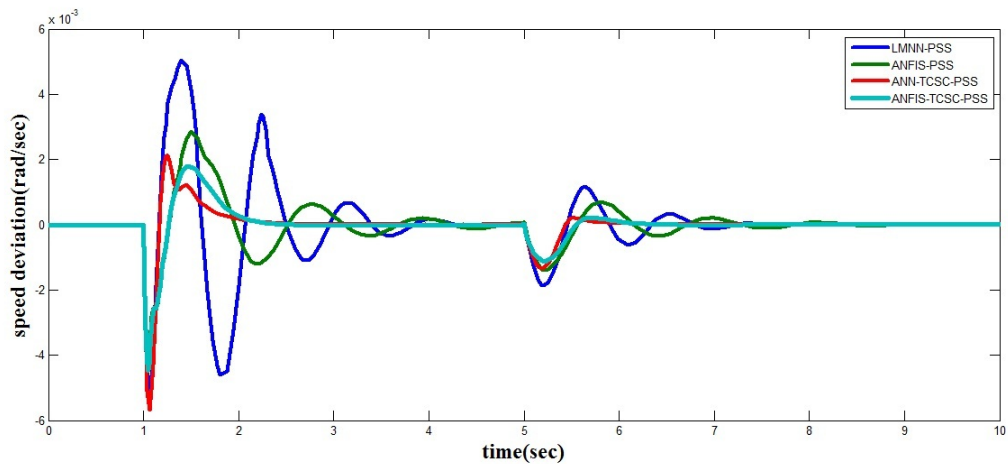


Figure 4.16: Case III: Speed response of ANFIS and LMNN based PSS-TCSC

#### 4.6.4 Case IV

$P_t = 1.2, Q_t = 0.2$ , A 0.1p.u. change in reference input voltage is applied at 1 s and removed at 5 s. The response of the  $\omega_m$  without and with presence of controllers has been shown in Figure 3.30 and 4.17 respectively. Figures 4.17 shows that the simultaneous application of ANFIS-TCSC-PSS controller has improved stability of the system compared to individual application of LMNN-PSS and ANFIS-PSS.

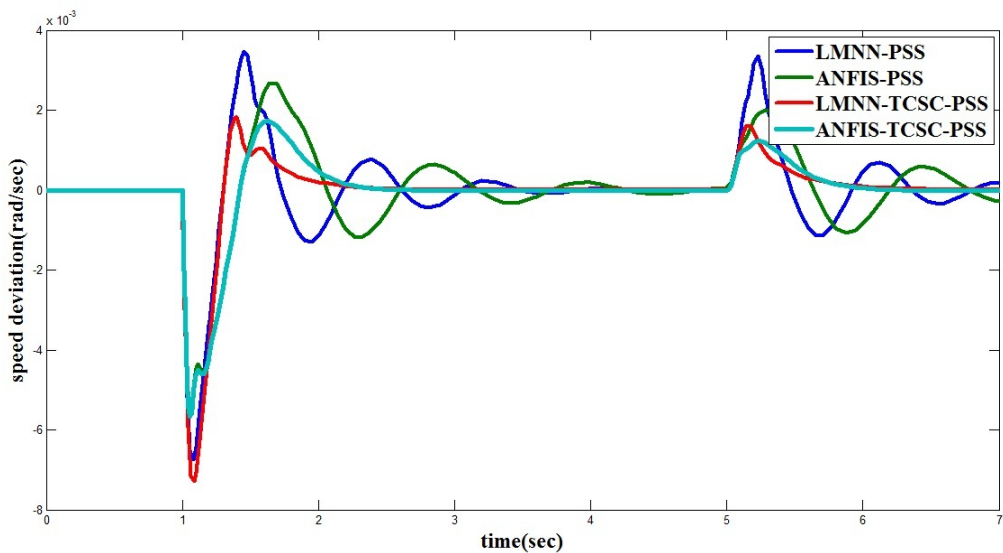


Figure 4.17: Case IV: Speed response of ANFIS and LMNN based PSS-TCSC

### 4.6.5 Case V

$P_t = 0.75, Q_t = 0.1$ , In this case another severe disturbance is considered. One of the transmission lines is permanently tripped at 1 sec. The line reactance is significantly increased. The speed response for the above contingency has been shown in Figure 3.34 and 4.18 without and with controller respectively. Figure 4.18 shows that ANFIS based simultaneously designed TCSC and PSS have provided good stability to system compared to individual neural network based power system stabilizer.

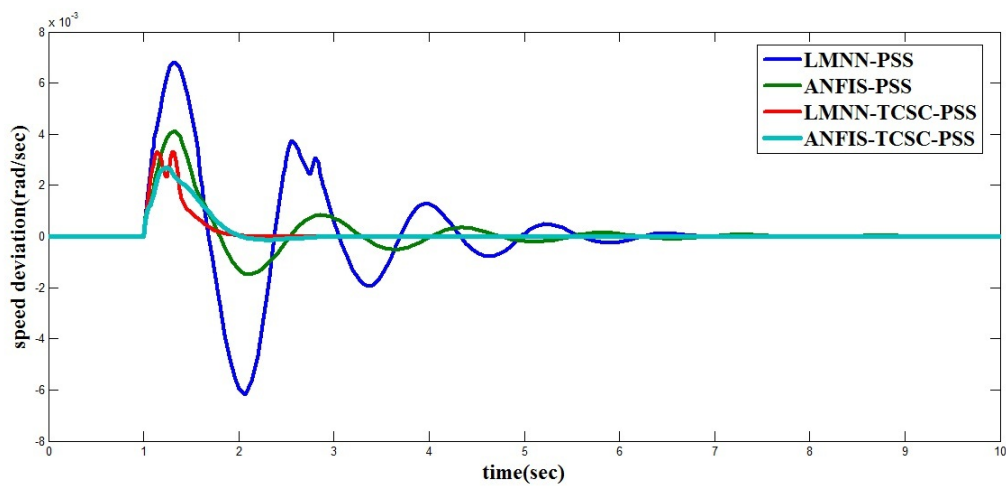


Figure 4.18: Case V: Speed response of ANFIS and LMNN based PSS-TCSC

## 4.7 Conclusion

In this study, the smart control strategies based TCSC damping controller and PSS have been designed. The ANFIS and LMNN based PSS, and simultaneously LMNN and ANFIS based TCSC-PSS have been applied to the dynamical power system. The non-linear simulations have been carried out for detailed analysis of the stability of the power system. The time response of speed deviation obtained by intelligent techniques based controller has been compared to the conventional power system stabilizer. Four different operating conditions are taken and the response of rotor speed deviation has been analyzed under different types of the disturbances and faults.

From the non - linear analysis,

1. Without the application of the controllers in the system, the oscillations in rotor speed deviation has been observed. Under the heavy loading condition, it has been observed that the active power and reactive power are increased; the oscillation in speed deviation is continuously growing which creates the instability of the system. The smart damping controllers have greatly diminished oscillations in system.
2. Conventional power system stabilizer does't produce satisfactory response under the different operating conditions. While simultaneous application of ANFIS and ANN based TCSC and PSS have provided very good damping characteristics compared to the individual application of PSS and almost eliminated the oscillations in system.
3. It has been observed that individual application of ANFIS-TCSC produces better response compared to the individual application of LMNN-TCSC.
4. As shown in figures, individual application of ANFIS-PSS produces better response compare to the individual LMNN-PSS.
5. Under the heavy loading condition, ANFIS based TCSC-PSS has produced good results compared to the LMNN based TCSC-PSS, and also improved the time response parameters such as settling time, rise time and delay time appreciably and decreased the overshoot in the system.

# Chapter 5

## Design of PSS Using NARMA-L2 and GA-ANN Controller with TCSC

### 5.1 Introduction

The power system stabilizer has been designed using Non Linear Autoregressive Moving Average-L2 controller and hybrid Genetic Algorithm based Network Network. In order to achieve appreciable damping, developed ANFIS based Thyristor control series capacitor has been suggested in addition to power system stabilizer. The non-linear simulations of single machine infinite bus system (SMIB) have been carried out using individual and simultaneous application of PSS and TCSC. Trained and optimized NARMA-L2 and GA-ANN based PSS have been tested with ANFIS-TCSC on non-linear power system dynamics under the different operating conditions, various disturbances and faults in the power system. The results have shown efficacy and capability of proposed control schemes under the various operating conditions and faults, and demonstrate the improvement in the dynamic performance of the system with proposed control algorithm.

## 5.2 Nonlinear Auto regressive Moving average -L2 Controller

Nowadays, artificial neural network controllers have been effectively introduced to improve the performance of nonlinear control systems. Unlike conventional controllers, no exact mathematical model is required for ANN controller, and it shows better results in terms of time response parameters such that settling time, delay time, overshoot and robustness. There are several approaches to neural network training [87] for determining an appropriate set of weights. The neural network based identification techniques successfully can be applied for non linear control problem as reported by [87][42].

### 5.2.1 NARMA-L2 (Feedback Linearization) Control

NARMA-L2 controller has been successfully applied for the identification and controller design. The execution of NARMA-L2 controller involves typically two stages. First stage is identification, which includes development of neural network model of the plant to be controlled. Second stage is controller design, in which training of neural network controller is carried out using developed neural network plant model. The identified NN plant model is used in neural network controller that transforms the non linear system into linear system through additive and multiplicative cancellation of nonlinearities.

#### 5.2.1.1 Identification Stage

The first stage of plant identification process is to generate input/output data pairs to train a neural network to represent the forward dynamics of the plant. The system identification stage has been represented by Figure 5.1. There are two sets of inputs to the plant model, one is delayed values of the plant output and other is delayed values of the controller output.

The model used for the plant identification is described as follow:

$$y(k+d) = N[y(k), y(k-1) \dots y(k-n+1), u(k), u(k-1) \dots u(k-n+1)] \quad (5.1)$$

Where  $u(k)$  is the system input,  $y(k)$  is the system output, and  $d$  is system delay. During the identification stage, the neural network training is realized in order to approximate the nonlinear function  $N$ . If the system follows a desired reference trajectory  $y_r$ , then the nonlinear controller can be written as follow:

$$u(k) = G[y(k), y(k-1) \dots y(k-n+1), y_r(k+d), u(k), u(k-1) \dots u(k-m+1)] \quad (5.2)$$

The neural network training could be performed to determine the function  $G$  that minimizes the mean square error using back propagation training algorithm. The dynamic of back propagation is slow and computationally demanding. To achieve faster response [19, 9, 87] proposed the use of NARMA-L2 controller approximate model in companion form and is represented as equation (5.3).

$$\hat{y}(k+d) = f[y(k), y(k-1) \dots y(k-n+1), u(k-1) \dots u(k-m+1)] + g[y(k), y(k-1) \dots y(k-n+1), u(k-1) \dots u(k-m+1)] \cdot u(k) \quad (5.3)$$

Here the next controller input  $u(k)$  is not contained in the nonlinearity. The advantage of this form is that user can solve for the control input that causes the system output to follow the reference  $y(k+d) = y_r(k+d)$ . The resulting controller would have the form as described by equation (5.4).

$$u(r) = \frac{y_r(k+d) - f[y(k), y(k-1) \dots y(k-n+1), u(k-1) \dots u(k-m+1)]}{g[y(k), y(k-1) \dots y(k-n+1), u(k-1) \dots u(k-m+1)]} \quad (5.4)$$

Using this equation directly can cause realization problems; the determination of the control input based on the output at the same time is not realistic and hence uses the following model:

$$y(k+d) = f[y(k) \dots y(k-n+1), u(k) \dots u(k-n+1)] + g[y(k) \dots y(k-n+1), u(k) \dots u(k-n+1)] \cdot u(k+1) \quad (5.5)$$

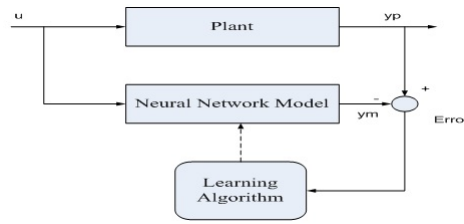


Figure 5.1: Identification Stage

### 5.2.1.2 Controller Stage

A more practical form of controller is given by (5.6). This controller is realizable for  $d \geq 2$ .

The controller structure [9] has been shown in Figure 5.2.

$$u(k+1) = \frac{y_r(k+d) - f[y(k) \dots y(k-n+1), u(k) \dots u(k-n+1)]}{g[y(k) \dots y(k-n+1), u(k) \dots u(k-n+1)]} \quad (5.6)$$

$$\Delta V_{pss}(k+1) = \frac{\Delta \omega_r(k+2) - F}{G} \quad (5.7)$$

Where,

$$F = G = f[\Delta \omega_m(k), \Delta \omega_m(k-1), \Delta \omega_m(k-2), \Delta V_{pss}(k), \Delta V_{pss}(k-1), \Delta V_{pss}(k-2)]$$

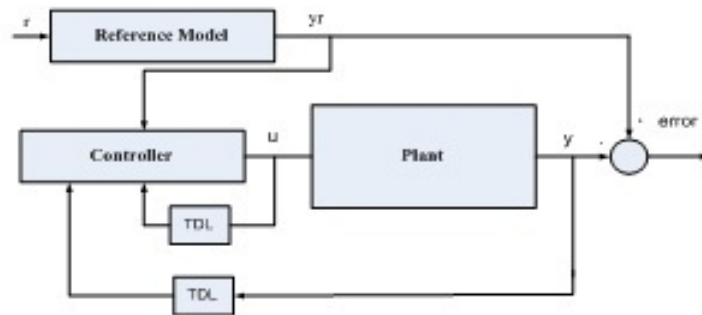


Figure 5.2: NARMA-L2 Controller

## 5.3 NARMA-L2 Controller based Power System Stabilizer

An indirect data based approach has been used for approximate linearization through feedback. Indirect data base technique is two step methodology, where a model of the plant is

identified on the basis of input output data and then used in model based design of a suitable controller.

### 5.3.1 Neural Network Identifier

NARMA-L2 neural controller has been proposed for the designing of the PSS for power system stability improvement. The identification of neural network base plant is developed using non linear auto regressive moving average model. For the particular system  $y$ ,  $u$  and  $\hat{y}$  are the speed deviation  $\Delta\omega_m(k)$  of the plant, output of the neural network controller  $\Delta V_{pss}(k)$ , and predicted plant output  $\Delta\hat{\omega}_m(k)$  by the neural network identifier respectively. The training process of the neural network identifier has been shown in Figure 5.3.

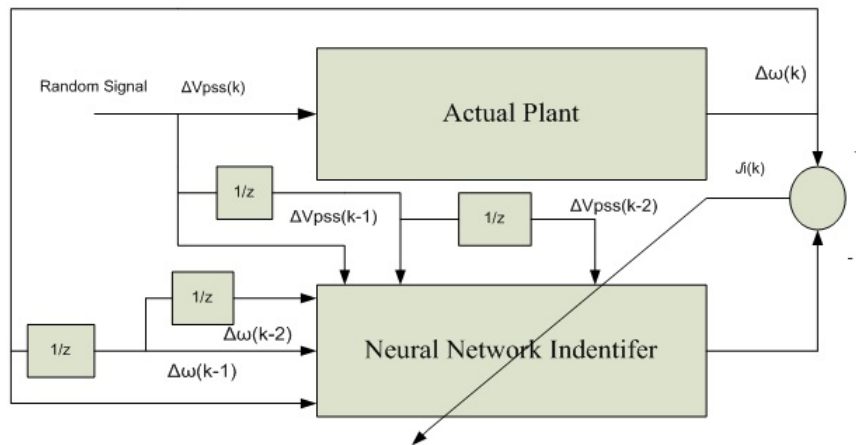


Figure 5.3: Identification of the Plant

Random inputs have been applied to the plant model to generate the input output data. The values of random signal are distributed between -0.04 to 0.04, which are taken from CPSS simulation. Here, 10000 data are used for the identification of the plant. The neural network plant model has two inputs available namely delayed controller outputs and delayed plant outputs. The inputs to the neural network identifier during this phase are  $\Delta\omega_m(k)$ ,  $\Delta\omega_m(k-1)$ ,  $\Delta\omega_m(k-2)$ ,  $\Delta V_{pss}(k)$ ,  $\Delta V_{pss}(k-1)$ ,  $\Delta V_{pss}(k-2)$ . The optimization function of the neural network identifier is given by equation (5.8). Where  $\Delta\hat{\omega}_m(k)$  is NN

identifier output.

$$J_i(k) = \frac{1}{2} [\Delta\omega_m(k) - \Delta\hat{\omega}_m(k)]^2 \quad (5.8)$$

The neural network identifier is a multilayer feedforward network which is trained by the Levenberge-Marquardt algorithm as described by Section (4.4.1). The feedforward network has been developed with 10 neurons in hidden layer and 1 neuron in output layer with hyperbolic tangent sigmoid and linear transfer functions in first layer and hidden layer, and output layer respectively. Figure 5.4 shows input data to the plant, actual plant output, NN plant output and error between actual plant output and NN plant output. The NN trained plant model is similar to actual plant and error is varied between -0.00004 to 0.00004 rad/sec.

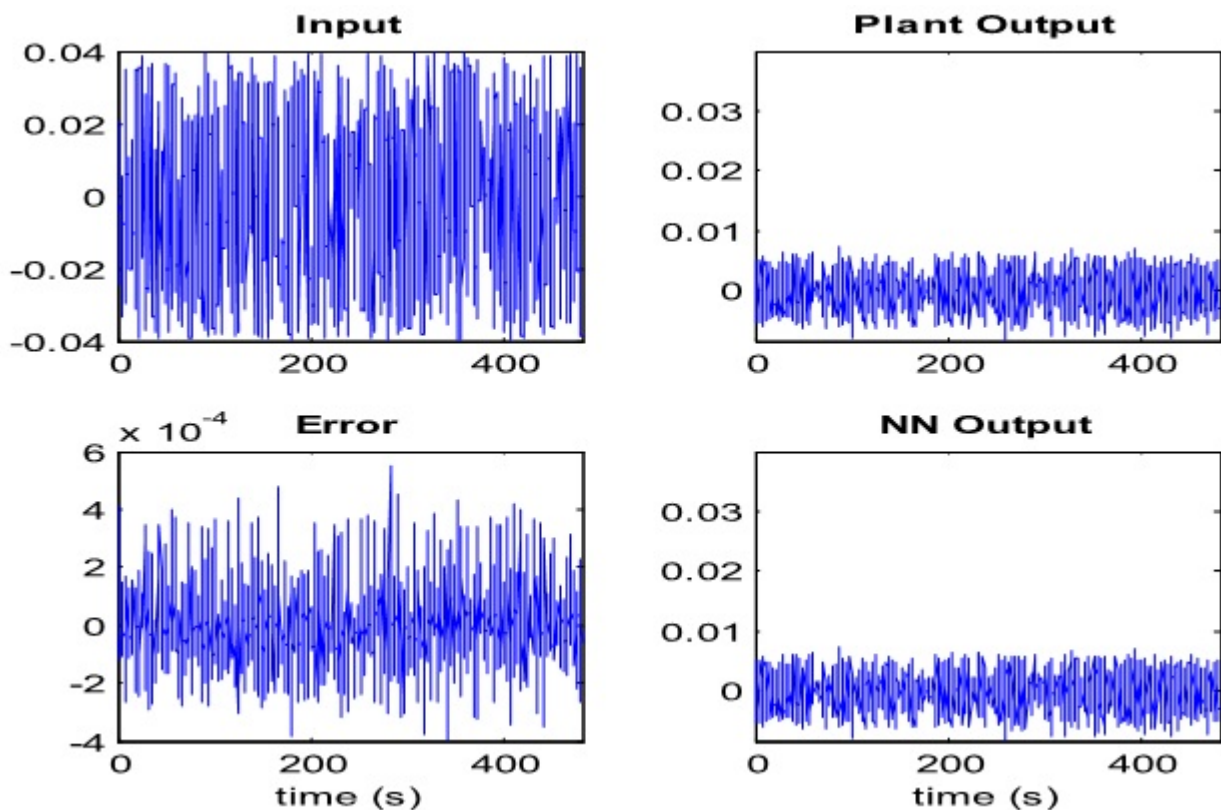


Figure 5.4: Plant Input, Plant Output, NN Output and Error

### 5.3.2 Neural Network Controller

The neural network controller has been implemented with the identified neural network plant model. The central idea of this controller is to transform nonlinear system dynamics by cancelling the nonlinearities. The neural network controller is also trained by the Levenberge-Marquardt algorithm with 10 neurons in hidden layer. The controller structure has been shown in Figure 5.5 and the controller can be written by the following equation.

$$\Delta V_{pss}(k+1) = \frac{(\Delta\omega_r(k+2) - F)}{G} \tag{5.9}$$

Where,

$$F = G = \Delta\omega_m(k), \Delta\omega_m(k-1), \Delta\omega_m(k-2), \Delta V_{pss}(k), \Delta V_{pss}(k-1), \Delta V_{pss}(k-2)$$

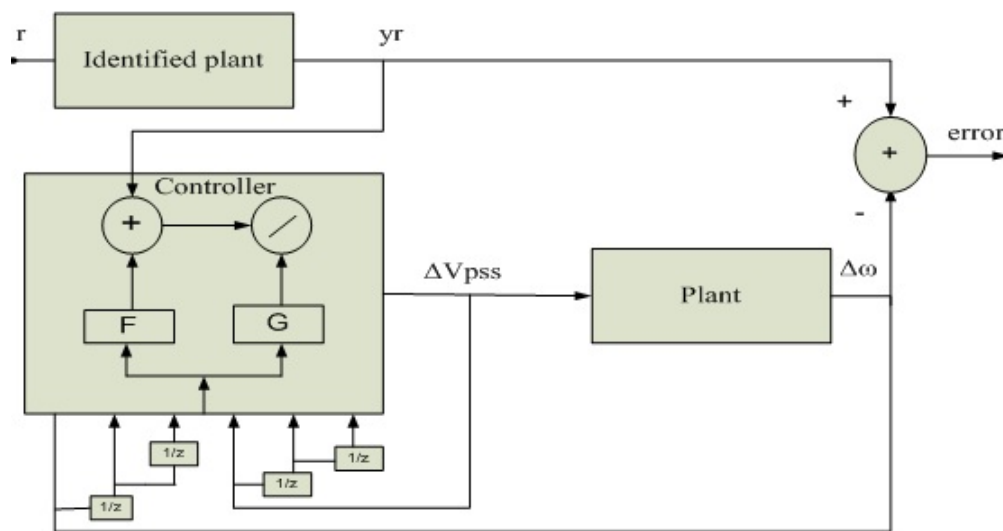


Figure 5.5: Implementation of NARMA-L2 Controller

### 5.4 GA-ANN Hybrid-Power System Stabilizer

Genetic Algorithm and Artificial Neural Network in the broad sense, reside in the class of the evolutionary computing algorithm. Both GAs and ANNs are adapting, they learn, and can deal with high non linear, complex model. The objective of the hybridization is to overcome the weakness in one technology during its application, with the strengths of the other by appropriately integrating them.

In this section, design of power system stabilizer using combination of genetic algorithm based neural network hybrid controller [94, 89] for analysis of dynamical power system has been discussed. Two different strategies have been used for designing of neural network through GA. In the first strategy, a genetic algorithm has been used to minimize the error before learning algorithm is applied and for second strategy, a genetic algorithm has been used to minimize the sum of square of error with respect to the ANN parameters [94]. Here, the calculation of weight and bias of ANN have been considered as an optimization problem. The weights and bias of the feed forward neural network have been identified and optimized using genetic algorithm. The trained and optimized GA-ANN based PSS has been tested on non-linear power system dynamics under the different operating conditions, various disturbances and faults in the power system.

### 5.4.1 Genetic Algorithm

Genetic algorithm has been proposed to calculate the initial values of parameters of neural network, the algorithm as follows:

1. Randomly generate the initial population for the parameter of initial weight and bias of NN.
2. Calculation of total number of weight and bias of NN for optimization.
3. Generate the fitness function to be evaluated.
4. Evaluate fitness function of each chromosome in population and select a new population from old population based on the fitness of individuals as given by the evaluation function.
5. Selection of appropriate value of genetic operators such as reproduction, crossover, mutation etc. to member of the population to create new solution.
6. Calculation of convergence rate of fitness function.
7. If expected convergence rate is achieved then stop the algorithm otherwise repeat from the step 4-7 and change the GA parameters.

By changing the GA parameters such as population size, crossover rate and function, mutation rate and function, No. of generation etc, the new set of NN parameters are developed, and best fitness values have been selected. The appropriate choice of the GAs parameters affects the convergence rate of the algorithm. The parameters are selected for expected solution as given in Table 5.1. Figure 5.6 shows the rate of the convergence of the optimization function, the best fitness value of the function 0.00021793 is achieved after the 51 generation has been reached. Figure 5.7 shows the total 81 best individual values of weight and bias of NN.

Table 5.1: GA Parameter and Value

Parameters	Values/Parameter
Popullation Size	50
Stopping Generation	100
Scaling Function	rank
Selection Function	Stochastic Uniform
Mutation Function	Gaussian
Crossover Function	Scattered

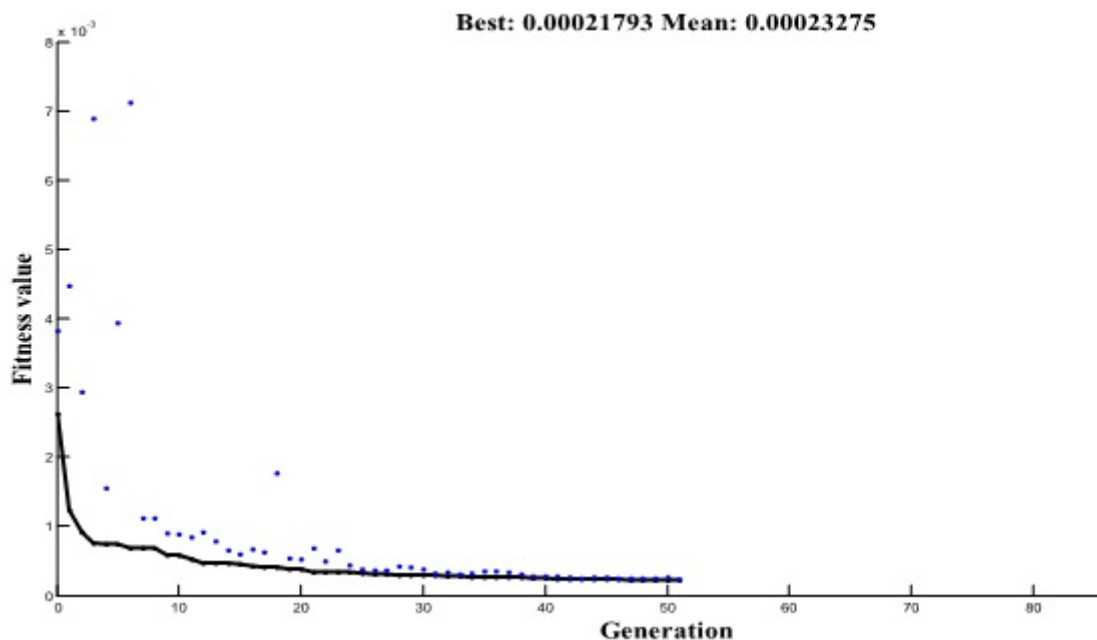


Figure 5.6: Convergence rate of GA

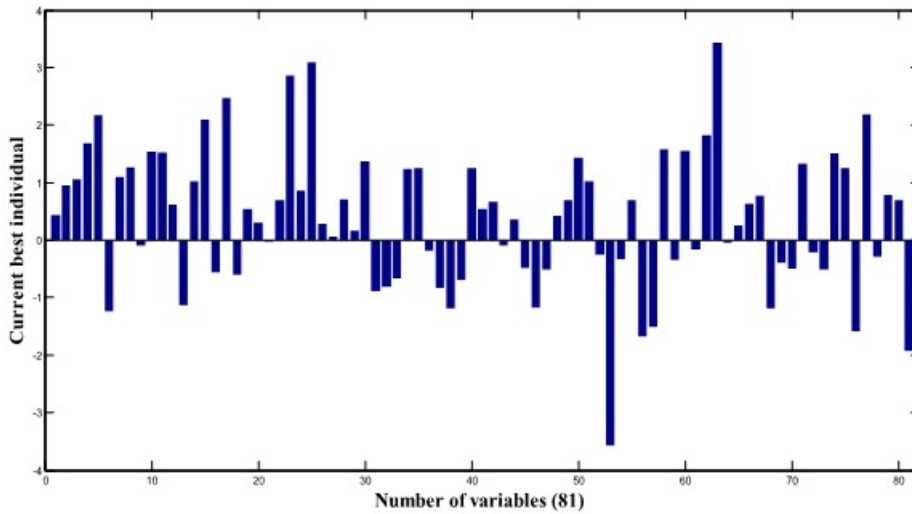


Figure 5.7: Best Value of NN Parameters

### 5.4.2 Neural Network

The training pattern for the feedforward neural network is dynamic inputs  $u(t)$  and corresponding outputs  $y(t)$  such that  $\omega_m(t), \omega_m(t-1), \omega_m(t-2), \omega_m(t-3)$  and  $V_{pss}$  respectively and targeted value of the neural network is  $\hat{y}(t)$ . The network has been trained using 8000 sample data, which are generated under the consideration of the different operating conditions and dynamic behavior of the power system. The feedforward network has been developed with 10 neurons in the first layer, 5 neurons in hidden layer and 1 neuron in output layer with hyperbolic tangent sigmoid transfer function between first layer and hidden layer, and linear transfer function between hidden layer and output layer. In this problem, derivative-based optimization Levenberg-Marquardt method is used for solving the nonlinear least squares problem.

The weights and bias of the network are adjusted such that the error between the actual output and targeted output is minimized and desired goal is achieved through Levenberg-Marquardt derivatives-based optimization. The optimization function can be represented mathematically by equation (5.10). Levenberg-Marquardt's direction [87, 14] that is determined by using equation (4.13) is an intermediate between the Gauss-Newton direction and the steepest descent direction. The optimization function can be represented by Equation

$$J_i(k) = \frac{1}{2} \sum [y(k) - \hat{y}(k)]^2 \quad (5.10)$$

The Gauss Newton Levenberg-Marquardt method works well in practice and has become standard of nonlinear least squares routines [87, 14].

The following steps are for implementation of neural network

1. The initial parameters of NN likes weights and bias are computed by GA.
2. Generate the input data pattern and corresponding the target data pattern.
3. Develop the feedforward neural net.
4. Train the neural network using Levenberg-Marquardt algorithm[14].
5. Update the NN parameters through equation of Levenberg-Marquardt Algorithm.
6. Calculation of mean square error between actual output and targeted output using Equation (5.10)
7. Compute the output of the NN network
8. If desired solution is achieved stop, else change the NN goal, learning rate, no. of epochs and repeat the algorithm from the step 4.

Figure 5.8 shows the error generated between actual data and target data and Figure 5.9 shows the relation between training data versus actual data and target data.

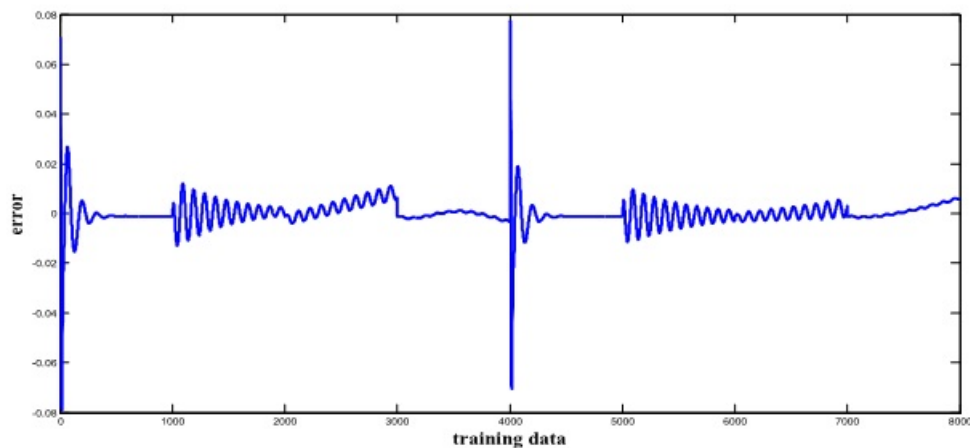


Figure 5.8: Error Between Actual and Target Value

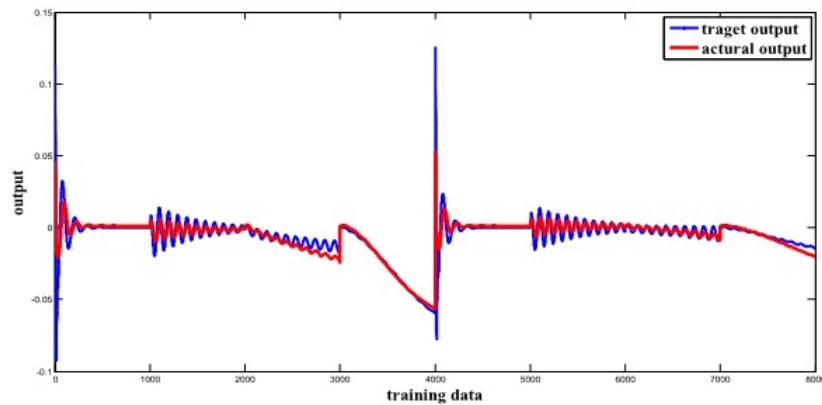


Figure 5.9: Output of GANN

## 5.5 Non Linear Simulation

The nonlinear model of the power system has been used for the stability analysis of the SMIB system with generator attached PSS and transmission line connected TCSC. The initial conditions of power system have been calculated using MATLAB programming. The non-linear simulation is carried out using non-linear dynamic model, which has been implemented using MATLAB/simulink environment. The non linear model and detailed data of the power system used in this study is given by Appendix A. The comparison analysis between (i) NARMA-L2 Controller and GA-ANN based PSS (ii) simultaneous application of ANFIS-TCSC with NARMA-L2-PSS and GA-ANN-PSS have been carried out under different operating condition, faults and disturbance. These disturbances considered are such as the three phase short circuit at the infinite bus, outage of transmission line, suddenly changes in mechanical input and step change in terminal voltage reference. The comparison study of smart techniques based TCSC and PSS has been carried out.

### 5.5.1 Case I

Considering operating condition 1 as defined in table 3.1  $P_t = 0.6, Q_t = 0.0224$ . A three phase fault is created at 1s at the sending end of one the circuits of the transmission line and

cleared after 100ms [33]. The original system restored after fault clearance. The response of speed deviation with the application of individual PSS, and simultaneous application of PSS with ANFIS controller has been shown by Figure 5.10 and 5.11 respectively. Figures 3.6 shows that without application of controllers the oscillation in speed deviation are observed while using simultaneous application of ANFIS-TCSC with NARMA-L2-PSS and GA-ANN-PSS have significantly diminished this oscillation in the system and provided very good damping characteristics.

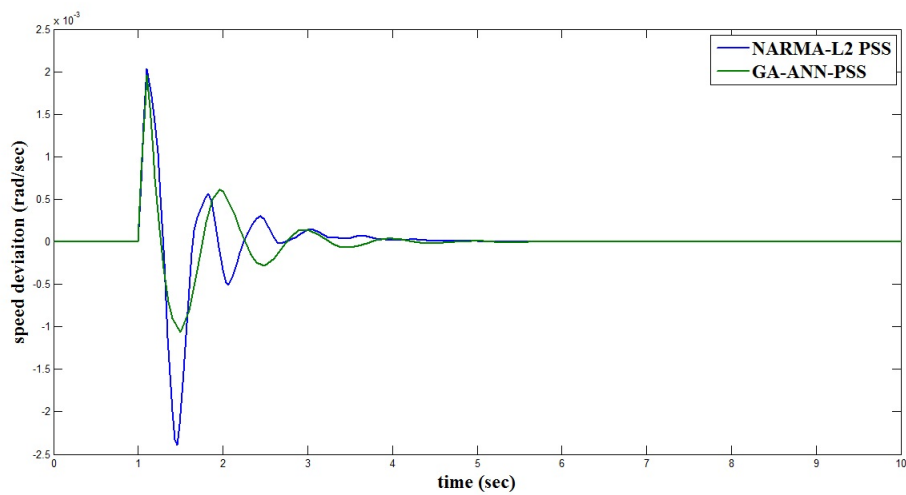


Figure 5.10: Case I: Speed response of NARMA-L2 and GA-ANN based PSS

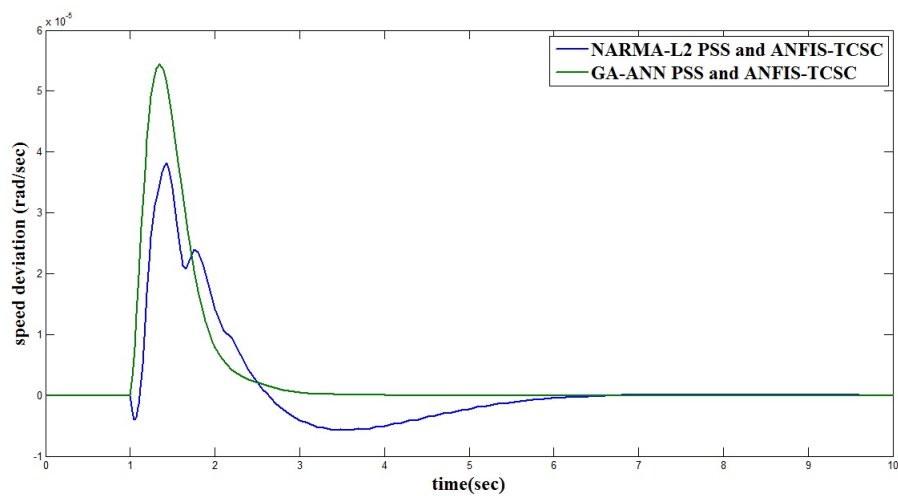


Figure 5.11: Case I: Speed response of NARMA-L2 and GA-ANN based PSS and ANFIS-TCSC

### 5.5.2 Case II

$P_t = 0.6, Q_t = 0.0224$ , A three phase fault is created at 1s at the middle of one transmission line and cleared after 50 ms by the disconnection of the faulted line, and then successfully reclosed at 5s [71]. Figure 3.15 shows the response of the rotor speed deviation without controllers. The response of the  $\omega_m$  with presence of NARMA-L2-PSS and GA-ANN-PSS has been shown in Figure 5.12. Figure 5.13 shows the response of  $\omega_m$  with simultaneous application of ANFIS-TCSC and PSS. Without application of damping controllers, the oscillations in speed deviation have been observed. These oscillation are continuous growing, which shows instability of system after 10s. While using individual PSS and simultaneous application of ANFIS-TCSC and PSS have significantly diminished this oscillations and improved stability of the system.

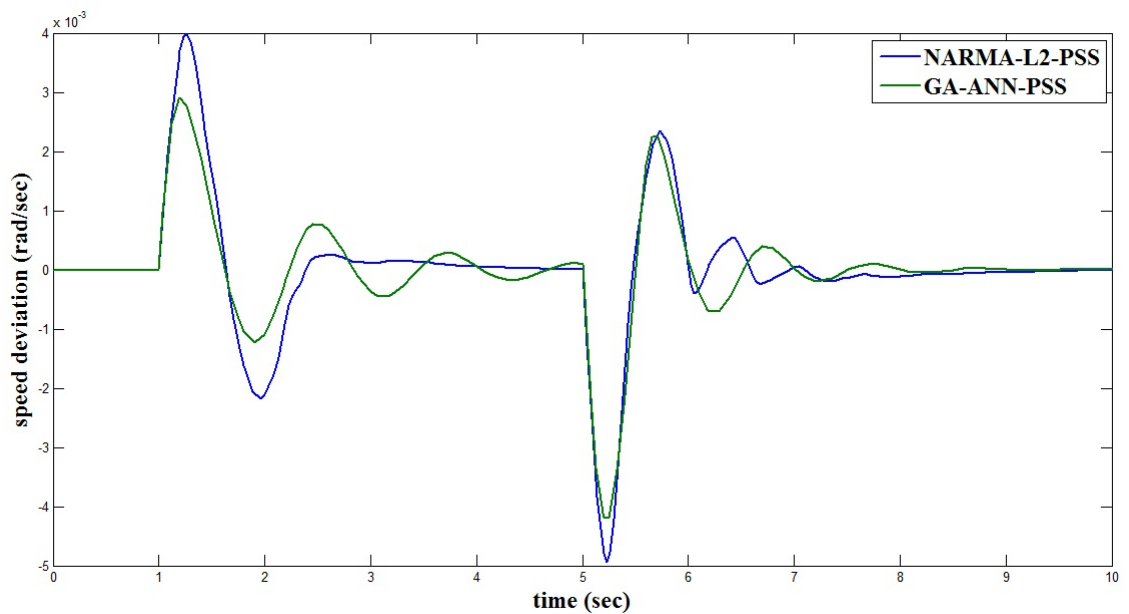


Figure 5.12: Case II: Speed response of NARMA-L2 and GA-ANN based PSS

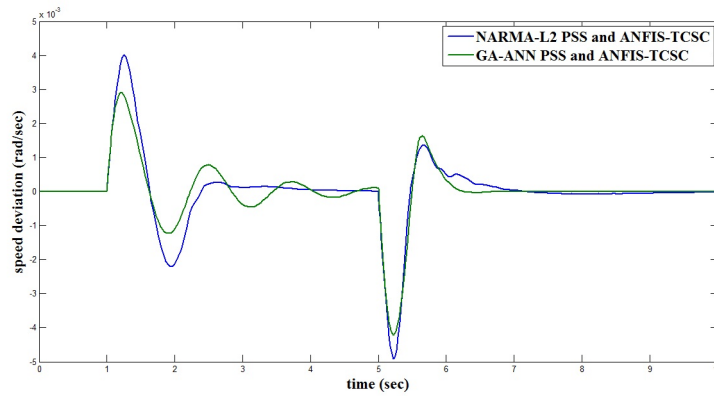


Figure 5.13: Case II: Speed response of NARMA-L2 and GA-ANN based PSS and ANFIS-TCSC

### 5.5.3 Case III

$P_t = 0.9, Q_t = 0.12$ , Here heavy loading condition is considered. A three phase fault is created at 1s at the sending end of one of the circuits of the transmission line and cleared after 50ms. The original system restored after the fault clearance. Figure 3.22 shows the response of the  $\omega_m(t)$  without controller, the oscillation in the power system continuously growing with respect to the time and system has become unstable. The speed response with NARMA-L2-PSS and GA-ANN based PSS, and simultaneously application of ANFIS-TCSC with NARMA-L2-PSS and GA-ANN-PSS has been shown in Figure 5.14 and 5.15 respectively. The simultaneous application of ANFIS-TCSC and PSS, and individual applications of PSS reduced the oscillations in the system and improved stability.

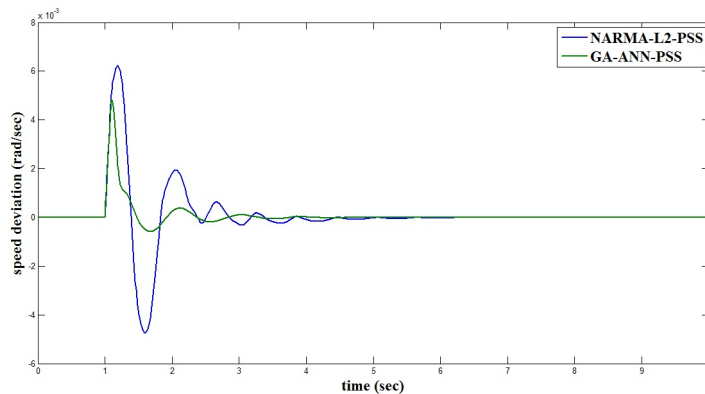


Figure 5.14: Case III: Speed response of NARMA-L2 and GA-ANN based PSS

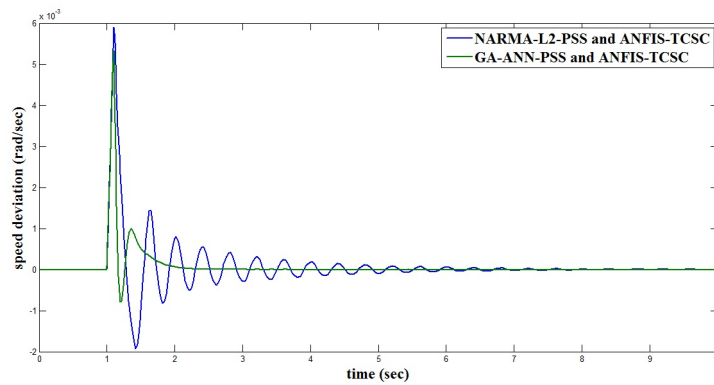


Figure 5.15: Case III: Speed response of NARMA-L2 and GA-ANN based PSS and ANFIS-TCSC

### 5.5.4 Case IV

$P_t = 0.9, Q_t = 0.12$ , Under the heavy loading condition a 10% mechanical change applied at 1s and removed at 5 s is considered. The system lost its stability at 4s without application of controllers, which has been shown by Figure 3.26. Figure 5.16 shows the response of  $\omega_m$  with individual and simultaneous application of PSS and TCSC. The simultaneous application of TCSC and PSS, and individual applications of PSS reduced the oscillations in the system and improved stability.

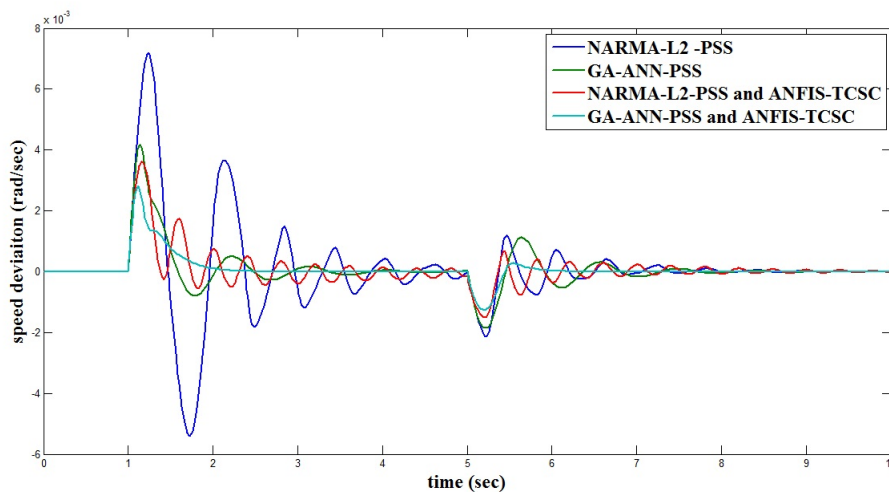


Figure 5.16: Case IV: Speed response of NARMA-L2 and GA-ANN based PSS and ANFIS-TCSC

### 5.5.5 Case V

$P_t = 1.2, Q_t = 0.2$ , A 0.1p.u. change in reference input voltage is applied at 1 s and removed at 5 s. The response of the  $\omega_m$  without and with presence of controllers has been shown in Figure 3.30 and 5.17 respectively. Figure 5.17 shows that GA-ANN-PSS has been produced better response than NARMA-L2-PSS. Simultaneous application of GA-ANN-PSS and ANFIS-TCSC have been produced best response compared to other controllers

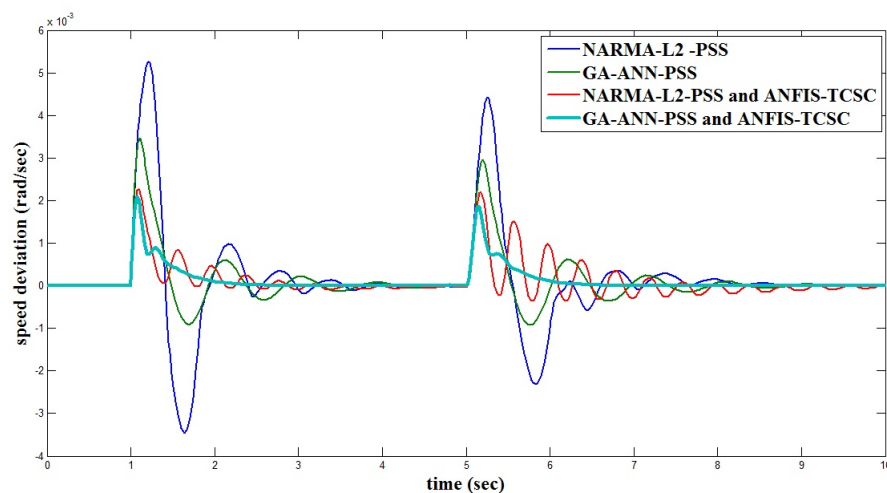


Figure 5.17: Case V: Speed response of NARMA-L2 and GA-ANN based PSS and ANFIS-TCSC

### 5.5.6 Case VI

$P_t = 0.75, Q_t = 0.1$ , In this case another severe disturbance is considered. One of the transmission lines is permanently tripped at 1 sec. The line reactance is significantly increased. The speed response for the above contingency has been shown in Figure 3.34 and 5.18 without and with controller respectively.

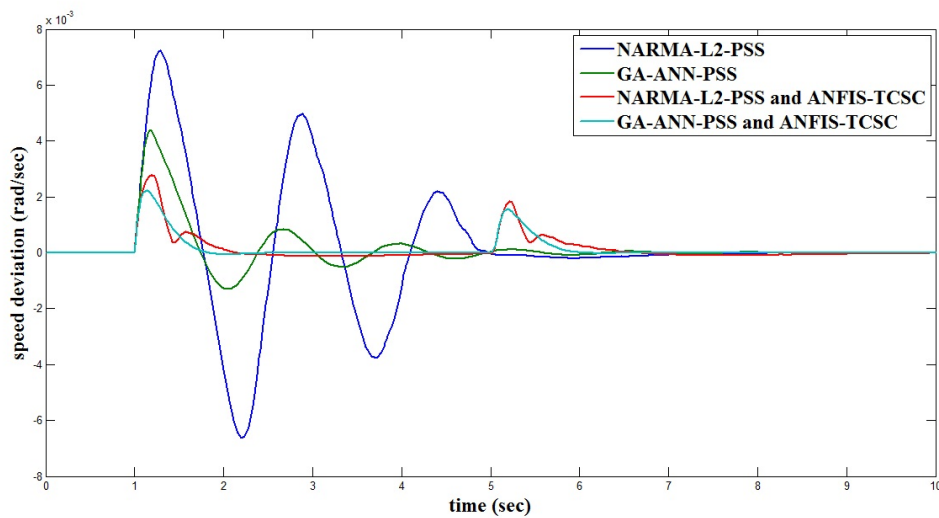


Figure 5.18: Case VI: Speed response of NARMA-L2 and GA-ANN based PSS and ANFIS-TCSC

## 5.6 Simulation of System with Intelligent Techniques based PSS and ANFIS-TCSC

Here five different types of intelligent controllers based PSSs have been tested under the heavy loading condition. For case I to case III, the operating condition  $P_t = 1.2, Q_t = 0.2$  and for case IV the operating condition  $P_t = 0.75, Q_t = 0.1$  have been selected for performance assessment of GA-CPSS, LMNN-PSS, ANFIS-PSS, NARMA-L2-PSS and GA-ANN-PSS with dynamic power system under different contingencies. For various cases, all intelligent techniques based PSS are tested with ANFIS-TCSC. The ANFIS-TCSC has been selected because its performance is better than compared to the GA-TCSC and LMNN-TCSC. ANFIS-TCSC has not required to tune for each and every operating conditions like GA-TCSC hence ANFIS-TCSC is better choice for simultaneous application with PSS.

### 5.6.1 Case I

$P_t = 1.2, Q_t = 0.2$ , A 10% mechanical change applied at 1s and removed at 5 s is considered. The speed response with five different types of intelligent techniques based PSS has been shown in Figure 5.19. Figure 5.20 shows all the intelligent PSS applied with ANFIS-TCSC.

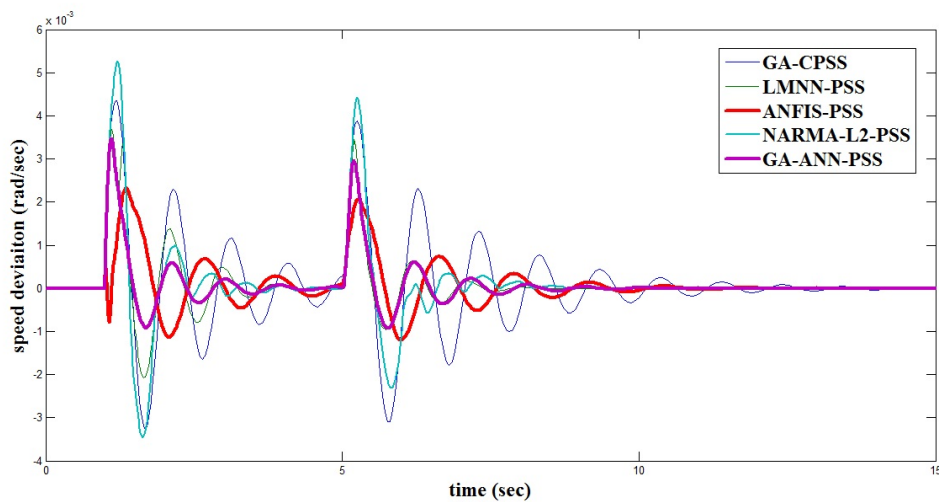


Figure 5.19: Case I: All Intelligent Techniques based PSS

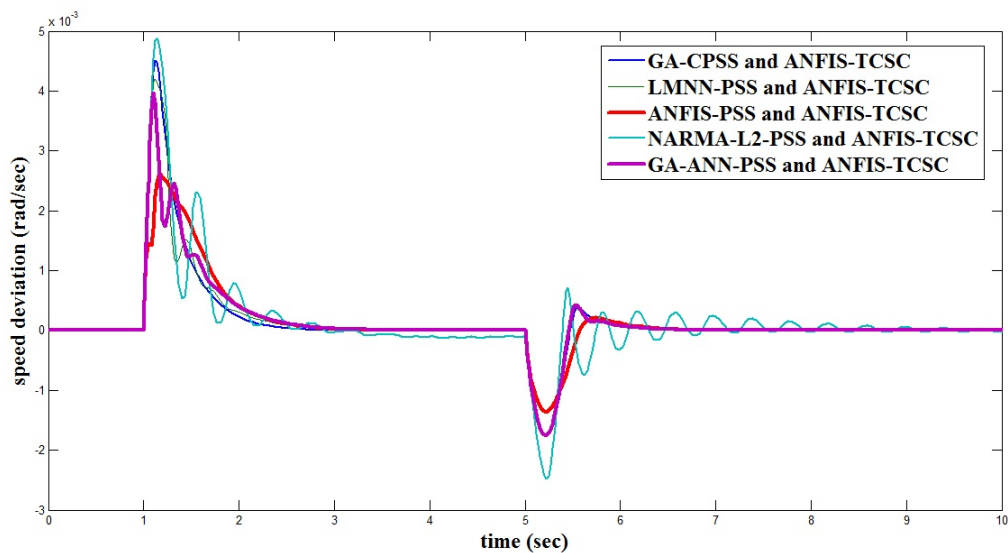


Figure 5.20: Case I: ANFIS-TCSC with Intelligent Techniques based PSS

### 5.6.2 Case II

$P_t = 1.2, Q_t = 0.2$ , A 0.1p.u. change in reference input voltage is applied at 1 s and removed at 5 s. The speed response with five different types of intelligent techniques based PSS has been shown in Figure 5.21. Figure 5.22 shows all the intelligent techniques based PSS applied with ANFIS-TCSC.

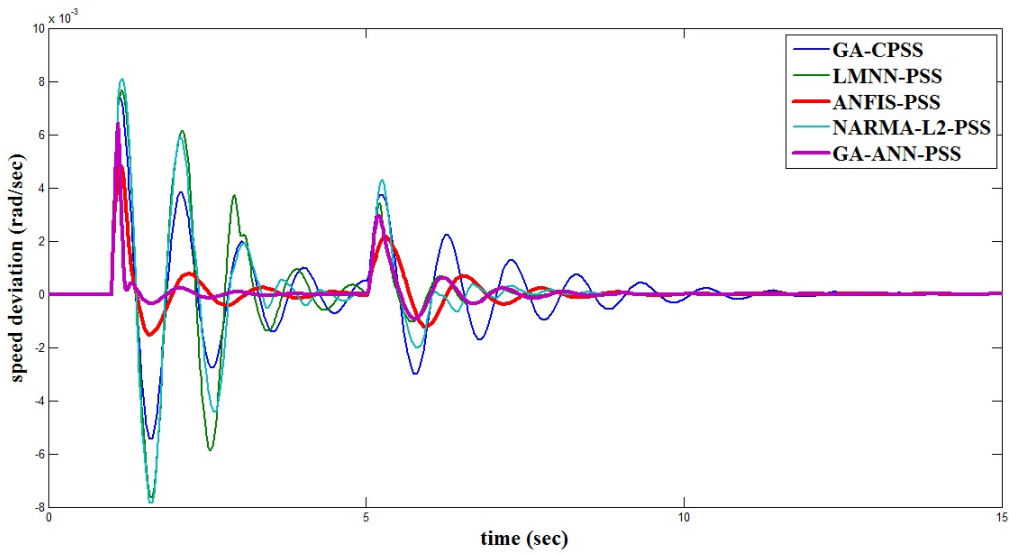


Figure 5.21: Case II: All Intelligent Techniques based PSS

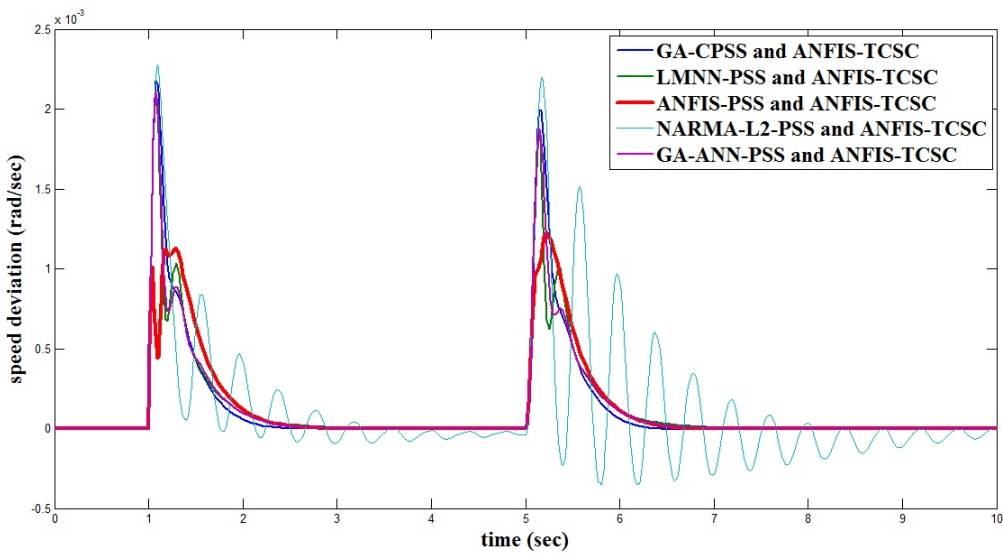


Figure 5.22: Case II: ANFIS-TCSC with Intelligent Techniques based PSS

### 5.6.3 Case III

$P_t = 1.2, Q_t = 0.2$ , A three phase fault is created at 1 s at the sending end of one of the circuits of the transmission line and cleared after 100ms. The speed response with five different types of intelligent techniques based PSS has been shown in Figure 5.23. Figure 5.24 shows the all intelligent techniques based PSS applied with ANFIS-TCSC.

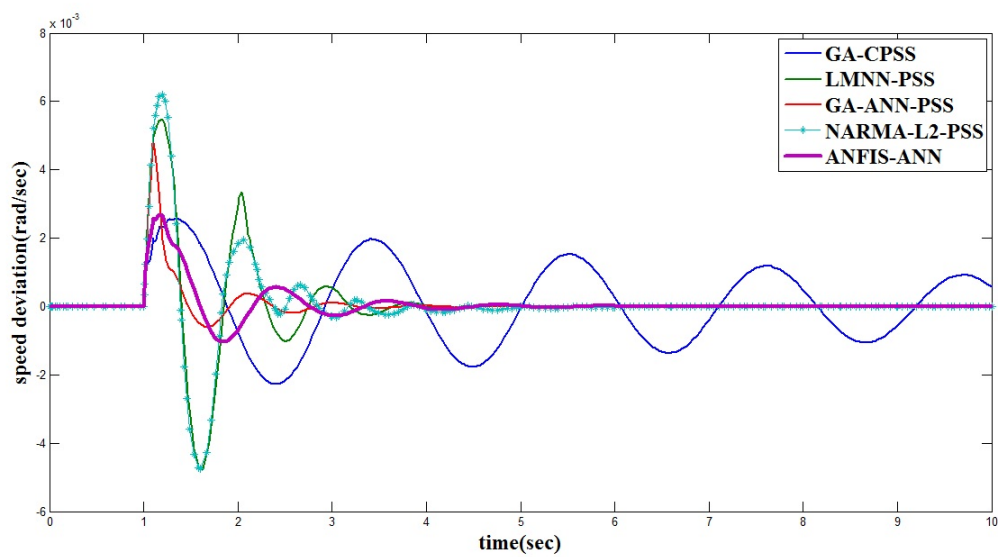


Figure 5.23: Case III: All Intelligent Techniques based PSS

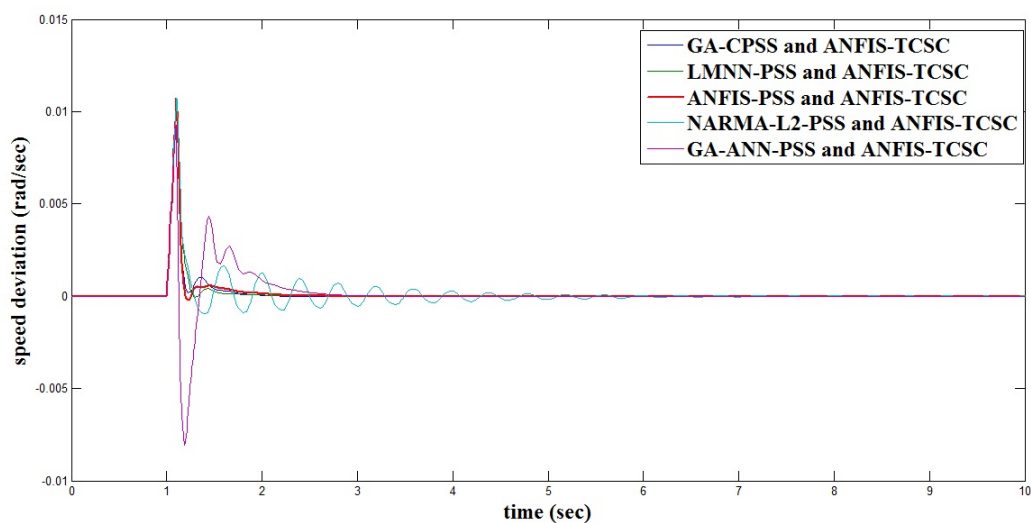


Figure 5.24: Case III: ANFIS-TCSC with Intelligent Techniques based PSS

### 5.6.4 Case IV:

$P_t = 0.75, Q_t = 0.1$ , A fault is created at 1 s at the middle of one transmission line and cleared after 50ms by disconnection of the faulted line, then successfully reclosed at 5s. Figure 5.25 shows the speed response with five different types of intelligent techniques based PSS. All intelligent techniques based PSS applied with ANFIS-TCSC has been shown in Figure 5.26.

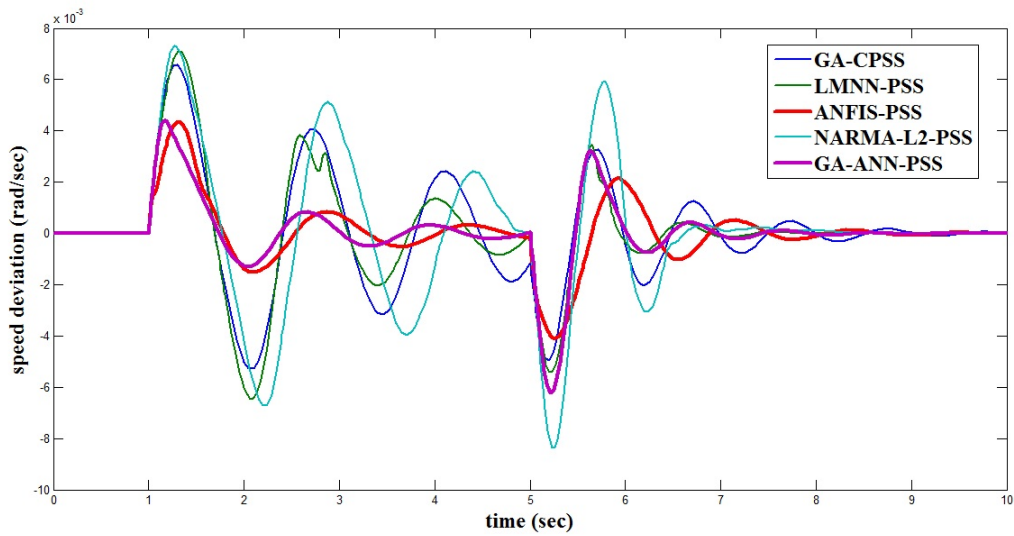


Figure 5.25: Case IV: All Intelligent Techniques based PSS

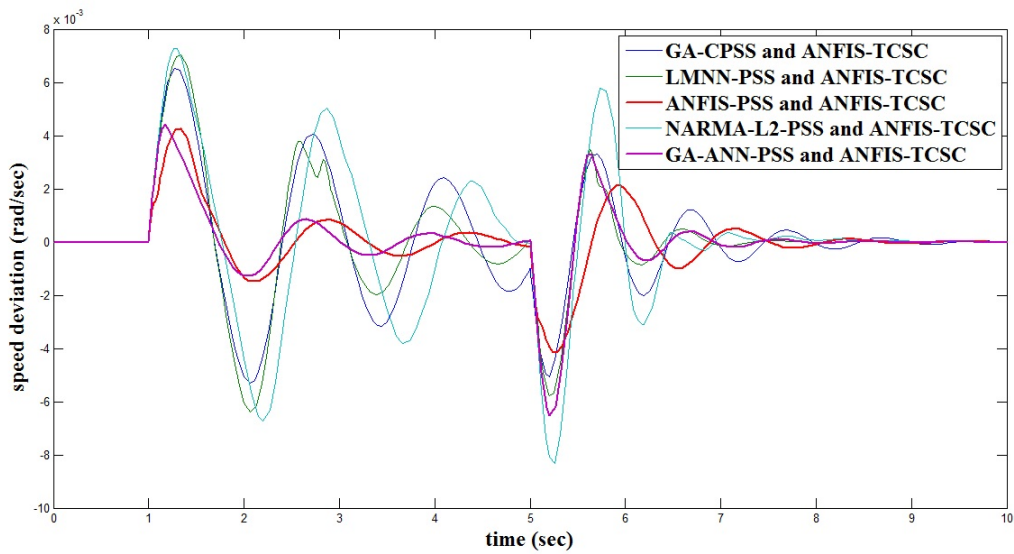


Figure 5.26: Case IV: ANFIS-TCSC with Intelligent Techniques based PSS

## 5.7 Conclusion

In this study, the smart control strategies based TCSC damping controller and PSS have been designed. The NARMA-L2 and GA-ANN based PSS, and simultaneously ANFIS-TCSC and PSS have been applied to the dynamical power system. The non-linear simulations have been carried out for detailed analysis of the stability of the power system. The time responses of speed deviation obtained by intelligent techniques based controller have been compared to the conventional power system stabilizer. Four different operating conditions are taken and the response of rotor speed deviation has been analyzed under different types of the disturbances and faults.

From the non - linear analysis,

1. Without the application of the controllers in the system, the oscillations in rotor speed deviation has been observed. Under the heavy loading condition, it has been observed that the active power and reactive power are increased; the oscillation in speed deviation is continuously growing which creates the instability of the system. The smart damping controllers have been greatly diminished oscillations in system.
2. Conventional power system stabilizer doesn't produce satisfactory response under the different operating conditions. While simultaneous application of ANFIS -TCSC and PSS have provided very good damping characteristics compared to the individual application of PSS and almost eliminated the oscillations in system.
3. Figures have shown that individual application of GA-ANN-PSS produces better response compare to the individual NARMA-L2-PSS.
4. Under the different loading conditions, It has been observed that simultaneous application of GA-ANN-PSS and ANFIS-TCSC produce better response compared to the simultaneous application of NARMA-L2-PSS and ANFIS-TCSC. It improved the time response parameters such as settling time, rise time and delay time appreciably and decreased the overshoot in the system.

In section (5.6), different Intelligent techniques based PSS are tested under heavy loading

conditions. Simultaneous ANFIS-TCSC with all PSS are also tested under heavy loading conditions. Following results are obtained from detailed study:

1. The GA-CPSS, ANFIS-ANN and GA-ANN are produced better response compared to the LMNN-PSS and NARMA-L2-PSS.
2. But GA-CPSS required different optimized parameters under different operating conditions and GA-ANN has needed more time for training of neural network. While ANFIS-PSS has been produced fast, adaptive and satisfactory response with less number of training data.
3. From figures (5.19) to (5.26), it has been observed that the ANFIS-TCSC produces better response with GA-CPSS, ANFIS-PSS and GA-ANN-PSS compared to the NARMA-L2-PSS and LMNN-PSS.
4. Finally it has been concluded that simultaneous application of ANFIS-TCSC with ANFIS-PSS produced good damping characteristics under all operating conditions and disturbances in power system.

# Chapter 6

## Design of Ancillary Controllers for Restructured Electric Market

### 6.1 Introduction

This chapter presents the application of ancillary services [54, 55, 25] such as power system stabilizers and thyristor control series capacitor in two area deregulated electric market with load frequency control loop. The first order linear model and fourth order model of synchronous machines have been considered for the performance evaluation of the dynamical two area power system. Fourth order model have been considered in the company of automatic voltage regulators. Both the power system stabilizers and thyristor control series capacitor have been simultaneously designed by genetic algorithm and their optimal parameters have been evaluated. The adaptive neuro fuzzy inference system based multiple power system stabilizer and series capacitor have been applied to multiple control area under deregulated electric environment. The distribution participation matrix has been considered according to the various correlative conditions of generating companies and distribution companies. To reflect the effectiveness of power system stabilizers and thyristor control series capacitor in two area of deregulated system, eigen value analysis and non-linear simulation have been performed using linear and non linear model of the synchronous machine respectively.

## 6.2 Restructured Power System

The traditional two area system of AGC has been modified in restructured electric market [92, 57, 32] to consider the effect of bilateral contracts. The dynamic response of the LFC has been analyzed under effect of bilateral contracts. In deregulated market, DISCO participation factor matrix (DPM) is introduced, which shows different contracts between GENCOs and DISCOs in the two area control loop. DPM consists  $n \times m$  matrix, where  $n$  is the number of GENCOs and  $m$  is the number of DISCOs in control area. DPM is composed of contract participation factor (cpf);  $cpf_{ij}$  corresponds to the fraction of the total load power contacted by DISCO  $j$  from GENCO  $i$ . Figure 6.1 shows schematic diagram of two GENCOs and two DISCOs in each area, according to that, the DPM is described by equation (6.1). The two area interconnected system with TCSC in series with tie line has been shown in Figure 6.2.

$$DPM = \begin{bmatrix} cpf_{11} & cpf_{12} & cpf_{13} & cpf_{14} \\ cpf_{21} & cpf_{22} & cpf_{23} & cpf_{24} \\ cpf_{31} & cpf_{32} & cpf_{33} & cpf_{34} \\ cpf_{41} & cpf_{42} & cpf_{43} & cpf_{44} \end{bmatrix} \quad (6.1)$$

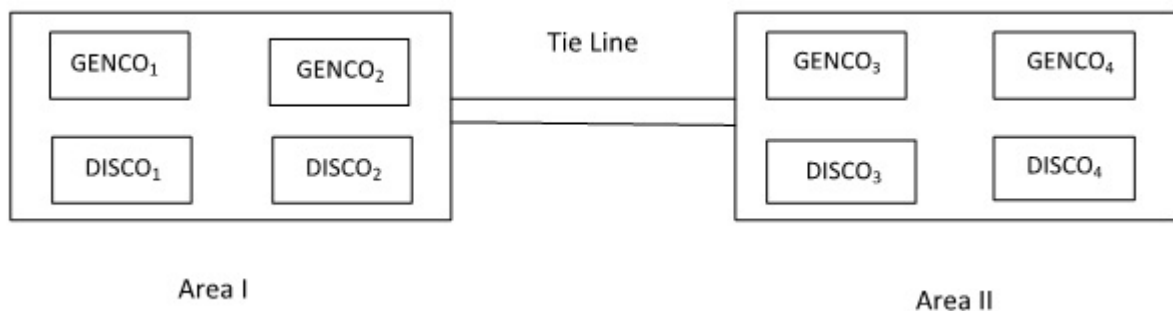


Figure 6.1: Schematic Diagram of Two area system in Restructured Market

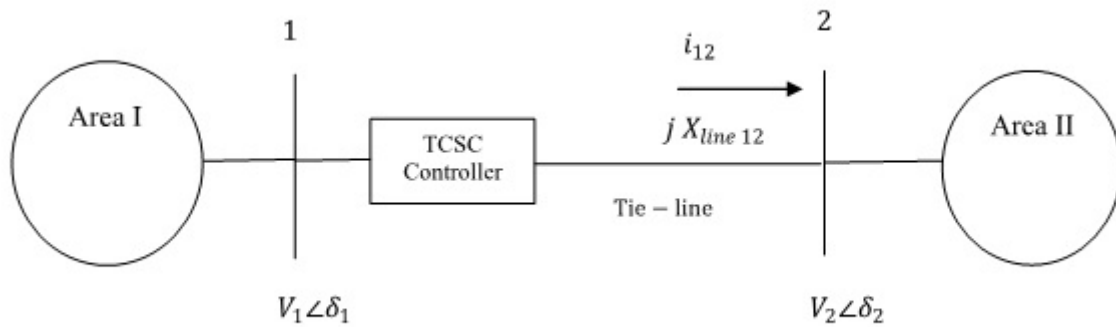


Figure 6.2: Restructured System with TCSC in Series with Tie-Line

Many GENCOs in each area so area control error (ACE) has been distributed among GENCOs. The coefficients that distribute ACE to several GENCOs are called ACE participation factors. According to their participation in the AGC, the ACE participation factors (apfs) distributes ACE to several GENCOs. In deregulated market, a DISCO prefers a particular GENCO for load flow. The scheduled steady state power flow on the tie-line can be given as

$\Delta P_{tie12}^{scheduled} = (\text{Demand of DISCOs in area 2 from GENCOs in area 1}) - (\text{Demand of DISCOs in area 1 from GENCOs in area 2})$

i.e.

$$\Delta P_{tie12}^{scheduled} = cpf_{12} \Delta P_{L2} - cpf_{21} \Delta P_{L1} \quad (6.2)$$

The tie line power error at any time is defined as :

$$\Delta P_{tie12}^{error} = \Delta P_{tie12}^{actual} - \Delta P_{tie12}^{scheduled} \quad (6.3)$$

When steady state is reached,  $\Delta P_{tie12}^{error}$  vanishes.

In the AGC scheme, contracted load is forward through the DPM matrix to GENCO set points. The actual load affects system dynamics via the input  $\Delta P_{L,LOC}$  to the blocks of the power system. The difference between actual and contracted load demands may results in a frequency deviation that will drive AGC to redispatch GENCOs according to ACE participation factors.

The ACE provides steady state response under normal conditions, but system performance gets affected under the dynamic environment of power system only with ACE in multiarea AGC. Therefore multiple PSS have been suggested with LFC loop. Moreover, in the restructured electric market, various kinds of large capacity equipments and fast power consumption can cause serious problem of frequency oscillation. If system has been not provided with adequate damping, then the oscillation of system frequency may sustain and grow hence, resulting in serious stability problem. The TCSC may be used as a new ancillary service for the stabilization of frequency oscillation of an interconnected thermal power system.

### 6.3 Design of TCSC Controller with First Order Power System Model

In this section, frequency deviation in two area restructured power system has been analyzed with TCSC controller. The TCSC controller has been used for controlling of tie-line power exchange between two area. The parameters of TCSC controller has been tuned using genetic algorithm. The ANFIS based TCSC controller has been designed from GA based controller. The first order model of power system with turbine and governor system are considered for linear analysis of the two area system. The eigen values analysis have been carried out for stability verification of two area AGC with FACTS controller. The simulation has been performed for analysis of frequency deviation and tie line power in each area with intelligent control techniques under consideration of different  $DPM$ . The load frequency controller has controlled the control valves associated with turbine at load variations [15]. Here it is assumed that small variations of load permit the linearization of system equations. The governor and turbine of the system is represented by first order transfer function. The power system is represented by first order model. Here the generator model considered in the present study are described below:

### 6.3.1 Power system model

The power system loads are composite of a variety of electrical devices. The frequency dependent characteristics of a composite load can be expressed as

$$\Delta P_e = \Delta P_L + D\Delta\omega_m \quad (6.4)$$

where  $\Delta P_L$  =non frequency sensitive load change,  $D\Delta\omega_m$  =frequency sensitive load change,  $D$  =load damping constant.

The damping constant is expressed as a percentage change in load for one percent change in frequency. The power system block diagram including the effect of the load damping is shown in Figure 6.3.

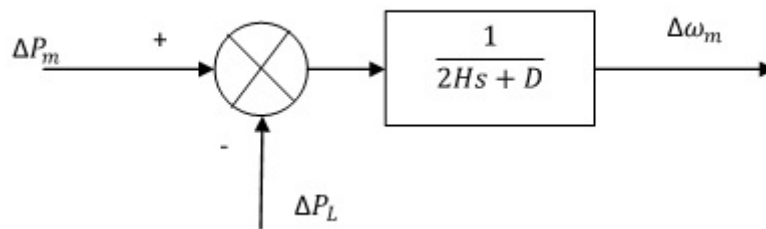


Figure 6.3: First Order Power System

### 6.3.2 Tie Line Power Flow Model With TCSC

Figure 6.2 shows the schematic diagram of two area interconnected thermal system with TCSC in series with the tie-line. Therefore real power flow can be controlled to mitigate the frequency oscillation and enhance power system stability. Without TCSC, the incremental tie line power flow from area 1 to area 2 under open market system can be expressed as equation

$$\Delta P_{tie12}(s) = \frac{2\pi T_{12}}{s} (\Delta F_1(s) - \Delta F_2(s)) \quad (6.5)$$

where  $T_{12}$  is the synchronising constant without TCSC.

When TCSC has been placed in series with the tie line as shown in Figure (6.2), the line resistance is to be zero. Current flowing from area 1 to area 2 is  $i_{12}$  and power flow equation can be written as follow:

$$P_{tie12} = \frac{|V_1| |V_2| \sin(\delta_1 - \delta_2)}{X_{net}} \quad (6.6)$$

where  $X_{net} = X_{line12} - X_{TCSC}$

Linearising equation (6.6) using  $\Delta X_{net} = -\Delta X_{TCSC}$ , equation (6.7) can be obtained. In equation (6.6) perturbing  $\delta_1, \delta_2$  from their nominal values  $\delta_1^0, \delta_2^0$  respectively, then

$$\Delta P_{tie12} = \frac{|V_1| |V_2|}{X_{net^0}} \cos(\delta_1^0 - \delta_2^0) \sin(\Delta\delta_1 - \Delta\delta_2) + \frac{|V_1| |V_2|}{X_{net^0}^2} \sin(\delta_1^0 - \delta_2^0) \Delta X_{TCSC} \quad (6.7)$$

But for a small change in real power load, the variation of bus voltage angles is very small. Therefore  $\sin(\Delta\delta_1 - \Delta\delta_2) \approx (\Delta\delta_1 - \Delta\delta_2)$ , so equation (6.7) is written as

$$\Delta P_{tie12} = \frac{|V_1| |V_2|}{X_{net^0}} \cos(\delta_1^0 - \delta_2^0) (\Delta\delta_1 - \Delta\delta_2) + \frac{|V_1| |V_2|}{X_{net^0}^2} \sin(\delta_1^0 - \delta_2^0) \Delta X_{TCSC} \quad (6.8)$$

Above equation is organized as follow:

$$\Delta P_{tie12} = T_{12} (\Delta\delta_1 - \Delta\delta_2) + K_{p1} \Delta X_{TCSC} \quad (6.9)$$

where  $T_{12} = \frac{|V_1| |V_2|}{X_{net^0}} \cos(\delta_1^0 - \delta_2^0) (\Delta\delta_1 - \Delta\delta_2)$  and  $K_{p1} = \frac{|V_1| |V_2|}{X_{net^0}^2} \sin(\delta_1^0 - \delta_2^0)$ , so tie line power can be controlled by  $\Delta X_{TCSC}$ .

But

$$\Delta\delta_1 = 2\pi \int \Delta f_1 dt \quad (6.10)$$

and

$$\Delta\delta_2 = 2\pi \int \Delta f_2 dt \quad (6.11)$$

Equation (6.9) is modified

$$\Delta P_{tie12} = T_{12} (2\pi \int \Delta f_1 dt - 2\pi \int \Delta f_2 dt) + K_{p1} \Delta X_{TCSC} \quad (6.12)$$

Laplace transform of equation (6.12)

$$\Delta P_{tie12} = \frac{2\pi T_{12}}{s} (\Delta F_1(s) - \Delta F_2(s)) + K_{p1} \Delta X_{TCSC} \quad (6.13)$$

As per equation (6.13), it can be observed that the tie line power can be controlled by line reactance. The stability loop of TCSC controller has been used for controlling the tie line power. The  $\Delta X_{TCSC}$  can be represented by

$$\Delta X_{TCSC}(s) = \frac{K_C T_{W1} s}{1 + T_{W1} s} \left[ \frac{(1 + T_{1T} s)(1 + T_{2T} s)}{(1 + T_{3T} s)(1 + T_{4T} s)} \right] \Delta Error(s) \quad (6.14)$$

If speed deviation  $\Delta \omega_{m1}$  is sensed, it can be used as control signal, so  $\Delta Error = \Delta \omega_{m1}$  to TCSC unit to control  $\Delta X_{TCSC}$ , which will change tie line power flow between two area and assist in stabilizing the frequency oscillations, Thus

Thus equation (6.13) can be written

$$\Delta P_{tie12} = \frac{2\pi T_{12}}{s} (\Delta F_1(s) - \Delta F_2(s)) + K_{p1} \frac{K_C T_{w1} s}{1 + T_{w1} s} \left[ \frac{(1 + T_{1T} s)(1 + T_{2T} s)}{(1 + T_{3T} s)(1 + T_{4T} s)} \right] \Delta \omega_1 \quad (6.15)$$

$$\Delta P_{tie12} = \frac{T_{12}}{s} (\Delta \omega_{m1}(s) - \Delta \omega_{m2}(s)) + K_{TCSC} \frac{T_{w1} s}{1 + T_{w1} s} \left[ \frac{(1 + T_{1T} s)(1 + T_{2T} s)}{(1 + T_{3T} s)(1 + T_{4T} s)} \right] \Delta \omega_1 \quad (6.16)$$

where  $K_{TCSC} = K_C K_{p1}$

But in the restructured market system the actual tie line power flow also includes the demand from DISCOs in one area to GENCOs in another area. It can be represented as

$\Delta P_{tie12,actual} = \Delta P_{tie12}(s) + (\text{demand of DISCOS in area 2 from GENCOs in area 1}) - (\text{demand of DISCOS in area 1 from GENCOs in area 2})$ .

### 6.3.3 Block Diagram and Model of Interconnected Two area System

Figure 6.4 represents block diagram of intelligent controller based TCSC in two area power system under restructured market. Figure 6.4 shows the transfer functions of power system, governor and turbine system with ACE and regulator system in two area AGC under open market scenario. The closed loop system in Figure 6.4 is characterized in state space form as

$\dot{x} = A^{decl}x + B^{decl}u$ . The two area system is represented by  $16 \times 16$  matrix with inclusion of TCSC. The state diagram of TCSC as shown in Figure 2.10 has been used for consideration of modeling for two area system with TCSC controller.

where  $x$  is the state vector and  $u$  is the vector of power demands of the DISCOs.  $A^{decl}$  and  $B^{decl}$  are developed from Figure 6.4. The  $A^{decl}$  is also defined as stability matrix. The eigen values of the system can be calculated using stability matrix. The eigen values shows the position of closed loop poles in s-plane, through these values effectiveness of TCSC in AGC system can be verified.  $A^{decl}$  and  $B^{decl}$  are represented by equation (6.17) and (6.18) respectively. The state matrix  $x$  of variables and input matrix  $u$  are mention.

$$A^{decl} = \begin{bmatrix} A_1 & A_2 \\ A_3 & A_4 \end{bmatrix}_{16 \times 16} \quad (6.17)$$

Where,

$$A_1 = \begin{bmatrix} -\frac{1}{T_{p1}} & 0 & \frac{K_{p1}}{T_{p1}} & \frac{K_{p1}}{T_{p1}} & 0 & 0 & 0 & 0 \\ 0 & -\frac{1}{T_{p2}} & 0 & 0 & \frac{K_{p1}}{T_{p2}} & \frac{K_{p2}}{T_{p2}} & 0 & 0 \\ 0 & 0 & -\frac{1}{T_{t1}} & 0 & 0 & 0 & -\frac{1}{T_{t1}} & 0 \\ 0 & 0 & 0 & -\frac{1}{T_{t2}} & 0 & 0 & 0 & -\frac{1}{T_{t2}} \\ 0 & 0 & 0 & 0 & \frac{1}{-T_{t3}} & 0 & 0 & 0 \\ 0 & 0 & 0 & 0 & 0 & \frac{1}{-T_{t4}} & 0 & 0 \\ -\frac{1}{2\pi R_1 T_{g1}} & 0 & 0 & 0 & 0 & 0 & -\frac{1}{T_{g1}} & 0 \\ -\frac{1}{2\pi R_1 T_{g2}} & 0 & 0 & 0 & 0 & 0 & 0 & -\frac{1}{T_{g2}} \end{bmatrix}$$

$$A_2 = \begin{bmatrix} 0 & 0 & 0 & 0 & 0 & 0 & -\frac{K_{p1}}{T_{p1}} & -\frac{K_{p1}}{T_{p1}} \\ 0 & 0 & 0 & 0 & 0 & 0 & -\frac{a_{12}K_{p1}}{T_{p1}} & -\frac{a_{12}K_{p1}}{T_{p2}} \\ 0 & 0 & 0 & 0 & 0 & 0 & 0 & 0 \\ 0 & 0 & 0 & 0 & 0 & 0 & 0 & 0 \\ -\frac{1}{T_{t3}} & 0 & 0 & 0 & 0 & 0 & 0 & 0 \\ 0 & -\frac{1}{T_{t4}} & 0 & 0 & 0 & 0 & 0 & 0 \\ 0 & 0 & -\frac{K_1 a_{p1} f_1}{T_{g1}} & 0 & 0 & 0 & 0 & 0 \\ 0 & 0 & -\frac{K_1 a_{p1} f_2}{T_{g2}} & 0 & 0 & 0 & 0 & 0 \end{bmatrix}$$

$$A_3 = \begin{bmatrix} 0 & -\frac{1}{2\pi R_1 T_{g3}} & 0 & 0 & 0 & 0 & 0 & 0 \\ 0 & -\frac{1}{2\pi R_1 T_{g4}} & 0 & 0 & 0 & 0 & 0 & 0 \\ \frac{B_1}{2\pi} & 0 & 0 & 0 & 0 & 0 & 0 & 0 \\ 0 & \frac{B_2}{2\pi} & 0 & 0 & 0 & 0 & 0 & 0 \\ \frac{-Kc}{T_{p1}} & 0 & \frac{K_{p1}Kc}{T_{p1}} & \frac{K_{p1}Kc}{T_{p1}} & 0 & 0 & 0 & 0 \\ \frac{(KcT_{1T})}{T_{2T}T_{p1}} & 0 & \frac{T_{1T}K_{p1}Kc}{T_{2T}T_{p1}} & \frac{T_{1T}K_{p1}Kc}{T_{2T}T_{p1}} & 0 & 0 & 0 & 0 \\ a & 0 & b & c & 0 & 0 & 0 & 0 \\ \frac{T_{12}}{2\pi} & -\frac{T_{12}}{2\pi} & 0 & 0 & 0 & 0 & 0 & 0 \end{bmatrix}$$

$$A_4 = \begin{bmatrix} -\frac{1}{T_{g3}} & 0 & 0 & -\frac{K_2apf_3}{T_{g3}} & 0 & 0 & 0 & 0 \\ 0 & -\frac{1}{T_{g4}} & 0 & -\frac{K_2apf_4}{T_{g4}} & 0 & 0 & 0 & 0 \\ 0 & 0 & 0 & 0 & 1 & 0 & 0 & 0 \\ 0 & 0 & 0 & 0 & -1 & 0 & 0 & 0 \\ 0 & 0 & 0 & 0 & -\frac{1}{T_w} & 0 & 0 & -\frac{K_{p1}Kc}{T_{p1}} \\ 0 & 0 & 0 & 0 & \frac{1/T_{2T}-T_{1T}}{T_{2T}T_w} & \frac{1}{T_{2T}} & 0 & \frac{K_{p1}KcT_{1T}}{T_{p1}T_{2T}} \\ 0 & 0 & 0 & 0 & m & n & -\frac{1}{4T} & p \\ 0 & 0 & 0 & 0 & 0 & 0 & 1 & 0 \end{bmatrix}$$

Where,

$$a = -\frac{KcT_{1T}T_{3T}}{T_{2T}T_{p1}T_{4T}}, b = \frac{T_{1T}K_{p1}KcT_{3T}}{T_{2T}T_{p1}T_{4T}}, c = \frac{KcK_{p1}T_{1T}T_3}{T_{4T}T_{p1}T_{2T}}, m = \frac{T_{3T}/T_{2T}T_{4T}}{T_1T_{3T}/T_{2T}T_{4T}T_w}, n = \frac{1/T_{4T}}{T_{3T}/(T_{2T}T_{4T})}, p = -\frac{KcT_{3T}T_1TK_{p1}}{T_{2T}T_{4T}T_{p1}}$$

$$B^{decl} = \begin{bmatrix} B_1 & B_2 \\ B_3 & B_4 \end{bmatrix}_{16 \times 6} \quad (6.18)$$

Where,

$$B_1 = \begin{bmatrix} -\frac{K_{p1}}{T_{p1}} & -\frac{K_{p1}}{T_{p1}} & 0 \\ 0 & 0 & -\frac{K_{p2}}{T_{p2}} \\ 0 & 0 & 0 \\ 0 & 0 & 0 \\ 0 & 0 & 0 \\ 0 & 0 & 0 \\ \frac{cpf_{11}}{T_{g1}} & \frac{cpf_{12}}{T_{g1}} & \frac{cpf_{13}}{T_{g1}} \\ \frac{cpf_{21}}{T_{g2}} & \frac{cpf_{21}}{T_{g2}} & \frac{cpf_{21}}{T_{g2}} \end{bmatrix}$$

$$B_2 = \begin{bmatrix} 0 & -\frac{Kp1}{Tp1} & 0 \\ -\frac{Kp2}{Tp2} & 0 & -\frac{Kp2}{Tp2} \\ 0 & 0 & 0 \\ 0 & 0 & 0 \\ 0 & 0 & 0 \\ 0 & 0 & 0 \\ \frac{cpf14}{Tg1} & 0 & 0 \\ \frac{cpf21}{Tg2} & 0 & 0 \end{bmatrix}$$

$$B_3 = \begin{bmatrix} \frac{cpf31}{Tg3} & \frac{cpf31}{Tg3} & \frac{cpf31}{Tg3} \\ \frac{cpf41}{Tg4} & \frac{cpf41}{Tg4} & \frac{cpf41}{Tg4} \\ cpf31 + cpf41 & cpf32 + cpf42 & -(cpf13 + cpf23) \\ -(cpf31 + cpf41) & -(cpf32 + cpf42) & cpf13 + cpf23 \\ 0 & 0 & 0 \\ 0 & 0 & 0 \\ 0 & 0 & 0 \\ 0 & 0 & 0 \end{bmatrix}$$

$$B_4 = \begin{bmatrix} \frac{cpf31}{Tg3} & 0 & 0 \\ \frac{cpf41}{Tg4} & 0 & 0 \\ -(cpf14 + cpf24) & 0 & 0 \\ cpf14 + cpf24 & 0 & 0 \\ 0 & 0 & 0 \\ 0 & 0 & 0 \\ 0 & 0 & 0 \\ 0 & 0 & 0 \end{bmatrix}$$

Where,

$$x = \left[ \Delta\omega_1 \quad \Delta\omega_2 \quad \Delta P_{GV1} \quad \Delta P_{GV2} \quad \Delta P_{GV3} \quad \Delta P_{GV4} \quad \Delta P_{M1} \quad \Delta P_{M2} \right]' \text{Contd...}$$

$$x = \left[ \Delta P_{M3} \quad \Delta P_{M4} \quad \int ACE_1 dt \quad \int ACE_1 dt \quad \Delta X_1 \quad \Delta X_2 \quad \Delta X_{TCSC} \quad \Delta P_{tie1-2} \right]'_{16 \times 1}$$

$$u = \left[ \Delta P_{L1} \quad \Delta P_{L1} \quad \Delta P_{L3} \quad \Delta P_{L4} \quad \Delta P_{L1,LOC} \quad \Delta P_{L2,LOC} \right]'_{6 \times 1}$$

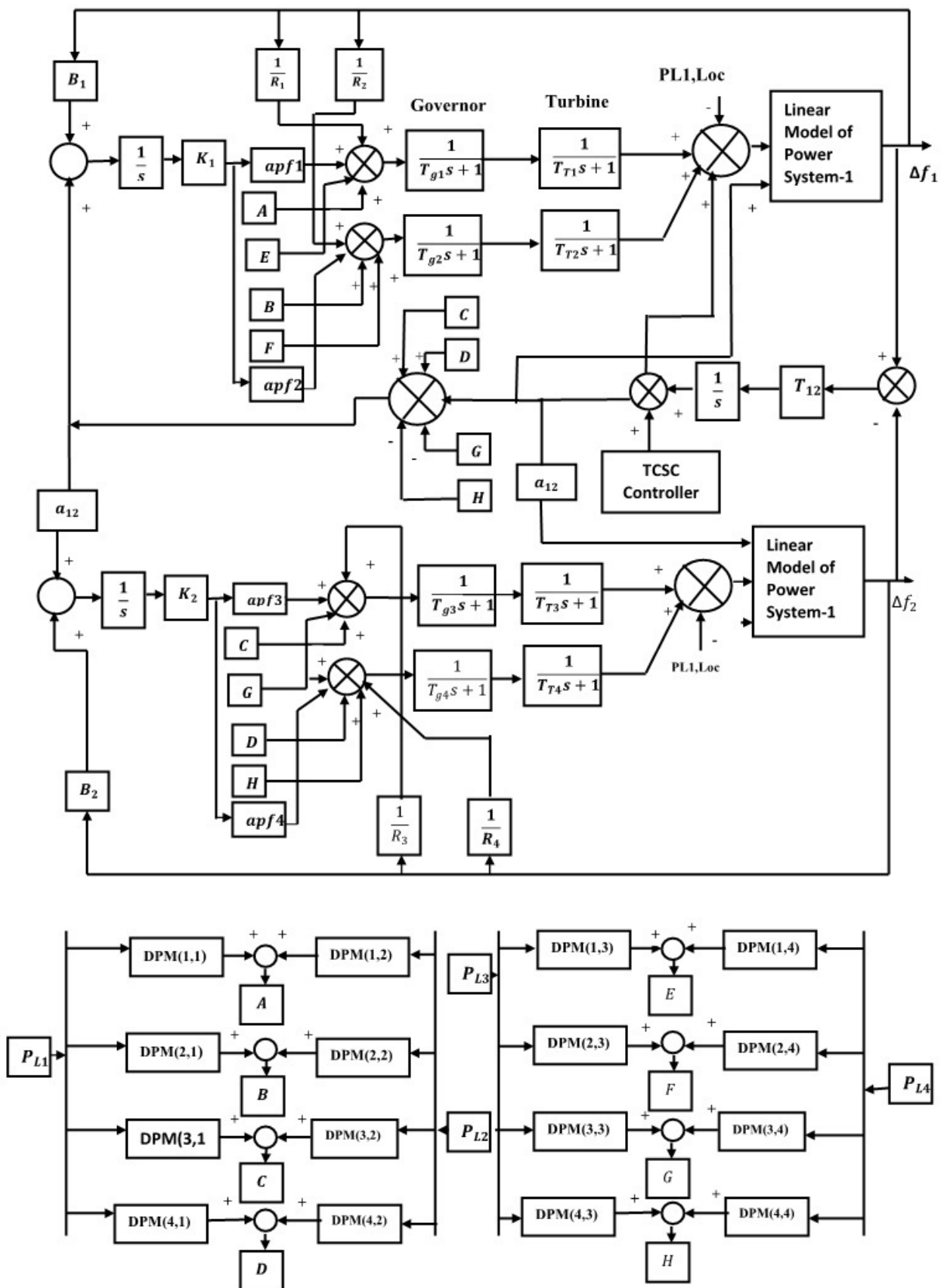


Figure 6.4: Intelligent techniques based TCSC for two area system under restructured market

### 6.3.4 GA- tie line TCSC Controller: Problem Formulation and Optimization Function

The stability loop equation (2.89) has been used for frequency stabilization. The input signal rotor speed deviation of area 1 or area 2 has been chosen for TCSC proposed controller. The equation (6.16) consists wash out filter time constant  $T_{w1}$ , gain  $K_{TCSC}$  and time constant of phase compensator  $T_{1T}, T_{2T}, T_{3T}$  and  $T_{4T}$ , which provides appropriate phase-lead characteristics to compensate for the phase lag between input and output signals. Thus, five parameters such as gain  $K_{TCSC}$  and time constant parameter  $T_{1T}, T_{2T}, T_{3T}, T_{4T}$  are required to be optimized for the optimal design of TCSC frequency controller. For TCSC, the time constant of wash out filter  $T_{w1}$  has been selected to be 10. The objective of LFC with tie line TCSC controller is, to reduce the oscillatory frequency in rotor mode and to minimize the tie line power oscillation in both control area. The goal can be achieved after minimizing the optimization function  $J$ , which is described by equation (6.19). The optimization function has been developed such that the damping factor of rotor mode in LFC be improved and minimization of real part of the eigen values associated with the rotor mode. Hence time response parameters such as settling time to be improved and overshoots to be reduced. The Time Multiplied by Absolute Error (ITAE) has been used as the performance index. The optimization function  $J$  follows the optimized performance of TCSC controlled system. The gains for the TCSC controller are adjusted such that the performance index be minimized. The performance index is calculated over a time interval  $T$ , normally in the region of, where  $t$  is the settling time of the system. The best system response is obtained when the tie line power controller TCSC parameters are optimized by minimizing the maximum eigen values over a certain range of operating conditions. The optimization flow chart for implementation of real coded GA is similar as shown in Figure 3.3. However, here only TCSC tie line controller parameters are required to be optimized as described by equations (6.20) to (6.24). The optimization function  $J$  is as follows :

$$J = \int_0^T t |\Delta\omega_{m1}(t)| dt \quad (6.19)$$

with

$$T_{1T}^{min} \leq T_{1T} \leq T_{1T}^{max} \quad (6.20)$$

$$T_{2T}^{min} \leq T_{2T} \leq T_{2T}^{max} \quad (6.21)$$

$$T_{3T}^{min} \leq T_{3T} \leq T_{4T}^{max} \quad (6.22)$$

$$T_{4T}^{min} \leq T_{4T} \leq T_{4T}^{max} \quad (6.23)$$

$$K_{TCSC}^{min} \leq K_{TCSC} \leq K_{TCSC}^{max} \quad (6.24)$$

### 6.3.5 ANFIS- Tie Line TCSC Controller

Here, GA-TCSC is replaced by the ANFIS based TCSC. The mathematical model of the two area LFC system with GA-TCSC as shown in Figure 6.4 has been used for the generation of the training data pair for the ANFIS-TCSC. The Takagi-Sugeno FIS is used for the design of ANFIS based TCSC. The ANFIS architecture and algorithm steps described by section (4.2) and section (4.3) have been implemented for designing of ANFIS based tie line TCSC respectively. The network has been trained using 1000 sample data, which are generated under the consideration of the different correlative conditions between GENCOs and DISCOs and different values of six inputs of the system. The two inputs and one output have been used for the training of ANFIS. The dynamic inputs are speed  $\Delta\omega_{m1}(t)$  and change in speed  $(\frac{\Delta d\omega_{m1}(t)}{dt})$ , and corresponding  $\Delta X_{TCSC}$  has been selected as output value of the ANFIS.

### 6.3.6 Simulation and Results

The model presented by Figure 6.4 has been used for stability analysis of the two area system with TCSC. The eigen values, damping factors and participation factors of the system are calculated using MATLAB programming. The objective function described by equations (6.20) to (6.24) have been optimized. The time domain simulation is performed and fitness value is determined through equation (6.19) for gain and time constant parameters of TCSC. By changing the GA parameters such as population size, crossover rate and function, mutation rate and function, number of generation, etc, the new set of gains and time constants have been developed and best fitness values have been selected. The optimized parameters of TCSC are tuned for expected solution which is given by Table 6.2. eigen values and damping factor without application of TCSC and with application of TCSC have been shown in Table 6.1.

Table 6.1: Eigen values without TCSC and with TCSC

	without TCSC		with TCSC	
	eigen values	$\zeta$	eigen values	$\zeta$
area 1	$0.2312 + 1.9285i$	-0.1191	$-0.0361 + 5.4791i$	0.0066
	$0.2312 - 1.9285i$	-0.1191	$-0.0361 - 5.4791i$	0.0066
area 2	$-0.5908 + 0.7397i$	0.6241	$-0.3780 + 0.9571i$	0.3673
	$-0.5908 - 0.7397i$	0.6241	$-0.3780 - 0.9571i$	0.3673

Table 6.2: Optimized Parameters of TCSC

Parameters	Values
$K_{TCSC}$	5.252
$T_{1T}$	0.01382
$T_{2T}$	0.01091
$T_{3T}$	0.01135
$T_{4T}$	0.01645

Attention to Table 6.1, Without TCSC, the eigen value associated with area 1 is positive and in area 2 is negative. With TCSC, eigen values and the damping factor associated to rotor mode in two area LFC have been significantly improved. hence, the TCSC tie line

power controller provides good stability to the multiple area power system and closed poles are far away in the left half of the s-plane using TCSC compared to without controller.

**Case I:**

A two area system is used to demonstrate the behavior of the AGC scheme with TCSC frequency stabilizer. The different cases [32] are considered according to the bilateral contract between GENCOs and DISCOs in restructured market. The comparison analysis between GA based TCSC and ANFIS based TCSC in restructured AGC scheme have been carried out. The data described by Appendix B are used for the simulation purpose. The governor and turbine units in each area assumed to be identical. In this case, the GENCOs in each area participate equally in AGC. ACE participation factors are  $apf_1 = 0.5, apf_2 = 0.5, apf_3 = 0.5, apf_4 = 0.5$ . Assume that the load change occurs only in area 1. Thus, the load is demanded only by DISCO1 and DISCO2. Load variation in area 1 is  $\Delta P_{L1} = 0.05$  p.u.,  $\Delta P_2 = 0.05$  p.u.,  $\Delta P_{L1,LOC} = 0.1$  p.u. are considered and no disturbances occur in area II. The optimal integral gain  $K_1 = 0.9$  and  $K_2 = 0.1$  are selected [76] The *DPM* is described by equation (6.25). Figure 6.5 shows the response of speed deviation without TCSC in both area. The response of speed deviation with GA and ANFIS based TCSC in both area has been shown in Figure 6.6 and 6.7 respectively. Figure 6.8 shows the tie line power oscillation response in both area with TCSC controller.

$$DPM = \begin{bmatrix} 0.50 & 0.50 & 0.00 & 0.00 \\ 0.50 & 0.50 & 0.00 & 0.00 \\ 0.00 & 0.00 & 0.00 & 0.00 \\ 0.00 & 0.00 & 0.00 & 0.00 \end{bmatrix} \quad (6.25)$$

**Case II:** In this case, where all the DISCOs contract with GENCOs for power as per *DPM* described by equation (6.26). ACE participation factors are  $apf_1 = 0.75, apf_2 = 0.25, apf_3 = 0.5, apf_4 = 0.5$ . The load variation are considered such as  $\Delta P_{L1} = 0.01$  p.u.,  $\Delta P_2 = 0.02$  p.u.,  $\Delta P_{L3} = -0.05$  p.u.,  $\Delta P_{L4} = 0.1$  p.u.,  $\Delta P_{L1,Loc} = -0.1$  p.u. and  $\Delta P_{L2,Loc} = 0$ . Figure 6.9 shows the response of speed deviation without TCSC in both area. The response

of speed deviation with GA and ANFIS based TCSC in both area has been shown in Figure 6.10 and 6.11 respectively. Figure 6.12 shows the tie line power oscillation response in both area with TCSC controller.

$$DPM = \begin{bmatrix} 0.50 & 0.25 & 0.00 & 0.30 \\ 0.20 & 0.25 & 0.00 & 0.00 \\ 0.00 & 0.25 & 1.00 & 0.70 \\ 0.30 & 0.25 & 0.00 & 0.00 \end{bmatrix} \quad (6.26)$$

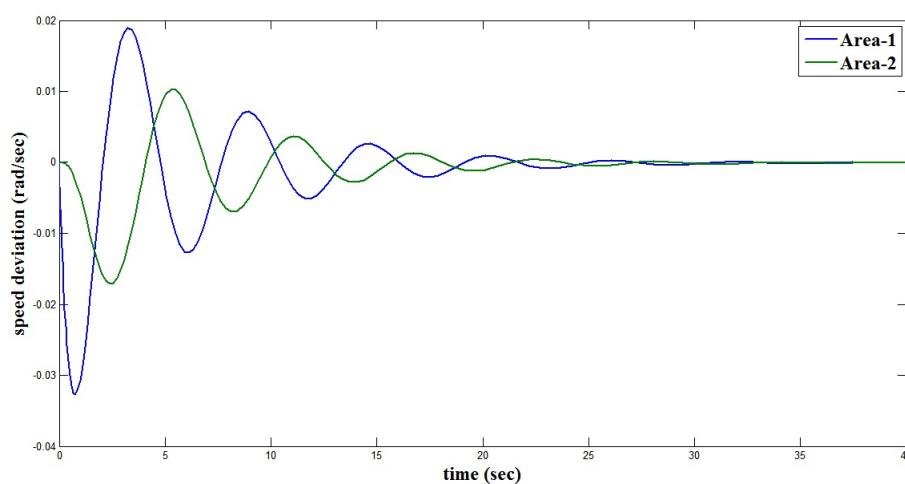


Figure 6.5: Case I: Speed deviation in Restructured Market without Tie Line Controller

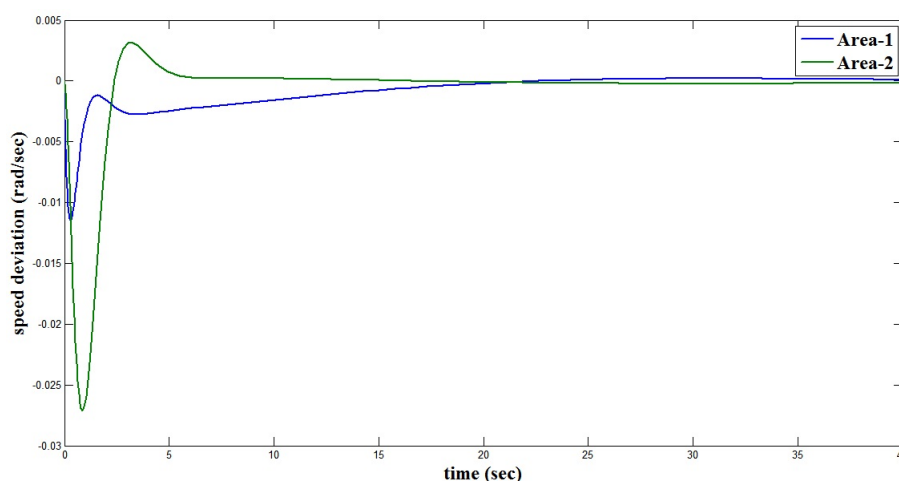


Figure 6.6: Case I: Speed deviation in Restructured Market with GA-TCSC Tie Line controller

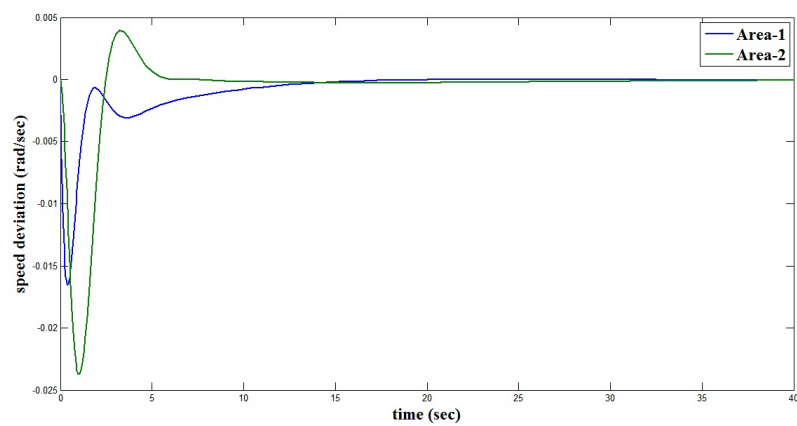


Figure 6.7: Case I: Speed Deviation in Restructured Market with ANFIS-TCSC Tie Line controller

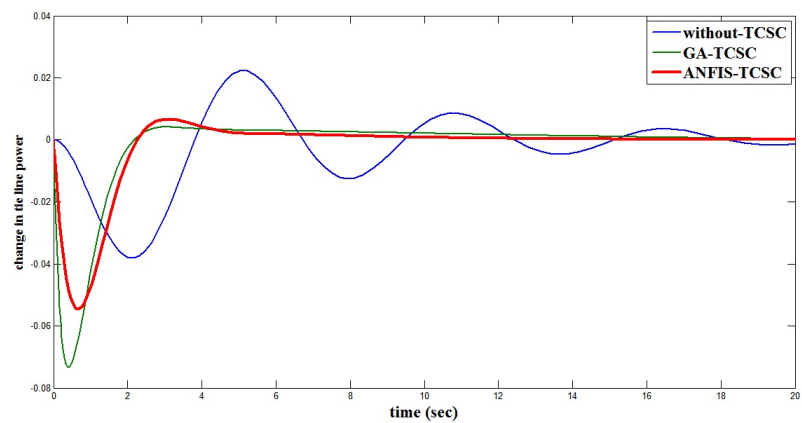


Figure 6.8: Case I: Tie Line Power Change with Controllers

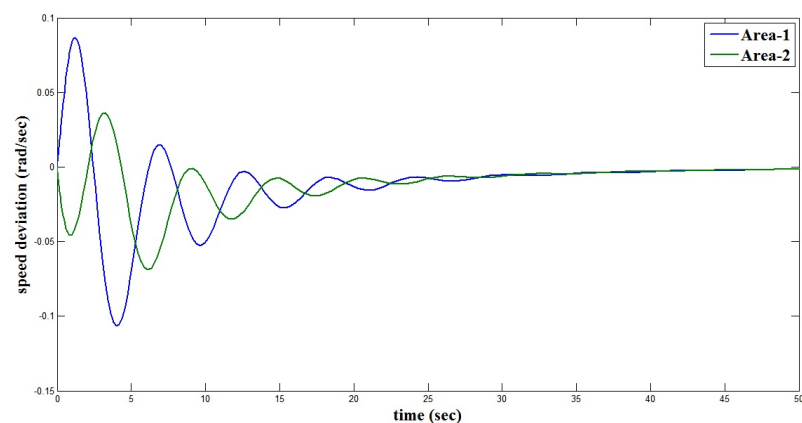


Figure 6.9: Case II: Speed deviation In Restructured Market without Tie Line Controller

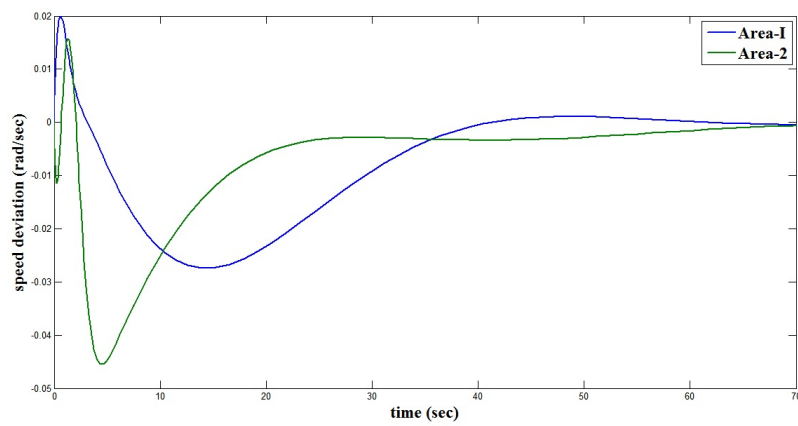


Figure 6.10: Case II: Speed deviation in Restructured Market with GA-TCS C Tie Line Controller

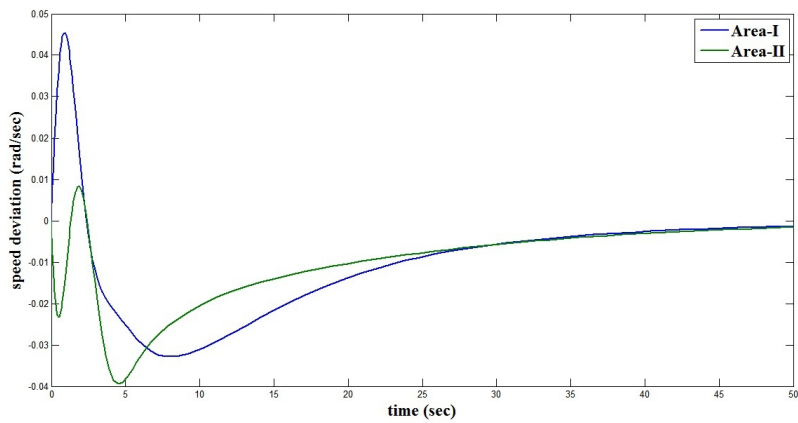


Figure 6.11: Case II : Speed deviation in Restructured Market with ANFIS-TCS C Tie Line Controller

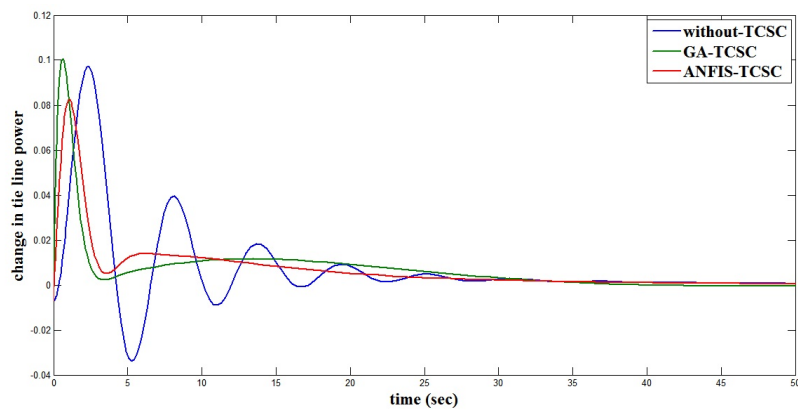


Figure 6.12: Case II: Tie Line Power Change With Controllers

### 6.3.7 Discussion

Here linear power system model has been used for two area LFC loop in deregulated electric market. The oscillatory frequency in two area have been controlled by tie line TCSC controller with different disturbances and consideration of various DPM. eigen values analysis show that the tie line power controller has provided good stability to the multiarea system. The effect of various *DPM* and variation of load have been clearly observed in the simulation results of speed deviation and change in tie line power. The simulation results show that the frequency oscillation as shown in Figures 6.6, 6.7, 6.10, 6.11 and tie line power oscillation as shown Figures 6.8 and 6.12 have been controlled through GA and ANFIS based TCSC in two area system. The settling time and overshoot in both control area without TCSC has been given in Table 6.3. Comparison analysis between GA and ANFIS based TCSC have been given in Table 6.4 and 6.5 respectively. In case II, ANFIS based TCSC has performed better than GA tuned TCSC controller. The responses of oscillation in speed deviation and tie line power have been improved using ANFIS-TCSC controller. Here TCSC controller has reduced oscillations significantly in speed deviation as well as tie line power in both area. The settling time of responses have been improved using TCSC tie line controller compared to that without TCSC.

Table 6.3: Time Response Parameters without Tie-Line TCSC Controller

Area		Speed deviation		Tie-line power	
		Settling time(s)	Overshoot(rad/sec)	Settling time(s)	Overshoot(p.u.)
Case I	area-1	38	-0.0327	35	-0.018
	area-2	38	-0.017		
Case II	area-1	50	0.08	45	0.098
	area-2	50	0.025		

Table 6.4: Time Response Parameters with Tie-line GA-TCSC Controller

Area		Speed deviation		Tie-line power	
		Settling time(s)	Overshoot(rad/sec)	Settling time(s)	Overshoot(p.u.)
Case I	area 1I	25	-0.0111	20	-0.072
	area 2	17.5	-0.0273		
Case II	area 1	60	0.02	40	0.1
	area 2	70	-0.045		

Table 6.5: Time Response Parameters with Tie-line ANFIS-TCSC Controller

Area		Speed deviation		Tie-line power	
		Settling time(s)	Overshoot(rad/sec)	Settling time(s)	Overshoot(p.u.)
Case I	area 1	28	-0.0166	16	-0.05
	area 2	28	-0.0238		
Case II	area 1	45	0.045	35	0.08
	area 2	45	-0.04		

However, effect of exciter and power system stabilizer can not be analyzed considering the first order linear model of power system. The non linear simulation and transient analysis can't be performed using same model. So, it is essential to consider higher order linear and non linear model of power system for depth analysis of multiarea power system for verification of role of tie line power controller as well as other supplementary controllers such as PSS.

## 6.4 Design of PSS and TCSC Controller with Fourth order Power System Model

In this section, frequency deviation in two area restructured power system has been analyzed with multiple PSS and TCSC controller. The parameters of PSS and TCSC controller have been tuned using genetic algorithm. The ANFIS based PSS and TCSC controllers have been designed from GA based controller. The fourth order power system a company of AVR with turbine and governor system have been considered for analysis of the two area system. The

eigen values analysis have been carried out for stability verification of two area AGC with PSS and FACTS controller. The non-linear simulation has been performed for analysis of frequency deviation and tie line power in each area with intelligent control techniques under consideration of different DPM.

## 6.4.1 Power System Model

### 6.4.1.1 Model of Power System with multiple PSS

Figure 6.13 represents block diagram of intelligent controller based PSS in two area power system under restructured market. The linear model of power system consists fifth order linear equations with AVR. The block diagram described by Figure 2.3 has been utilized as power system 1 and power system 2 in area control loop. The equation (2.78) of power system stabilizer is included in machine state equations and described in state space form  $\Delta\dot{x} = A\Delta x + B\Delta u$ . Here one stage phase compensator of PSS with gain and washout filter has been considered. The complete closed loop two area system AGC with PSSs can be represented by  $25 \times 25$  matrix. The closed loop system in Figure 6.13 is characterized in state space form as

$$\dot{x} = A^{declpss}x + B^{declpss}u \quad (6.27)$$

where  $x$  is the state vector and  $u$  is the vector of power demands of the DISCOs.  $A^{declpss}$  and  $B^{declpss}$  are developed from Figure 6.13. The  $A^{declpss}$  is also defined as stability matrix. The eigen values of the system can be calculated using stability matrix.  $A^{declpss}$  is represented by equation (6.28).

### 6.4.1.2 Model of Power System with PSSs and TCSC

The two area interconnected system with tie line TCSC controller is shown in Figure 6.4. The state diagram of TCSC as shown in Figure 2.10 has been used for consideration of

modeling for two area system with TCSC controller. The complete closed loop two area system with TCSC can be represented by  $24 \times 24$  matrix. Figure 6.13 has been modified with effect of TCSC controller and mathematical model of simultaneous application of TCSC and PSSs can be described by  $28 \times 28$  matrix.

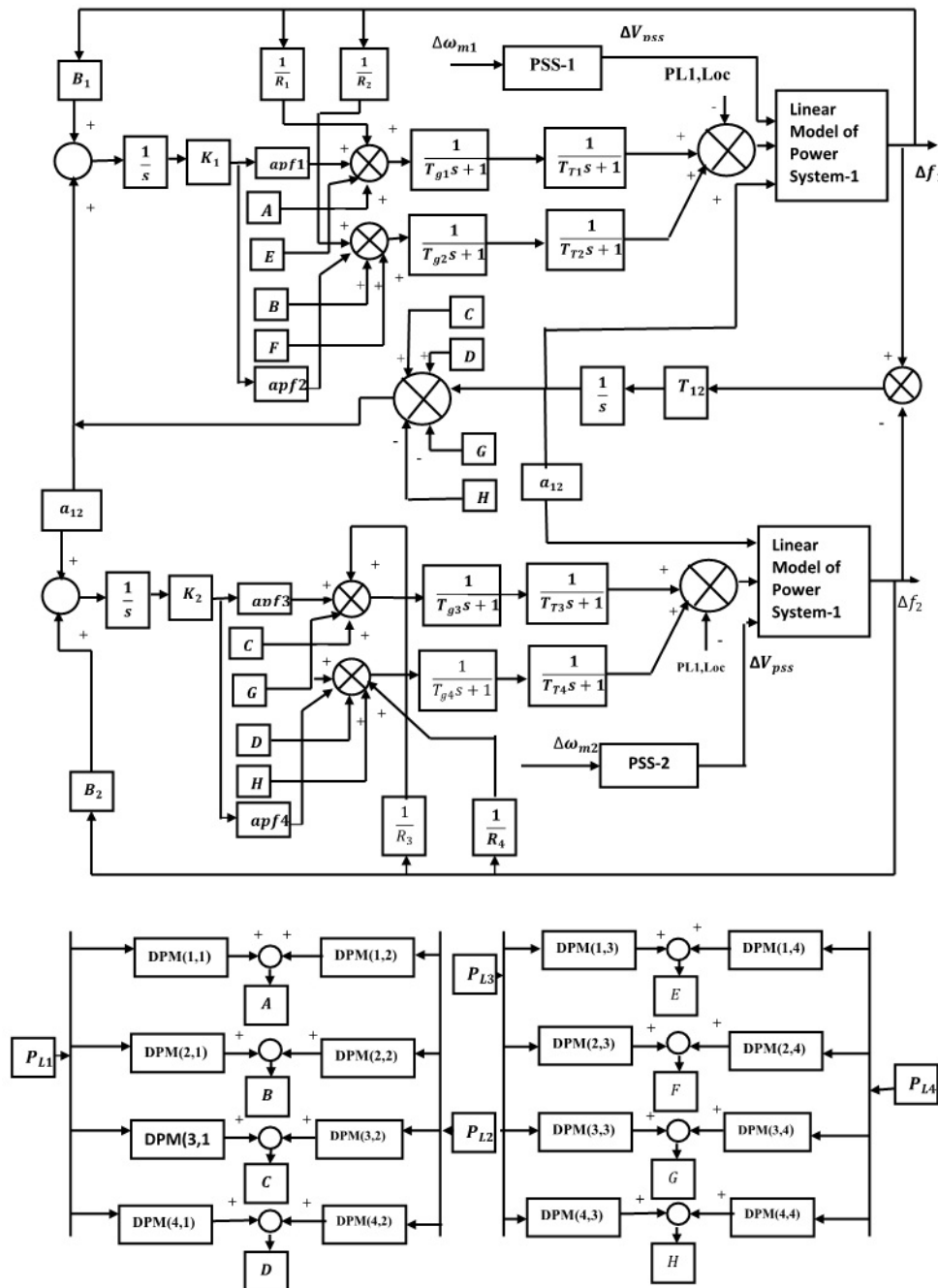


Figure 6.13: Two area interconnection system with multiple PSS in restructured market

$$A^{decpss} = \begin{bmatrix} \frac{-D}{2H} & 0 & \frac{-K_1}{2H} & 0 & \frac{-K_2}{2H} & 0 \\ 0 & -\frac{D}{2H} & 0 & -\frac{K_1}{2H} & 0 & \frac{-K_2}{2H} \\ wb & 0 & 0 & 0 & 0 & 0 \\ 0 & wb & 0 & 0 & 0 & 0 \\ 0 & 0 & -\frac{K_5}{T'_{d0}} & 0 & -\frac{1}{K_4 T'_{d0}} & 0 \\ 0 & 0 & 0 & -\frac{K_5}{T'_{d0}} & 0 & -\frac{1}{K_4 T'_{d0}} \\ 0 & 0 & -\frac{K_7}{T'_{q0}} & 0 & 0 & -\frac{1}{K_6 T'_{q0}} \\ 0 & 0 & 0 & -\frac{K_7}{T'_{q0}} & 0 & 0 \\ 0 & 0 & -\frac{K_A K_8}{T_A} & 0 & -\frac{K_A K_9}{T_A} & 0 \\ 0 & 0 & 0 & -\frac{K_A K_8}{T_A} & 0 & -\frac{K_A K_9}{T_A} \\ 0 & 0 & 0 & 0 & 0 & 0 \\ 0 & 0 & 0 & 0 & 0 & 0 \\ 0 & 0 & 0 & 0 & 0 & 0 \\ 0 & 0 & 0 & 0 & 0 & 0 \\ -\frac{1}{2\pi R_1 T_{G1}} & 0 & 0 & 0 & 0 & 0 \\ -\frac{1}{2\pi R_2 T_{G2}} & 0 & 0 & 0 & 0 & 0 \\ 0 & -\frac{1}{2\pi R_3 T_{G3}} & 0 & 0 & 0 & 0 \\ 0 & -\frac{1}{2\pi R_4 T_{G4}} & 0 & 0 & 0 & 0 \\ \frac{B1}{2\pi} & 0 & 0 & 0 & 0 & 0 \\ 0 & \frac{B1}{2\pi} & 0 & 0 & 0 & 0 \\ \frac{T_{12}}{2\pi} & -\frac{T_{12}}{2\pi} & 0 & 0 & 0 & 0 \\ -\frac{K_{pss} D}{2H} & 0 & -\frac{K_1 K_{pss}}{2H} & 0 & -\frac{K_2 K_{pss}}{2H} & 0 \\ -\frac{K_{pss} D T_1}{T_2 2H} & 0 & -\frac{K_{pss} K_1 T_1}{T_2 2H} & 0 & -\frac{K_2 K_{pss} T_1}{2H T_2} & 0 \\ 0 & a3 & 0 & b3 & 0 & c3 \\ 0 & a4 & 0 & b4 & 0 & c4 \end{bmatrix} \text{Contd....}$$

$$\begin{bmatrix}
 \frac{-K_3}{2H} & 0 & 0 & 0 & \frac{1}{2H} & \frac{1}{2H} & 0 & 0 & 0 & 0 \\
 0 & \frac{-K_3}{2H} & 0 & 0 & 0 & 0 & \frac{1}{2H} & \frac{1}{2H} & 0 & 0 \\
 0 & 0 & 0 & 0 & 0 & 0 & 0 & 0 & 0 & 0 \\
 0 & 0 & 0 & 0 & 0 & 0 & 0 & 0 & 0 & 0 \\
 0 & 0 & \frac{1}{T'_{d0}} & 0 & 0 & 0 & 0 & 0 & 0 & 0 \\
 0 & 0 & 0 & \frac{1}{T'_{d0}} & 0 & 0 & 0 & 0 & 0 & 0 \\
 0 & 0 & 0 & 0 & 0 & 0 & 0 & 0 & 0 & 0 \\
 0 & -\frac{1}{K_6 T'_{q0}} & 0 & 0 & 0 & 0 & 0 & 0 & 0 & 0 \\
 -\frac{K_A K_{10}}{T_A} & 0 & -\frac{1}{T_A} & 0 & 0 & 0 & 0 & 0 & 0 & 0 \\
 0 & -\frac{K_A K_{10}}{T_A} & 0 & -\frac{1}{T_A} & 0 & 0 & 0 & 0 & 0 & 0 \\
 0 & 0 & 0 & 0 & -\frac{1}{T_{R1}} & 0 & 0 & 0 & \frac{1}{T_{T2}} & 0 \\
 0 & 0 & 0 & 0 & 0 & -\frac{1}{T_{T2}} & 0 & 0 & 0 & \frac{1}{T_{T2}} \\
 0 & 0 & 0 & 0 & 0 & 0 & -\frac{1}{T_{R3}} & 0 & 0 & 0 \\
 0 & 0 & 0 & 0 & 0 & 0 & 0 & -\frac{1}{T_{T4}} & 0 & 0 \\
 0 & 0 & 0 & 0 & 0 & 0 & 0 & 0 & -\frac{1}{T_{G2}} & 0 \\
 0 & 0 & 0 & 0 & 0 & 0 & 0 & 0 & 0 & -\frac{1}{T_{G2}} \\
 0 & 0 & 0 & 0 & 0 & 0 & 0 & 0 & 0 & 0 \\
 0 & 0 & 0 & 0 & 0 & 0 & 0 & 0 & 0 & 0 \\
 0 & 0 & 0 & 0 & 0 & 0 & 0 & 0 & 0 & 0 \\
 0 & 0 & 0 & 0 & 0 & 0 & 0 & 0 & 0 & 0 \\
 0 & 0 & 0 & 0 & 0 & 0 & 0 & 0 & 0 & 0 \\
 0 & 0 & 0 & 0 & 0 & 0 & 0 & 0 & 0 & 0 \\
 -\frac{K_3 K_{pss}}{2H} & 0 & 0 & 0 & \frac{K_{pss}}{2H} & \frac{K_{pss}}{2H} & 0 & 0 & 0 & 0 \\
 -\frac{K_3 K_{pss} T_1}{T_2 2H} & 0 & 0 & 0 & \frac{K_{pss} T_1}{T_2 2H} & \frac{K_{pss} T_1}{T_2 2H} & 0 & 0 & 0 & 0 \\
 0 & d3 & 0 & 0 & 0 & 0 & e3 & f3 & 0 & 0 \\
 0 & d4 & 0 & 0 & 0 & 0 & e4 & f4 & 0 & 0
 \end{bmatrix}$$

Contd...

Where,

$$a3 = -DK_{pss1}/2H, b3 = -K_1 K_{pss1}/2H, c3 = -K_2 K_{pss1}/2H, d3 = -K_3 K_{pss1}/2H,$$

$$e3 = K_{pss1}/2H, f3 = K_{pss1}/2H, g3 = -a_{12} K_{pss1}/2H, h3 = -1/T_w$$

$$a4 = -DK_{pss2} T_1 / 2HT_2, b4 = -K_{pss2} K_1 T_1 / 2HT_2, c4 = -K_{pss2} K_2 T_1 / 2HT_2,$$

$$d4 = -K_{pss2} K_3 T_1 / 2HT_2, e4 = -K_{pss2} T_1 / 2HT_2, f4 = -K_{pss2} T_1 / 2HT_2,$$

$$g4 = -K_{pss2}T_1a_{12}/2HT_2, h4 = (1/T_2) - T_1/(T_2T_w)$$

$$\begin{bmatrix} 0 & 0 & 0 & 0 & \frac{-1}{2H} & 0 & 0 & 0 & 0 \\ 0 & 0 & 0 & 0 & \frac{-1}{2H} & 0 & 0 & 0 & 0 \\ 0 & 0 & 0 & 0 & 0 & 0 & 0 & 0 & 0 \\ 0 & 0 & 0 & 0 & 0 & 0 & 0 & 0 & 0 \\ 0 & 0 & 0 & 0 & 0 & 0 & 0 & 0 & 0 \\ 0 & 0 & 0 & 0 & 0 & 0 & 0 & 0 & 0 \\ 0 & 0 & 0 & 0 & 0 & 0 & 0 & 0 & 0 \\ 0 & 0 & 0 & 0 & 0 & 0 & 0 & 0 & 0 \\ 0 & 0 & 0 & 0 & 0 & 0 & \frac{K_A}{T_A} & 0 & 0 \\ 0 & 0 & 0 & 0 & 0 & 0 & 0 & 0 & \frac{K_A}{T_A} \\ 0 & 0 & 0 & 0 & 0 & 0 & 0 & 0 & 0 \\ 0 & 0 & 0 & 0 & 0 & 0 & 0 & 0 & 0 \\ \frac{1}{T_{T3}} & 0 & 0 & 0 & 0 & 0 & 0 & 0 & 0 \\ 0 & \frac{1}{T_{T4}} & 0 & 0 & 0 & 0 & 0 & 0 & 0 \\ 0 & 0 & -\frac{apf_1K_1}{T_{G1}} & 0 & 0 & 0 & 0 & 0 & 0 \\ 0 & 0 & -\frac{apf_2K_1}{T_{G2}} & 0 & 0 & 0 & 0 & 0 & 0 \\ -\frac{1}{T_{G3}} & 0 & 0 & -\frac{apf_3K_2}{T_{G3}} & 0 & 0 & 0 & 0 & 0 \\ 0 & -\frac{1}{T_{G4}} & 0 & -\frac{apf_3K_2}{T_{G3}} & 0 & 0 & 0 & 0 & 0 \\ 0 & 0 & 0 & 0 & 1 & 0 & 0 & 0 & 0 \\ 0 & 0 & 0 & 0 & -1 & 0 & 0 & 0 & 0 \\ 0 & 0 & 0 & 0 & 0 & 0 & 0 & 0 & 0 \\ 0 & 0 & 0 & 0 & -\frac{K_{pss}}{2H} & -\frac{1}{T_w} & 0 & 0 & 0 \\ 0 & 0 & 0 & 0 & -\frac{K_{pss}T_1}{T_22H} & 0 & 0 & 0 & 0 \\ 0 & 0 & 0 & 0 & g3 & 0 & 0 & h3 & 0 \\ 0 & 0 & 0 & 0 & g4 & 0 & 0 & h4 & -\frac{1}{T_2} \end{bmatrix}_{25 \times 25} \quad (6.28)$$

Where,

$$x = \left[ \Delta\omega_1 \Delta\omega_2 \Delta\delta_1 \Delta\delta_2 \Delta E'_{q1} \Delta E'_{q2} \Delta E'_{d1} \Delta E'_{d2} \Delta E_{fd1} \Delta E_{fd2} \right]' \text{Contd...}$$

$$x = \left[ \Delta P_{GV1} \Delta P_{GV2} \Delta P_{GV3} \Delta P_{GV4} \Delta P_{M1} \Delta P_{M2} \Delta P_{M3} \Delta P_{M4} \right]' \text{Contd...}$$

$$x = \left[ \int ACE_1 dt \int ACE_1 dt \Delta P_{tie1-2} \Delta v_1 \Delta \dot{V}_{pss1} \Delta v_2 \Delta \dot{V}_{pss2} \right]'_{25 \times 1}$$

## 6.4.2 Design of Ancillary controllers using GA

The multiple PSSs and tie-line power flow TCSC controllers have been designed using real coded genetic algorithm. The different parameters of PSSs and TCSC have been optimized for two area power system. Design of PSSs and TCSC are described as follow :

### 6.4.2.1 GA based Multiple PSS : Problem Formulation and Optimization Function

The power system stabilizer has been used for frequency stabilization in both area of power system. The rotor speed deviation of area 1 and area 2 have been chosen as input signal for PSS1 and PSS2 proposed controller. The equation (2.5) consists wash out filter time constant  $T_w$ , gain  $K_{pss}$  and time constant of phase compensator  $T_1, T_2, T_3$  and  $T_4$ . Here one stage phase compensator has been used for PSS1 and PSS2. Thus, four parameters such as gain  $K_{pss1}$  of PSS1 and  $K_{pss2}$  of PSS2, and time constant parameter of phase compensator  $T_1, T_2$ , are required to be optimized for the optimal design of both PSS. For both PSS, the time constant of wash out filter  $T_w$  has been selected to be 10. The objective of LFC with multiple area PSS is, to reduce the oscillatory frequency in rotor mode and also to minimize the tie line power oscillation in both control area. The goal can be achieved after minimizing the optimization function  $J$ , which is described by equation (6.29). The optimization function has been developed such that the damping factor of rotor mode in LFC be improved and minimization of real part of the eigen values associated with same mode. Hence time response parameters such as settling time to be improved and overshoots to be reduced. The Time Multiplied by Absolute Error (ITAE) has been used as the performance index. The optimization function  $J$  follows the optimized performance of PSSs controlled system. The gains for the PSSs are adjusted such that the performance index be minimized. The performance index is calculated over a time interval  $T$ , normally in the region where  $t$  is the settling time of the system. The best system response is obtained when PSSs parameters are optimized and minimizing the maximum real part of eigen values over a

certain range of operating conditions. The optimization flow chart for implementation of real coded GA is similar as shown in Figure 3.1. Only optimization parameters are different, which are described by equations (6.30) to (6.33). The optimization function  $J$  is described by following equation (6.29) :

$$J = \int_0^T t(|\Delta\omega_{m1}(t)| + |\Delta\omega_{m2}(t)|)dt \quad (6.29)$$

with

$$K_{pss1}^{min} \leq K_{pss1} \leq K_{pss1}^{max} \quad (6.30)$$

$$K_{pss2}^{min} \leq K_{pss2} \leq K_{pss2}^{max} \quad (6.31)$$

$$T_1^{min} \leq T_1 \leq T_1^{max} \quad (6.32)$$

$$T_2^{min} \leq T_2 \leq T_2^{max} \quad (6.33)$$

#### 6.4.2.2 GA based PSSs and TCSC : Problem Formulation and Optimization Function

The stability loop equation of TCSC (2.89) has been used for frequency stabilization. The input signal rotor speed deviation of area 1 or area 2 has been chosen for TCSC proposed controller. The equation (6.16) consists wash out filter time constant  $T_{w1}$ , gain  $K_{TCSC}$  and time constant of phase compensator  $T_{1T}, T_{2T}, T_{3T}$  and  $T_{4T}$ , which provides appropriate phase-lead characteristics to compensate for the phase lag between input and output signals. Five parameters such as gain  $K_{TCSC}$  and time constant parameter  $T_{1T}, T_{2T}, T_{3T}, T_{4T}$  are required to be optimized for the optimal design of TCSC frequency controller. Four parameters such as gain  $K_{pss1}$  of PSS1 and  $K_{pss2}$  of PSS2, and time constant parameter of phase compensator  $T_1, T_2$ , are required to be optimized for the optimal design of both PSS. For PSSs and TCSC, the time constant of wash out filter has been selected to be 10. The optimization function

described by equation (6.34) has been used for PSSs and TCSC parameters with following constraint as follows :

$$J = \int_0^T t(|\Delta\omega_{m1}(t)| + |\Delta\omega_{m2}(t)|) dt \quad (6.34)$$

$$T_{1T}^{min} \leq T_{1T} \leq T_{1T}^{max} \quad (6.35)$$

$$T_{2T}^{min} \leq T_{2T} \leq T_{2T}^{max} \quad (6.36)$$

$$T_{3T}^{min} \leq T_{3T} \leq T_{4T}^{max} \quad (6.37)$$

$$T_{4T}^{min} \leq T_{4T} \leq T_{4T}^{max} \quad (6.38)$$

$$K_{TCSC}^{min} \leq K_{TCSC} \leq K_{TCSC}^{max} \quad (6.39)$$

$$K_{pss1}^{min} \leq K_{pss1} \leq K_{pss1}^{max} \quad (6.40)$$

$$K_{pss2}^{min} \leq K_{pss2} \leq K_{pss2}^{max} \quad (6.41)$$

$$T_1^{min} \leq T_1 \leq T_1^{max} \quad (6.42)$$

$$T_2^{min} \leq T_2 \leq T_2^{max} \quad (6.43)$$

### 6.4.3 Design of Ancillary controllers using ANFIS

The multiple PSSs and tie-line power flow TCSC controllers have been designed using Adaptive Neur-Fuzzy Inference System. The PSSs and TCSC have been designed for two area power system. Design of PSSs and TCSC are described as follow :

### 6.4.3.1 ANFIS based Multiple PSS

In this work, GA based CPSSs are replaced by the ANFIS based PSSs. The Adaptive Neuro-Fuzzy Inference System based PSS has been developed and tested extensively in chapter 4. The model of ANFIS described in section (4.3.1) has been utilized as PSS1 and PSS2 in two area power system model. The inputs are speed  $\Delta\omega_m(t)$  and change in speed ( $\frac{\Delta d\omega_m(t)}{dt}$ ) and corresponding  $\Delta V_{pss}$  has been selected as output value for the ANFIS1 and ANFIS2 in two area power system model in restructured environment.

### 6.4.3.2 ANFIS based PSSs and TCSC

In this work, GA based TCSC is replaced by the ANFIS based TCSC. The Adaptive Neuro-Fuzzy Inference System based tie line TCSC has been developed and tested extensively in Chapter 4. The model of ANFIS described in section (4.3.2) has been utilized as TCSC tie line controller. The inputs are speed  $\Delta\omega_{m1}(t)$  and change in speed ( $\frac{\Delta d\omega_{m1}(t)}{dt}$ ) and corresponding  $\Delta X_{TCSC}$  has been selected as output value for the ANFIS controller in two area power system model in restructured environment.

## 6.4.4 Analysis

The linearized model presented by Figure 6.13 has been used for the stability analysis of the two area system without ancillary controllers and with multiple area PSS and tie line TCSC controller. The first and third operating conditions and corresponding values of machine constant  $K_1$  to  $K_{10}$  as shown in Table 3.2 are used for stability analysis of two area power system. For two operating conditions, the oscillations of the electromechanical modes of the machine are identified with PSSs and TCSC and stability of the system has been analyzed. The optimized parameters of PSSs are tuned for expected solution which is given by Table 6.6. Here eigen values and damping factors associated with electromechanical mode are mentioned. eigen values and corresponding damping factor without PSS and with GA based

PSSs are shown in Table 6.7 and Table 6.8 respectively. The optimized parameters of TCSC have been utilized from Table 3.12. eigen values and corresponding damping factor with GA based TCSC and simultaneous application of PSSs and TCSC are shown in Table 6.9 and Table 6.10 respectively.

Table 6.6: Optimized Parameters of PSSs

Parameters	Operating Conditions	
	1	2
$K_{pss1}$	2.568	4.56
$K_{pss2}$	2.280	2.69
$T_1$	0.97	1.83
$T_2$	0.994	2.419

Table 6.7: Eigen values without PSSs

O.C.	Area 1		Area 2	
	eigen values	$\zeta$	eigen values	$\zeta$
1	$0.0030 + 6.4053i$	-0.005	$0.0038 + 6.4237i$	-0.006
	$0.0030 - 6.4053i$		$0.0038 - 6.4237i$	
2	$0.1370 + 6.8954i$	-0.0199	$0.1365 + 6.8784i$	-0.0198
	$0.1370 - 6.8954i$		$0.1365 - 6.8784i$	

Table 6.8: Eigen values with PSSs

O.C.	Area 1		Area 2	
	eigen values	$\zeta$	eigen values	$\zeta$
1	$-2.8617 + 6.7807i$	0.3888	$-2.8629 + 6.7592i$	0.3900
	$-2.8617 - 6.7807i$		$-2.8629 - 6.7592i$	
2	$-3.2075 + 7.4701i$	0.3945	$-3.2085 + 7.4488i$	0.3956
	$-3.2075 - 7.4701i$		$-3.2085 - 7.4488i$	

Table 6.9: Eigen values with TCSC

O.C.	Area 1		Area 2	
	eigen values	$\zeta$	eigen values	$\zeta$
1	$-3.7524 + 7.5030i$	0.4473	$0.0017 + 6.4058i$	-0.0003
	$-3.7524 - 7.5030i$		$0.0017 - 6.4058i$	
2	$-7.1835 + 11.9598i$	0.5149	$0.1354 + 6.8788i$	-0.0197
	$-7.1835 - 11.9598i$		$0.1354 - 6.8788i$	

Table 6.10: Eigen values with PSSs and TCSC

O.C.	Area 1		Area 2	
	eigen values	$\zeta$	eigen values	$\zeta$
1	-10.2311 +10.4023i	0.7012	-2.8552 + 6.7546i	0.3893
	-10.2311 -10.4023i		-2.8552 - 6.7546i	
2	-10.1058 +19.1186i	0.4673	-3.2050 + 7.4454i	0.3954
	-10.1058 -19.1186i		-3.2050 - 7.4454i	

The participation factor method has been used for identification of eigen values and damping factors associated to electromechanical mode using TCSC, PSSs and PSSs-TCSC. With only TCSC as shown in Table 6.9, for the two operating conditions the eigen values associated with area 1 are negative and damping factors are positive, while with area 2, the eigen values and damping factor are positive and negative respectively. Hence eigen values show that only tie line power controller doesn't provide stability to multi area power system. Attention to Table (6.8), multiple area PSSs improved the eigen values, damping factor and reduced oscillatory frequency in rotor mode of area 1 and area 2. As shown in Table (6.10), the eigen value and damping factor are improved compared to individual application of PSSs and TCSC. So, simultaneous application of PSSs and TCSC have significantly enhanced stability of the system. The closed poles are very far away in the left half of the s-plane using ancillary controllers PSSs-TCSC compared to individual controllers.

#### 6.4.5 Non Linear Simulation

Here, nonlinear simulation has been performed under consideration of normal operating condition and heavy loading operating condition of power system. Here various *DPM* has been considered with variation of load in control area 1 and area 2. A two area system is used to demonstrate the behavior of the AGC scheme with multiple power system stabilizer and TCSC tie line power controller. The different cases [32] are considered according to the bilateral contract between GENCOs and DISCOs in restructured market. The comparison analysis between GA based PSSs and ANFIS based PSSs in restructured AGC scheme have

been carried out. The performance of simultaneous application of PSSs and TCSC have also been verified. The data described by Appendix A and Appendix B are used for the simulation purpose. The governor and turbine units in each area are assumed to be identical.

**Case I :**

In this case, the GENCOs in each area participate equally in AGC. ACE participation factors are  $apf_1 = 0.5, apf_2 = 0.5, apf_3 = 0.5, apf_4 = 0.5$ . Assume that the load change occurs only in area 1. Thus, the load is demanded only by DISCO1 and DISCO2. Load variation in area 1 is  $\Delta P_{L1} = 0.05$  p.u.,  $\Delta P_2 = 0.05$  p.u.,  $\Delta P_{L1,LOC} = 0.1$ p.u. are considered and no disturbances occur in area II. The optimal integral gain  $K_1 = 0.9$  and  $K_2 = 0.1$  are selected [76]. For this case, the *DPM* is described by equation (6.44).

For the normal operating condition, speed deviation in area 1 and area 2 has been observed in Figure 6.14. Figure 6.15, 6.16 and 6.17 show individual application of GA and ANFIS based PSSs, and simultaneous application of intelligent based ancillary controllers, which provided good damping characteristics for speed deviation as well as change in tie line power.

The response of speed deviation without ancillary controllers under heavy loading condition has been shown in Figure 6.18. System lost its stability very quickly at 4 second, which shows instability of two area system. The response of speed deviation with GA and ANFIS based PSSs has been shown in Figure 6.19 and 6.20. The response of tie line power changes in both area with TCSC has been shown in Figure 6.21. Responses show that simultaneous application of controllers reduce oscillation in both area and provide stability to system.

$$DPM = \begin{bmatrix} 0.5 & 0.5 & 0 & 0 \\ 0.5 & 0.5 & 0 & 0 \\ 0 & 0 & 0 & 0 \\ 0 & 0 & 0 & 0 \end{bmatrix} \quad (6.44)$$

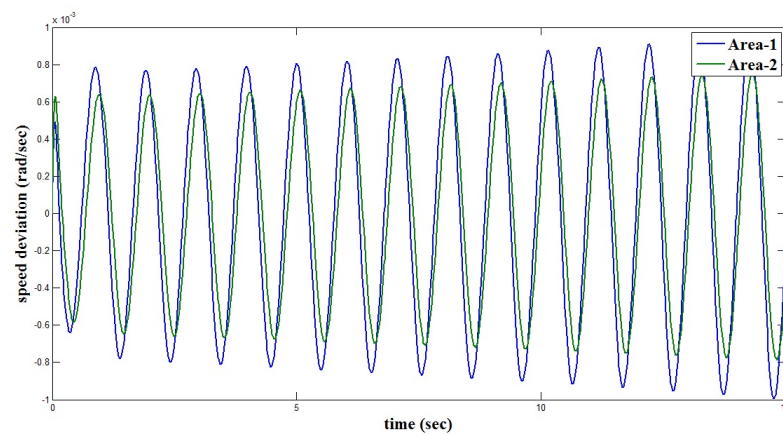


Figure 6.14: Case I: First O.C. : Response of speed deviation in Area 1 and Area 2

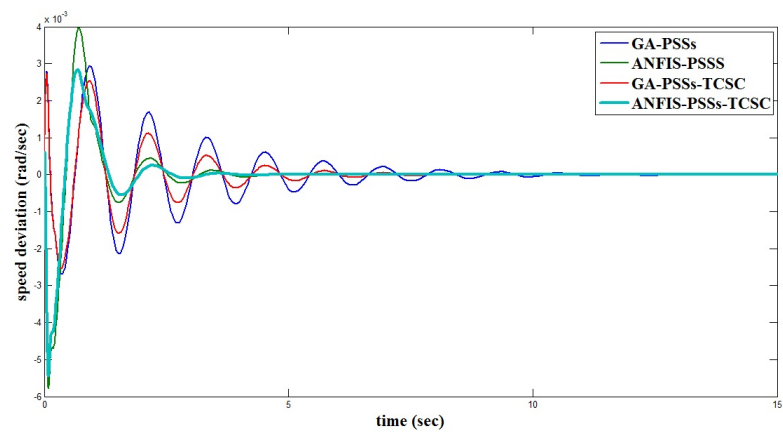


Figure 6.15: Case I : First O.C.: Response of speed deviation in Area 1 with Multiple PSS and TCSC

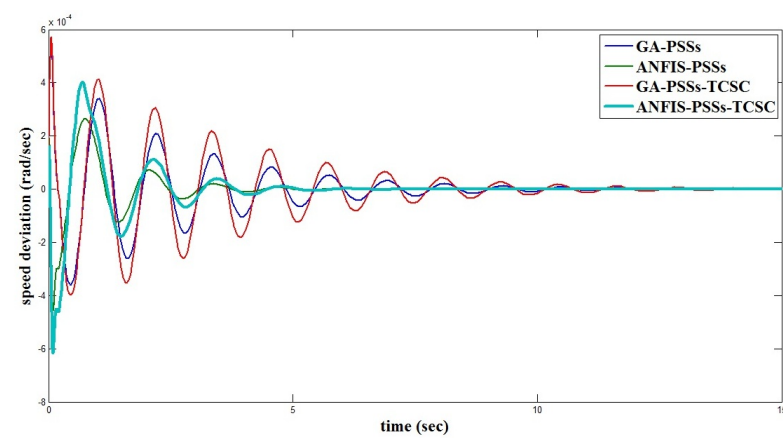


Figure 6.16: Case I: First O.C.: Response of speed deviation in Area 2 with Multiple PSS and TCSC

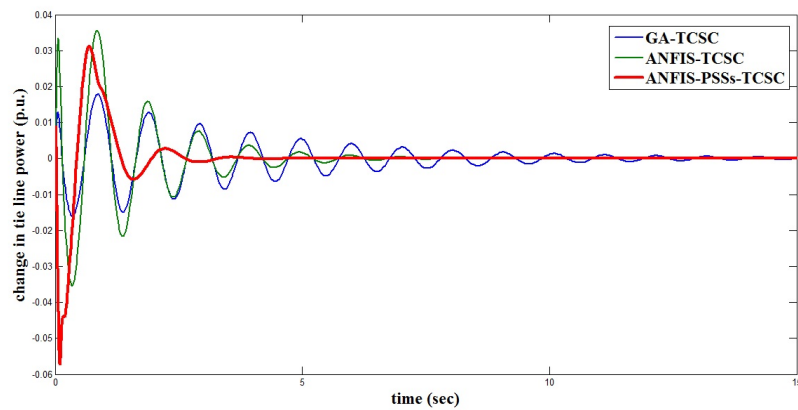


Figure 6.17: Case I: First O.C.: Change in Tie Line Power with Controllers

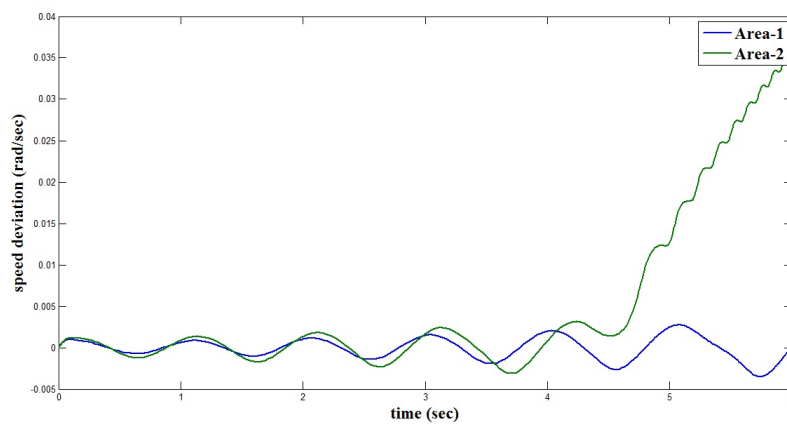


Figure 6.18: Case I: Second O.C.: Response of speed deviation in Area 1 and Area 2

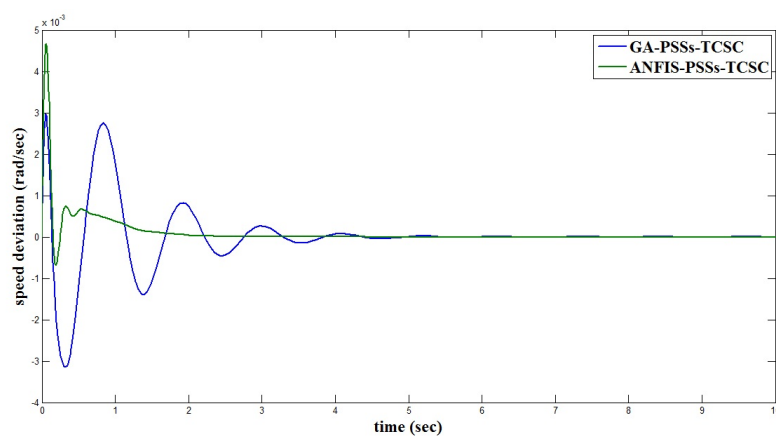


Figure 6.19: Case I: Second O.C.: Response of speed deviation in Area 1 with Multiple PSS and TCSC

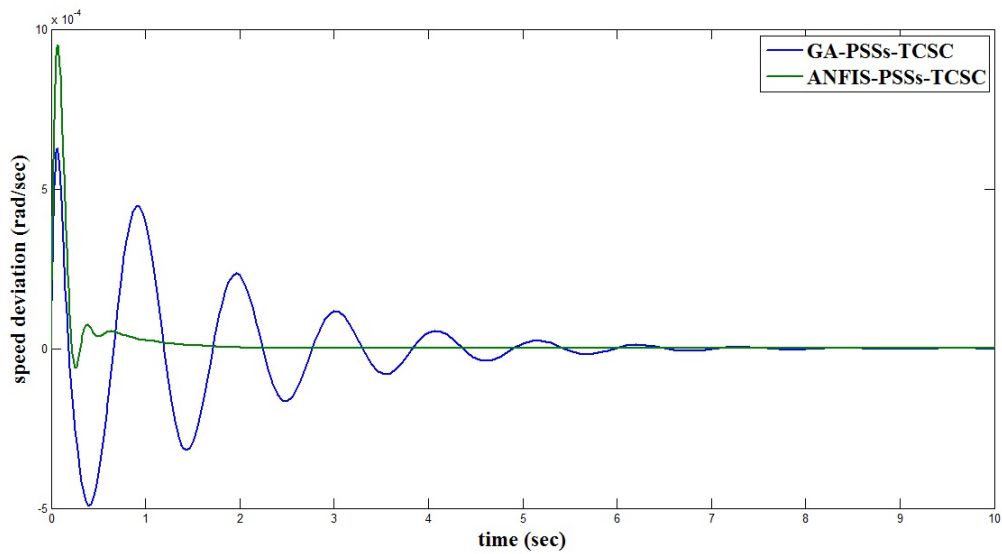


Figure 6.20: Case I: Second O.C.: Response of speed deviation in Area 2 with Multiple PSS and TCSC

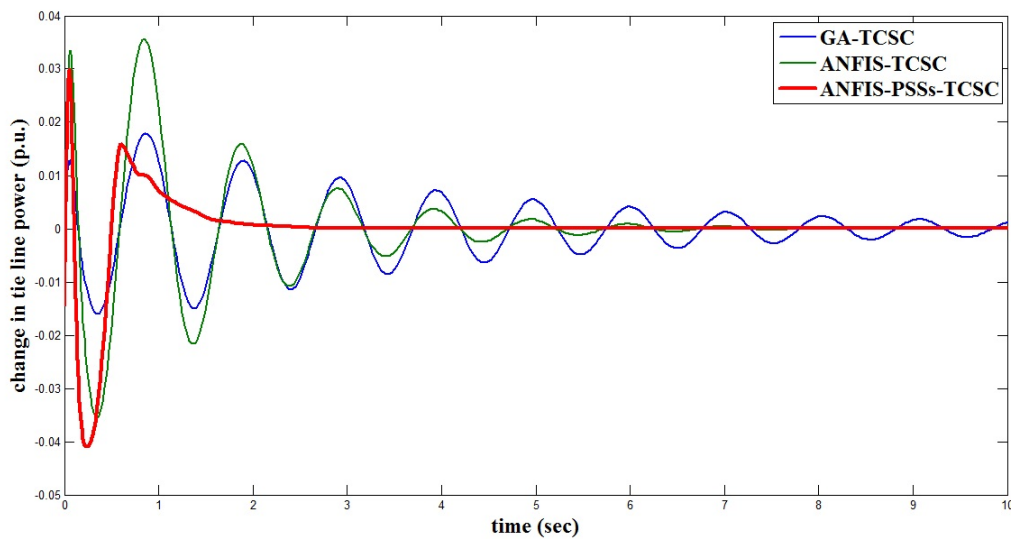


Figure 6.21: Case I: Second O. C.: Change in Tie Line Power with Controllers

### Case II:

In this case, where all the DISCOs contract with GENCOs for power as per *DPM* described by equation (6.45). ACE participation factors are  $apf_1 = 0.5, apf_2 = 0.5, apf_3 = 0.5, apf_4 = 0.5$ . The load variation are considered such as  $\Delta P_{L1} = 0.01$  p.u.,  $\Delta P_2 = 0.02$  p.u.,  $\Delta P_{L3} = -0.05$  p.u.,  $\Delta P_{L4} = 0.1$  p.u.,  $\Delta P_{L1,Loc} = -0.1$  p.u. and  $\Delta P_{L2,Loc} = 0$ . For the normal operating condition, speed deviation in area 1 and area 2 has been observed as

shown in Figure 6.22. Figure 6.22 shows that system become unstable and lost stability at 10 second under consideration of  $DPM$  described by equation (6.45) and variation of load in control area. Figure 6.23, 6.24 and 6.25 show individual application of PSSs and TCSC, and simultaneous application of intelligent techniques based ancillary controllers, which shows that ancillary controller has provided good damping characteristics for speed deviation as well as change in tie line power.

Under heavy loading conditions, different  $DPM$  and variation of load in control area, system comes under unstable mode very fast, which has been shown in Figure 6.18. The response of speed deviation in both area has been shown in Figure 6.27 and 6.28. Change in tie line power in both area with TCSC controller has been shown in Figure 6.29. Figures 6.27, 6.28 and 6.29 show that simultaneous application of intelligent techniques based controllers reduce oscillation in both area and provide stability to system.

$$DPM = \begin{bmatrix} 0.50 & 0.25 & 0.00 & 0.30 \\ 0.20 & 0.25 & 0.00 & 0.00 \\ 0.00 & 0.25 & 1.00 & 0.70 \\ 0.30 & 0.25 & 0.00 & 0.00 \end{bmatrix} \quad (6.45)$$

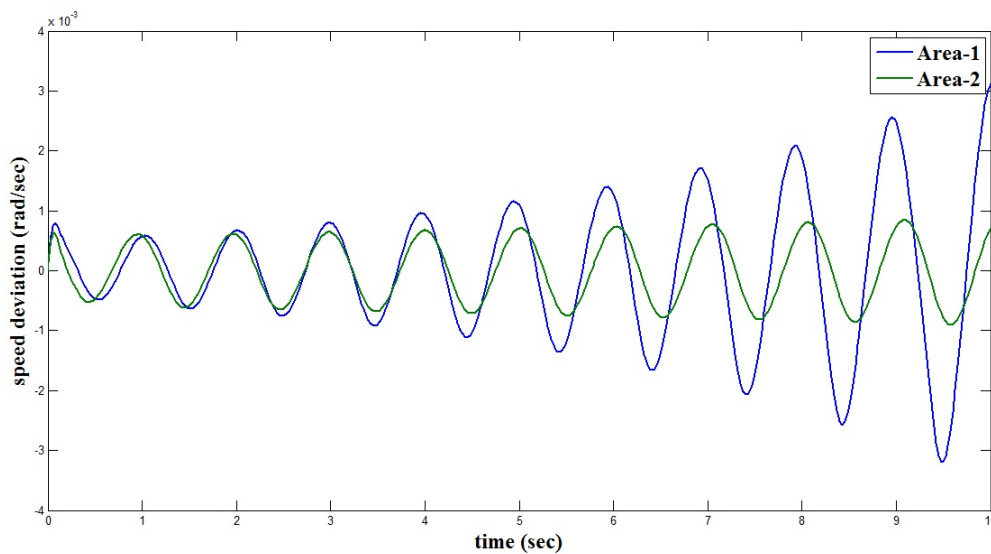


Figure 6.22: Case II: First O.C.: Response of Apeed deviation in Area 1 and Area 2

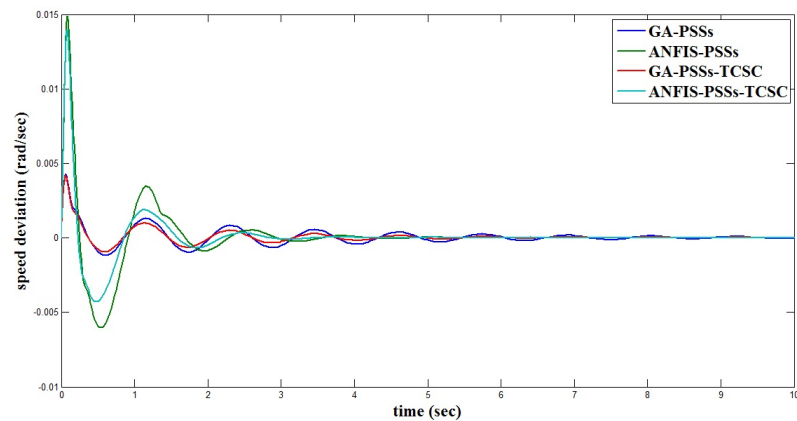


Figure 6.23: Case II: First O.C.: Response of Apeed deviation in Area 1 with Multiple PSS and TCSC

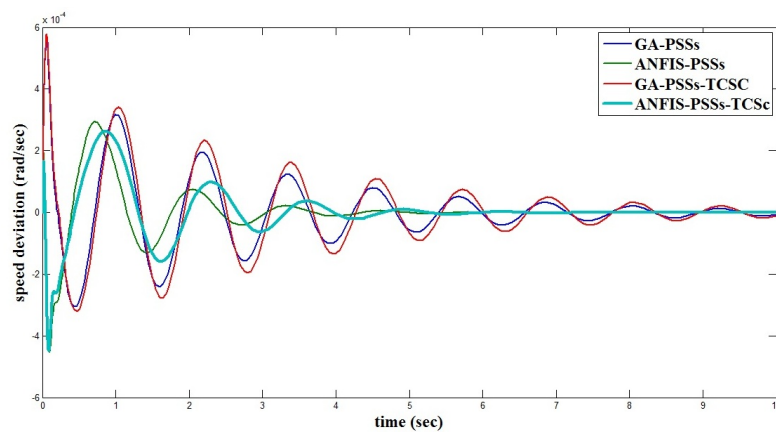


Figure 6.24: Case II: First O.C.: Response of Speed deviation in Area 2 with Multiple PSS and TCSC

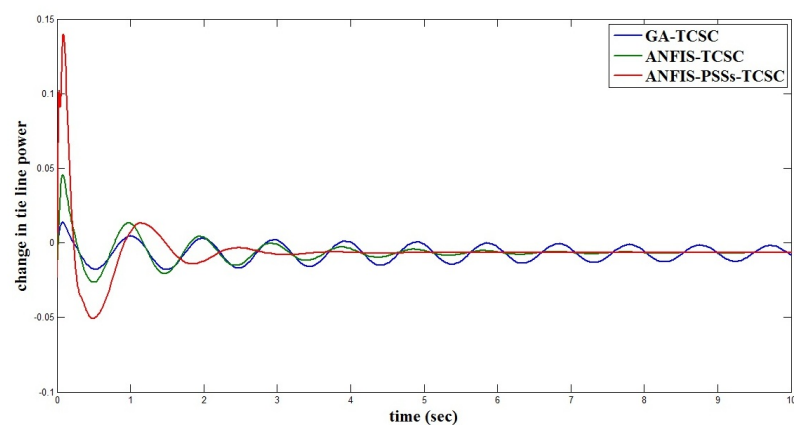


Figure 6.25: Case II: First O.C.: Change in Tie Line Power with Controllers

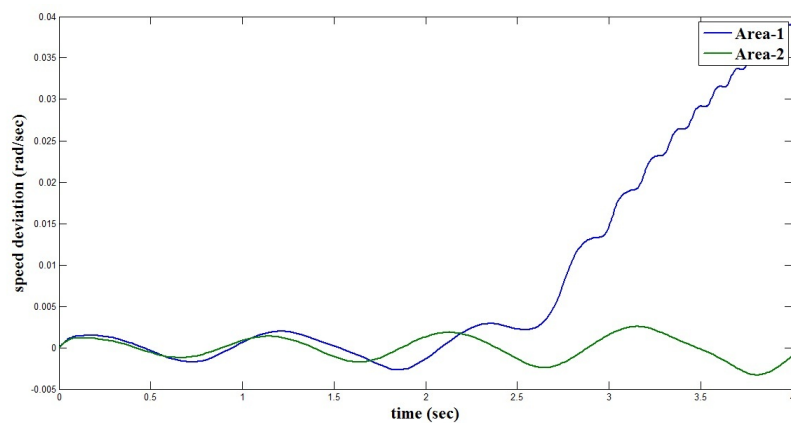


Figure 6.26: Case II: Second O.C.: Response of Speed deviation in Area 1 and Area 2

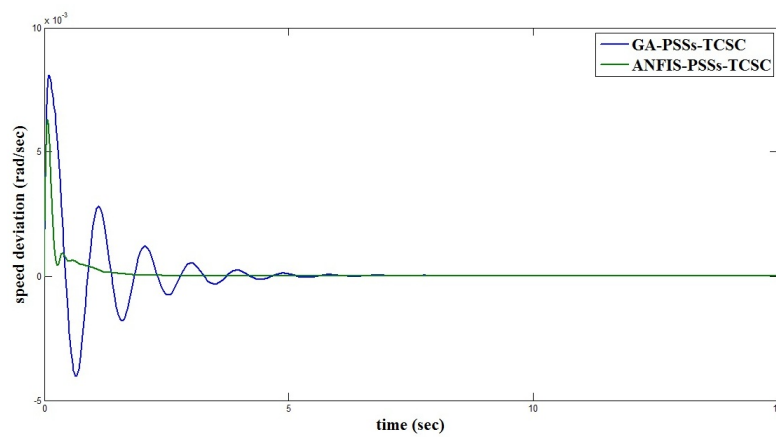


Figure 6.27: Case II: Second O.C.: Response of Speed deviation in Area 1 with Multiple PSS and TCSC

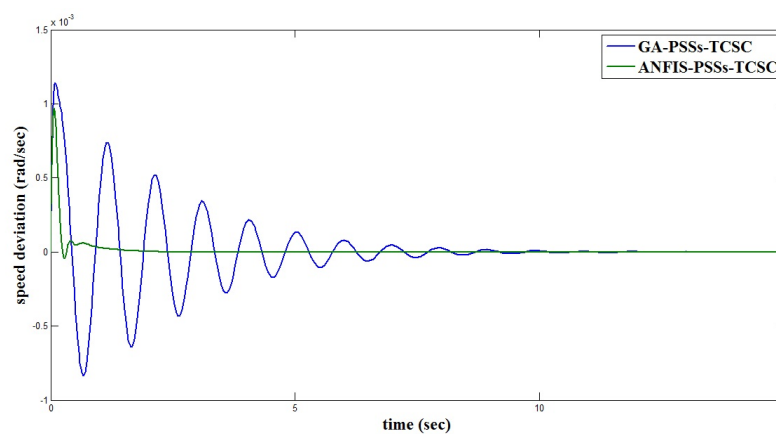


Figure 6.28: Case II: Second O.C.: Response of speed deviation in Area 2 with Multiple PSS and TCSC

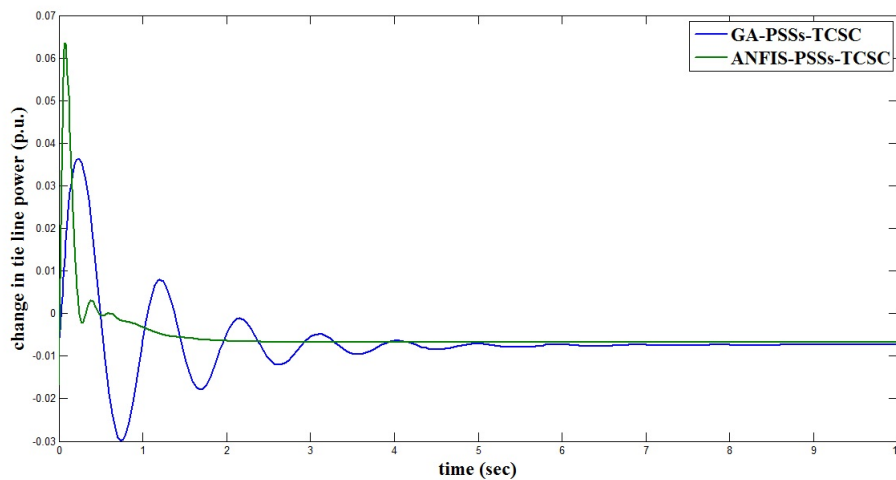


Figure 6.29: Case II: Second O.C.: Change in Tie Line Power with Controllers

## 6.5 Conclusion

In this study, performance and role of ancillary controllers such as PSS and TCSC have been analyzed in two area control system under restructured electric market. Low order power system model and higher order power system model have been considered for depth analysis of two area system with ancillary controllers. The small signal stability analysis and non-linear simulation for the transient stability analysis have been carried out for investigation of the power system stability issue. Two different operating conditions are taken with consideration of various *DPM* and load variation in both control area. The rotor speed deviation and change in tie line power have been analyzed under different types of *DPM* and variation of load in control area.

From first order power system model :

It has been shown that the eigen values associated to the electromechanical mode are more negative with presence of TCSC in two area system and poles in s-plane are far away from origin as shown in Table 6.1. The damping factor has been improved with TCSC compared to that without TCSC, which shows that the LFC system is more stable and TCSC has been provided good damping to oscillation in power system. The effect of various *DPM* and variation of load have been clearly observed in the simulation results of speed deviation and

change in tie line power. The simulation results have shown that the frequency oscillation and tie line power oscillation have been controlled through GA and ANFIS based TCSC in two area system. The ANFIS based TCSC has been reduced oscillation in speed deviation and tie line power compared to the GA based TCSC. The time response parameters such as settling time and overshoot have been improved using ANFIS based TCSC compared to the GA based TCSC in both control area.

From higher order power system model :

1. GA and ANFIS based control strategies have been developed for designing of multiple PSS and TCSC damping controller. The multiple PSS and simultaneous designed TCSC and PSS have been applied to the dynamical two area power system.
2. It has been shown that the eigen values associated to the electromechanical mode are more negative with presence of multiple PSS and TCSC in multi area power system and poles in s-plane are far away from origin. The damping factor has been improved with PSSs compared to that without PSSs, which has shown that the system is more stable and PSSs have provided good damping to oscillation in power system. It has also been observed that the with simultaneous application of multiple PSS and TCSC in power system, the eigen values are more negative and damping factor has been improved significantly, which shows good stability of system compared to the individual application of PSS and TCSC.
3. From the non - linear analysis, without the application of the controllers in the system, the oscillations in rotor speed deviation and tie line power have been observed. Under the heavy loading conditions in restructured environment, the oscillation in speed deviation are continuously growing which creates the instability of the restructured electric system. Simultaneously designed TCSC and PSS damping controller have significantly diminished oscillations in system. Simultaneous application of TCSC and PSS have provided very good damping characteristics compared to the individual application of PSSs or TCSC and almost eliminate the oscillations in system. Application of ANFIS

based TCSC and PSSs have improved the time response parameters such as settling time, rise time and delay time appreciably and also decreased the overshoot in the system compared to the GA based ancillary controllers.

# Chapter 7

## Conclusions

### 7.1 General

This thesis has addressed mathematical model of power system with power system stabilizer and thyristor control series capacitor, design of PSS and TCSC using different computational intelligent techniques, design of smart techniques based ancillary controllers with first order and fifth order linear and non linear power system model under restructured electric environment, and linear and non linear analysis of rotor angle stability issue under different operating conditions, contingencies, faults and various *DPM*.

The main contribution of the thesis include:

The development of the systematic procedure for conversion of non linear mathematical model into linear model of power system with both PSS, TCSC and simultaneous designing of PSS and TCSC as discussed in chapter 2.

The Genetic Algorithm Based control strategies have been developed for designing of PSSs and TCSC damping controller. The PSSs and simultaneous designed TCSC and PSS have been applied to the dynamical power system as discussed in chapter 3.

Adaptive Neuro-Fuzzy inference System and Levenberg-Marquardt Artificial Neural Network algorithm for the development of the control strategy for thyristor control series capacitor Based damping controller and power system stabilizer has been discussed in chapter 4.

Identification method such as Non Linear Auto regressive Moving Average-L2 based controller and hybrid controller such as Genetic Algorithm Based Network Network has been discussed for the development of the control strategy for power system stabilizer , and developed ANFIS Based Thyristor control series capacitor has been suggested in addition to power system stabilizer in chapter 5.

A new control strategy for designing of Ancillary controllers such as power system stabilizers and thyristor control series capacitor in two area deregulated electric market with load frequency control loop with low and higher order power system model has been discussed in chapter 6.

## 7.2 Summary of Important Findings

Chapter 2 has presented the fourth order non linear mathematical model of the power system with IEEE-ST1 excitation system. The systematic procedure for conversion of non linear model into linear model with both PSS, TCSC and simultaneous designing of PSS and TCSC have been discussed. Using Taylor's series method, a new fourth order linearized model of the power system with exciter has been derived and the equations of machine constant  $K_1$  to  $K_{10}$  have been calculated. The linerized mathematical model and state space form of power system with conventional power system stabilizer and a new PID- power system stabilizer have been described. The linearized state space form of power system with individual TCSC and simultaneous CPSS and TCSC have been also derived. The block diagram representation of system with PSSs and TCSC are included.

In chapter 3, genetic algorithm based control strategies have been developed for designing of PSSs and TCSC damping controller. The PSSs and simultaneous designed TCSC and PSS have been applied to the dynamical power system. The small signal stability Analysis and non-linear simulation for the transient stability analysis have been carried out for details investigation of the power system stability issue. Four different operating conditions are taken and the responses of the rotor Angle, rotor speed deviation, terminal voltage and net reactance have been analyzed under different types of the disturbances and faults.

- It has been shown that the eigen values associated to the electromechanical mode are more negative with presence of CPSS and PID-PSS in power system and poles in s-plane are far away from origin. The damping factor has been improved with PSSs compared to that without PSSs, which has shown that the system is more stable and PSSs have provided good damping to oscillation in power system. It has also been also observed that with the simultaneous application of PSS and TCSC in power system, the eigen values are more negative and damping factor has been improved significantly, which shows good stability of system compared to the individual application of PSS and TCSC.
- From the non - linear Analysis, without the application of the controllers in the system, the oscillations in rotor angle, rotor speed deviation have been observed. Under the heavy loading conditions, it has been observed that as the active power and reactive power are increased, the oscillation in rotor angle and speed deviation are continuously growing which creates the instability of the system under the contingencies. While simultaneously designed TCSC and PSS damping controller have significantly diminished oscillations in system, simultaneously application of TCSC and PSS have provided very good damping characteristics compared to the individual application of PSSs or TCSC and almost eliminated the oscillations in system. Application of GA Based TCSC and PSSs have improved the time response parameters such as settling time, rise time and delay time appreciably and also decreased the overshoot in the system.

In chapter 4, the smart control strategies based TCSC damping controller and PSS have been designed. The ANFIS and LMNN based PSS, and simultaneous LMNN and ANFIS based TCSC-PSS have been applied to the dynamical power system. The non-linear simulations have been carried out for detail analysis of the stability of the power system. The time responses of speed deviation obtained by intelligent techniques based controller has been compared to the conventional power system stabilizer. Four different operating conditions are taken and the response of rotor speed deviation has been analyzed under different types of the disturbances and faults.

From the non - linear Analysis,

- Without the application of the controllers in the system, the oscillations in rotor speed deviation has been observed. Under the heavy loading condition, it has been observed that if the active power and reactive power are increased; the oscillation in speed deviation is continuously growing which creates the instability of the system. The smart damping controllers have greatly diminished oscillations in system.
- Conventional power system stabilizer does't produce satisfactory response under the different operating conditions. Simultaneous application of ANFIS and ANN based TCSC and PSS have provided very good damping characteristics compare to the individual application of PSS and almost eliminated the oscillations in system.
- It has been observed that individual application of ANFIS-TCSC produces better response compared to the individual application of LMNN-TCSC.
- Figures have shown that individual application of ANFIS-PSS produces better response compared to the individual LMNN-PSS.
- Under the heavy loading condition, ANFIS based TCSC-PSS has produced good results compared to the LMNN based TCSC-PSS, and also improved the time response parameters such as settling time, rise time and delay time appreciably and decreased the overshoot in the system.

In chapter 5, the smart control strategies based TCSC damping controller and PSS have been designed. The NARMA-L2 and GA-ANN based PSS, and simultaneously ANFIS-TCSC and PSS have been applied to the dynamical power system. The non-linear simulations have been carried out for detail analysis of the stability of the power system. The time response of speed deviation obtained by intelligent techniques based controller has been compared to the conventional power system stabilizer. Four different operating conditions are taken and the response of rotor speed deviation has been analyzed under different types of the disturbances and faults.

From the non - linear analysis,

- Without the application of the controllers in the system, the oscillations in rotor speed deviation has been observed. Under the heavy loading condition, it is clear that if

the active power and reactive power are increased; the oscillation in speed deviation is continuously growing which creates the instability of the system. The smart damping controllers have greatly diminished oscillations in system.

- Convention power system stabilizer doesn't produce satisfactory response under the different operating conditions, while simultaneously application of ANFIS -TCSC and PSS been provided very good damping characteristics compared to the individual application of PSS and almost eliminate the oscillations in system.
- Figures have shown that individual application of GA-ANN-PSS produces better response compare to the individual NARMA-L2-PSS.
- Under the different loading conditions, It has been observed that simultaneous application of GA-ANN-PSS and ANFIS-TCSC produce better response compare to the simultaneous application of NARMA-L2-PSS and ANFIS-TCSC. Also it has improved the time response parameters such as settling time, rise time and delay time appreciably and decreased the overshoot in the system.

In the section (5.6), different Intelligent techniques based PSS are tested under heavy loading conditions. Simultaneously ANFIS-TCSC with all PSS are also tested under heavy loading conditions. Following results are obtained from details study:

- The GA-CPSS, ANFIS-ANN and GA-ANN have produced better response compared to the LMNN-PSS and NARMA-L2-PSS.
- But GA-CPSS has required different optimized parameters under different operating conditions and GA-ANN needed more time for training of neural network. ANFIS-PSS has provided fast, adaptive and satisfactory response with less number of training data.
- From figures (5.19) to (5.26), it has been observed that the ANFIS-TCSC produces better response with GA-CPSS, ANFIS-PSS and GA-ANN-PSS compared to the NARMA-L2-PSS and LMNN-PSS.
- Finally it has been concluded that simultaneous application of ANFIS-TCSC with ANFIS-PSS produce good damping characteristics under all operating conditions and disturbances in power system.

In chapter 6, a performance and role of ancillary controllers such as PSS and TCSC have been analyzed in two area control system under restructured electric market. Low order power system model and higher order power system model have been considered for depth Analysis of two area system with Ancillary controllers. The small signal stability analysis and non-linear simulation for the transient stability analysis have been carried out for investigation of the power system stability issue. Two different operating conditions are taken with consideration of various *DPM* and load variation in two control area. The rotor speed deviation and change in tie line power have been analyzed under different types of *DPM* and variation of load in control area.

From first order power system model :

It has been shown that the eigen values associated to the electromechanical mode are more negative with presence of TCSC in two area system and poles in s-plane are far away from origin as shown in Table 6.1. The damping factor has been improved with TCSC compared to that without TCSC, which has shown that the LFC system is more stable and TCSC has been provided good damping to oscillation in power system. The effect of various *DPM* and variation of load have been clearly observed in the simulation results of speed deviation and change in tie line power. The simulation results have shown that the frequency oscillation and tie line power oscillation have been controlled through GA and ANFIS based TCSC in two area system. The ANFIS based TCSC has reduced oscillation in speed deviation and tie line power compared to the GA based TCSC. The time response parameters such as settling time and overshoot have been improved using ANFIS based TCSC compared to the GA Based TCSC in both control area.

From higher order power system model :

1. GA and ANFIS based control strategies have been developed for designing of multiple PSS and TCSC damping controller. The multiple PSS and simultaneous designed TCSC and PSS have been applied to the dynamical two area power system.
2. It has been shown that the eigen values associated to the electromechanical mode are more negative with presence of multiple PSS and TCSC' in multi area power

system and poles in s-plane are far away from origin. The damping factor has been improved with PSSs compared to that without PSSs, which has shown that the system is more stable and PSSs have provided good damping to oscillation in power system. It has also been observed that with the simultaneous application of multiple PSS and TCSC in power system, the eigen values are more negative and damping factor has been improved significantly, which shows good stability of system compared to the individual application of PSS and TCSC.

3. From the non - linear analysis, without the application of the controllers in the system, the oscillations in rotor speed deviation and tie line power have been observed. Under the heavy loading conditions in restructured environment, the oscillation in speed deviation are continuously growing which creates the instability of the restructured electric system. While simultaneously designed TCSC and PSS damping controller have significantly diminished oscillations in system. Simultaneous application of TCSC and PSS have provided very good damping characteristics compared to the individual application of PSSs or TCSC and almost eliminated the oscillations in system. Application of ANFIS based TCSC and PSSs have improved the time response parameters such as settling time, rise time and delay time appreciably and also decreased the overshoot in the system compared to the GA based Ancillary controllers.

### 7.3 Scope of Future Research

As consequence of investigations carried out in this thesis, the following aspects are being suggested as future research work to be carried out.

Modeling of PSS and TCSC controller with fifth order power system has been presented. However, the modeling of system can be extended for other FACTS controllers for stability analysis and sensitivity of power system.

Chapter 3 has been restricted to genetic algorithm based controllers. The different evolutionary algorithms such as cultural, ant colony, and hybrid algorithms can be applied for designing of PSS and different FACTS controllers for parameters optimization.

The highly dynamic power system, the recurrent dynamic neural network with non linear

system identification techniques can be applied for PSS and FACTS controllers. Neural network based system identification for non linear power system is new research area for designing of PSS and FACTS controllers. The non linear power system stability also can be analyzed using non linear Liyapunov's stability method.

The work presented by chapter 6 can be extended for three and four areas power system with four GENCOs and four DISCOs in each area. The optimized location of PSS and FACTS controllers can be identified using evolutionary algorithms in multi area power system. Considering dynamical situation in power system, the adaptive neural networks based ancillary controllers can be developed for stability issues and tie line power control in restructured electric market. The concept described by chapter 6 can be applied to large integrated hybrid power system.

# Bibliography

- [1] L.A.Zadeh, *Fuzzy Sets.*, Journal on Information and Control, Vol. 8, pp. 338-353,1965
- [2] De Mello, F.P., and Concordia, C., *Concepts of Synchronous Machine Stability as Affected by Excitation Control*, IEEE Transaction on Power System Apparatus and System, Vol. 88, pp. 316-329, 1969.
- [3] O.I. Elgerd, C. Fosha, *Optimal Megawatt-frequency Control of Multiarea Electric Energy System*, IEEE Transaction on Power System Apparatus and System, Vol. 89, No. 4, pp. 556-563, 1970.I
- [4] G.C.Verghese, I.J.perez-Arriaga and F.C.Schweppe, *Selective Model Analysis with Application to Electric Power Systems, Part II: The Dynamic Stability Problem*, IEEE Transaction Power Apparatus and System, Vol. 101, No-9, pp.3126-3134, 1982.
- [5] O.I. Elegerd, *Electric Energy system Theory: Introduction*, McGraw-Hill inc., New York, 1982.
- [6] Y. N. Yu, *Electric Power System Dynamics*, Academic Press, New York, 1983.
- [7] Caudil.M., *Neural Networks Primer*, San Francisco, CA: Miller Freeman Publication, 1989.
- [8] D.E.Goldberg, *Genetic Algorithm in Search ,Optimization and Machine Learning*, Addison-wesley, 1989.
- [9] K.S.Narendra and K.Parthasarthy, *Identification and Control of Dynamic System using Neural Network*, IEEE, Transaction on Neural Networks, Vol. 1, No. 1, pp.4-27, 1990.
- [10] Patrick K.Simpson, *Artificial Neural System*, Pergamon press, New York, 1990.

- [11] Hertz J., Krogh A., & Palmer R. G., *Introduction to the Theory of Neural Computation*, MA, Addison Wesley, 1991
- [12] Caudil M. and C.Butler, *Understanding Neural Networks : Computer Exploration*, Vols. 1 & 2, Cambridge, MA: the MiT Press, 1992.
- [13] Jang J.-S.R., *ANFIS: Adaptive-network-Based Fuzzy Inference System*, IEEE Transaction on System, Man and Cybernetics, Vol.23, No. 3, pp. 665-685, 1993.
- [14] Martin T.HagAn and Mohmmaad B.Menhaj, *Training Feedforward Networks with the Marquardt Algorithm*, IEEE Transaction on Neural Networks, Vol. 5, No. 6 , pp-989-993, 1994.
- [15] P. Kundur, *Power System Stability and Control*, McGraw-Hill, 1994.
- [16] J. Kennedy and R. Eberhart, *Particle Swarm Optimization*, in Proc. of the IEEE international conference on neural networks, pp. 1942-1948, 1995.
- [17] Satish Joshi, *Voltage Stability and Contingency Selection Studies in Electric Power Systems*, Ph.D thesis, 1995.
- [18] F. ShabAni, N.R.Prasad, H.A.Smolleck, *A Fuzzy Logic Supported Weighted Least Squares State Estimation*, International Journal on Electric Power Systems Research, Vol. 39, pp55-60, 1996.
- [19] K.S.Narenda and S.M.Mukhopadhyay, *Adaptive Control using Neural Networks and Approximate Models*, IEEE, Transaction on Neural Networks, Vol. 8, No. 3, pp. 475-485, 1997.
- [20] Curtis Johnson, *Process Control instrumentation Technology*, fourth Edition, PHi, 1998.
- [21] F.D. Galiana and M. Ilic, *A Mathematical Framework for the Analysis and Management of Power Transactions Under Open Access*, IEEE Trans. on Power Systems, vol. 13, no. 2, pp. 68- 687, 1998.
- [22] M. Ilic, F.D. Galiana and L. Fink, *Power System Restructuring Engineering and Economics*, Kluwer Academic Publishers, 1998.

- [23] D.K.Chaturvedi, P.S.Satsangi, P.K.Kalra, *Load frequency control : A Generalized Neural Network Approach*, International Journal on electrical power and energy system, Vol. 21, pp. 405-415, 1999.
- [24] M.A.Abido, *Robust Design of Multi-machine Power System Stabilizer using Simulated Annealing*, IEEE Transaction on Energy Conversion, Vol. 15, No. 3, pp. 297-304, 2000.
- [25] N.G.Hingorani and L.Gyugyi, *Understanding FACTS: Concepts and Technology of Flexible AC Transmission System*, IEEE Press, 2000.
- [26] N.G.Hingorani, *Role of FACTS in a Deregulated Market*, IEEE, pp. 1463-1467, 2000.
- [27] J. Kennedy, R. Eberhart, *Swarm intelligence*, Academic press, San Diego, CA, 2001.
- [28] K.A.El-Metwally, *A Fuzzy Logic Based PID power system stabilization*, International Journal on Electric Power Components and Systems, Vol. 29, No. 7, pp. 659-669, 2001.
- [29] Loi Lei Lai, *Power System Restructuring and Deregulation*, Johns Wiley and sons, Ltd, 2001.
- [30] Mei S., Chen J., Lu Q., Song Y.H., Goto M., Yokoyama A., *Nonlinear Multitarget  $H_\infty$  Controller for Thyristor-controlled Series Compensation*, IET Journals and Magazines, Vol. 148, No. 6, pp. 557-561, 2001.
- [31] QiAng Lu, YuanzhAng sun, shengwei Mei, *Non Linear Control System and Power System Dynamics*, Kluwer Academic Publishers, 2001
- [32] Vaibhav Donde, M.A.Pai, An A.Hiskens, *Simulation and Optimization in an AGC System After Deregulation*, IEEE Transaction on Power System, Vol. 16, No. 3, pp.481-489, 2001.
- [33] K.R.Padiyar, *Power System Dynamics Stability and control*, BS Publications, 2nd Hyderabad, India, 2002.
- [34] K. M. Passino, *Biomimicry of Bacterial foraging for Distributed Optimization and Control*, IEEE Control System. Mag., Vol. 22, No. 3, pp., 52-67, 2002.

- [35] Li G, Lie TT, soh CB, YAng GH, *Design of State Feedback Decentralized Non Linear  $H_\infty$  Controllers in Power System*, International Journal on Electrical power and Energy system, Vol.24, pp. 601-610, 2002.
- [36] Mishra,S., Dash,P.K.,Hota ,P.K.,Tripathy,M., *Genetically Optimized Neuro-fuzzy IPFC for Damping Modal Oscillations of Power System*, IEEE Transaction on Power System, Vo-17, issue-4, pp-1140-1147,2002.
- [37] Vijay Vittal, *Consequence and impact of Electric Utility Industry Restructuring on Transient Stability and Small Signal Stability Analysis*, Proceedings of the IEEE, Vol.88, No. 2, pp. 196-207, 2002.
- [38] Alberto D.Del Rosso, Claudio A.Canizares, Victor M.Dona, *A Study of TCSC Controller Design for Power System Stability Improvement*, IEEE transactions on power system, Vol. 18, No.4, pp: 1487-1496, 2003.
- [39] ChuAn-Te ChAng.YuAn-Yih Hsu, *Design of An ANN Tuned Adaptive UPFC Supplementary Damping Controller for Power System Dynamic Performance Enhancement*, international Journal on Electric Power Systems Research, Vol. 66 , pp. 259–265, 2003.
- [40] D.Rerkpreedapong, A.Hasanovic, A.Feliachi, *Robust Load Frequency Control Using Genetic Algorithms and Linear Matrix inequalities*, IEEE Transaction on power system, Vol.18, No.2, pp. 855-861, 2003.
- [41] Hadi Sadat, *Power System Analysis*, McGraw-Hill, 2003.
- [42] M Gopal, *Digital Control and State Variable Methods : Conventional and Neuro Fuzzy Control system*, Tata McGraw Hill, Second Edition, 2003
- [43] P.M.anderson, A.A.Fouad, *Power System Control and Stability*, Wiley Interscience, IEEE Press, Second Edition, 2003.
- [44] R.Mohan Mathur, Rajiv K. Verma, *Thyristor-Based FACTS controllers for Electrical Transmission Systems*, IEEE Press, 2003.

- [45] Wenxin Liu, Ganesh K. Venayagamoorth, Donald C. Wunsch II, *Design of An Adaptive Neural Network Based Power System Stabilizer*, Science Direct, Neural Network, Vol. 16, pp. 891-898, Special issue, 2003
- [46] Y. L. Abdel-Magid and M. A. Abido, *Optimal Multiobjective Design of Robust Power System Stabilizer Using Genetic Algorithm*, IEEE Transaction on Power systems, Vol. 18, No. 3, pp. 1125-1132, 2003.
- [47] Y. TAnga, H. Chenb, H.F. WAnga, R. Aggarwala, A.T. Johnsa, X.Z. Daic, N.H. Lib, *implementation and Test of a TCSC ANN-Based  $\alpha$ th Order inverse Control System*, International Journal on Electrical Power and Energy Systems, Vol. 25, pp. 309-317, 2003.
- [48] B. S. Grewal, *Numerical Methods*, KhAnna publishers, Sixth Edition, 2004.
- [49] DANiele Menniti, Anna Pinnarelli, Nadia Scordino, Nicola Sorrentino, *Using a FACTS Device Controlled by a Decentralized Control Law to Damp the Transient Frequency Deviation in a Deregulated Electric Power System*, International Journal on Electric Power Systems Research, Vol. 72, pp. 289-298, 2004.
- [50] IEEE/CIGRE Joint Task Force on Stability Terms and Definitions, *Definition and classification of power system stability*, IEEE Transaction On Power System, Vol. 19, No.3, pp. 1387-1401, 2004.
- [51] M.Dobrescu and I.Kamwa, *A New Fuzzy Logic Power System Stabilizer Performances*, Power System Conference and Exposition, Vol. 2, pp. 1056-1061, IEEE PES, 2004.
- [52] Ravi Segala, Avdhesh Sharma, M.L. Kothari, *A Self-tuning Power System Stabilizer Based on Artificial Neural Network*, International Journal on Electrical Power and Energy Systems, Vol. 26, pp. 423-430, 2004.
- [53] S.P.Ghosal, *Optimization of PID Gains by Particle Swarm Optimization in Fuzzy Based Automatic Generation Control*, International Journal on Electric Power System Research, Vol. 72, No. 3, pp. 203-212, 2004.

- [54] Adrian andreoiu,Kamkar Bhattacharya, *PSS-Control as an Ancillary Service*, International Journal on Electric Power System Research, Vol.74, pp. 391-399, 2005.
- [55] C.K. Panigrahi, P.K. Chattopadhyay, R.N. Chakrabarti, *FACTS in Deregulated Market Scenario*, Inaugural IEEE PES Conference and Exposition in Africa, IEEE, 2005.
- [56] I.Kamwa, R. Grondin, and G. Trudel, *IEEE PSS2B Versus PSS4B: The Limits of Performance of Modern Power System Stabilizers*, IEEE Transaction on Power Systems, Vol. 20, No. 2, pp. 903-915, 2005.
- [57] Ibraheem, Kumar Prabhat, Kothari D.P., *Recent Philosophies of Automatic Generator Control Strategies in Power Systems*, IEEE Transaction on Power System, Vol. 20, No. 1, pp. 346-357, 2005.
- [58] Jensen R. & Shen Q., *Fuzzy-Rough Data Reduction With Ant Colony Optimization*, IEEE Transaction on Fuzzy Sets & Systems, Vol. 149, No. 1, pp. 5-20, 2005.
- [59] Joe H. Chow, Felix F. Wu, James A Momoh, *Applied Mathematics for Restructured Electric Power Systems: Optimization, Control and Computational Intelligence*, Springer,2005.
- [60] Mara Lucia M. Lopes, Carlos R. Minussi, Anna Diva P. Lotufo, *Electric Load forecasting Using A Fuzzy ART & ARTMAP Neural Network*, Applied intelligent Techniques, Vol. 5, pp. 235-244, 2005.
- [61] TamerAbdelazim & O.P.Malik, *Power System Stabilizer Based on Model Reference Adaptive Fuzzy Control*, International Journal on Electric Power Components and Systems, Vol. 37, No. 9, pp. 985-998, 2005.
- [62] Xiao-ping zhang, Christian Rehtanz, Bikash Pal, *Flexible AC Transmission System : Modeling and Control*, Springer, 2006.
- [63] Andre M.D. Ferreira, Jos e A.L. Barreiros, Walter Barra Jr., Jorge Roberto Brito-de-Souza, *A Robust Adaptive LQG/LTR TCSC Controller Applied to Damp Power System Oscillations*, International Journal on Electrical Power System Research, Vol. 77, pp. 956-964, 2007.

- [64] Faa-Jeng Lin, Po-Kai HuAng, Chin-Chien Wang, Li-Tao Teng, *An induction Generator System Using Fuzzy Modeling and Recurrent Fuzzy Neural Network*, IEEE Transaction on Power Electronics, Vol. 2, No. 1, pp. 260-271, 2007.
- [65] I.J.Nagrath, M.Gopal, *Control System Engineering*, New Age international Publisher, Fifth Edition, 2007
- [66] Sidhartha Panda, N.P.Padhy, *Coordinated Design of TCSC Controller and PSS Employing Particle Swarm Optimization Technique*, World academy of Science, Engineering and Technology, Vol. 28, pp. 428-436, 2007.
- [67] A.Karami, M.S. Mohammadi, *Radial Basis Function Neural Network for Power System Load-flow*, International Journal on Electrical Power and Energy Systems, Vol. 30, pp. 60-66, 2008.
- [68] D. K. Chaturvedi, O. P. Malik, *Neurofuzzy Power System Stabilizer*, IEEE Transaction on Energy Conversion, Vol. 23, No. 3, pp. 887-894, 2008.
- [69] Faa-Jeng Lin, Li-TaoTeng, Meng-HsiungYu, *Radial Basis Function Network Control with Improved Particle Swarm Optimization for induction Generator System*, IEEE Transcation on Power Electronics, Vol. 23, No. 4, pp-2157-2169, 2008.
- [70] K. ShAnti Swarup, *Artificial Neural Network Using Pattern Recognition for Security Assessment and Analysis*, International Journal on Neurocomputing, Vol. 71, pp-983-998, 2008.
- [71] Miguel Ramirez-Gonzalez, O.P. Malik, *Power System Stabilizer Design using an Online Adaptive Neurofuzzy Controller with Adaptive Input Link Weights*, IEEE transaction on Energy Conversation, Vol.23, No.3, pp.914-922, 2008.
- [72] M. Carolin Mabel, E. Fernandez, *Analysis of Wind Power Generation and Prediction Using ANN: A Case Study*, International Journal on Renewable Energy, Vol. 33, pp. 986-992, 2008.
- [73] R. Bayindir, S. Sagioglu, I. Colak, *An intelligent Power Factor Corrector for Power System Using Artificial Neural Networks*, International Journal on Electric Power Systems Research, pp. 152-160, 2008.

- [74] Michael J. Basler, Richard C. Schaefer, *Understanding Power-System Stability*, IEEE Transaction on Industry Applications, Vol. 44, No. 2, pp. 463-474, 2008.
- [75] Salman Hameed, Biswarup Das, Vinay Pant, *A Self-tuning Fuzzy Pi Controller for TCSC to improve Power System Stability*, International Journal on Electrical Power System Research, Vol. 78, pp. 1726-1735, 2008.
- [76] S.H.Hosseini, A.H.Etemadi, *Adaptive Neuro-fuzzy inference System Based Automatic Generation Control*, International Journal on Electric Power Systems Research, Vol. 78 , pp.1230-1239, 2008.
- [77] C.Srinivasa Rao, S.Siva Nagaraju, P.Sangameswara Raju, *Automatic Generation Control of TCPS Based Hydrothermal System Under Open Market Scenario: A Fuzzy Logic Approach*, Vol. 31, pp. 315-322, 2009.
- [78] H.Shayeghi, H.A.Shayanfar, A.Jalili, *LFC Design of a Deregulated Power System With TCPS Using PSO*, international Journal of Electrical and Electronics Engineering, Vol. 3:10, 2009, pp.632-640
- [79] J.Nanda, S.Mishra, L.C.Saikia, Maiden, *Application of Bacterial foraging Based Optimization Techniques in Multiarea Automatic Generation Control*, IEEE Transaction on Power System, Vol. 24, No. 2, pp. 602-609, 2009.
- [80] Lachman, T., Mohamad, T.R., *Neural Network Excitation Control System for Transient Stability Analysis of Power System*, TENCON, IEEE Conference, 2009.
- [81] Shaoru Zhang and Fang Lin Luo, *An improved Simple Adaptive Control Applied To Power System Stabilizer*, IEEE Transaction on Power Electronics, Vol. 24, No. 2 pp. 369-375, 2009.
- [82] S.R. Samantaray , P.K. Dash , S.K. Upadhyay, *Adaptive Kalman Filter and Neural Network Based High impedance Fault Detection in Power Distribution Networks*, Electrical Power and Energy Systems, Vol. 31, pp. 167-172, 2009.
- [83] Ai-Hinai, *Dynamic Stability Enhancement Using Genetic Algorithm Power System Stabilizer*, International Conference on Power System Technology, IEEE, 2010.

- [84] Adam Dysko, William E. Leithead, John O' Reilly, *Enhanced Power System Stability by Coordinated PSS Design*, IEEE Transaction on Power systems, Vol. 25, No. 1, pp. 413-422, 2010.
- [85] Elyas Rakhshni, Javed Sadeh, *Practical Viewpoints on Load Frequency Control Problem in a Deregulated Power System*, International Journal on Energy Conversion and Management, Vol. 51, pp. 1148-1156, 2010.
- [86] Gong Li, Jing Shi, *on Comparing Three Artificial Neural Networks for Wind Speed forecasting*, International Journal on Applied Energy, Vol. 87, pp-2313-2320, 2010.
- [87] J-S.R JAng, C.-T.Sun, E-Mizutani, *Neuro-Fuzzy and Soft Computing : A Computational Approach to Learning and Machine intelligence*, PHI, 2010.
- [88] Katsuhik Ogata, *Modern Control Engineering* , PHI, Fifth Edition, 2010.
- [89] S.Rajasekaran, G.A. Vijayalakshmi Pai, *Neural Networks, Fuzzy Logic, and Genetic Algorithm Synthesis and Applications*, PHI, 2010.
- [90] S.Sumathi and Surekha P., *Computational intelligence Paradigms Theory and Application Using MATLAB*, CRC Press, Taylor and Francis Group ,2010.
- [91] V.Jayasankar, N.Kamaraj, N.VAnaja, *Estimation of Voltage Stability index for Power System Employing Artificial Neural Network Technique and TCSC Placement*, International Journal on Neurocomputing, Vol. 73, pp-3005-3011, 2010.
- [92] D.P.Kothari and i.J. Nagrath, *Modern Power System Analysis*, Tata McGraw-Hill, fourth edition, 2011.
- [93] Datta S., Roy, A.K., *Radial Basis Function Neural Network Based STATCOM Controller for Power System Dynamic Stability Enhancement*, IICPE , pp.1-5, 2011.
- [94] Chin-Hsing Cheng, Jian-Xun Ye, *GA-Based Neural Network for Energy Recovery System of the Electric Motorcycle*, International Journal on Expert Systems with Applications, Vol.38, pp. 3034-3039, 2011.

- [95] N.B. Dev Choudhury , S.K. Goswami, *Artificial intelligence Solution to Transmission Loss Allocation Problem*, International Journal on Expert Systems with Applications, Vol. 38, pp. 3757-3764, 2011.
- [96] Praghnesh Bhatt, Ranjit Roy, S.P. Ghoshal, *Comparative Performance Evaluation of SMES-SMES, TCPS-SMES and SSSC-SMES Controllers in Automatic Generation Control for a Two-area Hydro-Hydro System*, International Journal on Electrical Power and Energy Systems, Vol. 33, pp. 1585-1597, 2011.
- [97] Richard C.Dorf, Robert H.Bishop, *Modern Control System*, Pearson, 2011
- [98] Sachin K. Jain, S.N. Singh, *Harmonics Estimation in Emerging Power System: Key issues and Challenges*, International Journal on Electric Power Systems Research, Vol. 81, pp. 1754-1766, 2011.
- [99] Tripathy M, Mishra S., *Interval Type-2 Based Thyristor Controlled Series Capacitor to improve Power System Stability*, IET Journal on Generation, Transmission and Distribution, Vol. 5, No. 2, pp. 209-222, 2011.
- [100] V.Shanmuga Sundaram, and T.Jayabarathi, *An Artificial Neural Network Approach of Load Frequency Control in a Multi Area interconnected Power System*, Journal of Electrical Engineering, Elixir online Journal, Vol.38, pp. 4394-4397, 2011
- [101] Bayram Akdemir, Nurettin Çetinkaya, *Long-term Load forecasting Based on Adaptive Neural Fuzzy inference System Using Real Energy Data*, Energy Procedia, Elsevier, pp-794-799, 2012.
- [102] E.S.Ali,S.M.Abd-Elazim, *TCSC Damping Controller Design Based on Bacteria foraging Optimization Algorithm for a Multimachine Power System*, International Journal on Electrical power and Energy systems, Vol. .37, pp. 23-30, 2012.
- [103] E.S. Ali, S.M. Abd-Elazim, *Coordinated Design of PSSs and TCSC via Bacterial Swarm Optimization Algorithm in A Multimachine Power System*, International Journal on Electrical Power and Energy Systems, Vol. 36, pp. 84-92, 2012.

- [104] O.P. Rahi, Amit Kr Yadav, Hasmat Malik, Abdul Azeem, Bhupesh Kr, *Power System Voltage Stability Assessment through Artificial Neural Network*, Procedia Engineering, Elsevier, pp. 53-60, 2012.
- [105] Swati R.Khuntia, Sidhartha Panda, *Simulation Study for Automatic Generation Control of a Multi-area Power System by ANFIS Approach*, International Journal on Applied soft computing, Vol. 12, pp. 333-341, 2012
- [106] S.M. Radaideh, I.M. Nejdawi, M.H. Mushtaha, *Design of Power System Stabilizers using Two Level Fuzzy and Adaptive Neuro-fuzzy inference Systems*, International Journal on Electrical Power and Energy Systems, Vol.35, pp.47-56, 2012.
- [107] Swasti R. Khuntia , Sidhartha Panda, *ANFIS Approach for SSSC Controller Design for the Improvement of Transient Stability Performance*, International Journal on Mathematical and Computer Modelling, Vol.57, pp. 289-300, 2013.
- [108] S.M. Abd-Elazim, E.S.Ali, *A Hybrid Particle Swarm Optimization and Bacterial foraging for Optimal Power System Stabilizers Design*, International Journal Electrical. Power and Energy system, Vol. 46, pp. 334-341, 2013.
- [109] Najeh Chaabane, *A Hybrid ARFIMA and Neural Network for Electricity Price Prediction*, International Journal on Electrical Power and Energy Systems, Vol. 55, pp. 187-194, 2013

# Appendix A

## Data of Single machine Infinite Bus system

The system data on 1000 MVA base are given below[33] :

Generator								Transformer	
$x_d$	$x_q$	$x'_d$	$x'_q$	$T'_{d0}$	$T'_{q0}$	$H$	$\omega_B$	$R_t$	$X_t$
1.7572	1.5845	0.4245	1.04	6.66	0.44	3.542	314 rad/sec	0.00	0.1364

Transmission Line			Excitation		Operating Data			
$R_l$	$x_l$	$B_c$	$K_A$	$T_A$	$E_b$	$V_t$	$\theta$	$X_{TH}$
0.08593	0.8125	0.1184	400	0.025	1.0	1.05	21.65 <sup>0</sup>	0.13636

TCSC Data:

$T_{TCSC}$	$\alpha_0$	$X_{TCSC0}$	$p$	$X_{max}$	$X_{min}$
15ms	142 <sup>0</sup>	0.62629	2	0.8 $X_L$	0

## Appendix B

# Numerical Values of the Restructured Model

System frequency $f$	50 Hz
Inertia Constant $H$	5 s.
Regulation $R$	2.4 Hz/pu.
Load frequency characteristics $D$	0.0083 pu/Hz
Speed governor time constant $T_g$	0.08 s
Turbine time constant $T_t$	0.3 s
Power system time constant $T_p$	20 s
Power system gain $K_p$	120 Hz/pu
Frequency bias control $B$	0.425 pu
Synchronizing power coefficient	0.545 pu
$a_{12}$	-1

# Curriculum-Vitae

Pimal R.Gandhi

Assistant Professor  
Electrical Engineering Department  
Sardar Vallabhbhai Patel Institute of Technology  
Vasad, Gujarat-388 306, INDIA

## Educational Qualifications:

Sr.No	Examination Passed	Board/University	Years of Passing	% of marks	Main Subject
1	B.E.	North Guj., Modasa	1999	67.42%	Electrical
2	M.E.	MS Univ. Baroda	2006	61.67%	Electrical

## Research Papers:

1. *GA based Conventional and PID Power System Stabilizer for Stability Analysis of SMIB System*, Elixir International Journal on Electrical Engineering, Vol.40, pp.5229-5233, 2011.
2. *Design of PID Power System Stabilizer using GA for SMIB System: Linear and Non-Linear Approach*, 2011 International Conference on Recent Advancements in Electrical, Electronics and Control Engineering, Sivakasi, Dec. 15-17, IEEE, 2011.
3. *Non Linear Auto Regressive Moving Average Controller based PSS for Dynamic Power System*, International Conference on Power System Technology, POWERCON, Auckland, Oct. 30 to Nov. 2, IEEE, 2012 ,
4. *GA and ANFIS based Power System Stabilizer*, 2013 IEEE Power and Energy Society Meeting, Vancouver, July 21-25, IEEE, 2013.
5. *Design of Power System Stabilizer using Genetics Algorithm Based Neural Network*, International Journal on Electrical Engineering, ISBN: 1582-4594, Vol. 14(2), pp.1-13, 2014.
6. *Design of Ancillary Controller using GA and ANFIS in Restructured Electric Market*, 18<sup>th</sup> Power System Computing Conference (PSCC'2014), Poland, (Abstract Accepted and full paper submitted)
7. *Smart Control Techniques for Design of TCSC and PSS for Stability Enhancement of Dynamical Power System*, International Journal on Applied Soft Computing, Elsevier ,ISSN:1568-4946 (Paper Accepted)
8. *Computational Intelligent Paradigms for Design of Power System stabilizer*, International Journal on Electrical Power and Energy System, Elsevier (Under review)